Author/s:
Richardson, Zuwena Akilah

Title:
Using multiparameter imaging to understand HIV persistence in tissue in people living with HIV on antiretroviral therapy

Date:
2021

Persistent Link:
https://hdl.handle.net/11343/275134

USING MULTIPARAMETER IMAGING TO UNDERSTAND HIV-1 PERSISTENCE IN TISSUE IN PEOPLE LIVING WITH HIV-1 ON ANTIRETROVIRAL THERAPY

Zuwena Akilah Richardson

MSc, BSc

Submitted in fulfilment of the requirements for the degree of

Doctor of Philosophy

Date: 04/01/2021

Department of Microbiology and Immunology

Faculty of Medicine, Dentistry and Health Science

Abstract

Antiretroviral therapy (ART) has dramatically reduced morbidity and mortality for people living with HIV-1 (PLWH) however treatment is life long and there is no cure. The main barrier to an HIV-1 cure is the persistence of long lived and proliferating latently infected $CD4^+$ T-cells. These cells are more commonly found in tissue such as lymph node (LN) or the gastrointestinal (GI) tract. Latency can be established in multiple T-cell subsets, but the contribution of regulatory T-cells (Tregs) as targets for HIV-1 infection and latency are not well defined. These cells express the transcription factor FoxP3 as well as the immune checkpoint (IC) markers programmed death (PD-1) and cytotoxic T lymphocyte associated protein (CTLA-4) that both potentially play a role in maintaining HIV-1 latency. We hypothesized that IC markers define subsets of latently infected T-cells in LN tissue and that Tregs are an important reservoir that persists in PLWH on ART.

We first developed a method to detect HIV-1 RNA and HIV-1 DNA and multiple cellular markers in LN tissue from PLWH on ART. To optimise the method, productive and latent HIV-1 infection were first examined in two latently infected cell lines (ACH2 and J-Lat) and a model of latency using primary $CD4^+$ T-cells co-cultured with monocytes and infected with a virus that expresses green fluorescent protein (GFP). We used flow cytometry to sort GFP^+ (productively infected) and GFP- (latently infected) cells. GFP- cells were then stimulated with phorbol myristate acetate (PMA). Cells from each condition were collected and embedded into paraffin and then single slides were prepared. HIV-1 RNA and DNA were quantified using *in situ* hybridization (ISH) with anti-sense probes targeting HIV-1 RNA and sense probes targeting HIV-1 DNA. When either cell line was stimulated with PMA and then mixed with an increasing number of uninfected cells at a ratio of 1:1 and 1:10, detection of both HIV-1 RNA and DNA with the probes was clearly demonstrated. Using the *in vitro* infection model, stimulation of GFP- cells resulted in a significant increase in detection of HIV-1 RNA relative to HIV-1 DNA consistent with clear discrimination of the RNA and DNA probes.

Having demonstrated the HIV-1 RNA and DNA probes were sensitive and specific in paraffin embedded samples of cell lines, we then assessed formalin fixed paraffin embedded (FFPE) LN tissue collected from PLWH both on and off ART. We quantified HIV-1 RNA and DNA using the same fluorescent probes, in combination with antibodies to the cell proteins (CD4, PD-1, FoxP3 and CTLA-4) using a novel multiplex detection system (Vectra multispectral immunohistochemistry) and analysed expression of the probes using Halo software. In all samples, we detected both HIV-1 RNA and DNA in LN, but in individuals on ART compared to individuals off ART there was a lower ratio of RNA: DNA.

We successfully detected cells that co-expressed HIV-1 RNA and DNA (active replication) and DNA only (latently infected cells) in combination with FoxP3, CD4, CTLA-4 and PD-1 both on and off ART. We observed significantly more frequent cells expressing both RNA and DNA in the B –cell follicle (BCF) compared to the T-cell zone (TCZ) when corrected for the total number of cells in each region. Tregs were defined by expression of FoxP3 and were mainly distributed within the TCZ. Tregs represented only a small proportion of the infected cells but HIV-1 infection was more frequent in Tregs compared to nonTregs, in participants on and off ART. Most of the expression of ICs was in nonTregs. Although the difference of HIV-1 between IC^+ and IC^- expressing cells was minimal on ART, virus was detected in CTLA-4^+ Tregs and these cells were distributed between the BCF and the TCZ cells in PLWH on ART. Taken together, these data demonstrated that Tregs and cells expressing the ICs PD-1 and CTLA-4 are infected and ART reduced the frequency of infection in all subsets, but virus persisted in all subsets.

Finally, we aimed to compare the relative sensitivity of ISH for detection of HIV-1 RNA and DNA to cell sorting and PCR quantification. In a separate cohort of PLWH on ART, we collected blood and LN (n=8) and sorted cells into four populations based on expression of PD-1 and CTLA-4 and compared the frequency of cells with HIV-1 DNA, unspliced and multiply spliced RNA using PCR. In two participants we also examined LN tissue using combined RNA/DNAscope with multiplex immunohistochemistry (mIHC). We found enrichment of HIV-1 DNA in memory $CD4^+$ T-cells expressing CTLA-4^+ cells compared to other cell subsets, but there was no significant difference between the blood and the LN. Using IHC, we

found enrichment of HIV-1 in CTLA-4^+ cells that are either nonTregs or Tregs located in either the BCFs or the TCZs.

Combining HIV-1 RNA and DNA identification by ISH with immunohistochemistry allows identification of HIV-1 persistence in specific cell populations within tissue samples. Using this technique, we have shown that CTLA-4^+ Tregs compared to nonTregs expressing ICs are more frequently infected in PLWH on and off ART. Although the Treg contribution to the HIV-1 reservoir remains small, their expression of immune checkpoints may allow them to play a disproportionate role in the persistence of the HIV-1 reservoir. Immune checkpoint inhibitors could potentially target both Tregs and nonTregs that express ICs and reverse HIV-1 latency and could therefore be used as a component of a combination cure strategy.

Declaration

I declare that this thesis:

I. Comprises of my original work towards the Doctor of Philosophy except where indicated in the Preface

II. Due acknowledgment has been made in the text to all other material used

III. This thesis is less than 100,000 words in length, exclusive of tables, figures, references and the appendices

Signature: Zuwena Richardson

Date: 4/01/2021

Preface

Most of the work for this thesis was carried out under the supervision of A/ Prof Paul U. Cameron, with co-supervision of Professor Sharon R. Lewin in the Lewin/Cameron Laboratory at the Peter Doherty Institute for Infection and Immunity and the Department of Microbiology and Immunology, Faculty of Medicine, Dentistry and Health Sciences at the University of Melbourne, Australia. Most of this work was carried out in the laboratory of Professor Johnathon Cebon and Dr. Andreas Behren at the Olivia Newton-John Cancer Centre Research Institute, Austin Hospital, Heidelberg, Australia. Three weeks was spent at the Frederick National Laboratories for Cancer Research, Frederick, Maryland, United States in the Laboratory of Dr. Jacob Estes and Dr. Claire Deleage. In addition, most of the analysis took place in the Laboratory of Professor Sarah Ellis at the Peter MacCallum Cancer, Melbourne, Australia.

Chapter 2 has been formatted according to requirements for publication to the Journal of Immunological Methods.

Multiparameter immunohistochemistry analysis of HIV-1 DNA, RNA and immune checkpoints in lymph node tissue.

Zuwena A. Richardson†, Claire. Deleage‡, Candani S A. Tutuka§,¶, Marzena. Walkiewicz§,||, Perla M. Del Río-Estrada¦, Rachel D. Pascoe†, Vanessa A. Evans†, Gustavo. Reyesteran¦, Michael. Gonzales*, Samuel. Roberts-Thomson*, Jacob D. Estes‡‡, Sharon R. Lewin†, #, || || & Paul U. Cameron†,**

Components of the work in this thesis were carried out by the following individuals, as detailed below Dr. Mauricio González-Navarro and Dr. Fernanda Torres-Ruiz for performing the LN biopsies (Centro de Investigación en Enfermdades Infecciosas, Mexico City, Mexico) (Chapter 2). We thank Caroline Tumpach and Michael Roche (Peter Doherty Institute) for providing us with cells (Chapter 2, Fig. 2.2 A&B) and Rachel Pascoe for providing me with cells for the *in vitro* model of latency (Chapter 2, Fig. 2.3). In addition, Claire Deleage, Jacob Estes (Frederick National Laboratories for Cancer Research) and Metta Jana (Peter MacCallum Cancer Centre) contributed intellectually to the analysis portion (Chapter 2). Thomas Rasmussen (Peter Doherty Institute) for his guidance on the analysis (Chapter 3) and as one of the contributors in the study design and analysis portion (Chapter 4). Vanessa Evans, Ashanti Dantanarayana, Rachel Pascoe performed processing of LN biopsies and cell sorting on biopsy samples (Chapter 4). Ajantha Rhodes performed PCR analyses of CA-US HIV-1 RNA (Chapter 4.3).

Acknowledgements

I would like to take time now to thank the people that significantly contributed to me reaching this far. Herewith, being so grounded in my faith, I would like to start by thanking God, for being the source of my strength and peace.

Secondly, I would like to thank my supervisors Paul Cameron and Sharon Lewin. Paul, thank you for your invaluable insight in formulating the research questions. At first, it was really hard for me to see you retire towards the end of my PhD, as I missed the option, I had of just popping in your office to ask you a question. Nevertheless, thank God for technology as we found a way to make it work. Therefore, I'm grateful to you for providing me with the opportunity to call you whenever I needed your help (including the weekends), not many students have that option. Also, thank you for asking me critical questions and pushing me to resolve issues on my own but also helping me when needed. Although it was time-consuming some days, I am grateful as it made me the independent person that I am today. I also appreciate you supporting me whenever I would tell you about a meeting or conference that I think might benefit me or my work.

I am very appreciative of my second supervisor Sharon for allowing me to join her lab after leaving the Department of Medicine at the Austin Hospital to join the Department of Microbiology and Immunology at the Peter Doherty Institute. This was a huge move for me, but it has always been my dream to work on HIV-1/AIDS, so thank you for allowing that transition to happen so smoothly. Your insightful feedback pushed me to sharpen my thinking and brought my work to a higher level. Also, thank you for finding a way to collaborate with my former lab at the Austin Hospital and with other experts in this field such as Jake Estes, who have significantly helped with my PhD. As a somewhat shy person, this meant I was out of my comfort zone and that I would have to meet new people or be in a new working environment. Looking back, I can say that I have grown so much and became independent, and as a result, I was able to foster and maintain collaborations. I would also like to thank Sharon for her support when my health wasn't optimal, this contributed to my recovery and my eagerness in returning to the lab and

finishing. Empathy goes a long way! Sharon, I want to thank you for your support and for all the opportunities I was given to further my research.

I would like to also thank Vanessa Evans for co-supervising me after Paul's retirement. I appreciate you travelling to The Austin Hospital to meet me and your input in my research. You have been also so supportive, thanks for also being a listening ear when I needed it. I would also like to thank Thomas Rasmussen for assisting me towards the end with helping me to organize my results and proof-reading my thesis. I have always been amazed at how quickly you would get back to me, and for that, I am truly appreciative of. I am very thankful for our lab manager Ajantha Solomon and our research manager Jasminka Sterjovski (Peter Doherty Institute). Aj, thanks for assisting me and being so supportive when I was working at the Austin, I will miss our little walks. Jas, you have been so supportive and understanding. I will never forget when the Hurricane destroyed 90% of my island back home and I was unable to contact my family for a few weeks. This was one of the scariest moments in my life, but you were there every day checking to see if I was okay and offering me to go for a walk in the park. I will forever be appreciative of your kindness, empathy and support, you are one of a kind!

Special thanks to my collaborators at Olivia Newton-John Cancer Centre Research Institute, Austin Hospital, Australia. Marzena Walkiewicz (my lab aunty), thanks for teaching me all there is to know about immunohistochemistry and for all the delicious treats. I would also like to thank Dani for training me on the Vectra imaging platform and Johnathon Cebon and Katherine Woods for being so graceful when I decided to switch to HIV-1 research and welcoming me back for collaboration, it felt as if I have never left!

I would also like to thank my collaborators Claire Deleage and Jake Estes (Frederick National Laboratories for Cancer Research, USA), thank you for picking me up every morning and teaching me RNA/DNAscope and imaging. On the same note, I would also like to thank my other collaborators, Gustavo Reyesteren and Perla Del-Rio (Instituto Nacional de Enfermedades Respiratoriras, Mexico), Michael Gonzales, Samuel Thomson (Pathology Department, The Royal Melbourne Hospital, Australia) and Metta Jena and Rejhan Idrizi (Peter MacCallum Cancer Centre, Australia).

In addition, I am greatly appreciative of the immunomodulation group (Peter Doherty Institute), who contributed to my research, particularly Judy and former member Renee, who has trained me so quickly on getting PC3 certified and on the *in vitro* model of Latency. I also owe gratitude to our research assistants, especially Caroline and former research assistant Surekha for always following up on my orders and contacting me if there were any issues. I would also like to thank present and former members of the lab Simin, Hao, Sandy and Jenny.

To my parents, O'Neil Richardson and Julienne van der Leeuw-Richardson, thank you for the encouragement, sacrifices made and for permitting me to leave my Island at a young age to pursue my dreams. To my big sister Nyakomi, thanks for always being my hype man and believing in me, and to my other siblings, Glenroy and Abigail, my intelligent nephew Amaziah and friends overseas and the ones I've made in Australia (too numerous to mention), thank you for supporting me in every aspect during the completion of my PhD.

After completing my masters, I was fortunate to work in my hometown St. Maarten (which has the largest amount of people living with HIV-1/AIDS in the Dutch Caribbean islands) at the HIV-1/AIDS foundation, interviewing patients suffering in secret. This has also contributed to me pursuing a PhD in this field. Therefore, I would like to acknowledge those living with HIV-1, particularly in places where stigma and discrimination are at the highest.

I've learned that people will forget what you said, people will forget what you did, but people will never forget how you made them feel.' *M. Angelou*

Thank you for all the positivity and support throughout this journey.

Table of Contents

List of Figures

Chapter 1

Chapter 2

Chapter 3

Chapter 4

List of Tables

Chapter 1

Chapter 2

Chapter 3

Chapter 4

List of Abbreviations

ART	Antiretroviral therapy
AMPK	adenosine monophosphate-activated kinase
AP	alkaline phosphatase
APC	antigen-presenting cell
APOBEC	apolipoprotein B mRNA editing enzyme, catalytic polypeptide
ARV	antiretroviral
BBB	blood brain barrier
BCF	B-cell follicle
Bcl-2	B-cell lymphoma gene
BET	bromodomain and extra terminal domain
BIR	baculoviral IAP repeat
BMI	body mass index
BTLA	B and T-lymphocyte attenuator
cAMP	cyclic adenosine monophosphate
CAR	chimeric antigen receptor
CA-US	cell-associated unspliced
CCL19	C-C motif ligand 19
CCL20	C-C motif ligand 20
CCN3	Cellular Communication Network Factor 3
CCR5	C-C Motif receptor 5
CCR6	C-C Motif receptor 6
CCR7	C-C Motif receptor 7
CCR8	C-C Motif receptor 8
CD62L	L-selectin
CMV	cytomegalovirus
CNS	central nervous system
CSF	cerebrospinal fluid
CTLA-4	cytotoxic T lymphocyte associated protein
CTLs	cytotoxic T-lymphocytes
CXCL13	C-X-C motif ligand 13
CXCR3	C-X-C motif receptor 3
CXCR4	C-X-C motif receptor 4
CXCR5	C-X-C motif receptor 5
Cy	Cyclophosphamide
DAB	diaminobenzidine
DCs	dendritic cells
ddH_2O	double-distilled H2O
ddPCR	droplet digital PCR
ECs	endothelial cells
Env	envelope
eTfr	effector follicular regulatory
FDA	Food and Drug Administation
FDCs	follicular dendritic cells
FFPE	Formalin-fixed paraffin embedded
FIs	fusion inhibitors
FISH	Fluorescence *in Situ* Hybridization
FMO	fluorescence minus one
FoxP3	forkhead box P3

FTR	fostemsavir
GALT	gut-associated lymphoid tissue
GCs	germinal centres
GFP	green fluorescent protein
GI	gastrointestinal
GITR	glucocorticoid-induced tumour necrosis factor receptor
H&E	hematoxylin and eosin
HDACi	histone deacetylase inhibitor
HEPES	N-2-Hydroxyethylpiperazine-N′-2-ethanesulfonic acid
HEV	high endothelial venules
HIV-1	Human Immunodeficiency virus
HLA-DR	human leukocyte antigen–DR
HRP	horseradish hydrogen peroxidase
HSPCs	Hematopoietic stem progenitor cells
IAP	inhibitors of apoptosis
IC	immune checkpoint
ICB	immune checkpoint blockers
ICOS	inducible costimulatory
IL-10	interleukin-10
IL-2	interleukin-2
IL-7	Interleukin-7
IN	integrase
IPDA	intact proviral DNA assay
IRES	internal ribosome entry site
ISH	*in situ* hybridization
iTregs	induced regulatory T-cells
kb	kilo byte
LAG-3	Lymphocyte-activation gene 3
LAP	latency-associated peptide
LN	lymph node
LP	lamina propria
LTRs	long terminal repeats
mAB	monoclonal antibody
mDC	myeloid dendritic cell
mIHC	multiplex immunohistochemistry
mRNA	messenger RNA
MS	multiply-spliced
MWT	microwave treatment
NFAT	nuclear factor of activated T-cells
NF-κB	nuclear factor kappa B
NNRTIs	non-nucleoside reverse transcriptase inhibitors
NRTIs	nucleoside reverse transcriptase inhibitors
nTregs	natural Tregs
PAMPs	pathogen-associated molecular patterns
PBMCs	peripheral blood mononuclear cells
PD-1	programmed death
PFA	paraformaldehyde
PHA	phytohemagglutinin
PIC	pre-integration complex
PIs	protease inhibitors
PLWH	people living with HIV-1
PMA	phorbol myristate acetate
PPAR	peroxisome proliferator-activated receptor

PPs	peyer’s patches
PR	protease
PRRs	Pathogen-recognition receptors
P-TEFb	transcriptional elongation factor b
QVOA	quantitative viral outgrowth assay
RM	rhesus macaques
ROI	Region of Interest
RORγt	RAR-related orphan receptor gamma
RT	reverse transcriptase
RT-PCR	polymerase chain reaction
SEB	Staphylococcus enterotoxin B
SIV	simian immunodeficiency virus
SP1	spacer peptide 1
SS	single spliced
ssRNA	single stranded ribonucleic acid
STAT5	signal transducer and activator of transcription 5
TBS	Tris Buffered saline
T_{CM}	central memory T-cell
TCR	T-cell receptor
TCZ	T-cell zone
T_{EM}	effector memory T-cell
Tfh	T-follicular helper
Tfr	follicular regulatory
TGF-β	transforming growth factor beta
Th17	T-helper 17
Th3	T-helper 3
TIM-3	T-cell immunoglobulin and mucin-domain containing-3
T_N	naïve T-cell
Tr1	regulatory type 1
Tregs	regulatory T cells
TSA	tyramide system amplication
T_{SCM}	stem memory T-cells
TSDR	T-cell specific demethylation region
T_{TD}	terminally differentiated
T_{TM}	transitional memory
UNAIDS	United Nations Programme on HIV-1/AIDS
US	unspliced
VAT	Visceral adipose tissue
vDNA	viral DNA
VISTA	V-domain Ig suppressor of T-cell activation
vRNA	viral RNA
XIAP	X-linked IAP
γδ	gamma delta
Δ32	delta 32

Chapter 1: **Literature review**

1.1 THE BURDEN OF HIV-1

The Human Immunodeficiency virus (HIV-1) epidemic continues to be one of the major challenges globally, causing significant morbidity and mortality. The virus can eventually lead to Acquired Immune Deficiency Syndrome (AIDS) and to date has resulted in over 39 million HIV-1/AIDS related deaths [1,2]. So far, there are more than 38 million people living with HIV-1 (PLWH) according to the United Nations Programme on HIV-1/AIDS (UNAIDS) with the majority living in developing countries of Sub-Saharan Africa, Asia and South America [2]. According to UNAIDS reports, there has been a decrease in HIV-1 mortality from 1.95 million deaths in 2006 to 0.69 million deaths in 2019. This trend follows with the number of new cases globally decreasing in 1997 from 3.16 million down to 1.7 million in 2019. In many countries, the foundation for ending the AIDS epidemic is through the provision of antiretroviral therapy (ART) and implementing early screening. Though ART has reduced morbidity for PLWH and restricted the spread of HIV-1, there still remain several challenges, one of which is access to ART.

Moreover, studies have shown that HIV-1 testing and treatment programmes often fail to reach key populations and the prevalence of HIV-1 is estimated to be higher in men who have sex with men, sex workers and people who inject drugs. Unfortunately these groups of people sometimes suffer discrimination and experience hostility and service denial [3,4]. Despite the progress made in reducing HIV-1-related deaths with the success of ART, the burden of HIV-1 remains high even in some countries with good access to ART [5].

Despite the great successes of ART, treatment remains life-long as interruption of ART leads to viral rebound in nearly all people [6,7]. This is because the main barrier to an HIV-1 cure is the persistence of long-lived infected cells, also known as latently infected cells. Importantly, there has been an increased risk of kidney, cardiovascular, obesity and bone diseases associated with treatment despite ART becoming more effective and safer, therefore a cure for HIV-1 remains crucial, [8,9]. Moreover, the cost of providing ART globally remains a burden, particularly in high

burden countries, i.e. Africa with an increase reported in some of the countries [10]. Therefore, it is vital to develop tools to accurately identify and quantify these infected cells in PLWH on ART and to understand the exact molecular mechanism responsible for establishing and maintaining HIV-1 latency to develop eradication strategies.

1.2 THE VIRUS

HIV-1-1 consist of two single stranded ribonucleic acid (ssRNA) molecules with a ribonucleic acid (RNA) genome of approximately 9.8 kilobases in length [11]. Retroviral particles use cell-surface proteins as specific receptors to enter their host cells [12]. In HIV-1, these viral proteins are embedded in a lipid bilayer. The surface viral glycoprotein gp120 and transmembrane glycoprotein gp41 are composed of trimers of non-covalently linked heterodimers [13]. The viral core contains the capsid protein, nucleocapsid protein and the matrix protein. The capsid core is protected by a matrix protein, anchored to the inside of the viral lipid bilayer. A protective case surrounds HIV-1 genomic material and forms the capsid protein[14]. The capsid protein is comprised of a viral core and contains the RNA genome as well as three viral enzymes required for viral replication such as integrase (IN), reverse transcriptase (RT) and protease (PR) [15].

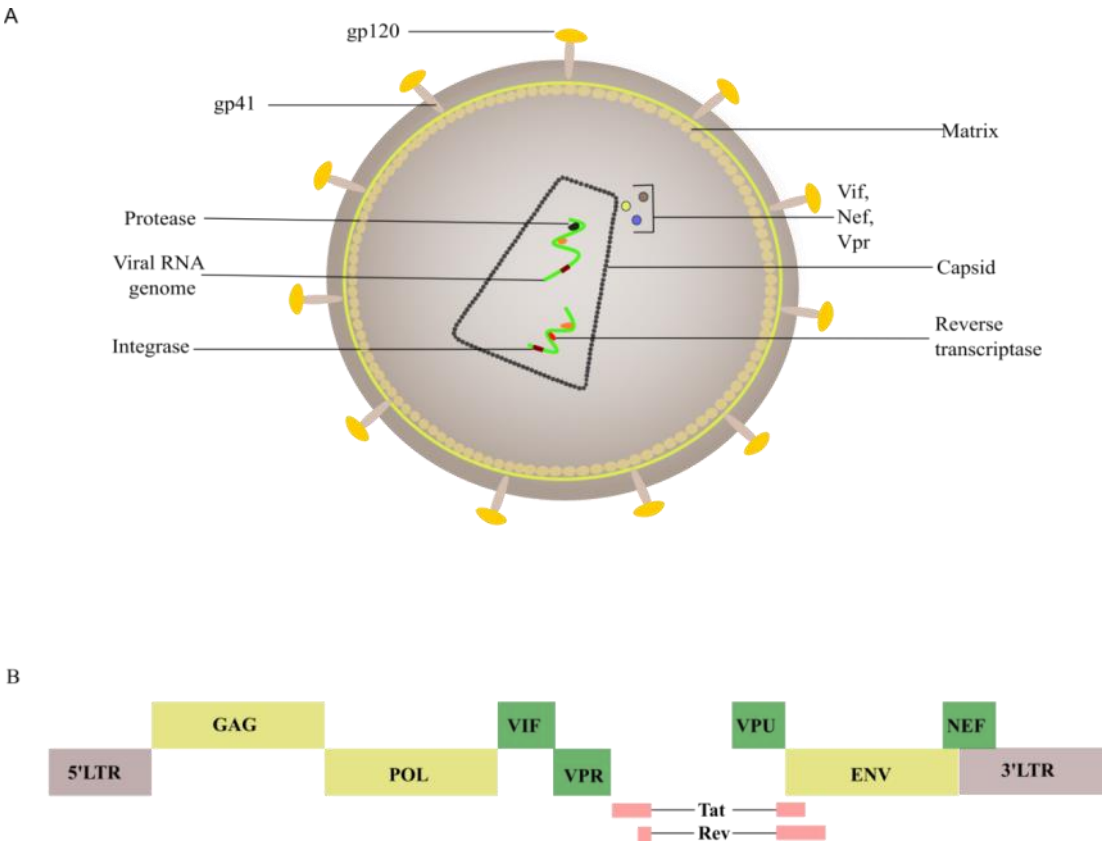

Figure 1.1 Structure of a mature HIV-1 virus and the organization of the HIV-1 genome. (a) The HIV-1 viral envelope has a lipid bilayer which consists of an outer glycoprotein gp120 and a transmembrane domain gp41, including several host proteins. HIV-1 RNA, various proteins such as Vif, Vpr, Vpu, Nef and enzymes such as protease, integrase and reverse transcriptase are covered by a cylindrical core, consisting of the matrix and the capsid proteins. (b) Representative image of the composition of the nine-reading frame from of the HIV-1-1 genome showing genes coding for the structural proteins (gag, pol and env), the accessory proteins (vpr, vif, vpu and nef) and lastly, the regulatory proteins (tat and rev). The location of the genes of HIV-1 are in the central region of the proviral DNA and codes nine proteins [16]. These proteins are divided into three classes: firstly, the structural proteins such as the viral envelope Env protein [17], the polyprotein Gag and reverse transcriptase Pol, secondly, regulatory proteins, Tat and Rev, thirdly, the accessory proteins Vpu, Vpr, Vif, and Nef [18–20]. Like most retroviruses, HIV-1-1 has the ability to reverse transcribe RNA into DNA during viral replication. Both ends of the provirus are flanked by a repeated sequence, also known as the long terminal repeats (LTRs) at the 5' and 3' ends (Figure 1.2) [16].

1.2.1 HIV-1 REPLICATION CYCLE

Following the initial step of binding, retroviral particles use cell-surface proteins as specific receptors to enter their target cells through interactions with the viral envelope (Env) glycoproteins [21,22]. The cycle of HIV-1-1 begins when gp120 binds to CD4 on the target cell surface resulting in conformational changes leading to binding to a second chemokine receptor and then fusion between the host and viral cell membrane and release of the viral core into the cytoplasm.

When the surface receptor CD4 interacts with gp120, it induces the formation of a bridging sheet between the inner and outer domains of the gp120 monomer [23]. This then triggers the binding site for a secondary coreceptor surface molecule, chemokine C-C motif receptor 5 (CCR5) or C-X-C motif receptor type 4 (CXCR4). Viruses that bind to CCR5 are called R5-tropic and viruses that bind to CXCR4 are called X4-tropic. Binding of gp120 to the coreceptors triggers membrane fusion of the viral and cellular membrane and entry of the viral RNA into the target cell [24]. Partial uncoating of the capsid allows for the viral RNA to undergo reverse transcription from single stranded viral RNA to double stranded DNA. The double stranded DNA interacts with essential viral proteins and forms a structure known as the pre-integration complex (PIC). The enzyme integrase (IN) allows for PIC to get imported to the nucleus and integrated into the viral genome, where the viral DNA is called the provirus [25].

Following import into the host cell nucleus, the viral DNA is integrated into the host DNA, transcribed, and translated with messenger RNA (mRNA). mRNA serving as a template for protein production leads to the translation of structural and non-structural proteins [26]. The new viral RNA expressed by HIV-1 is divided into three classes, unspliced (US) RNA, serving as genomic RNA, encoding Gag and Pol precursor proteins, single spliced (ss) RNA, encoding the envelope and accessory proteins. Lastly, multiple spliced RNA, encoding additional accessory proteins [27–29]. New viral particles are packaged after the processing and production of new viral proteins and genetic material. Subsequently, new viral particles are encompassed in the capsid, and as the virus is released out of the cell to become a new virion, they become surrounded by an envelope at the cell surface [30]. Finally, maturation of the virus takes place following protease (PR)-mediated cleavage, an enzyme that cleaves

two precursor proteins into smaller fragments to form mature Gag proteins; and as a result, a new infectious virion is created (Figure 1.3) [31].

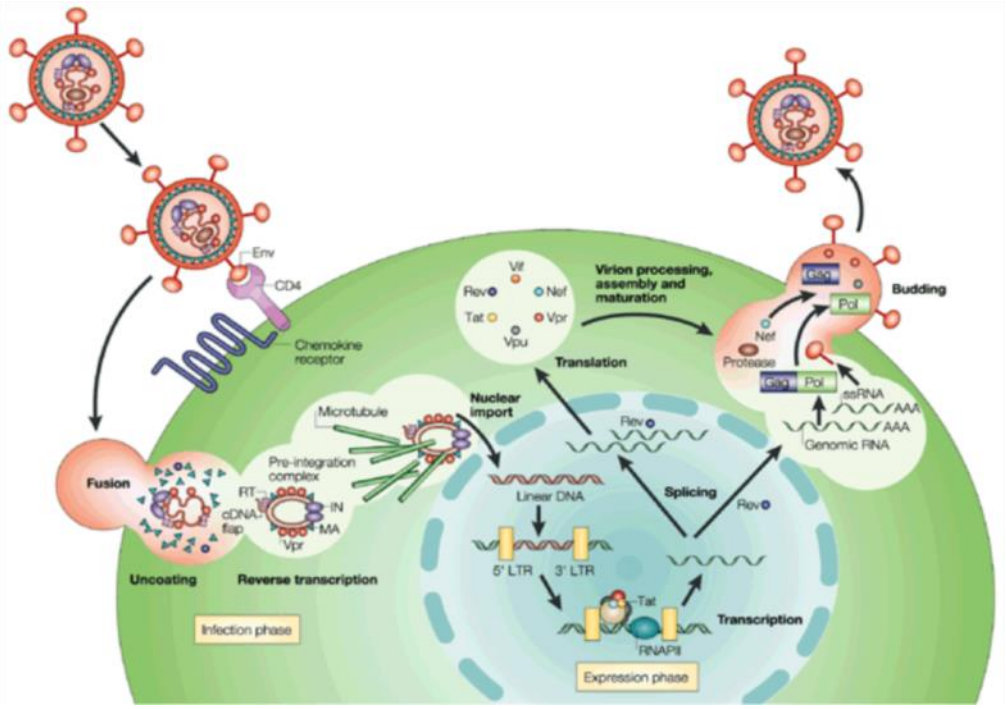

Figure 1.2 HIV-1 life cycle. HIV-1 enters the cell through the virus glycoproteins receptors where it binds to the host CD4 and co-receptor CCR5 or CXCR4. The virus enters the cell following fusion of the virus with the host cell membrane, resulting in the release of the viral nucleocapsid. Reverse transcriptase then coverts the viral single stranded RNA into double stranded DNA. The viral DNA is then transported to the host nucleus, where it uses the integrase enzyme to integrate into the host DNA. Transcription of the HIV-1 DNA leads to the production of viral RNAs, which are then transported into the cytoplasm and undergo translation leading to production of proteins. Lastly, maturation occurs, allowing for the viral RNA and proteins to assemble at the surface, leaving the cell by budding off the cellular membrane (Figure adapted from [32]).

1.3 ANTIRETROVIRAL THERAPY

ART is used to treat HIV-1 and consists of at least two or three antiviral agents that target viral enzymes or proteins required for HIV-1 replication [33]. There are now six classes of antiretrovirals based on their molecular targets: (1) the, nucleoside reverse transcriptase inhibitors (NRTIs) and (2) non-nucleoside reverse transcriptase inhibitors (NNRTIs), (3) integrase inhibitors, (4) protease inhibitors (PIs), (5) fusion inhibitors (FIs) and (6) the CCR5 co-receptor antagonist(reviewed in [34]. Recent new classes of antivirals that are progressing through clinical development include attachment inhibitors [35,36], maturation inhibitors [37], capsid assembly inhibitors [38,39] as well as long acting injectable and oral forms of antivirals [40] and broadly neutralising antibodies (reviewed in [41]).

Attachment inhibitors, also known as anti-CD4 inhibitors, inhibit HIV-1 entry by firmly binding to HIV-1 gp120 protein onto the target cells [35,36]. Before fusion of the virion and the CD4 receptor takes places, gp120 monomers of the Env form trimers based on three-fold symmetry [42]. Once attached, viral attachment to the host cell membrane becomes weakened by binding to the positively charged region of env and oppositely charged proteoglycans on the host cell membrane, preventing viral entry [36]. Successful clinical trials of attachment inhibitors in humans were first reported for the humanized monoclonal antibody (mAB) ibalizumab. Nine weeks of intravenous treatment led to a reduction in HIV-1 RNA levels in 20 of the 22 study participants off ART with no serious drug-related adverse effects [43]. In a more recent phase III study, the attachment inhibitor fostemsavir (FTR) demonstrated a decrease in plasma viral RNA in up to 82% of participants treated for 48 weeks [36].

HIV-1-1 maturation, the final stage of proteolytic cascade that leads to the formation of virus particles [44] can be blocked by maturation inhibitors. Maturation inhibitors belong to a class of small-molecule compounds which block maturation by interfering with the HIV-1-1 protease-mediated capsid protein p24 and spacer peptide 1 (SP1) [45,46]. Blocking the activity of the protease enzyme, results in the production of immature, non-infectious virus particles [38]. In a phase I and II study one of the first HIV-1-1 maturation inhibitors, bevirimat was well tolerated in combination with ART and effective in reducing plasma HIV-1 RNA [47]. However, it was discontinued due to naturally occurring sequence polymorphisms within capsid protein and the SP1 cleavage site, resulting in resistance in 50% of participants [48].

Since then, improved maturation inhibitors were developed and referred to as second generation inhibitors [37]. The development of the second generation inhibitor GSK3532795 demonstrated efficacy in reducing plasma HIV-1 RNA and coverage of naturally occurring Gag polymorphisms was more potent than bivirimat in participants on ART[49].

The viral assembly and maturation step of the HIV-1 life cycle offers the possibility of developing new classes of drugs. Specific inhibitors in these steps prevent the release of mature capsid proteins from its precursor, by blocking the activity of the protease enzyme, resulting in the production of immature, non-infectious virus particles [50]. GS-CA1, a small molecule capsid inhibitor, had potent antiviral activity by binding to the capsid and interfering with the capsid-mediated nuclear import of viral DNA [51].

1.4 HIV-1 LATENCY

HIV-1 latency is defined as the integration of a provirus in the host genome, that is replication-competent but transcriptionally silent. This means that viral proteins are not produced so latently infected cells are not visible to the immune system. In PLWH on long-term ART, latency is characterised by the detection of integrated HIV-1 DNA but minimal or no cell associated HIV-1 RNA, proteins or free virions.

1.4.1 ESTABLISHMENT OF LATENCY

HIV-1 latency may consist of two forms, based on whether or not the provirus is integrated into the host genome. The first form, pre-integration latency is when the viral life cycle is partially or completely blocked at steps such as incomplete reverse transcription or incomplete integration [52]. This form of latency exists for a short period in the cytoplasm of $CD4^+$ T-cells and appears to be clinically irrelevant [53–55]. There are two ways in which the establishment of latency can occur, referred to as pre-activation or post-activation latency (Figure 1.4).

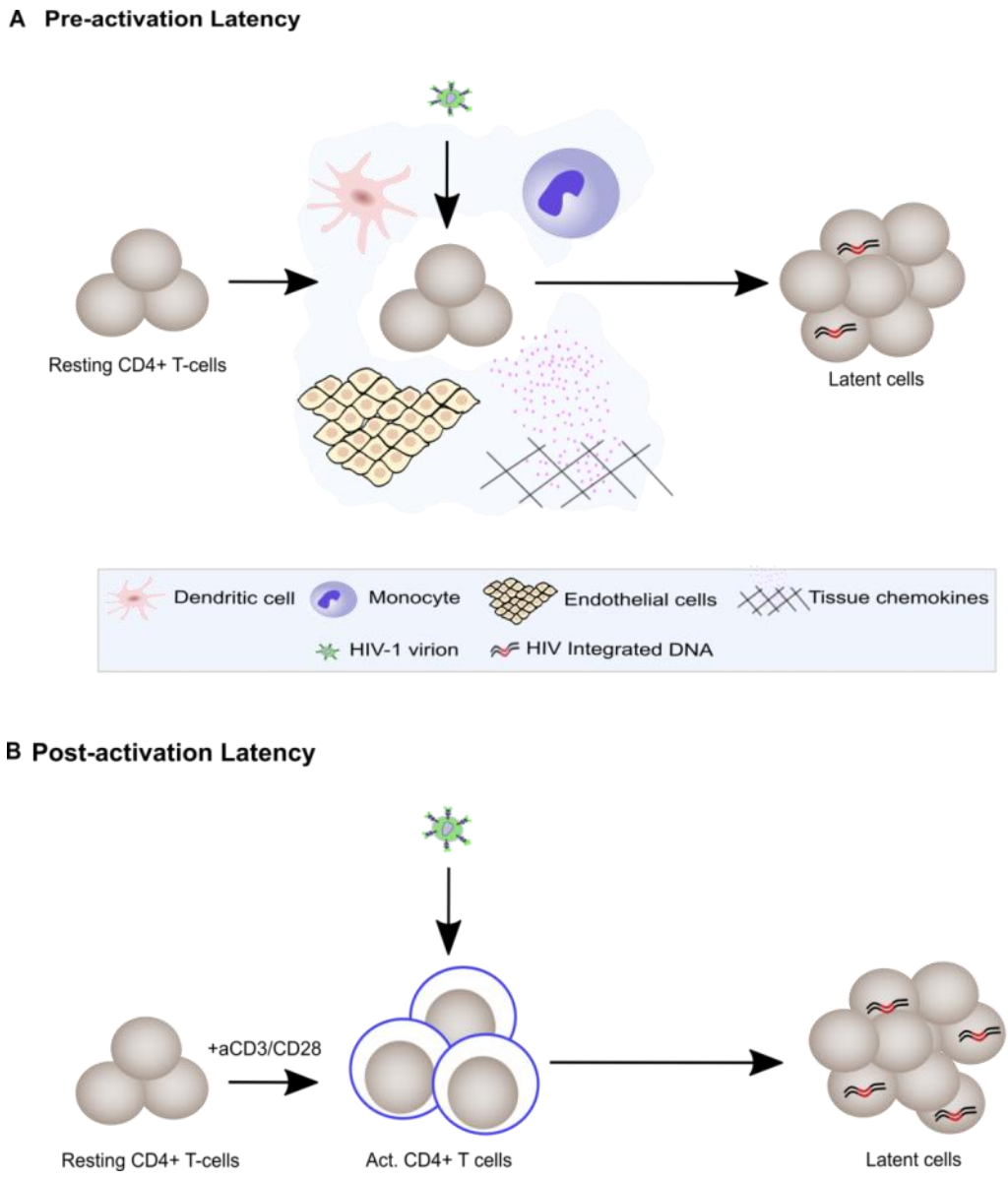

Figure 1.3 Mechanisms in which the establishment of latent infection may occur. The establishment of latency may follow two pathways. A) In the first instance, latency can be established when a resting $CD4^+$ T-cell becomes directly infected with HIV-1 in the presence of chemokines, monocytes and dendritic cells and may facilitate pre-activation latency. As a result, HIV-1 DNA integrates into resting $CD4^+$ T-cells resulting latent cells that do not express viral proteins. This process is known as pre-activation latency. B) Post-activation latency is established when resting $CD4^+$ T-cells in the presence of anti-CD3/CD28 become activated $CD4^+$T-cell, When directly infected with HIV-1, these activated $CD4^+$ T-cells may revert to a latent state.(Adapted from [56]).

1.4.2 PRE AND POST-ACTIVATION LATENCY

The process by which an activated $CD4^+$ T-cell with integrated HIV-1 DNA reverts to a resting state is termed post-activation latency [57]. Central memory (T_{CM}) $CD4^+$ T-cells are an important reservoir of HIV-1 that persists in PLWH on ART, therefore suggesting that the process by which a $CD4^+$ T-cell gets infected and returns to a quiescent state is significant for the formation of latency *in vivo* [58]. A few studies have looked at the mechanisms that drive post-activation latency. These studies suggest that cell activation is a requirement for RT and integration of HIV-1 DNA. These studies suggest that when an HIV-1 infected activated $CD4^+$ T-cells reverts into a resting state, this promotes a transcriptionally quiescent state of the HIV-1 genome [59,60]. Once latency is established, these cells are stable, long-lived with a half-life of 44 months. These cells do not produce viral proteins and therefore evade the immune system and death due to limited expression of viral proteins. Therefore, long-term treatment of ART alone would not be able to eradicate these cells [61].

Another mechanism for the establishment of latently infected $CD4^+$ T-cells is when a resting $CD4^+$ T-cell becomes directly infected. A few studies have confirmed this by looking at the establishment of latency by direct infection of a resting $CD4^+$ T-cell. This could explain why transcriptionally silent T-cell subsets such as naïve cells harbour proviral DNA [62–65]. Also, a recent study has shown that HIV-1 integration in resting T-cells is maintained in active chromatin regions in resting $CD4^+$ T-cells, however transcription of the provirus in resting $CD4^+$ T-cells repress productive HIV-1 infection [66]. Despite the non-permissive nature of $CD4^+$ T-cells, viral proteins such as Gag and Nef, have been observed in these cells, and to a lesser extent Tat, Rev and Env [67,68].

Resting $CD4^+$ T-cells can become infected in several ways, including cell to cell contact in the presence of APCs such as dendritic cells (DCs), mDCs and monocytes [69,70] but in the absence of APCs, $CD4^+$ T-cells can become activated with endothelial cells (ECs) [71] or through incubation of chemokines such as chemokine C-C motif ligand 19 (CCL19) or chemokine C-C motif ligand 20 (CCL20) [62,72,73].

1.4.3 MAINTENANCE OF LATENCY

Multiple mechanisms maintenaning post-integration latency are active at the transcriptional level of an HIV-1 infected cell [74]. These include epigenetic silencing, transcriptional interference, insufficient levels of transcriptional activators, the presence of transcriptional repressors, HIV-1 transcript elongation inefficiency and unproductive control of viral RNA splicing (reviewed in [75]). Notably, the use of ART can block new infection of permissive cells but unfortunately does not act on latently infected cells containing integrated proviruses.

The HIV-1 provirus remains stable in PLWH on ART for years due to the longevity of resting $CD4^+$ T-cells, as these cells have a long half-life [61]. HIV-1 latency is also maintained in resting $CD4^+$ T-cells as a consequence of proliferation, evidenced by identical integration sites of the virus in multiple cells [76]. Although the main driver for proliferation is unclear, potential mechanisms include homeostatic proliferation through interleukin-7 (IL-7), antigen-driven stimulation and integration site-driven proliferation (reviewed in [77]).

1.4.4 MODELS OF HIV-1 LATNECY

Several models of HIV-1 latency exist and have mimicked *in vitro* infection of the exogenous virus, though up to this day no model has completely replicated latently infected cells *in vivo* [78].

Transformed cell lines have been particularly useful in studying HIV-1-1 latency [79]. To present a more relevant representation of latency and to resemble what takes places *in vivo*; this section will focus exclusively on latency models using primary cell lines.

As mentioned earlier, primary resting $CD4^+$ T-cells constitute the major latent reservoir for HIV-1 latency and, several models have been developed to mirror what takes place *in vivo* (Table 1). Each of these cell models used to establish latency differ in the cell subsets they use to infect or the type of viral strain they use (reviewed in [80]). Despite these novel strategies for latency, each model comes with its limitation. The interaction between DC and T cell has previously shown to be potent inducers of antigen-specific T-cells and productive infection in activated $CD4^+$ T cells [81]. In addition, a recent *in vitro* model of HIV-1 latency showed that

myeloid dendritic cell (mDC) co-cultured with resting $CD4^+$T-cells could increase the frequency of HIV-1 DNA integration and latent HIV-1 infection in non-proliferating memory $CD4^+$ T-cells [69]. This model was modified by using monocytes instead of DCs to induce latency [69,82].

Table 1.1 In vitro models of latency

Model	Latency establishment	Virus	Advantages	Disadvantages
Marini *et al.*[83]	Naïve $CD4^+$ T-cells co-cultured with DC's and IL-7	NL4.3	Reflects latency *in vivo*	IL-7 which can lead T-cell activation
Karn *et al.*[84]	Infected activated $CD4^+$T-cells co-cultured with feeder cells	VSV-G pseudo-typed GFP reporter	Longevity and a large population of cells generated	Mutated virus limits the resemblance of latency
Sillicano *et al.* [85]	$CD4^+$ T-cells transduced with BCL-2 and infected	NL4-3-Δ6–drEGFP	Longevity in the absence of cytokine stimulation	Usage of mutated virus limits the resemblance of latency
O'Doherty *et al.*[86]	Direct infection of resting $CD4^+$T-cells by spinoculation	NL4.3	Reflects latency *in vivo*	Limited cell numbers and short longevity
Lewin *et al.* [73]	Resting $CD4^+$ T-cells stimulated with CCL19	NL4.3	Longevity, enhanced infection with chemokines	CCR7 is not expressed on every T-cell subset
Lewin *et al.* [69]	Resting $CD4^+$ T-cells cocultured with primary DCs or monocytes	NL(AD8)Δ*nef*	mimics physiological events in LNs by using DCs and T-cells	Limited DCs and technically challenging
Planelles *et al.*[87]	naïve $CD4^+$ T-cells activated with α-CD3/α-CD28 in the presence of IL-2	NL4.3Δ*env*	Large number of latently infected cells	Latently infected naïve cells are rarely observed in PLWH

BCL-2: B-cell lymphoma gene; CCR7: C-C Motif Chemokine Receptor 7; CCL19: chemokine (C-C motif) ligand 19; DCs: dendritic cells; VSV-G: vesicular stomatitis virus G; IL-7: interleukin 7

1.5 IMMUNOLOGICAL CONTROL OF HIV-1 IN UNTREATED INFECTION

Immunological mechanisms involved in the generation and maintenance of memory $CD4^+$ T-cells also control the persistence of the HIV-1 reservoir [88]. HIV-1 production in primary $CD4^+$ T-cells are induced by T-cell receptor (TCR) engagement together with IL-7 *in vitro* and this suggests that replication-competent HIV-1-infected memory $CD4^+$ T-cells may be continuously exposed to reactivation signals [89,90]. As a result, viral latency can be maintained by positive signals from cytokines or TCR stimulation that can be balanced out by negative signals that would interfere with reactivation of the viral reservoir and $CD8^+$ T-cells cytopathic effects or cytotoxic killing of infected cells.

1.5.1 $CD8^+$ T-CELL RESPONSES IN HIV-1

$CD8^+$ T-cells are essential mediators of adaptive immunity against viral and tumour cells. These cells require signals from activated DCs before they become cytotoxic T-lymphocytes (CTLs), enabling them to execute their killing properties. During primary infection, HIV-1 specific $CD8^+$ T-cells have the ability to decrease viral load, however, their cytotoxic function, in particular antiviral cytokines, drastically decreases and reduces their ability to exert a antiviral responses [91,92]. Compared to uninfected individuals, $CD8^+$ T-cells have been reported to be significantly elevated in untreated PLWH and expanded numbers do not normalize following suppressive ART [93,94]. In addition, due to constant exposure to viral antigens from HIV-1, $CD8^+$ T-cell function is impaired as demonstrated by presence of an exhausted phenotype in untreated PLWH. In PLWH off ART, there is increased expression of multiple immune checkpoints (ICs), including programmed cell death protein 1 (PD-1) [95] and T-cell immunoglobulin and mucin-domain containing-3 (TIM-3). Expression of TIM-3 has been directly correlated with HIV-1-1 plasma RNA [96].

In contrast to PLWH off ART, HIV-1 specific $CD8^+$ T-cells from elite controllers (ECs; individuals who maintain the virus in the absence of treatment) have increased cytolytic function by producing significant amounts of cytotoxic granule proteins, i.e granulysins, perforin and granzyme B [97,98]. Initiation of ART leads to significant improvement in $CD8^+$ T-cell function. Early initiation of ART, within 6 months of infection, compared to initiation of ART at a later stage was

shown to be associated with increased $CD8^+$ T-cell function measured by intracellular cytokine production [99].

Although HIV-1-specific $CD8^+$ T-cells have improved function in PLWH following ART, they have a lower proliferative function and cytolytic production than ECs. This was further demonstrated in an *in vitro* study in which the presence of HIV-1 $CD8^+$ T-cells did not lead to cytopathic effects of activated $CD4^+$ T-cells, but instead resulted in their survival [100]. Finally, the surface expression of PD-1 on $CD8^+$ T-cells was found to be reduced in PLWH treated earlier compared to those treated after a year with ART [101].

1.5.2 $CD4^+$ T-CELL RESPONSES IN HIV-1

$CD4^+$ T -cells play a crucial role in HIV-1 infection, providing optimal help to other cells, especially DCs, monocytes, B-cells for the induction of $CD8^+$ T-cells and antibodies and the ability to limit HIV-1-specific immune responses (reviewed in [102]. HIV-1-1 selectively infects $CD4^+$ T-cells and is associated with a massive increase of cytokines and chronic immune activation that lead to severe depletion of $CD4^+$ T-cells, particularly in untreated PLWH [103]. Impaired interleukin-2 (IL-2) production as a result of persistent immune activation had a deleterious effect on $CD4^+$ T-cells and reduced their capacity to proliferate [99,104]. $CD4^+$ T-cell proliferation was maintained in ECs and with the ability of these cells to produce more IL-2 and be more polyfunctional compared to untreated PLWH [105]. A more recent study found several elevated cytokines, amongst those were chemokine C-C motif ligand 21 (CCL21) and chemokine C-C motif ligand 17 (CCL17) which were able to suppress virus replication in resting $CD4^+$ T-cells of untreated and treated PLWH [106].

A few studies have confirmed restoration of $CD4^+$ T-cell that mediated aviremia in PLWH on ART [107,108] and reduced T-cell immune activation [109]. Burgers and colleagues showed that although ART led to $CD4^+$ T-cell recovery, not all cells were restored and that restoration of $CD4^+$ T-cells was dependent on their memory phenotype [107].

1.5.3 ONGOING INTERACTIONS BETWEEN THE IMMUNE SYSTEM AND THE HIV-1 RESERVOIR ON ART

The ongoing interaction between the immune system and HIV-1 persistence has been investigated in non-human primates [110,111]. SIV-infected RMs were infected with SIV and treated with ART to investigate the contribution of $CD8^+$ T-cells to latency maintenance. Six SIV-infected RMs received a single dose of anti-CD8α depleting Ab, following five weekly doses of a Smac mimetic inhibitor (inhibitor of apoptosis protein, which functions by activating the NF- κB pathway) [110]. This study showed that the combination of treatment increased plasma SIV RNA levels in all six RMs, suggesting that depletion of $CD8\alpha^+$ may enhance latency reversal by activating the NF-κB pathway [110]. Similar findings were also demonstrated in a recent study in which SIV-infected RM treated ART, receiving IL-15 and depleted of $CD8^+$ T-cells induced latency reversal [111].

Moreover, increasing evidence have shown that $CD8^+$ T- cells from PLWH who initiate ART in early infection exhibit a decrease in $CD8^+$ T-cell dysfunction and have a broader function of these cells. [112,113]. One study reported that PLWH treated during the acute phase were less likely to develop escape mutations directed to $CD8^+$ T-cell epitopes [114]. To circumvent this issue, $CD8^+$ T-cells that could target epitopes from latent HIV-1-1 were identified in chronically infected PLWH on ART [114]. Additional *in vitro* studies performed with humanized mice showed that stimulation of $CD8^+$ T-cells eliminated cells infected with autologous virus [114]. Altogether, this data suggests that despite the presence of CTL escape mutations, chronically infected PLWH on ART retain a broad spectrum of viral-specific $CD8^+$ T-cell responses. Strategies should focus on augmenting $CD8^+$ T-cells responses to non-escape epitopes for eradication of latency HIV-1.

Additionally, it has been shown that HIV-1 control is mediated by $CD8^+$ T-cells targeting specific epitopes [115]. Therefore, HLA presentation of HIV-1-1 epitopes to CTLs have been investigated for its role in HIV-1 control. This was demonstrated in one study which developed a method that screened the entire HIV-1-1 proteome for disease-relevant peptides from PLWH, by integrating their viral load data and HLA genotypes. Investigators show in a large dataset consisting of >6,000 chronically infected PLWH that both quantity and quality of HLA-bound HIV-1

epitopes contribute to controlling a patient's viral load. Altogether these findings confirmed the association between HLA genes and HIV-1-1 infection outcome [116].

1.6 PERSISTENCE OF HIV-1 ON ART

Despite years of continuous optimal suppressive therapy, interruption or discontinuation of ART can lead to persistent HIV-1, in which re-emergence of the virus occurs. One of the main mechanisms underlying HIV-1 persistence during ART therapy is the persistence of memory $CD4^+$ T-cells, also known as latently infected cells which can exist in a range of anatomical sites and different cell subsets [61,117,118]. Therefore, understanding the cell types and anatomical sites that harbour latent HIV-1 proviruses is essential for the design of therapeutic strategies to eradicate HIV-1 in PLWH.

1.6.1 CELLULAR RESERVOIR

As mentioned, an important source of HIV-1 persistence is the re-emergence of the virus, predominantly in long-lived and proliferating memory $CD4^+$ T-cells that harbor integrated latent proviruses but can also emerge from non $CD4^+$ T-cells. The HIV-1 provirus lies in a pool of transcriptionally silent cells. $CD4^+$ T-cells enter a cellular state that promotes the capacity for these cells to produce infectious virus particles upon stimulation, making them replication-competent [119–121]. These cells have the ability to remain invisible and escape viral cytopathic effects and CTL killing [122,123]; therefore, it is crucial to identify and eliminate HIV-1 latent cells. The most prominent cellular reservoirs of HIV-1 are T_{CM} $CD4^+$ T-cells but HIV-1 persists in naïve (T_N), effector memory (T_{EM}), transitional memory (T_{TM}) and terminally differentiated (T_{TD}) $CD4^+$ T-cells [124–127]. In addition, T_{TM} $CD4^+$ T-cells contained high levels of latency, however, other subsets such as T_{TD} ,T_N and T_{EM} are reduced over time [128]. Recently studied subsets of T-cell, the stem memory T-cells (T_{SCM}) which are long-lived are capable of spreading the provirus to other types of memory T-cells and with the potential of self-renewal and differentiation upon stimulation [129]. T_{SCM} are just as susceptible to infection as T_{CM} $CD4^+$ T-cells, despite having a lower surface expression of CCR5 [130].

1.6.2.1 OTHER $CD4^+$ T-CELL SUBSETS

$CD4^+$ T-follicular helper (Tfh) cells, a subset of memory $CD4^+$ T-cells which are found in lymph nodes (LNs) and peripheral blood mononuclear cells (PBMCs)

have been shown to be a reservoir for HIV-1 persistence in PLWH on ART [131]. Tfh cells can be distinguished from other $CD4^+$ T-cells by their low level expression of IFN- γ and IL-17 and are further characterized by expression of C-X-C Motif Chemokine Receptor 5 (CXCR5) and ICs, PD-1 [132,133]. In addition, the role of Tfh cells during HIV-1 showed that these cells are highly susceptible to HIV-1-1 infection *in vivo*, leading to viral replication and production *in vitro* and are a major site of viral replication [134,135].

In addition, a recent study has proposed another $CD4^+$ T-cell subset characterized by the surface expression of CD161 as a reservoir. $CD4^+$ $CD161^+$T-cells share their lineage with T-helper 17 (Th17) cells [136], while the majority of these cells have a T_{CM} phenotype and have been reported to be long-lived while harbouring replication competent latent HIV-1 compared to $CD4^+$ CD161neg T-cells [137]. Other cellular reservoirs amongst $CD4^+$ T-cell subsets include Th17 cells and regulatory T-cells, also known as Tregs [138,139].

1.6.1.2 NON-T-CELL RESERVOIRS

Besides T-cells, macrophage-derived monocytes have also shown to be susceptible to HIV-1 in PLWH on ART. These cells have the potential of contributing to the spread of HIV-1 as they migrate and circulate in tissue, but whether these include latently infected cells or contain replication competent virus remains unclear [140,141]. So far two recent studies have identified another subset of T-cells known as gamma delta (γδ) T-cells together with its subset Vγ9Vδ2 T-cells as a cellular reservoir in PLWH on ART[142,143]. Hematopoietic stem progenitor cells (HSPCs) have been another confirmed subset that is a reservoir to HIV-1 [144–148]. It has been demonstrated that these cells serve as an HIV-1 reservoir and harbour replication competent HIV-1 proviral genomes in PLWH on ART [149]. Other cells which have also been implicated as reservoirs include; astrocytes [150–152], microglia [153] in the brain and fibrocytes, blood and tissue [154].

Cells expressing surface receptors have also been investigated for their contribution to the HIV-1 reservoir. These include the expression of ICs on T-cells (which will further be discussed in this chapter) [124,155,156] as well as chemokine receptors C-C Motif Chemokine Receptor 6 (CCR6), C-C Motif chemokine Receptor 7 (CCR7) and C-X-C Motif Chemokine Receptor 3 (CXCR3) [157,158]. Benkirane and colleagues have proposed CD32a as a marker on $CD4^+$ T-cells and myeloid cells as

a reservoir enriched in inducible replication proviruses in PLWH on ART [137,159]. These findings have since then been challenged as these results could not demonstrate enrichment for HIV-1 DNA in $CD4^+CD32^+$ cells [160]. These cells are phenotypically diverse as a result of doublets formed with T and B-cells, potentially dismissing CD32 as a marker for latency [161,162]. A more recent study reaffirmed these findings in an *ex vivo* study confirming that $CD32^+$ $CD4^+$ T-cells contain HIV-1 proviruses and that the purity and isolation of these cells using flow cytometry play an major role in the enrichment of HIV-1 DNA [137].

1.6.2 ANATOMIC RESERVOIRS

Both human and non-human primates (NHP) studies have highlighted the importance of both the lymphoid and non-lymphoid tissue as reservoirs for HIV-1 persistence. Studies have shown that lymphoid tissues are essential anatomical sites for HIV-1 as the majority of $CD4^+$ T-cells are localised in lymphoid tissues. Moreover, a large population of these infected cells are known to reside in the main anatomical compartments such as the spleen, lungs, LNs and gut-associated lymphoid tissue (GALT) in humans and NHPs [121,163]. Anatomical compartments such as non-lymphoid tissue including the central nervous system (CNS) has not been extensively studied compared to peripheral blood and lymphoid tissue as these samples are more difficult to obtain but are documented as a potential reservoir for HIV-1 [164–166].

1.6.2.1 NON-LYMPHOID TISSUE: CNS DURING HIV-1 PERSISTENCE

The CNS is considered one of the sanctuary sites for latently infected cells and presents obstacles in cure strategies. Recognised as an immune-privileged site, the CNS has a low drug penetration to the brain with barriers such as the blood brain barrier (BBB) and reactivation due to inflammation in the CNS [167–170]. The main cellular reservoir represented in the CNS are the microglia cells with a half-life of several years [170,171], other subsets include astrocytes [164] and macrophages[153], both having half-lives of months [172,173]. One particular study showed that the CNS contained lower HIV-1 DNA compared to the LNs and GALT which has the highest level of HIV-1 DNA [174]. Sarah Joseph and colleagues illustrated a detectable higher level of HIV-1 RNA in the cerebrospinal fluid (CSF) compared to plasma, also known as CSF escape in three PLWH on ART. In one individual, there was

evidence of CSF escape produced by persistent viral replication in the CNS, with these latently infected cells sharing characteristics of a macrophage/microglia phenotype. CSF escape in the other two individuals was more likely to be caused by proliferation and trafficking of these latent cells [175].

1.6.2.2 LYMPH NODE (LNS) DURING HIV-1 PERSISTENCE

Lymphoid tissue such as LNs provides an environment for T_{CM} T-cells through the expression of lymphoid homing CCR7 and adhesion molecule L-selectin (CD62L) to recirculate through the LNs and blood [176,177]. Moreover, studies have reported that LNs contain a higher frequency of HIV-1 DNA and RNA per $CD4^+$ T-cell compared to blood [178–181].

Lymph nodes

Infected T-cells enter the LNs through the high endothelial venules (HEV), where close contact between T-cell and APC, DCs or virions leads to viral transmission [182–184]. These cells migrate to specific compartments in the LNs. This includes two main regions: the cortex which can be subdivided into the paracortex or inner cortex; T-cell zone (TCZ) and outer cortex; the B-cell follicle (BCF). These compartments are surrounded by an inner medulla which contains plasma cells, macrophages and T_{CM} T-cells (reviewed in [185]. Upon entry through the HEV, B-cells reside in the outer cortex region of the LNs as well as follicular dendritic cells (FDCs) and macrophages to form follicles. LNs consist of two types of follicles, primary and secondary follicles. Primary follicles do not contain germinal centres (GCs) whereas secondary follicles are composed of a GCs and a mantel zone region after a B-cell encounters an antigen resulting in a network of FDCs, macrophages (Figure 1.4) [186].

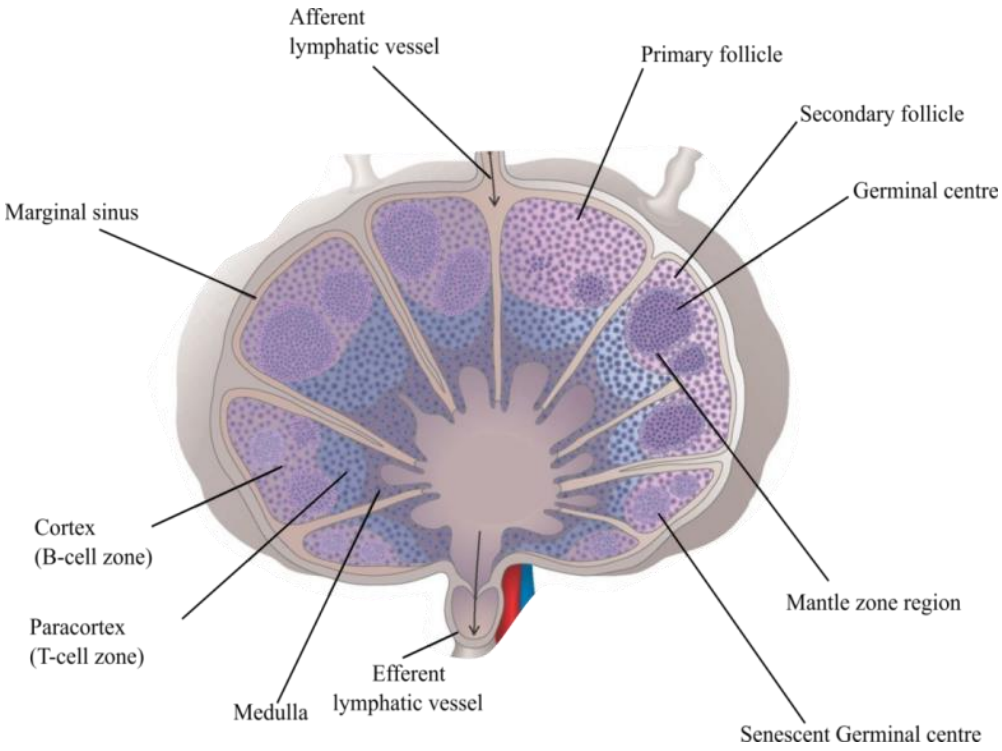

Figure 1.4 Schematic representation of a lymph node internal architecture. The two main regions of the LNs can be distinguished: the medulla and the cortex. The cortex can be divided into an inner cortex and outer follicle. LNs contain a primary follicle which do not have a germinal centre and secondary follicles with a germinal centre which are surrounded by a mantle zone region. The major route into the LNs is through the afferent and the major exit route where lymph and cells leave are via the efferent lymphatic vessels. The marginal sinus in turn receives lymph from afferent lymphatic vessels (adapted from [187]).

A potential source of HIV-1 persistence in the LNs might be due to the substantially lower concentrations of ART. There is a correlation between low concentration levels of ART and ongoing HIV-1 replication in these sites [188]. Another contributing factor to ongoing viral replication in Tfh cells in BCF has been explained in of HIV-1- simian immunodeficiency virus (SIV) infection, in which HIV-1-specific CTL $CD8^+$ T-cells and antiretroviral (ARV) drugs were limited in entering the BCFs despite ART [189]. Moreover, this has also been highlighted in a previous study, showing that the majority of HIV-1-specific $CD8^+$ T-cells are mainly found in the TCZ, and are largely excluded from the BCF region, immune privileged site, where HIV-1-specific $CD8^+$ T-cells cannot enter and clear up infected cells [190]. The block is explained by the lack of expression in follicular homing molecule CXCR5 on most $CD8^+$ T-cells, thus contributing to low levels of follicular HIV-1 specific $CD8^+$ T-cells. Nevertheless, a few SIV-specific $CD8^+$ T-cells were found within the follicles in close contact with forkhead box P3 $(FoxP3)^+$ T-cells and were able to suppress viral replication *in vivo* despite their expression of $CD8^+$ T-cells and showing an exhausted profile. Although these cells would need further characterization to confirm their phenotype, these $FoxP3^+$ T-cells were likely to be a subset of Tregs, known as follicular regulatory T-cells (Tfr) [191]. These specialized subsets of $CD8^+$ T-cells can also express $CXCR5^+$ and represent between 20-60% of $CD8^+$ T-cells in tonsil and LNs [192,193]. Additionally, $CXCR5^+$ $CD8^+$ T-cells found in the GCs of LNs were more frequently expressed in HIV-1-infected individuals compared to non-infected individuals [193]. A few of these T-cell subsets can be found within the TCZ, BCZ and the GC (Table 1.2).

Moreover, high numbers of Tregs previously reported in LN [194] correlate with HIV-1 viral load in PLWH [195]. This was extensively studied by one group demonstrating that although *in vivo* membrane expression of integrin α4β7, homing receptor CD62L and anti-apoptotic gene B-cell lymphoma gene (Bcl-2) led to the survival of Tregs,. As a result, Tregs accumulate in LNs [196]. In contrast, a more recent study demonstrated that the frequencies of Tregs within the LNs compared to blood remained unchanged, despite early initiation of ART in SIV-infected rhesus macaques (RMs) [197]. Altogether, these findings showcase the importance of the BCF as it constitutes sanctuaries for HIV-1 persistence.

Table 1.2 Anatomic locations of T-cells and functions during HIV-1 persistence

T-cells	Lymph node regions			Function during HIV-1 persistence	Ref
	TCZ	BCZ	GC		
$CD4^+$ T-cell	+	-	-	Decrease in $CD4^+$ T-cell count, leads to immunodeficiency and serves as a reservoir for HIV-1	198–200
Tregs	+	-	-	Suppress HIV-1-specific T-cell responses leading to the inhibition of T-cell responses to HIV-1, increase of HIV-1 persistence, reduces immune activation and is a HIV-1 reservoir	201–204
Tfh cells	-	+	+	Interacts with B-cells to generate high affinity antibodies and memory B-cells and is a reservoir for HIV-1	199,205,205–207
Tfr cells	-	+	-	Inhibits Tfh cells and B-cells and are susceptible to HIV-1	208–210
CXCR5- $CD8^+$ T-cell	+	-	-	Less suppressive function compared to $CXCR5^+$ $CD8^+$ T-cell function	211
$CXCR5^+$ $CD8^+$ T-cell	-	+	+	Suppress viral replication, cytopathic mediated killing via granzyme	212–215

TCZ: T-cell zone, BCZ: B-cell zone, GC: Germinal centre, CXCR5: CXC chemokine receptor 5; regulatory T-cells: Tregs; Follicular helper cells: Tfh cells; follicular regulator T-cells: Tfr cells

1.6.2.3 GUT-ASSOCIATED LYMPHOID TISSUE (GALT) DURING HIV-1 PERSISTENCE

Gut-associated lymphoid tissue (GALT), which is known as the largest immune organ in the body (reviewed in [216,217]), also serves as one of the main anatomical compartments for HIV-1 persistence [218–221] and is one of the first sites to become exposed and infected [222–224]. GALT is made up of four compartments: the lamina propria (LP), located beneath the intestinal epithelium; peyer's patches (PPs) in the small intestine; lymphoid follicles (also known as lymphoid aggregates) and; mesenteric LNs [225]. Antigens are largely delivered in PPs or by antigen loaded DCs in the LP [226]. Most $CD4^+$ T-cells are in the LP and $CD8^+$ T-cells between epithelial cells. Moreover, migration of both T and B-cells occurs out of the epithelium, towards lymphoid follicles [217].

GALT association with HIV-1 has been examined in SIV-infected macaques and PLWH, in which severe depletion of $CD4^+$ T-cells within the gut has been reported [227,228]. One study showed enrichment of HIV-1 DNA in T_{CM} $CD4^+$ T-cells expressing chemokine receptors CXCR3 and CCR6 in PLWH on ART [117]. This was also confirmed in a follow up study, where integrated HIV-1 DNA was found in $CD4^+$ T-cells expressing $CCR6^+CXCR3^+$, with increased chemokine receptor CCL20 in rectal tissue in PLWH receiving ART [220].

Despite treatment, the gastrointestinal immune system is not fully restored, even when early treatment is initiated with long-term ART. Low ART penetration into the gut compartment is also one of the many challenges contributing to residual replication [188]. Another possible explanation for ongoing viral replication could be due to the high $CD4^+$ T-cell frequency expressing CCR5 and GALT being one of the first tissues of exposure and early infection [229].

Moreover, PD-1 expression on $CD4^+$ T-cells in rectal tissue has also been proven to represent a marker for HIV-1 persistence [230]. As mentioned previously, CD32 expression, a suggested marker of the HIV-1 reservoir, was also looked at in a recent study in GALT. This study reported that a population of T-cells expressing $CD3^+CD4^+CXCR5^+$ $PD\text{-}1^+$ Bcl-6 (ruling out B-cells and confirming that they were not the source for signal), consistent with the cellular characteristics used to define Tfh cellscorrelated significantly with rectal HIV-1 DNA and CD32 expression of Tfh cells in PLWH on ART [231].

Besides the LNs, there have also been ongoing studies performed to understand the impact of treatment within GALT during HIV-1 persistence. These studies have reported substantially reduced concentration levels of treatment, leading to insufficient suppression of HIV-1 replication, and as a result leading to incomplete inhibition of viral replication in GALT [232,233]. In addition, a correlation was made with reduced concentrations of ART and HIV-1 accumulation present in the FDCs network, as detected by HIV-1 RNA by *in situ* hybridization (ISH) [188].

1.6.3 DEFECTIVE AND INTACT VIRUS

Studies have shown that the majority (over 90%) of HIV-1 proviruses in $CD4^+$ T-cells are defective in PLWH on ART [234–236]. Notably, HIV-1 genes can be expressed by defective proviruses due to integration into active transcription sites, LTR promotor function and the lack of promotor methylation [237]. HIV-1-promotor function was found in cells carrying both defective and intact proviruses and these cells were able to express viral antigens upon reactivation [238,239]. Moreover, cells containing defective proviruses may induce alternative splicing events, leading to the expression of viral proteins such as Tat and Rev and clearance by the host immune system [239]. Defective proviruses contain mutations mediated by deletions, insertions, apolipoprotein B mRNA editing enzyme, catalytic polypeptide-like (APOBEC) hypermutations and packaging signal defects [240]. In addition, defective proviruses with large deletions or point mutations may halt viral protein production and as a result, evade recognition and clearance by $CD8^+$ T-cells [239].

Defective viruses can potentially overestimate the frequency of the true reservoir if DNA is quantified using qPCR and droplet digital PCR (ddPCR) with primers in the LTR or gag region [241,242]. Recently, a novel assay was developed that discriminates the presence of intact or defective viruses using the intact proviral DNA assay (IPDA), which includes primers that bind to regions of the virus which are commonly deleted or hypermutated latently infected cells that persist on ART [243]. This method separates intact and defective viruses by using different fluorescent probes in ddPCR format [243]. In a recent study of PLWH on ART, IPDA demonstrated that intact and defective proviruses have different decay rates with intact virus decaying more rapidly than defective proviruses [244].

1.6.4 NON-INDUCED VIRUSES

The frequency of cells infected with replication competent virus can be measured using a quantitative viral outgrowth assay (QVOA). In this assay, dilutions of $CD4^+$ T-cells are stimulated with mitogen phytohemagglutinin (PHA) to induce T-cell activation. Virus production is then detected by quantification of viral proteins such as p24 [245], viral RNA [246] or capacity to infect a reporter cell line [247]. This assay quantifies the frequency of infected cells following a single round of $CD4^+$ T-cell activation.

Although the QVOA is considered the gold standard to measure the replication competent reservoir, there are proviruses that are completely intact but seem to not respond to T-cell activation. These are now termed non-inducible proviruses. Intact viruses with a non-inducible phenotype will lead to an underestimation of the true frequency of replication competent proviruses using the QVOA [248,249]. More recently, Yu and colleagues demonstrated that in elite controllers, intact proviral sequences can be integrated in parts of the genome, known as gene desert sites which are highly resistant to gene expression [250]. In these sites, the HIV-1 reservoir remained "locked", and as a result is resistant to expression of virions. Notably, although the intact proviruses were thought to be in a state of deep latency, they could eventually be induced when activating T-cells using the QVOA [250].

1.6.5 HIV-1 PERSISTENCE IN TISSUE

There have been several reports on whether HIV-1 persistent in anatomical compartments is genetically different or the same as that observed in peripheral blood. In the first proof of concept, one particular study looked at the LN and GALT, pre- and post-treatment and demonstrated that viral rebound did not solely arise from these sites but from multiple sources associated with multifocal infection in lymphoid tissue and latently infected cells [251]. Additionally, these results were further supported with viral sequence analysis from PLWH, post-treatment interruption, revealing that GALT was not the primary source of plasma viremia rebound [252]. Genetic characterization of HIV-1 DNA in infected cells from peripheral blood and lymphoid tissues in PLWH on ART had similar viral sequences [253–256], with one study demonstrating replication-competent clonal populations from reactivation of

latently infected cells during viral rebound [257]. Other studies have shown that both blood and LNs contained proviruses with identical sequences, integration sites and RNA expression in PLWH on ART [258]. In summary, it is unclear if there is true compartementalisation of latent viruses in blood and different tissue sites. The tissues environment may be important in determining the likelihood of whether viral proteins or virions are expressed [219].

1.6.6 ONGOING VIRUS PRODUCTION AND REPLICATION

There has been a long-standing debate on whether there is persistent virus replication on ART. Some groups have reported changes in viral sequences in blood and lymphoid tissue over time, potentially consistent with ongoing viral replication [259–263]. One proposed explanation is inadequate tissue penetration of treatment in anatomical compartments which is insufficient to stop virus replication but not high enough to generate drug resistance [264,265]. ART intensification studies have also helped understand whether ongoing replication exists on ART. In one study, ART intensification with the integrase inhibitor raltegravir resulted in an increase in 2-long terminal repeats (LTR) circles, a dead end product of unintegrated HIV-1 DNA, consistent with residual virus replication on ART [266]. The increase in 2-LTR was potentially more notable in participants receiving PI-based ART prior to intensification. However, results from another study using the integrase inhibitor dolutegravir for intensification observed no change in levels of 2-LTRs. Differences between findings of dolutegravir and raltegravir may be related to the high concentrations of raltegravir in the GI tract. In addition, the two studies only looked at blood and not tissue such as LNs or GALT [267].

Another potential strategy to understand virus replication on ART is to assess differences in low level plasma HIV-1 RNA. Commercial assays can detect plasma HIV-1 RNA down to 20 copies/ml [268]. However, supersensitive assays, often called single copy assays, can detect HIV-1 RNA to 1 copy/ml [269]. Although detected in nearly all PLWH on ART, the source of residual low level viremia is unclear [270]. A recent study assessed residual viremia therapizing PLWH on integrase, protease and NRTI based therapy. Notably, the probability of having a detectable plasma HIV-1 RNA of >20 copies/ml was higher on PI-based treatment, potentially consistent with residual virus replication in this setting [271].

1.6.7 CLONAL PROLIFERATION DURING HIV-1 PERSISTENCE

HIV-1-infected cells can also persist on ART through clonal expansion, identified as cells containing an identical integration site [272] or an identical virus sequence [273]. Potential drivers of clonal expansion of infected cells on ART include homeostatic proliferation, antigen driven proliferation and integration mediated proliferation. Antigen-specific $CD4^+$ T-cells undergoing clonal expansion are driven following exposure to different pathogens, such as cytomegalovirus (CMV) or influenza [274,275].

Identifying clonal expansion of cells infected with replication competent HIV-1 requires simultaneous analysis of the integration site and virus sequence. It was initially assumed that clonally expanded cells mainly harbor defective HIV-1 proviruses [248]. Since then a few studies have confirmed this observation and demonstrated that ~50% of HIV-1 infected cells undergo clonal expansion and harboured replication competent proviruses [237,276–278] and that these cells accumulate within the first week of infection [234]. However, a more recent study found clonal expansion of both defective and intact proviruses in PLWH on ART [279]. Interestingly, a significant variation in reservoir decay was found in two PLWH on ART [279]. This data suggest that expression of viral proteins from intact proviruses could potentially lead to proviral clearance therefore selecting for defective proviruses over time [279].

Whether clonally expanded cells contribute to low level HIV-1 plasma viremia has been investigated in a recent study. For this study, samples were collected from eight PLWH who had viremia that was not suppressed by ART for more than 6 months to determine the origin of this persisting low level viremia. The authors found identical gag-pro-pol sequence in both plasma and p24+ wells following amplification of virus using QVOA. The authors concluded that clonally expanded infected cells in blood in all four PLWH, referred to as repliclones, carried replication-competent virus. Additionally, in three out of four PLWH, the clones were found to produce enough virions to cause clinically detectable nonsuppressible viremia [280]. A few studies have shown that HIV-1 RNA obtained from blood, plasma and lymphoid tissue does not diverge and that highly proliferated cell clones contribute to viral rebound [281–283]. Subsequent studies have validated these results in LNs and GALT and have confirmed that all observed sequences are derived from

cellular proliferation and are all members of clonal populations [174,258,284]. Moreover, the effect of ART has been reported to be caused by clonal expansion of cells in LNs and blood and not ongoing HIV-1 replication in two recent studies [174,285]. Together, these findings highlight the importance of clonal expansion during HIV-1 persistence and targeting these cells is crucial for HIV-1 eradication.

1.7 DETECTION AND QUANTIFICATION OF HIV-1

Accurate methods are critical for measuring the reservoir in PLWH on ART. HIV-1 persists in PLWH despite the initiation of ART. However, this does not describe whether or not the virus is capable of replicating, as both defective and intact proviral DNA can be found in infected individuals [286–288]. Thus far, there has been no convincing surface marker that distinguishes uninfected cells from latently infected cells. The QVOA is used to quantify replication competent virus in resting $CD4^+$ T-cells harbouring latent HIV-1-1 [289] while other assays that quantify nucleic acid are more high throughput. In Table 1.3, we provide a summary of the various assays that have been developed for the quantification of HIV-1 during ART in blood as well as tissue. Additionally, RNA and DNAscope are now being used to study HIV-1 persistence in tissue and will be the main focus of this thesis.

Table 1.3 | Methods used to detect HIV-1

Assay	Measures	Method	Pros	Cons	Ref
VOA	Replication-competent virus after activation induced by a single round of T cell activation.	ELISA or RT-PCR p24	Measures only induced replication competent virus; excludes detection of defective proviruses	Labour intensive; (requires 2–3 weeks of tissue culture in a PC3 laboratory). Expensive and requires a large blood volume. Not all intact viruses are guaranteed to get reactivated	[290]
qPCR for HIV-1-1 DNA	Total proviral DNA including replication-competent proviruses, defective proviruses, and unintegrated forms of HIV-1-1 DNA	qPCR	Sensitive, easy, and fast	Detects many proviruses that are defective	[291]
ddPCR for HIV-1-1 DNA	Total proviral DNA including replication-competent proviruses, defective proviruses, and unintegrated forms of HIV-1-1 DNA	ddPCR	Highly precise; provides absolute quantitation rather than relative	Detects many proviruses that do not pose a barrier to a cure	[292]
qPCR for 2-LTR circles	2-LTR circles	qPCR	Used to measure ongoing replication	Does not detect integrated proviruses.	[293]
Full genome sequencing	Residual viremia	Sanger sequencing and next generation sequencing	Intact virus	Labour intensive. Does not determine if the virus is inducible. Expensive.	[294]

Inducible transcription assays	Proviruses induced after activation to produce cell-associated RNA	RT-PCR or ddPCR for CA-RNA (us and ms)	Faster than VOA and requires less cells (Tat/rev induced limiting dilution assay, TILDA)	May detect some defective proviruses. Does not measure replication competency viruses.	[295]
Residual viremia	Virus particles	qRT-PCR	Measures residual virus production during ART	Labour intensive, unclear what the source of virus is and whether it is replication competent	[296]
RNA/DNA scope and	HIV-1 DNA and RNA	*In-situ* hybridization	Can detect HIV-1 DNA and RNA individually or simultaneously	Does not determine if the virus is replication competent. Labour intensive. Patient tissue might not always be easily obtained, and it might not be stored correctly, leading to over fixation.	[297]
Basescope	Exon splice junctions	*In-situ* hybridization	Visualize gene expression of short RNA target sequences (as short as 50 bp). Target regions in the 3′ HIV-1/SIV genome that have been demonstrated to be deleted or hypermutated	Does not determine if the virus is replication competent. Labour intensive.	[298]

ELISA: enzyme-linked immunosorbent assay; qPCR: quantitative polymerase chain reaction; IHC: immunohistochemistry; VOA: Viral outgrowth assay; bp: base pair

1.7.1 IN SITU HYBRIDIZATION

Over the years, a number of studies focusing on the HIV-1 reservoir in tissues have generated useful knowledge on what takes place within tissue; however, each approach has their limitations. Peripheral blood during HIV-1 persistence has been more extensively studied, with peripheral blood being easier to obtain compared to tissue [299]. Another approach to study the tissue reservoir is using single-cell analysis of tissue-derived cells, which has been able to provide insight into eradication strategies [300–302]. However, this is limited in providing spatial information regarding the exact location in tissue and not all tissue resident cells are easy to isolate [300–302]. One of the first techniques that was able to visualize viral RNA in formalin-fixed, paraffin embedded (FFPE) tissues used radiolabelled *in situ* hybridization (ISH). This technique has contributed to the understanding of the tissue reservoir by its sensitivity in ability to detect productively infected cells as well as virions. Nevertheless, this technique has it's disadvantages, such as using radioactive material and long incubation periods that make it labour intensive, as well as high background [297,303]. These limitations have led to the development of ISH assays focusing on increasing the high signal-to-noise ratio. However, these approaches were even less sensitive, time consuming, and with high background due to off target probe binding compared to radiolabelled ISH [304,305]. The use of these assays has been limited to genes that are highly expressed, such as transcripts of the Epstein-Barr virus [306].

Most recently, a new next-generation ISH approach, RNAscope, has been investigated, delivering hope in studying the tissue reservoirs, while promising to deliver sensitivity and a high signal-to-noise ratio. RNA ISH method, RNAscope, allows for single molecule visualization in each cell by using a unique probe design together with an amplification system while offering a high signal-to-noise-ratio and preserving tissue morphology. This can be done on intact FFPE tissue samples, or fresh tissue (cryopreserved) and visualized using a bright-field microscope (for chromogenic detection), or a fluorescent microscope (for fluorescent labels) [307].

1.7.1.1 RNA/DNA SCOPE

One of the many interesting features of RNAscope ISH is that it uses a unique probe design, consisting of two independent probes (double Z, or "ZZ" probes). The target probes consist of two oligonucleotides with a region complementary and highly specific to hybridize to the RNA target, a short linker, and a preamplifier sequence (depicted in a general scheme in Figure 1.5).

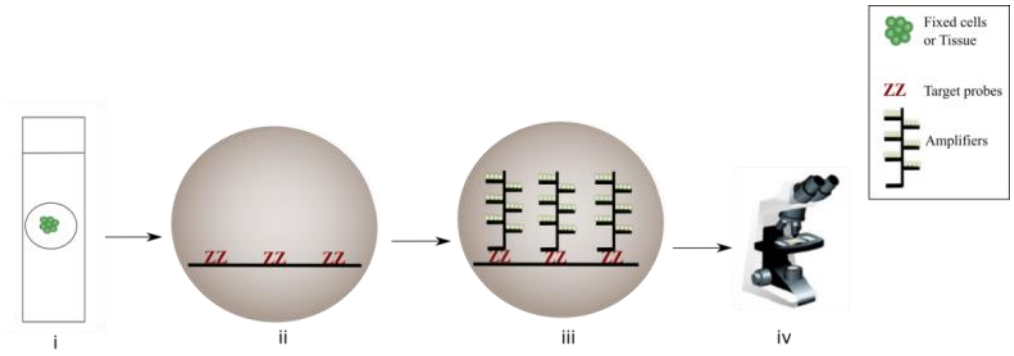

Figure 1.5 Schematic representation of RNA/DNAscope ISH technique. i) Formalin-fixed, paraffin embedded cell pellets or tissues are fixed onto the slide, followed by pre-treatment to remove paraffin and to expose RNA or DNA. ii) Next, hybridization of the target double Z probe takes place to target RNA or DNA. iii) The top part of the double Z probes then binds to the amplifiers to hybridize signals with attached labelled probes. iv) Lastly, labelled probes allow for chromogenic or fluorescence signals to be visualised using a microscope. (Image modified from ACD RNAscope®).

Moreover, this ensures specificity as the possibility of two probes binding simultaneously to non-specific target is extremely low. Each target RNA is designed with 20 double Z pairs, covering over one kilo byte (kb) region. Once hybridization takes place, both oligonucleotides of the target probe on a target RNA joins the two halves of the preamplifier. As a result, a cascade of signal amplification takes place, and with each label probe containing chromogenic enzymes, catalysing the deposition of chromogens such as diaminobenzidine (DAB) which uses horseradish peroxidase (HRP) and alkaline phosphatase (AP) based fast red chromogens. Lastly, the coloured signals can be detected by either bright field or fluorescence microscope are both highly specific and sensitive. Importantly, RNAscope can be used for the

detection of viral targets as well any cellular RNA for which target probes are available and validated. In addition, RNAscope is highly sensitive and enables the detection of low-copy transcripts in FFPE samples [308].

Advanced usage of RNAscope has opened doors to further study the HIV-1 reservoir in tissue. This has allowed investigators to successfully examine both viral RNA using RNAscope and viral DNA using a modified version of the RNAscope assay, known as DNAscope. So far only a limited number of of RNAscope probes have been designed covering the HIV-1/SIV genome and targeting 5' and 3' gene regions that bind to spliced and unspliced RNA transcripts; i.e HIV-1 clades A, CRF_AE, B, C, and D, SIVmac239, SIVagm and SHIV-1-C1157 [297].

The combination of both RNA^- and DNA^- scope in tissue from SIV-infected non-human primate (NHP) as well as LN tissue from PLWH has been investigated. This showed the discrimination of viral DNA $(vDNA)^+$ cells that are transcriptionally silent viral RNA $(vRNA)^-$, from those that are actively transcribing $vRNA^+$. These findings detected productively infected vRNA and $vDNA^+$ cells in tissue reservoirs and demonstrated the importance of the BCFs as an important anatomical compartment during treatment [297].The same group of investigators also quantified SIV in lymphoid tissue (i.e. LN, gut, lungs and spleen) of SIV-infected NHP, which contained >98% of SIV RNA and DNA cells before ART. The administration of ART substantially decreased the amount of SIV RNA and DNA cells; however, SIV RNA and DNA remained detectable, with the presence of lower drug concentrations in LN tissue than peripheral blood. Notably, these findings highlight the challenges faced in developing cure strategies that must target several anatomical compartments of infected cells that harbor replication competent virus [163].

With successful detection of both vRNA and vDNA, advances have been made to develop an assay which combines both RNAscope and/or DNAscope with the combination of immunofluorescent cellular markers in FFPE tissue or cell pellets using confocal microscopy. This assay was performed using the Opal-TSA system from Perkin-Elmer®, allowing for simultaneous detection to characterize distinct immune cells within tissue. This was demonstrated recently, in which two immunofluorescently labelled cellular markers; PD-1, cytotoxic T-lymphocyte-associated protein 4 (CTLA-4) and $CD4^+$ T-cell, in combination with DNAscope

have been used to study SIV tissue reservoirs. In SIV-infected RM on ART, SIV DNA was detected with infectious virus in CTLA-4^{+}PD-1^{-} cells, primarily outside the BCF region of LN tissue [309].

Although the usage of confocal microscopy delivers specificity in viral detection, it is unfortunately limited by the available wavelengths of light produced by lasers. This is not the case when using the conventional fluorescence microscope which makes use of a mercury lamp and offers a range of excitation wavelengths [310].

To date, most studies focusing on HIV-1 persistence in tissue have investigated the reservoir using confocal microscopes, limiting the number of markers for cellular phenotyping in combination with both HIV-1 RNA and/or DNAscope. Given that there is persistence of HIV-1-1 in the setting of ART, it is therefore important to obtain a better understanding with detailed immunophenotypic information of the viral reservoir in tissue.

We therefore optimized and developed an assay which will allow us to combine both HIV-1 RNA and/ or DNAscope with IHC. This will allow us to detect multiple antigens such as CD4, FoxP3, CTLA-4 and PD-1 in FFPE tissue sections to define and understand HIV-1 in PLWH on ART.

1.8 AN OVERVIEW OF REGULATORY T-CELLS (TREGS)

The earliest discovery of Tregs in 1969 demonstrated a suppressive T-cell function as a result of neonatal thymectomy in mice [311]. Since then, Sakaguchi and colleagues identified a subset of CD4^{+} T-cells expressing CD25 (the alpha chain of the IL-2 receptor) in the thymus that can prevent autoimmunity in mice [312]. Development of T-cells occurs in the thymus with their T-cell lineage regulated by the notch pathway [313]. In the thymus these cells develop into four T-cell types, these include; naïve CD8^{+} T-cells, naïve CD4^{+} T-cell, natural killer T-cells and natural Tregs (nTregs), also known as naïve Tregs. The development of nTregs is initiated through the interaction between TCR and MHC II with the self-peptides from APCs in the thymus. Based on a strong TCR signal with self-peptide, CD4^{+} thymoctyes undergo positive selection and differentiate into nTregs and CD4^{+} T-cell in the thymus. Lower affinity of the T-cell receptor with self-peptide leads to positive selection of CD4^{+} T-cells.

Most naïve $CD4^+$ single positive cells either undergo negative selection as a result of a weak TCR signal or with a high affinity for TCR undergo positive selection. As a result, these cells escape deletion and differentiate into Tregs [314]. Unlike nTregs which fulfil their suppressive role immediately, naïve $CD4^+$ T-cells, on the other hand, rely on other signals for their activation. Naïve $CD4^+$ T-cells expression is triggered when MHC II interacts with T-cell receptor [315–317] on the surface of an APC, following co-stimulatory signalling by CD28 interaction with CD80 or CD86. Lastly the secretion of cytokines by the APCs, leading to the differentiation of induced regulatory T-cells (iTregs) where they mature in the periphery (reviewed in [318]).

The role of FoxP3 has shown to play an essential role in the development and function of Tregs. Foxp3 has been demonstrated to be key regulator and a reliable signature of Treg lineage (mostly in the thymus) [319]. In mice, FoxP3 is constitutively expressed in Tregs and is the most specific marker [320]. However, this is the opposite in humans as not all Tregs express FoxP3, which is also upregulated in non-CD4 Tregs or B-cells [321–324]. The induction of peripheral FoxP3 can occur through transforming growth factor (TGF)-β, promoting Treg induced suppression [325–327]. In addition, induction of FoxP3 occurs in the Treg precursors as in either the thymus or in naïve $CD4^+$ T-cells. Their expression can also become triggered when MHC II interacts with TCR [315–317] together with an APC, resulting in a phenotypically heterogeneous populations. As a result, there are factors that block nuclear factor kappa B (NF-κB), resulting in the inhibition of cytokine expression [328] and transcription factor nuclear factor of activated T-cells (NFAT) which regulates gene expression and differentiation of Tregs [329,330]. Previous studies have also highlighted the role of vitamin D as a supplementary candidate for the expansion of Tregs and the maintenance of FoxP3. These observations were confirmed with a positive correlation with vitamin D concentration levels in serum and the frequency of Tregs in PBMC [331–333].

1.8.1 PHENOTYPIC DIVERSITY IN TREG SUBSETS

Tregs constitute up to 5-10 % of total $CD4^+$ T-cells [319,334] and can be divided into two main groups; these are the nTregs, which leave the thymus to become effector Tregs (also referred to as peripheral Tregs) and induced Tregs (iTregs).

nTregs develop in the thymus through interaction between TCR and MHC II with self-peptides from APCs. Upon antigen stimulation by an APC within the peripheral lymphoid organs, T-cells within the thymus differentiate into effector T-cells and iTregs. iTregs are further divided into transforming growth factor beta (TGF-β) secreting T helper 3 (Th3) cells [335] and interleukin-10 (IL-10) secreting regulatory type 1 (Tr1) T-cells [336] where they are matured in the periphery (Figure 1.6).

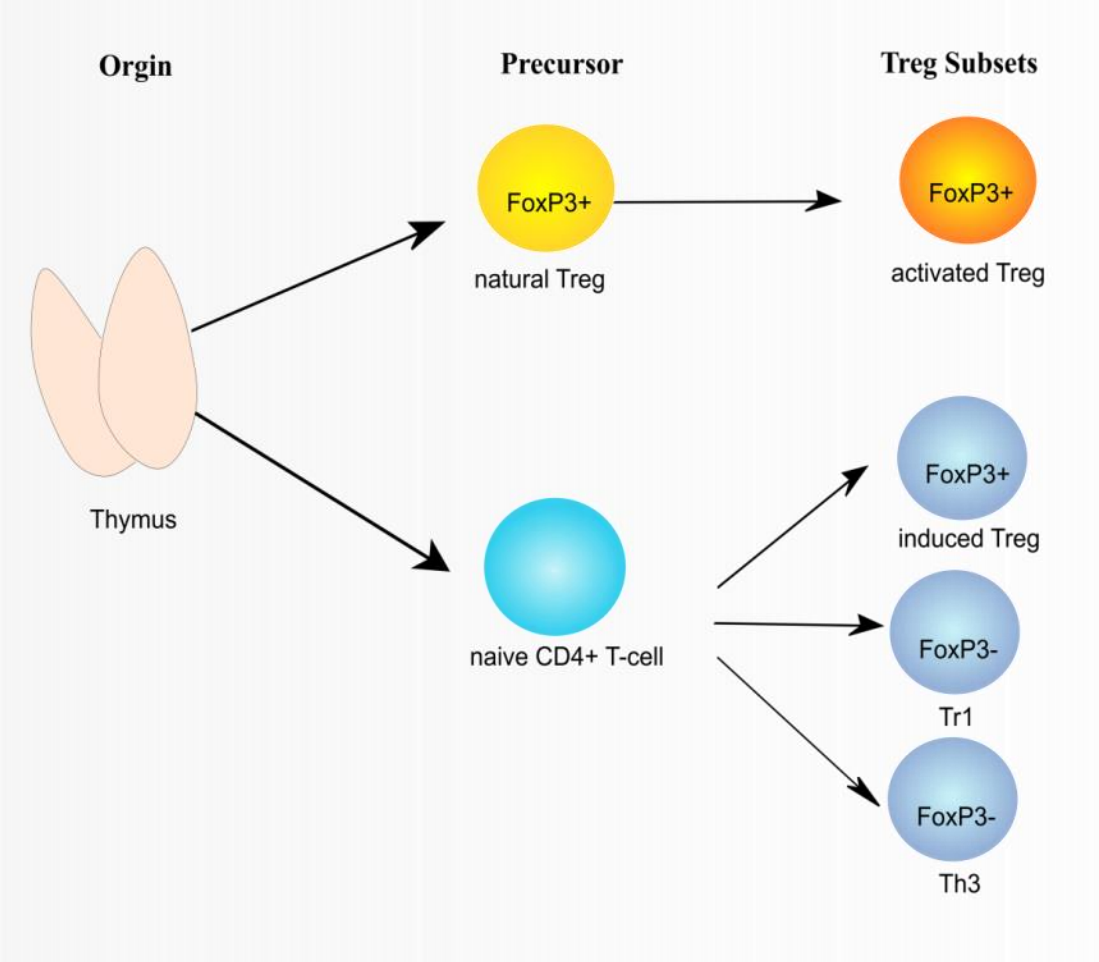

Figure 1.6 Differentiation of Tregs into subsets. The maturation of nTregs and Tregs derived from naïve $CD4^+$ T-cells takes places once these cells leave the thymus. There, nTregs differentiate into effector Tregs and naïve $CD4^+$ T-cells into iTregs, or Tr1 and Th3 T-cells. Tregs represent a heterogeneous population are distinctively phenotyped based on intracellular or surface markers. (Adapted from [337]). Abbreviations: nTregs: natural Tregs; Tr1: regulatory type 1; Th3: T helper 3; iTregs: inducible Tregs.

Because FoxP3$^+$ marks heterogeneous populations constituted of nTregs and iTregs, other markers have been identified and used to distinguish the different Treg sub-populations [338]. One of the earliest markers used to identify Tregs is CD25 [339,340]; however, CD25 is also a marker for T-cell activation and is therefore not exclusive to Tregs, rendering it an unsuited marker for characterizing Tregs [341]. In addition, the IL-7 receptor (CD127) is used as an additional marker of Tregs, and has shown to inversely correlate with FoxP3 and suppression on Tregs [342,343]. This has promoted the consistent identification of Tregs in combination with FoxP3 expression, and surface expression of CD4, CD25 and CD127 as key markers in past and recent studies to dissect populations of Tregs. A variety of other markers have been used to identify Tregs such as TIM-3, TIGIT, CD39, CD45RO, PD-1, CTLA-4 latency-associated peptide (LAP) and C-C Motif Chemokine Receptor 8 (CCR8), all which are not specific for iTregs, as they can also be expressed on other activated T-cells [344–350].

The combination of CD25 high, CD127 low and FoxP3$^+$ are the first group of Treg subset classification and are the most commonly used markers used to sort and study Tregs. However, FoxP3$^+$ is excluded for sorting Tregs as they require intracellular staining, which leads to non-viable cells [351–356]. Although combining CD127 with other markers has been highly beneficial to identify and sort Tregs, high CD127 expression on iTregs were reported [357]. In addition, several studies have also reported downregulation of CD127 on naïve T-cells [358] and other nonTregs in PLWH [359,360]. Thus, CD127 low expression is not an intrinsic characteristic of Tregs as it is unable to distinguish between activated T-cells, particularly during HIV-1 infection, indicating possible contamination with CD4$^+$CD25$^+$ T-cells [361].

The second classification of Treg subsets proposed was based on the expression of CD45RA, CD25 and FoxP3. CD45RA can be used for the distinction of naive and effector Tregs and can be further divided into three fractions: (i) naïve/resting Tregs (CD25low FoxP3low CD45RA-), (ii) effector Tregs (CD4$^+$ CD25high FoxP3high CD45RAhigh) and (iii) non-Tregs (CD4$^+$ CD25low CD45RA-FoxP3low CD25low) [362] (Figure 1.8). To date, there is not enough evidence to determine if these effector Treg subsets are thymic derived or if these Tregs are iTregs developed in the periphery. A recent *in vitro* study combined CD4, CD45RA, CD25, CD127 and FoxP3 to identify distinct Treg subsets with naïve phenotype

($CD4^+$ $CD25^+$ CD127low $CD45RA^+$ $FoxP3^+$) and Tregs with a memory phenotype ($CD4^+$ $CD25^+$ CD127low CD45RA- $FoxP3^+$). In addition, naïve/resting Tregs also possess and maintain a $FoxP3^+$ regulatory T-cell specific demethylation region (TSDR) demethylated phenotype. This phenotype is associated with the stability of FoxP3 and is exclusive for Tregs [363] during *in vitro* expansion [364]. Notably, sorting for a purified population of nTreg from total Tregs by combining CD45RA with CD4, CD25 and CD127 may be potentially beneficial for targeting in therapeutic immune interventions such as the depletion of Tregs in tumours [365,366].

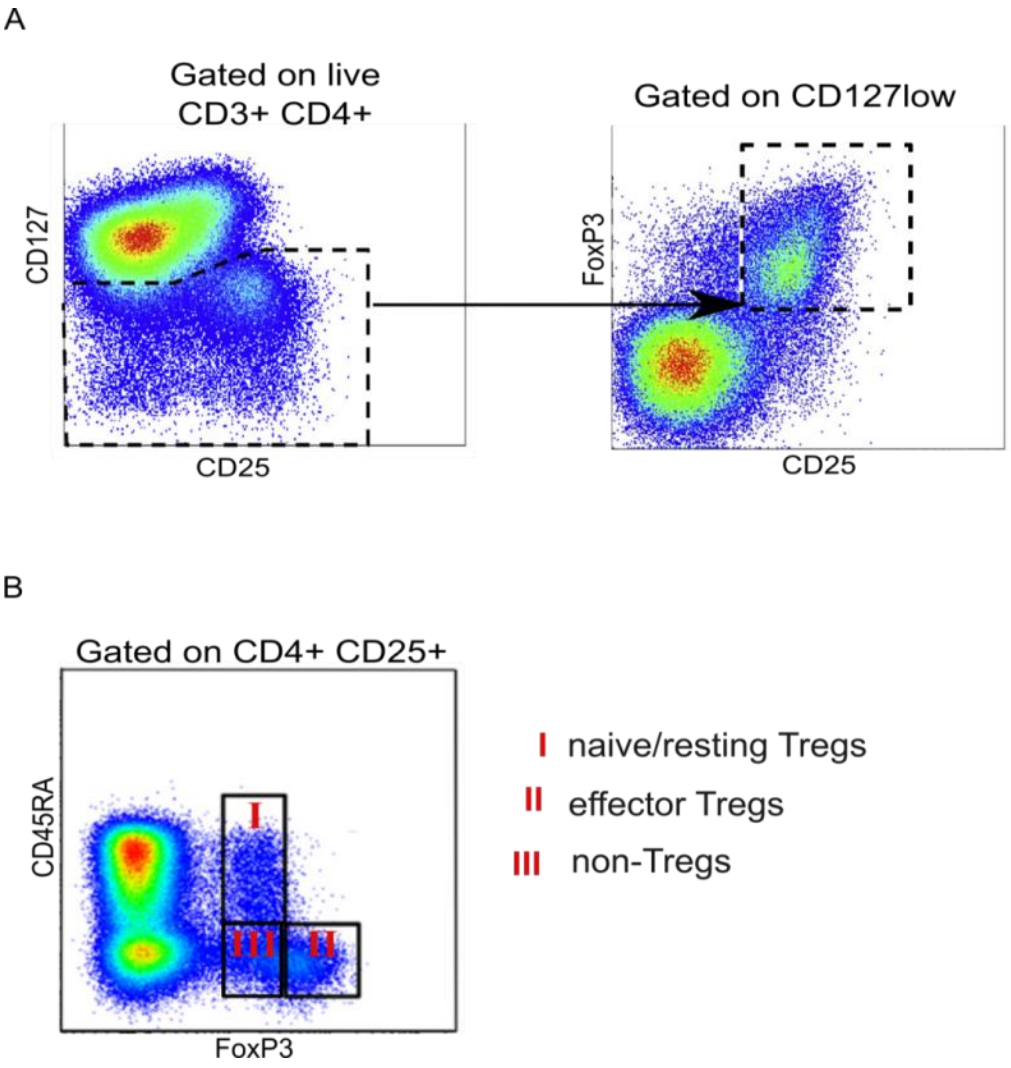

Figure 1.7 Flow cytometry profiling of phenotypically distinct Treg groups. Phenotypic markers enriched on Tregs were used to establish two distinct groups of Tregs based on gating strategies. A) First group of Tregs were sorted based on the expression of CD3, CD4, CD25, CD127 and FoxP3. Gating strategies identified total Tregs that were $CD3^+$ $CD4^+$ CD127low $CD25^+$ and $FoxP3^+$. B) Alternatively, Tregs can be divided using CD45RA. Here, $CD4^+$ $CD25^+$ T-cells can be fractioned into three groups, (i) $CD45^+$ FoxP3 naïve/resting Tregs, (ii) CD45RA- $FoxP3^+$ effector/activated Tregs and (iii) CD45- FoxP3- nonTregs.(Adapted from [367,368]).

1.8.2 THE PHYSIOLOGICAL FUNCTION OF TREGS

nTregs are co-stimulated by the CD28 molecule with paracrine IL-2 playing an essential role in maintaining thymic development and peripheral homeostasis [32,369]. iTreg differentiate from thymic derived naïve $CD4^+$ T-cells upon stimulation or in the presence of cytokines, following upregulation of FoxP3 in the periphery [370]. The presence of TGF-β promotes the development of these cells to become $CD25^+$ cells through binding of transcription factors NFAT and SMAD (an acronym from the fusion of *Caenorhabditis elegans Sma* genes) and as a result leading to the induction of FoxP3 [371,372]. *In vitro* studies have shown that Tregs in the absence of APCs can suppress $CD4^+$ and $CD8^+$ T-cells in a contact-dependent, antigen-independent manner [373,374]. Unlike nTregs, iTregs have a reduced dependency on IL-2 which is not required for their maintenance, and are instead maintained by inducible costimulatory (ICOS) [369].

Unlike other iTregs, IL-10 producing Tr1 cells are unable to express FoxP3 constitutively and are defined based on their coexpression of lymphocyte-activation gene-3 (LAG-3) and CD49b [375] and through IL-10 and TGF-β carry out their suppressive function through a contact independent pathway as well cell dependent inhibition, metabolic disruption and cytolysis [376].

TGF-β producing cells Th3, which are derived from naïve $CD4^+$ T-cells, are identified based on the expression of CD4 and LAP. *In vitro* studies have shown that Th3 can be generated in the presence of TGF-β, IL-4, and IL-10, while potentially shifting towards a $FoxP3^+$ iTreg phenotype. Th3 is associated with oral tolerance of self-antigen where they exhibit TGF-β suppression [377,378].

Thus, Tregs can be defined based on the expression of markers and cytokines they release, allowing the classification on Treg populations, denoting their suppressive profile in each subset.

1.8.3 TISSUE RESIDENT TREGS

As mentioned earlier, the expression of chemokines promotes the migration of Tregs from the thymus to lymphoid and non-lymphoid tissue. CD62Lhigh, CCR7high and cell surface adhesion receptor CD44low on nTregs, allows them to actively migrate through lymphoid organs before exiting the thymus. In addition, the downregulation of CD62L, CCR7 and the upregulation of CD44 expression on

iTregs as a result of antigenic simulation are associated with reduced non-lymphoid tissue homing potential [369,379]. Thus, the expression of chemokines and adhesion molecules may promote trafficking to various lymphoid and non-lymphoid tissues, demonstrating that Tregs are able to adapt to their environment and promote tissue homeostasis in several settings (Figure 1.9).

This can be further explained by looking at Th17-like Tregs, which mediate immunosuppression in the gut [343,344] and the relationship between the expression of Th17 key regulators, transcription factors RAR-related orphan receptor gamma (RORγt) and FoxP3. Notably, the microbiota may provide signals to induce these FoxP3$^+$ Th17-like Tregs to activate signal transducer and activator of transcription 5 (STAT5) or generate Th17 in the gut through interleukin 1 beta (IL-1β)/ interleukin 6 (IL-6) signalling. Visceral adipose tissue (VAT) FoxP3$^+$Tregs and peroxisome proliferator-activated receptor (PPAR)-γ in adipose tissue expresses high levels of the enzyme 15-hydroxyprostaglandin dehydrogenase which allows them to inhibit effector T-cells [380]. The secretion of amphiregulin produced by FoxP3$^+$ Tregs is essential for the regeneration of muscle cells, repairing lung damage and the secretion of the growth factor cellular communication network factor 3 (CCN3) in the CNS used to develop the brain (reviewed in [381]). As mentioned earlier, a specialized subset of Tregs, Tfr cells play a role in limiting the function of Tfh cells in the GCs and are driven by transcription regulators including FoxP3$^+$ [382].

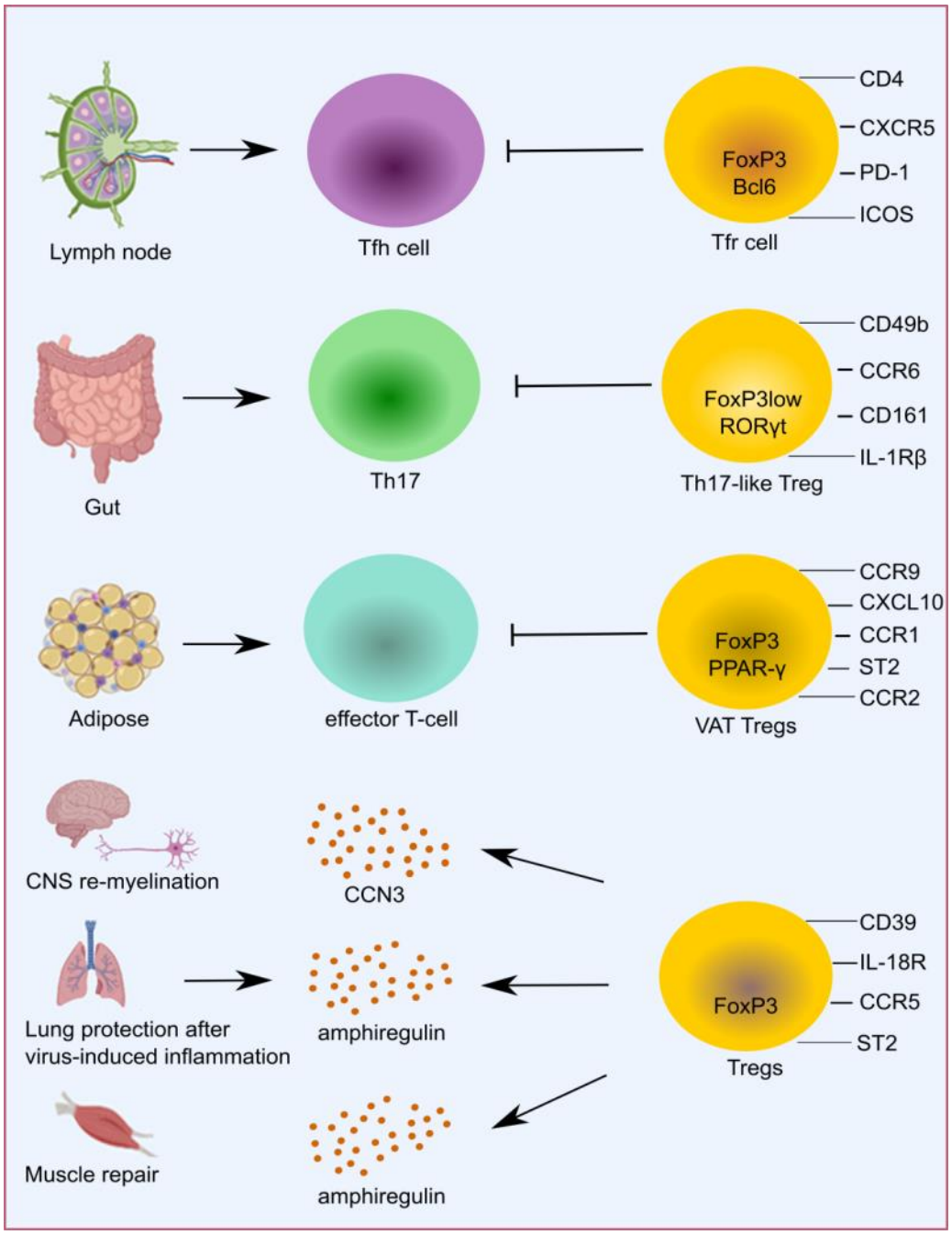

Figure 1.8 Tregs displayed in lymphoid and non-lymphoid tissue. The phenotype of Tregs and the mechanism they use to exert their suppressive function enable them to adapt to their environment. Tregs upregulate various chemokine receptors and transcription factors supporting their function and navigating to guide these cells towards lymphoid tissue such as LNs and the gut and non-lymphoid tissues; adipose tissue, CNS, lungs or muscles where they can localize. Treg subsets can suppress Tfh cells, Th17 cells, and effector cells or release the growth regulatory protein CCN3 or the secretion of amphiregulin. (Adapted from [383]). Abbreviations: LNs: lymph nodes; CNS: Central Nervous System; Tfh cells: T follicular helper cells; Th17: T helper 17; CNS: Central Nervous System; CCN3: Cellular Communication Network Factor 3.

1.8.3.1 FOLLICULAR TREGS

It was not until less than ten years ago that the physiology of Tfr cells was described in mice [382,384,385]. Tfr cells share similar phenotypes with Tregs and Tfh but differ in their transcriptional profile compared to the traditional Tregs described earlier [382]. NFAT allows for the upregulation of CXCR5 expression on Tfr cells which allows trafficking into C-X-C motif chemokine ligand 13 (CXCL13) enriched regions towards the GCs and is maintained by the expression of Bcl6 [386].

In addition, Tfr cells express transcription repressor protein B lymphocyte-induced maturation protein 1 (Blimp1), which is known for its suppressive function on Bcl6 [387]. These cells also express markers similar to Tfh such as PD-1, Bcl6 and ICOS and traditional Tregs including FoxP3 glucocorticoid-induced tumour necrosis factor receptor (GITR) and CTLA-4 [382,384,388]. One study found two distinct subpopulations of Tfr cells, $CD25^+$ and $CD25^-$ cells. Unlike $CD25^+$Tfr cells, $CD25^-$ Tfr cells are able to expand independent of IL-2, while stably expressing FoxP3 and Bcl, allowing them to migrate towards the GCs [389] $CD25^+$. Notably, Tfr cells are also the only $FoxP3^-$ cells that expressed $CD25^+$ and are able to produce high levels of Bcl6 [389,390]. This phenotype allows Tfr cells to modulate B-cells and the formation of autoreactive Tfh cells in the thymus and periphery.

The mechanism by which Tfr cells can suppress Tfh cells has not been well defined. To further understand this, one study demonstrated that Tfr cells derived IL-10 in response to an acute viral infection which promoted GC response [391]. Another study showed that Tfr cells in the GCs that correlated with a suppressed development of granzyme B expressing Tfh cells [392]. Moreover, the exposure of Tfr cells to antigens, allows these cells to differentiate with DCs initiating this process [382,390,393]. In addition, they also shape the quantity and quality of B-cells by suppressing humoral immune responses in the GCs (reviewed in [394]). Tfr cells can be found in the blood, spleen and lymphoid tissues such as PPs and LNs [395].

1.8.3.2 PERSISTENCE OF HIV-1 ON ART

Both eTregs and Tfr cells are found in LNs, where the majority of eTregs reside in the TCZ. Tfr cells reside between the T-B cell zone and a few found in GCs [391,396,397]. A few studies have shown that Tfr cells are differentiated from either nTregs precursor cells in the thymus [384,398] or similar to Tfh cells, naïve $CD4^+$ T-cells [390]. Here these cells undergo differentiation and migrate to different zones of the LNs

(reviewed in [399]) (Figure 1.8). Similar to Tfh cells, Tfr cells also require the LN microenvironment for their differentiation and function as these cells rely on signals such as ICOS and Bcl6 [382,384].

So far two models have been proposed to explain the differentiation that Tfr cells undergo while entering follicle compartments. One proposed model suggests that upon stimulation, nTregs in the thymus can differentiate into Tfr cells in the TCZ as a result of DCs priming before receiving further stimulation from B-cell interactions as they migrate towards the follicles and GCs.

Moreover, one proportion of these cells will remain localized in the TCZ, while other cells may become effector Tfr (eTFr) cells and recirculate to PBMCs. The circulating eTfr cells have shown to have a rapid memory response to Tfh cells but are less suppressive than LNs Tfr cells [400]. Next, Tfr cells in the TCZ can migrate between the TCZ and the BCZ where these cells interact with B-cells, while lastly migrating to the GC [401]. Similarly, another model suggests that key events from Tfr cells primarily take place in the follicles before they reach the GCs. Thymic derived $CXCR5^{-}CD25^{+}$ nTregs may also differentiate into $CXCR5^{+}CD25^{+}$Tfr cells in the follicles to $CXCR5^{-}$ $CD25^{+}$ Tfr cells in the GCs. Alternatively, microscopic analysis of LN tissues showed that nTregs in the thymus are also able to differentiate into $CD25^{+}$ $CXCR5^{-}$ while residing within the follicles and controlling the formation of Tfh cells by suppressing the interaction between the DCs and naïve T-cells [402] .

A

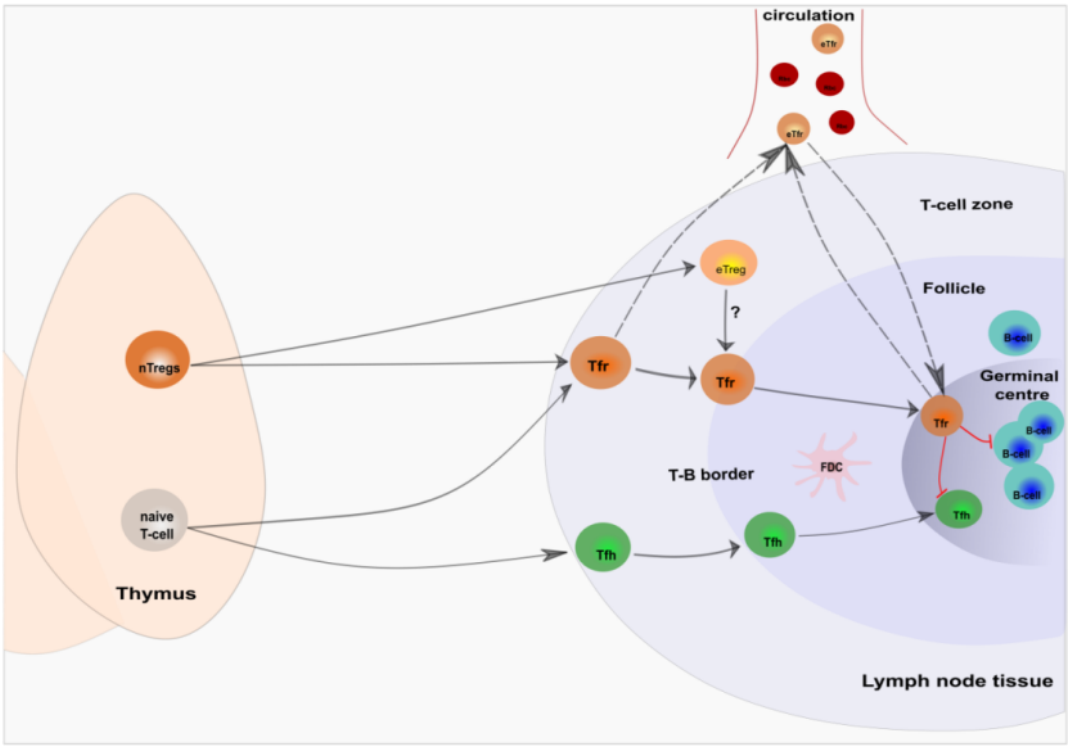

B

Location	T-cell zone		T-B border	Follicle	Germinal centre	Circulation
Subset	Tfr	eTreg	Tfr	Tfr	Tfr	eTfr
Markers	CD25+ FoxP3+ Blimp1- CXCR5+ PD-1- Bcl6- ICOS-	CD25+ FoxP3+ Blimp1+ CXCR5+ PD-1low Bcl6- ICOS+	CD25+ FoxP3+ Blimp1+ CXCR5- PD-1low Bcl6- ICOS+	CD25+/- FoxP3+ Blimp1+ CXCR5- PD-1low Bcl6+ ICOS+	CD25+/- FoxP3+ Blimp1- CXCR5high PD-1high Bcl6high ICOS+	CD25+ FoxP3+ Blimp1+ CXCR5+ PD-1low Bcl6- ICOS+

Figure 1.9 Schematic overview of the differentiation of Tfr cells in different region of the LNs. Tfr cells may either be generated from natural Tregs (nTregs) or naïve T-cells in the thymus. Thymic derived naïve T-cell can differentiate into Tfr cells upon signals from DCs during the interaction of T-cell receptor and MHCII in the TCZ. Alternatively, Tfr cells may also develop as a result of natural Tregs interacting with DCs through the signals provided by these cells in the TCZ. These cells then migrate from the TCZ, follicles into the GC where they may encounter other APCs such as B-cells or follicular dendritic cells. Alternatively, Tfr cells may also recirculate and become eTregs or migrate to the GCs where they suppress Tfh and GCs responses on B-cells. Transcription factors FoxP3 and Blimp-1 in Tfr cells direct the expression of Tfr key genes such as CXCR5, CD25, Bcl6 and ICOS. Abbreviations: nTregs: natural Treg; Tfr: T-follicular regulatory T-cell; eTreg: effector Treg; Tfh: T-follicular helper cell: FDC: Follicular dendritic cell; cTfr: central T-follicular regulatory T-cell; RBC: Red blood cell; TCZ: T-cell zone; DC: dendritic cell; GC: germinal centre (Adapted from [399]).

1.8.4 TREGS DURING HIV-1

1.8.4.1 SUSCEPTIBILITY OF TREGS DURING HIV-1

CCR5 and CXCR4 have been identified as receptors expressed on Tregs [403,404] and showed to be susceptible to HIV-1 infection, with their susceptibility to either CXCR4-using (X4) or CCR5-using (R5) HIV-1 strains. Moreno and colleagues demonstrated in an *in vitro* study using either X4 or R5 viruses, that Tregs were more susceptible to X4 viruses compared to R5 viruses can infect Tregs and were not preferentially infected with HIV-1 compared to other $CD4^+$ T-cell subsets [405]. In a humanized mice model, Tregs was rendered more susceptible to R5 viruses as a result of Vpr stimulating R5 HIV-1 replication, expanding Treg viral production [406]. In tissue, Tfr cells were shown to be highly susceptible to R5 viruses in PLWH on ART [407].

1.8.4.2 TREGS FREQUENCY IN TREATED AND UNTREATED PLWH

There have been several conflicting results in regards to the proportion of Tregs among $CD4^+$ T-cells in PLWH compared to healthy controls [408–413]. The frequency of Tregs and cell cycle marker for proliferation Ki67 was higher in untreated PLWH in comparison to other memory $CD4^+$ T-cell subsets [414]. This was also demonstrated in another study in which the proportion of Tregs within $CD4^+$ T-cells populations increased and correlated positively with HIV-1 viral load in untreated PLWH [415]. These observations were recently followed up demonstrating that Tregs defined as $CD4^+CD25^+CD127^-$ are increased in untreated PLWH during chronic infection compared to healthy individuals [416].

Besides peripheral blood, GALT which contains a significant amount of Tregs as previously mentioned was also investigated during SIV chronic infection. This study demonstrated an increase in the frequency of Tregs in GALT of SIV-infected RM off ART [417]. In contrast, another study showed no difference between the frequency of Tregs in untreated PLWH and uninfected individuals [418].

In one study in PLWH off ART, the frequency of Tregs was shown to have an inverse relationship with plasma viral load [419]. The authors identified a decrease in the total number of Tregs, which correlated with viremia and immune activation [419]. Two more studies also documented a decrease in the frequency of Tregs in untreated PLWH during chronic infection, compared to healthy donors [420–422].

In PLWH on ART, the frequency of Tregs increased and immune activation significantly decreased six months post ART [423]. Several groups have reported that the number of Tregs and immune activation normalized in PLWH on ART [424–426], while others have shown an increase during treatment [418,425,427,428] with higher levels of Tregs compared to uninfected controls [429]. In a recent study of PLWH on stable suppressive ART, ART intensification decreased the frequency of Tregs compared to untreated individuals, indicating the effectiveness of ART [430]. In summary, these findings suggest that uninterrupted ART may reduce the expansion of Tregs during HIV-1 infection. These results were all assessed by flow cytometry and IHC; however, each study used different markers to define Tregs, making cross study comparisons difficult.

Table 1.4 Frequency of Tregs in PLWH on and off ART

Cohort	Effect on Tregs	Method	Treg marker	Ref
Off ART				
PLWH (n=21)	Decrease in Treg frequency in blood compared to HD	Flow gating	$CD4^+$ $CD25^+$ $FoxP3^+$	419
PLWH (n=16)	Decrease in Treg frequency in blood compared to HD	Flow gating	$CD4^+$ CD45RA-$FoxP3^+$	420
PLWH (n=15)	Decrease in Treg frequency in blood compared to PLWH on ART	Flow gating	$CD4^+$ $CD25^+$ $FoxP3^+$	422
PLWH (n=38)	Decrease in Treg frequency in blood compared to HD	Flow gating	$CD4^+$ $CD25^+$	421
PLWH (n=131)	Increase in Treg frequency in blood compared to HD	Flow gating Isolation/flow gating	$CD4^+CD25^+$ FoxP3/ $CD4^+CD25^+$ CD127lo	414
NHP (n=8)	Increase in Treg frequency in GALT	Isolation/flow gating/IHC	$CD4^+CD25^+$ $FoxP3^+$	417
PLWH (n=10)	No difference in Tregs frequency in GALT compared to HD and ECs	IHC	$CD4^+$ $FoxP3^+$	418
On ART				
PLWH (n=12)	Decrease in Treg frequency in blood compared to HD	Isolation/flow gating	$CD4^+CD25^+$ CD127low $FoxP3^+$	423
PLWH (n=18)	Normalized Treg frequency in blood	Flow gating	$CD4^+$ $CD25^+$ CD127- $FoxP3^+$	424

	compared to HD			
PLWH (n=20)	Normalized Treg frequency in blood compared to ECs	Flow gating	$CD4^+$ $CD25^+$ $CD127^-$	426
PLWH (n=21)	Increase in Treg frequency in blood compared to PLWH off ART	Flow gating	$CD4^+CD25^+$ $FoxP3^+$	430
PLWH (n=12)	Increase in Treg frequency in blood compared to HD	Flow gating	$CD4^+$ $CD25^+$ $CD127^-$	427
PLWH (n=18)	Increase in Treg frequency in blood compared to PLWH on ART and IL-2	Flow gating	$CD4^+$ $CD25^+$ $CD127^-$	428
PLWH (n=32)	Increase in Treg frequency in blood compared to HD	Flow gating	$CD4^+$ $CD25^+$ $FoxP3^+$	429

HD: healthy donor; ECs: elite controllers; NHP: non-human primate; GALT; gut-associated lymphoid tissue; PLWH: people living with HIV-1

1.8.4.3 Effect of HIV-1 on Treg function

Of note, there has been conflicting evidence on the suppressive activity of Tregs during HIV-1. Two *in vitro* studies reported that HIV-1 had no effect on the suppressive function of Tregs [405,431], while another study showed that these cells had a lower suppressive capacity and a decrease in Foxp3 suppression when compared to uninfected Tregs [432].

1.8.4.4 Tregs as a reservoir during art

There are multiple studies that have investigated whether Tregs are a reservoir during HIV-1 persistence on ART. Resting Tregs defined by the expression of $CD4^+$ $CD25^+$ $HLADR^-CD69^-$ contained more HIV-1 compared to non-Tregs, suggesting that Tregs contribute to the viral reservoir [433]. These findings were also confirmed in a more recent study where $CD4^+$ $CD25^+$ CD127low Tregs harbouring higher levels of HIV-1-DNA were more abundant compared to non-Tregs in PLWH on and off treatment. In this study, intracellular HIV-1-1 p24 levels as well as p24 antigen levels in cell culture supernatant were examined in PBMCs, PBMCs depleted of Tregs, and Tregs. The p24 levels in Tregs, as well as the supernatant culture of Tregs were higher compared to PBMCs and PBMCs depleted of Tregs [434].

So far, one study measured replication competent provirus in Tregs compared to other $CD4^+$ T-cell subsets using droplet digital PCR (ddPCR), as well as total HIV-1 DNA. The Tregs in this study were sorted based on the expression of $CD4^+CD25^+$ CD127low and showed no difference in the total amount of HIV-1 DNA in Tregs compared to T_{CM} or T_{EM}. Notably, this study led to a skewed representation of the replication competent provirus in these T-cells, as this assay was limited due to a low yield of Tregs, resulting in results from two of the ten study participants on ART [435].

Recently, analysis in LNs from SIV-infected macaques confirmed that a subset of Tregs expressing ICs $CD4^+CTLA\text{-}4^+$ contained significantly more SIV DNA compared to $CD4^+$ $CTLA\text{-}4^-$ cells. Due to the anatomical location, these cells were suggested to be Tfr cells, however, this study was unable to validate this finding due to the limitations such as including the intracellular marker FoxP3 used to define Tregs [155].

In addition, one *in vivo* study showed that Tregs can inhibit HIV-1 through cyclic adenosine monophosphate (cAMP) dependent protein kinase A pathway to suppress HIV-1 infection in humanized mice. This study reported HIV-1 gene expression and replication inhibition by Tregs via Adenylyl Cyclase–Dependent cAMP and a decrease of the HIV-1 reservoir during ART as a result of Treg depletion [436].

Table 1.5 Summary of studies examining Tregs as a potential reservoir during HIV-1

Phenotype of Tregs	Assay	Main Findings	Ref
$CD4^+CD25^+$ $HLADR^-CD69^-$ $FoxP3^+$	Limiting cell dilution PCR	Abundant HIV-1 DNA in Tregs compared to nonTregs from sorted PBMCs	437
$CD4^+CD25^+$ CD127low	qPCR, ELISA for p24	HIV-1 DNA levels in Tregs were 10 fold higher than nonTregs	438
$CD4^+CD25^+$ CD127low	droplet digital PCR VOA	no difference in the total amount of HIV-1 DNA in Tregs compared to T_{CM} or T_{EM} in PBMCs	439
$CD4^+$ CTLA-4^+ PD-1^-	DNAscope, IHC, qPCR droplet digital PCR	$CD4^+$ CTLA-4^+ contained significantly more SIV DNA compared to $CD4^+$ CTLA-4^- in LN, PMBCs and spleen	155

ELISA: enzyme-linked immunosorbent assay; qPCR: quantitative polymerase chain reaction; IHC: immunohistochemistry; VOA: Viral outgrowth assay; PMBCs: peripheral blood mononuclear cells

1.9 IMMUNE CHECKPOINTS (ICS)

During ART, HIV-1 persists in $CD4^+$ T-cells that express immune checkpoints (ICs). ICs provide feedback responses that keep T-ells in check by maintaining self-tolerance, preventing autoimmunity and minimize collateral tissue damage (reviewed in [440]). Some ICs are expressed in peripheral tissues. Moreover, IC proteins and their respective ligands vary in their level of expression on immune cells (reviewed in [441]). Recently, studies have shown that cells that express multiple ICs compared to cells that don't express these ICs are more likely to harbour latent HIV-1 in PLWH on ART [156,199,309,442,443].

Thus far, several ICs have been identified with the most studied molecules including CTLA-4, PD-1, LAG-3, TIM-3 (reviewed in [440]). Other ICs include, B and T-lymphocyte attenuator (BTLA) and V-domain Ig suppressor of T-cell activation (VISTA) that are expressed on several immune cell subsets (reviewed in [444]). Figure 1.10 is an overview of some of the identified ICs pathway and their receptor.

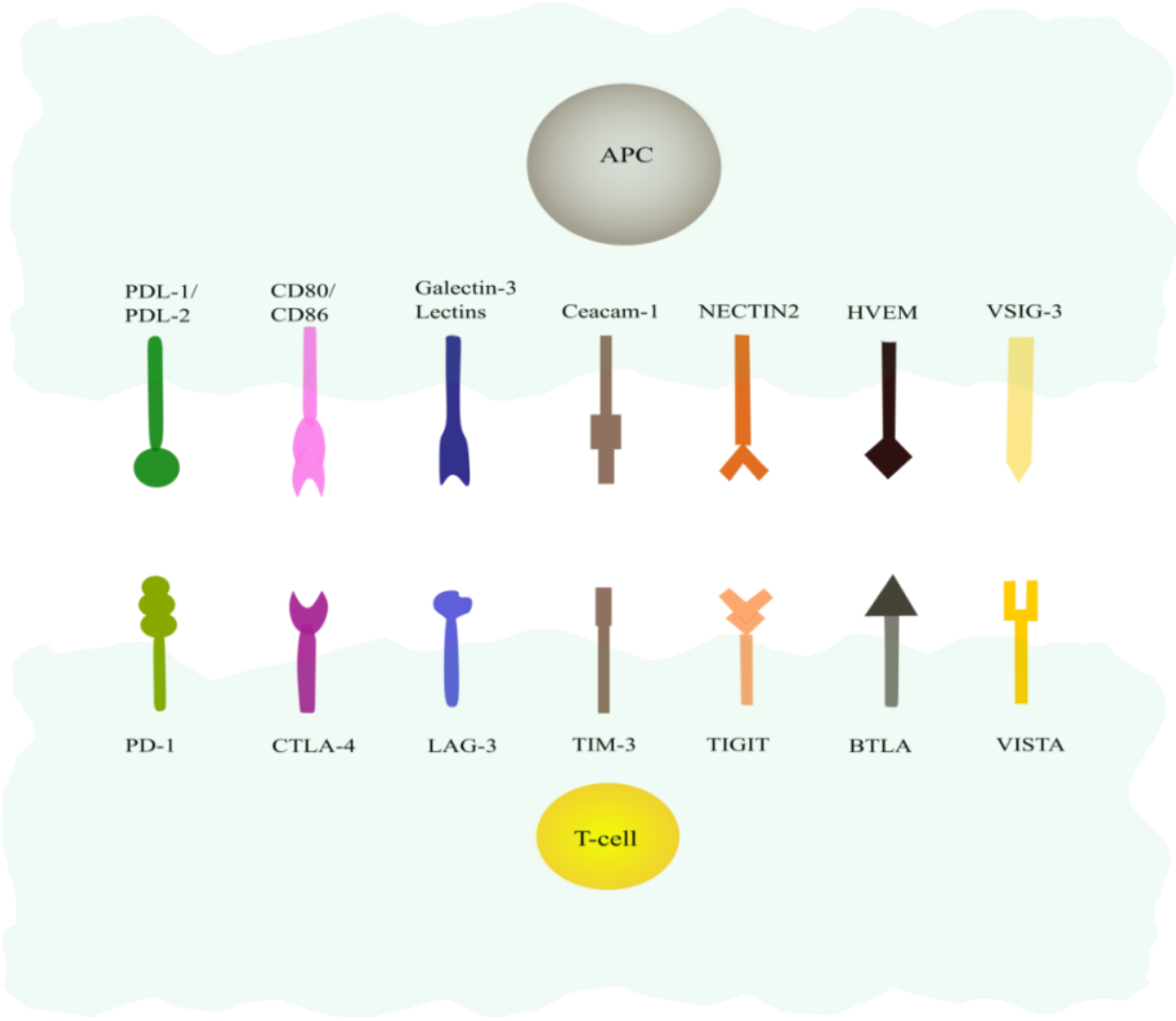

Figure 1.10 Immuno-stimulatory checkpoints and their targets on T-cells and APCs. Immune checkpoints bind to ligands delivering an inhibitory signal. These include PD-1, CTLA-4, LAG-3, TIM-3, TIGIT, BTLA and VISTA with their respective ligands. Abbreviations: APC: antigen presenting cell; CTLA-4: cytotoxic T lymphocyte antigen-4; PD-1: Programmed cell death protein 1; LAG-3: Lymphocyte-activation gene 3; BTLA: B and T-lymphocyte attenuator; VISTA: V-domain Ig suppressor of T-cell activation; CEACAM1: Carcinoembryonic antigen-related cell adhesion molecule 1; VSIG-3: V-Set and immunoglobulin domain containing 3; NECTIN2: Nectin cell adhesion molecule 2; Galectin-3: Galactose specific lectin 3 (Adapted from [440]).

Both PD-1 and CTLA-4 regulate immune responses, however operating by different mechanisms. They are so far the two most actively studied ICs, particularly in the context of cancer and persistent pathogens [445]. CTLA-4 is primarily localized in several intracellular compartments such as the endosomes, lysosomes and the *trans*-Golgi network [446,447]. Factors such as endocytosis and intracellular trafficking to the cell surface determine the overall level of expression of CTLA-4 on the surface of a T-cell (reviewed in [448]). CTLA-4 is predominantly expressed on $CD4^+$ T-cells, and is retained considerably longer on the surface of memory T-cells such as Tregs, compared to activated effector T cells [449].

CTLA-4 functions by regulating early stages of T-cell activation through binding of CTLA-4 to their ligands CD80/86, inducing a potent negative signalling cascade. By preventing the interaction of CD28 and CD80/86, which is required for T-cell activation, CTLA-4 binding to CD80/86 consequently results in tolerance [450]. Moreover, blocking CTLA-4 engagement with its ligand CD80/86 reduces the interaction of Tregs and T-cells, while increasing the T-cell proliferation [451]. Engagement of CTLA-4 binding to its ligand prevents the TCR stop signal, which is involved in sustaining the immunological synapse for the interactions between TCR and its peptide-MHC ligand. Moreover, both naïve and resting memory T-cells express CD28. In contrast to CD28, CTLA-4 is only expressed upon antigen engagement, and as a result, feedback inhibition can occur. Moreover, CTLA-4 is also involved in modulating T-cell responses against cancer and persistent pathogenic infections. Whereas the role of CTLA-4 in $CD4^+$ T cells is shown to downmodulate its activity, the role of CTLA-4 in Tregs is to enhance its suppressive function. Additionally, LN and blood showed similar levels of CTLA-4 expression in Tregs [452,453].

In contrast to CTLA-4, PD-1 is expressed on T-cells that have been in contact with an antigen in the periphery, such as activated T- and B-cells, but is absent in resting naïve memory T cells [454,455]. The expression of PD-1 can result in the inhibition of T-cell activation kinases when binding of PD-1 to either one of its two ligands, PD-L1 and PD-L2, takes place. Once binding takes place, PD-1 forms a cluster with TCR while activating phosphatase SHP2 (Src homology 2 domain-containing tyrosine phosphatase 2) and induces the dephosphorylation of the

proximal TCR signalling molecules. Continuous chronic antigen exposure can lead to persistently high levels of PD-1, resulting in anergy or exhaustion of $CD4^+$ or $CD8^+$ T-cells. However, more studies need to be done in order to understand the molecular mechanisms by which these pathways function and how and when T-cell exhaustion is initiated [456,457].

1.9.1 ICS AND HIV-1 PERSISTENCE ON ART

The relationship between expression of ICs on $CD4^+$ T-cells and HIV-1 persistence in PLWH on ART has been explored in several studies. This relationship can be assessed *in vitro* using different HIV-1 latency models or assessing blood or LN tissue from PLWH or SIV-infected NHP on ART. Our laboratory demonstrated using an *in vitro* model of co-culture of dendritic cells with T-cells that inhibition of PD-1 during infection favoured the establishment of latency [458]. In this model, cells expressing PD-1 compared to cells that didn't express PD1 were enriched for HIV-1. Finally we also demonstrated in the same *in vitro* model that cells expressing PD-1 and TIM-3 were highly enriched for latent HIV-1 [458].

Using $CD4^+$ T-cells from PLWH on ART, HIV-1 proviral DNA is harboured by memory $CD4^+$ T-cells expressing PD-1 compared to cells that don't express PD-1 [128]. A subsequent study in PLWH on ART showed that $CD4^+$ T-cells that expressed ICs compared to cells that didn't express ICs contained a higher frequency of cells infected with replication competent virus [156]. Correspondingly, Banga and colleagues also found replication competent virus in PD-1^+Tfh cells isolated from LNs in PLWH on ART [199].

In addition to PD-1, other ICs have also been shown to be expressed on cells enriched for HIV-1 in PLWH on ART. We showed that HIV-1 was enriched in cells that express PD1, TIGIT and TIM-3 [459]. In SIV-infected NHP on ART, imaging analysis of $CD4^+$ T-cells expressing CTLA-4^+ from LNs showed colocalization and enrichment of HIV-1 DNA [155]. Similar studies of the relationship between CTLA4 and HIV-1 in tissue have not been performed in PLWH.

1.10 CURE STRATEGY

Ten years after the Berlin patient was reported cured, a second individual known as the London patient on ART was effectively cured of HIV-1 infection [460]. These two individuals underwent a risky process for treating malignancy. This was achieved by allogenic stem-cell transplant from compatible donors who were homozygous for CCR5-delta 32 (Δ32) deletion, preventing HIV-1 infection susceptibility [460,461]. Although this intervention shows that curing HIV-1 is possible, such interventions are not feasible as they are also associated with high morbidity and mortality rates [462]. Therefore, less invasive strategies will be required for an effective cure to be developed to eliminate latently infected cells.

Several approaches are being investigated for eradicating the HIV-1 reservoir. These include strategies that can reverse HIV-1 latency, also known as the "shock and kill" strategy [463]. This strategy uses compounds to reactivate the integrated proviral DNA called latency reversing agents (LRAs), forcing the latently infected cell to express HIV-1 proteins or virions allowing for recognition and clearance by HIV-1-specific T-cells [464]. If this is done in PLWH on ART, uninfected cells are protected from further rounds of infection (reviewed in [465,466]). To date, this approach has not led to clearance of infected cells. Whether this is because more potent latency reversal is needed, more cells need to express HIV-1 proteins or that the latently infected cells are primed to survive remains unclear. [467]. As a consequence of these findings, current approaches include the combination of LRAs with strategies that induce immune function (reviewed in [468]). Another strategy which aims to control the HIV-1 reservoir is the "block and lock" approach. Block and lock functions by "blocking" HIV-1 transcription, resulting in the suppression of latency and "locking" the HIV-1 promoter in a deep latent state via epigenetic modifications (review in [469]).

1.10.1 SHOCK AND KILL STRATEGY

1. Epigenetic modifiers

The first LRAs investigated in clinical trials were the anti-cancer agents, Histone Deacetylase Inhibitors (HDACi). HDACs deactylate lysine residues on histones, inducing chromatic condensation and repression of gene expression, and thus packaging DNA in a silent state [470]. In addition, HDACs have also been shown

to be involved in the active repression of HIV-1 expression in its latent state. This was confirmed with vorinostat, the first potent HDACi investigated in clinical trials [471], which increased the expression of HIV-1 RNA in resting memory $CD4^+$ T-cells by an average of 4.8 fold [472]. Similarly, this was confirmed in another *in vivo* study which found that multiple doses of vorinostat resulted in an increase in viral RNA transcription in $CD4^+$ T-cells but had no effect on viral DNA in PLWH on ART [473]. In a clinical trial study in PLWH on ART, the use of HDACi panobinostat resulted in reactivation of the latent HIV-1 reservoir which was measured by a significant increase of cell-associated unspliced (CA-US) HIV-1 RNA and plasma HIV-1 RNA [474]. In the same way, romidempsin, a more potent HDACi shown to induce HIV-1 expression *ex vivo* [475], demonstrated induction of HIV-1 transcription with a significant increase in HIV-1 RNA in plasma [476].

2. PKC agonists

Another potential strategy to overcome latency involves the transcription factors that are down-regulated in latently infected $CD4^+$ T-cells. Protein Kinase C (PKC) agonists have been found to be highly potent in inducing proviral expression through NF-κB pathways. Prostratin and byrostatin-1 are the two well-known PKC activators, and have shown to play a role in latency reactivation of HIV-1 [477]. Unlike prostratin, which has not yet reach clinical studies due to its toxicity, byrostatin appears to be non-toxic and has been shown to reactivate latently infected cells by PKC and 5' adenosine monophosphate-activated kinase (AMPK) pathways, with and without the combination of HDACis [478–480].

3. Bromodomain inhibitors

The LRA JQ1 is a small molecule bromodomain inhibitor that has demonstrated its potential in inducing viral expression. Additionally, JQ1 has the ability to interact with BRD4 a member of bromodomain and extra terminal domain (BET) family, with the positive transcriptional elongation factor b (P-TEFb) and to compete with Tat for binding to P-TEFb at the HIV-1-1 promoter. Although JQ1 has demonstrated low toxicity and has potential to be used as a reactivating agent, studies have shown that *in vitro* results with primary cell and patients gave diverse results [481,482].

1.10.2 BLOCK AND LOCK STRATEGY

1. siRNA

One of the first studies on "block and lock" investigated strategies to silence the HIV-1 promoter using small interfering RNA (siRNA), also known as siPromA [483]. In an *in vitro* study, siPromA "blocked" HIV-1 transcription in a latently infected cell line, J-Lat, for more than 21 days. In the presence of LRAs, these cells remained resistant to reactivation, promoting their lock effect [484]. 2. nullbasic

Another "block and lock" effect that inhibits HIV-1-1 transcription and replication is the mutant form of Tat, also referred to as nullbasic [485]. When expressed in cell lines [486] or human cells [487], nullbasic can target cellular factors such as P-TEFb[488]. In a mouse model engrafted with human $CD4^+$ T-cells, the effect of nullbasic was further investigated as a small molecule gene therapeutic agent, referred to as NB-ZSG. In vivo, using a pre-infection model, $CD4^+$ T-cells were transduced with nullbasic, then sorted and infected with HIV-1, and then engrafted into mice. This approach inhibited virus replication in the mice. In a second approach, referred to as the post-infection model, infection of $CD4^+$ T-cells with HIV was performed first, followed by the delivery of nullbasic into infected cells using a retroviral vector. When these cells were engrafted in mice, HIV replication was delated compared with untreated mice [489].

3. dCA

didehydro-Cortistatin A (dCA), a small molecule inhibitor of Tat, functions by binding to the TAR-binding domain of Tat, inhibiting its interaction with TAR and blocking Tat transactivation of the HIV promoter [490]. Moreover, studies showed that dCA had an inhibitory effect on HIV reactivation from latency *in vitro* [491] and *in vivo* [492]. So far, dCA is the only "block and lock" therapeutic to advance to NHP studies. In an *ex vivo* study, dCA potentially inhibited SIV reactivation from latently infected Hut78 cells and from primary $CD4^+$ T-cells from $SIV_{mac}239$-infected RM [493]. Altogether, these data demonstrate the use of dCA in preclinical evaluation and the potential of "block and lock" in cure strategies.

1.10.3 SECOND MITOCHONDRIAL-DERIVED ACTIVATOR OF CASPASES MIMETICS

Tumour cells can resist apoptosis (programmed cell death) by increasing expression of proteins that block pro-apoptotic pathways. Survival signalling and apoptosis in cancer cells are regulated by members of inhibitors of apoptosis (IAP) protein family (reviewed in [494]). Overexpression of IAP may interrupt apoptosis of cancer cells, consequently leading to resistance of tumour treatment and are therefore considered as therapeutic targets [495]. Novel approaches that promote cell death and mimic IAP antagonists have been made, such as Smac mimetics [496].

Smac mimetics are small pro-apoptotic proteins which function as endogenous inhibitors [496]. Moreover, Smac contains a four-amino acid sequence which binds to a direct antagonist of caspase-3, -7, and -9, X-linked IAP (XIAP), baculoviral IAP repeat (BIR) 2 (also known as cellular inhibitor of apoptosis; c-IAP1) and baculoviral IAP repeat (BIR) 3 (also known as cellular inhibitor of apoptosis; c-IAP2) domain of IAPs [495]. Upon its release from the mitochondria, Smac mimetics alters c-IAP1 and c-IAP2 which in turn results in proteasomal degradation and XIAP, allowing apoptosis to occur (reviewed in [497]).

Originally developed for cancer treatment, Smac mimetics are being studied in reversing HIV-1 latency. In a recent study, macrophages which are permissive to HIV-1 and serve as important site of viral persistence [498] were infected with HIV-1 and treated with small molecule direct inhibitor of apoptosis protein-binding protein with low pl (DIABLO)/Smac mimetics to induce cell death. HIV-1-infected macrophages were selectively targeted when treated with DIABLO/Smac, resulting in BIRC2 and XIAP degradation and inducing autophagy-dependent apoptosis [499].

Smac mimetics SBI-0637142 were found capable of reversing latency in J-Lat cell lines, resulting in an increase of HIV-1 transcription. The same group demonstrated synergistic activation and induced apoptosis in isolated resting $CD4^+$ T-cells from PLWH on ART using SBI-0637142 and panobinostat [500]. A recent follow-up study using humanized mice on ART demonstrated an increase of latent HIV-1 expression when treated with Ciapavir (SBI-0953294), a more potent Smac mimetic compared to SBI-063714. In addition, Ciapavir used in combination with LRAs JQ-1 and BET protein inhibitor I-BET-151 acted synergistically to reverse

HIV-1 latency [501]. These studies highlight Smac mimetics as LRAs and efficacious therapeutic targets that can eliminate the HIV-1 reservoir.

1.10.4 TOLL-LIKE RECEPTOR AGONIST

Pathogen-recognition receptors (PRRs) which are expressed on immune subsets are capable of sensing small molecular motifs by recognizing pathogen-associated molecular patterns (PAMPs) that transduce signals derived from pathogenic infections (reviewed in [502]). Over the years, PRR ligands have received attention as therapeutic drugs against cancers and infectious diseases. The majority of PPRs used to treat diseases are agonists of TLRs. TLRs are transmembrane PPRs and consist of two groups based on their location within the cells and their cognate PAMP. The first subgroup of TLRs: 1, 2 4, 5, 6 and 10 are located on the surface of cells and recognize PAMPs present on fungi, protozoa and bacteria. On the contrary, the second group of TLRs: TLR3, 7, 8 and 9 are localised within intracellular endosomal structures and recognizes bacteria and viruses.

Increasing numbers of evidence have demonstrated that TLRs agonists function as unique LRAs. However, the role of TLR agonists in reversing latency has been largely restricted to *in vitro* studies. TLRs signalling has been shown to lead to activation of nuclear factor kappa B (NF-κB) and reactivation of latent HIV-1 proviruses in combination with other LRAs known to activate the NF-κB pathway, such as bryostatin and prostratin [503]. Interestingly, a recent study using J-Lat cells showed reactivation of HIV-1 latency in the absence of NF-κB activation, indicating NF-κB independent signalling of the latent provirus [504]. The TLR7 agonist, GS-9620 a potent compound originally used to treat chronic hepatitis [505] has also been tested as a LRA in SIV-infected RMs on ART, showing a decrease of viral DNA in LNs and blood [506]. In addition, Lim and colleagues also showed promising results when treating SIV-infected RMs with GS-9620 once every two weeks [507]. The authors showed that GS-9620 led to reduction in CA-SIV DNA in sorted $CD4^+$ T-cells from blood and tissue. Inconsistent results have been reported with GS-9620 treatment which did not result in a decrease in viral DNA blood or tissue nor plasma viremia or changes in the viral RNA to DNA ratio in blood and tissue in SIV-infected RMs [508]. However, both studies had several differences such as ART initiated at different

times after initial infection (65 versus 13 days) and treatment with GS-9620 at different times post ART (60 versus 75 weeks).

Additionally, TLR8 ligand CL75 enhanced HIV-1 replication and induced reactivation of latent HIV-1 in $CD4^+$ T-cells isolated from blood in two out nine PLWH on ART in the presence of PHA and from one patient when acting alone [509].

1.10.5 IMMUNE THERAPY

In conjunction with the above-mentioned strategies, a variety of immune-based therapies are also being investigated to eradicate HIV-1-infected cells. These include gene editing, bi-specific antibodies, broadly neutralising antibodies (bNAbs), chimeric antigen receptor (CAR) T-cells, therapeutic vaccines, Treg depletion, immune checkpoint blockers (ICB) [510] (reviewed in [468]). Because Tregs have been identified as a reservoir for HIV-1 during HIV-1 persistence and a decrease in Tregs has been associated with HIV-1 progression, the following section will focus on depleting these cells [437,438]. Additionally, novel strategies that can block ICB will also be discussed based on emerging data that HIV-1 is enriched in cells expressing ICs and therefore ICBs could potentially reverse latency and enhance HIV-1-specific T-cell function (reviewed in [468]).

1.10.5.1 ALTERNATIVE CURE STRATEGIES

The recent development of anti-tumour immunity using Treg depletion to facilitate cancer treatment has been another area of interest for HIV-1 cure. Depletion of Tregs have been tested in regulating anti-tumour immunity in mice by using antibodies or targeting surface receptors such as CD25, GITR and ICs. In addition, as stated previously (section 1.8.4), HIV-1 can alter Tregs suppressive function, which has led to targeting and manipulating these cells. However, this may be associated with some major challenges when directly targeting FoxP3 Tregs *in vivo* as activated T-cells transiently express Foxp3 [511]. A recent study has addressed this issue by suggesting an approach using a mAB which selectively targets Tregs expressing $CD4^+CD25^+CD127low$ by mediating antibody dependent cellular cytotoxicity (ADCC) [512].

A few surface markers have been investigated and administered for depleting or blocking Tregs in several diseases including HIV-1 infection. Tregs can be

depleted by targeting their surface maker CD25. The monoclonal antibody Daclizumab binds to CD25, which then blocks binding of the receptor IL-2 [513]. So far, Daclizumab has been successfully used in multiple immunological disorders including multiple sclerosis [513], but to date, little is known about its role in HIV-1. Denileukin diftitox (Ontak) is another component which binds to CD25 with IL-2 fused with diphtheria toxin, subsequently leading cell death as a result of diphtheria entering the cell in cancer [514]. Unlike Daclizumab, this compound has also been used in studies to deplete Tregs during HIV-1. In a study performed on SIV-infected African green monkeys, the use of Ontak resulted in a significant decrease of Tregs while reducing $CD4^+$ and $CD8^+$ T-cell activation [515]. In addition, Ontak led to a decrease in disease progression, increased immune activation [516,517] and, boosted SIV-specific T-cells in peripheral blood and LNs in in SIV infected RM [518]. Of importance, these two drugs were discontinued and replaced with an improved drug, bivalent human IL-2 fusion toxins [514] .

Another strategy to deplete Tregs is through targeting CCR4 with a diphtheria toxin based anti-human CCR4 immunotoxin, which leads to inhibition of protein synthesis [519]. A significant decrease of Tregs in LNs was demonstrated when depleting Tregs with this drug in NHP [520].

Cyclophosphamide (Cy), a drug used for chemotherapy, decreased the proportion of nTregs and aTregs in meseothelioma patients [521]. In addition, results from one study also reported a decrease in the frequency of aTregs, which was lower in LNs that were surgically removed from patients with melanoma cancer [522].

So far, only one study has looked at the effect of Cy on the HIV-1 reservoir and no significant difference was reported in HIV-1 DNA in LNs and PBMCs between ART treat alone and ART treated group with Cy. Notably, these patients had a detectable plasma viral load, with half of the participants admitting to nonadherence to ART, potentially explaining why a decrease of HIV-1 DNA in these patients was not detected [523]. Further studies are needed to investigate whether Cy could be used as a promising treatment for decreasing the HIV-1 reservoir.

1.10.5.2 IMMUNE CHECKPOINT BLOCKERS (ICB) IN CANCER

Cancer cells evade immune destruction by continuously inducing inhibitory signals such as ICs. As a result, this has led to studies of ICs, demonstrating that blocking these can result in antitumor immunity in preclinical models [524,525].

The ICs PD-1 and CTLA-4 both play distinct roles in T-cell immunity. In cancer, ICs become upregulated causing an inhibitory response and therefore limiting the ability of the immune system to produce an effective anti-tumour response. Therefore, blocking ICs has gained a tremendous amount of attention in anti-tumour immunity. This was demonstrated by Honjo and colleagues whereby blocking PD-1 led to long-term remission in melanoma [526,527]. The basic understanding of CTLA-4 functioning as a negative regulator of T-cells has led to preclinical observation that blocking its negative regulatory function can dramatically enhance anti-tumour activity in mouse models, then moving into the successive clinical trials that tested this in advance melanoma. Food and Drug Administration (FDA) approved CTLA-4 IgG1antibody and inhibitor, ipilimumab, was one of the first ICs therapeutic antibodies to be investigated in advanced melanoma, showing improved survival in phase III clinical trial [528,529]. Tumour-reactive T-cells have shown to be highly upregulated in melanoma patients; however, this has a beneficial effect due to the high proportion of these tumour-reactive T-cells, balance autoimmune toxicity.

Another immune checkpoint inhibitor, PD-1 and its ligand PD-L1 have been demonstrating even more exciting results by elevated anti-tumor activity and reduced toxicity, than for the anti-CTLA-4. Anti-PD-1, nivolumab, has shown an effective anti-tumor activity in melanoma as well as various cancers [530].

Although ipilimumab and nivolumab monotherapies may have an impact on survival rate, the majority of patients that undergo treatment unfortunately do not achieve objective responses to treatment; rather tumour regressions are partially eradicated. This has led to immunologic observation, suggesting that treatment combination of CTLA-4 and PD-1 could have an additive or synergistic potential. Studies in mouse models demonstrated that treatment combination of anti-CTLA-4 and anti-PD-1 may be synergistic [531,532]. Furthermore, combination treatment of ipilimumab and nivolumab showed early tumour regression in advanced melanoma. The five-year survival rate in patients who received ipilimumab and nivolumab was

52%, ipilimumab alone 26% and nivolumab 44%; treatment was related with no new side effects, also known as immune-related adverse events [530].

1.10.5.3 ICB IN HIV-1

Clinical trials of PD-1and CTLA-4 inhibitors in treated HIV-1-1 disease have been initiated, these are summarised in Table 1.4. Animal studies of SIV infection in macaques, which is a much closer model to humans than murine, has brought a better understanding of the role of ICs pathways in HIV-1. A recent study led by Paiardini and colleagues, demonstrated that inhibition of CTLA-4 and/or PD-1 using ipilimumab and nivolumab was well tolerated in SIV-infected RM on ART [533]. Inhibition of CTLA-4 alone or in combination with anti-PD-1 led to an increase in $CD4^+$ T-cell activation, proliferation and expanding T_{EM} and $CD8^+$ T-cells in peripheral blood and LNs. Notably, the combination of anti-PD-1 and anti-CTLA-4 increased viral reactivation, SIV-RNA and unparalleled HIV-1- specific $CD8^+$ T-cell responses in RM on ART. In addition, this combination also showed a decrease in total SIV-RNA or DNA in LNs, particularly in the BCZ [533].

In a small randomized study the effect of anti-PDL-1 showed promising results by enhancing HIV-1-specific T-cell responses in healthy PLWH without malignant cancers on ART, however, this study was discontinued as this antibody was related with immune-related adverse events in macaques [534]. The impact of ipilimumab and nivolumab on the HIV-1 reservoir in an HIV-1-infected patient on ART with metastatic melanoma [535,536] and lung cancer [537,538] was studied showing that these ICBs were well tolerated and reduced the HIV-1 reservoir [537], consistent with previous reports in HIV-1-infection. A study in our lab reported an increase in CA-US HIV-1 RNA after treatment with ipilimumab and nivolumumab in a HIV-1-infected individual treated for melanoma [539]. Furthermore, *ex vivo* blockade of PD-1 pathway with mAb pembrolizumab has shown promising results by enhancing HIV-1 production without increasing T-cell activation when used in combination with bryostatin [540].

In summary, these results suggest that ICBs PD-1 and CTLA-4 may have a significant impact on HIV-1 that persists on ART, including LN tissue. However, the

underlying mechanism of how there is depletion of infected cells needs to be further explored.

Table 1.4 | Summary of recent studies on the effects of anti-CTLA-4 and anti-PD-1on HIV-1 *in vivo*

Compound	Source	Cohort	Effect on the HIV-1 reservoir	Comments	Ref
Anti-CTLA-4					
Ipillimumab MDX-010	BMS[c]	SIV-infected RM on ART (n=10)	Significant increase in plasma viremia	Significant increase level of T-cell activation	541
Ipillimumab	BMS[c]	PLWH on ART treated for melanoma (n=1)	Increase in CA-US HIV-1 RNA and Transient increase in $CD8^+$ T-cells	No change in T-cell activation No change in CA-HIV-1 DNA but assay used was unable to pick up HIV-1 DNA containing inducible proviruses	539
Anti-PD-1					
Anti-PD-1	clone: EH12-1540	SIV-infected RM on ART (n=9)	Decrease in plasma viral load. RNA copies reduced post-treatment and delayed disease progression	Proliferation of memory B cells and increase in SIV envelope specific anti-body	542
Nivolumab[b]	BMS[c]	PLWH on ART treated for NSCLC(n=10)	Viral load remained undetectable	$CD4^+$ T-cells remained unchanged	543
Nivolumab[b]	BMS[c]	PLWH on ART treated for NSCLC (n= 1)	Increase in CA-HIV-1 DNA	Increase in HIV-1-specific $CD8^+$ and $CD4^+$ T-cells and decrease in $PD\text{-}1^+$ T-cells	538

Nivolumab[b]	BMS[c]	PLWH on ART treated for NSCLC (n=1)	Reduced the HIV-1 reservoir	Increase in HIV-1-specific $CD8^+$ T-cells	537
Pembrolizuma or Nivolumab[b]	BMS[c]	PLWH on ART treated for malignancy (n=3)	No changes in $CD4^+$ T-cell CA-HIV-1 RNA and DNA or plasma viremia	No consistent changes in the frequency of total or activated $CD4^+$ or $CD8^+$ T-cells	544
Pembrolizumab bryostatin	BMS[c]	PLWH on ART treated for melanoma (n=1)	Increase HIV-1 production	No increase in T-cell activation	540
Combination					
Ipilimumab Nivolumab	BMS[c]	PLWH on ART treated for melanoma and HCV (n=2)	No effect on the HIV-1 reservoir	No immune related adverse events	545
Ipilimumab Nivolumab	BMS[c]	SIV-infected RM on ART (n=34)	Induced SIV reactivation Increase in $CD4^+$ T-cell activation, proliferation and decreased SIV in the BCZ	No effect on SIV specific $CD8^+$ T-cells	533

[a]Ipilimumab isotype fully human IgG1 [b] Nivolumab isotype fully human IgG4 [c]BMS (Bristol-Myers Squibb)

CA-US: cell-associated unspliced; BCZ: B-cell zone; NSCLC: non-small cell lung cancer

1.11 HYPOTHESIS AND AIMS

Hypothesis:

Tregs are an important reservoir that persists in PLWH on ART and ICs define subsets of latently infected T-cells

Main Aim:

Determine the relationship between expression of ICs and HIV-1 persistence in blood and tissue from PLWH on ART

Aims:

1. Establish a method to identify HIV-1 RNA and DNA in combination with cellular markers used to define Tregs expressing PD-1 and CTLA-4 in LN tissue

2. Define the expression of CTLA-4 and PD-1 on T-cell subpopulations in LN tissue from PLWH on and off ART

3. Determine the relationship between detection of HIV-1 DNA and RNA using IHC and PCR based quantification in LN tissue from PLWH on ART

Chapter 2: Multiparameter immunohistochemistry analysis of HIV-1 DNA, RNA and immune checkpoints in lymph node tissue

Zuwena A. Richardson[†], Claire. Deleage[‡], Candani S A. Tutuka[§,¶], Marzena. Walkiewicz[§,‖], Perla M. Del Río-Estrada[¦], Rachel D. Pascoe[†], Vanessa A. Evans[†], Gustavo. Reyesteran[¦], Michael. Gonzales*, Samuel. Roberts-Thomson*, Jacob D. Estes[‡‡], Sharon R. Lewin[†,#,‖ ‖] & Paul U. Cameron[†,]**

[†]The Peter Doherty Institute for Infection and Immunity, The University of Melbourne and Royal Melbourne Hospital, Melbourne, Australia

[‡]Frederick National Laboratories for Cancer Research, Frederick, Maryland, USA

[§]Olivia Newton John Cancer Centre Research Institute, Austin Hospital, Heidelberg, Australia

[¶]La Trobe School of Cancer Medicine, La Trobe University, Melbourne, Australia

[‖]Murdoch Children's Research Institute, Royal Children's Hospital, Melbourne, Australia

[¦]Centro de Investigación en Enfermdades Infecciosas, Instituto Nacional de Enfermedades Respiratoriras, Mexico City, Mexico

*Pathology Department, The Royal Melbourne Hospital, Melbourne, Australia

[‡‡] Vaccine and Gene Therapy Institute and Oregon National Primate Research Center, Oregon Health Science University, Portland, Oregon

[#]Department of Infectious Diseases, Alfred Hospital and Monash University, Melbourne, Australia

[‖ ‖] Victorian Infectious Diseases Service, Royal Melbourne Hospital, Melbourne, Australia

**Launceston General Hospital, Tasmania, Launceston, Australia

Journal: Journal of Immunological Methods

Abstract word count: 239

Article word count: 7000

Conflict of interest: No conflict of interest to declare

Corresponding author: paul.cameron@unimelb.edu.au (Paul Cameron)

Abstract

The main barrier to a cure for HIV-1 is the persistence of long-lived and proliferating latently infected $CD4^+$ T-cells despite antiretroviral therapy (ART). Latency is well characterized in multiple $CD4^+$ T-cell subsets, however, the contribution of regulatory T-cells (Tregs) expressing FoxP3 as well as immune checkpoints (ICs) programmed cell death protein 1 (PD-1) and cytotoxic T-lymphocyte-associated protein 4 (CTLA-4) as targets for productive and latent HIV-1 infection in people living with HIV-1 on suppressive ART is less well defined. We used multiplex detection of HIV-1 DNA and RNA with immunohistochemistry (mIHC) on formalin-fixed paraffin embedded (FFPE) cells to simultaneously detect HIV-1 RNA and DNA and cellular markers. HIV-1 DNA and RNA were detected by *in situ* hybridization (ISH) (RNA/DNAscope) and IHC was used to detect cellular markers (CD4, PD-1, FoxP3, and CTLA-4) by incorporating the tyramide system amplification (TSA) system. We evaluated latently infected cell lines, a primary cell model of HIV-1 latency and excisional lymph node (LN) biopsies collected from people living with HIV-1 (PLWH) on and off ART. We clearly detected infected cells that coexpressed HIV-1 RNA and DNA (active replication) and DNA only (latently infected cells) in combination with IHC markers in the *in vitro* infection model as well as LN tissue from PLWH both on and off ART. Combining ISH targeting HIV-1 RNA and DNA with IHC provides a platform to detect and quantify HIV-1 persistence within cells identified by multiple markers in tissue samples from PLWH on ART or to study HIV-1 latency.

Introduction

Antiretroviral therapy (ART) has led to a significant decline in mortality and morbidity in people living with HIV-1 (PLWH), however treatment is life long and there is no cure. Despite rapid decline of HIV-1 RNA in plasma to undetectable levels following ART, virus persists in long lived and proliferating latently infected $CD4^+$ T-cells [6,546]. Latency is defined as the integration of intact virus into the host genome but failure to complete the virus life cycle in the absence of T-cell stimulation [547,548] and can be distinguished by detection of HIV-1 DNA but not HIV-1 RNA [61,549]. Latently infected cells are rare in blood and are found at far higher frequency in tissue such as lymph node (LN) and the gastrointestinal (GI) tract [230,550–552]. Identification of specific subpopulations of latently infected cells by multiple markers, specifically in tissue from PLWH on ART, is of high interest but better tools are needed for such studies.

New strategies are needed to understand the complexity of HIV-1 persistence in tissue sites to allow analysis of the cell phenotype in situ and provide spatial information about the exact location of the infected cell in tissue structures [300–302]. The lack of sensitivity of traditional *in situ* hybridisation (ISH) approaches has led to development of a new and more sensitive ISH method of RNAscope and DNAscope. These use fluorescents labelled probes in either formalin-fixed, paraffin embedded (FFPE) tissues samples or fresh cryopreserved tissue. This method identifies RNA and DNA in individual cells and uses bright-field microscope (for chromogenic detection), or a fluorescent microscope (for fluorescent labels) [307].

The combination of both DNA and RNAscope in the same tissue section collected from either simian immunodeficiency virus (SIV) infected non-human primates

(NHP) or PLWH allows for the discrimination of viral DNA (vDNA) $^{+}$ cells that are transcriptionally silent, from those that are actively transcribing viral RNA (vRNA) $^{+}$ cells. These methods demonstrate the importance of the B-cell follicles (BCFs) as an important site for persistence of vRNA^{+} cells in LN from PLWH on ART [297] and in all lymphoid tissue (i.e. LN, gut, lungs and spleen) in NHP even after years of ART[163].

There is currently no surface marker that can distinguish latently infected from productively infected cells in PLWH on ART. There are many cellular markers that are enriched for HIV-1 persistence and these include immune checkpoint (IC) markers which can be found on certain CD4^{+} T cell subsets, including regulatory T-cells (Tregs) [553,554]. We and others have shown that on ART, virus can persist in cells that express PD-1 [555,556] and these PD-1hi cells are frequently found in the BCFs [199,557] and have features consistent with T follicular helper (Tfh) cells. However, HIV-1 can persist in cells other than PD-1 hi cells, including cells that express other IC markers such as TIM-3[558], TIGIT[559], and CTLA-4[155], which are largely found in the extrafollicular areas. Therefore characterization of HIV-1 and multiple markers in tissue is of great importance and has been studied in FFPE tissue[155], however, further progress to stain more antigens on the same tissue has been limited.

Advances in immunohistochemistry (IHC) now allows simultaneous *in situ* detection of RNA and multiple surface proteins in FFPE tissues [561], using the Tyramide signal amplification (TSA) Opal system and the Vectra multispectral IHC (mIHC) imaging system from Perkin-Elmer and could potentially be applied to fully understand where HIV-1 persists in LN tissue in PLWH on ART. In this study, we report the development of a seven-color mIHC panel, combining both HIV-1 DNA and RNAscope with IHC, allowing us to simultaneously characterize HIV-1 RNA, HIV-

1 DNA, CD4, FoxP3, PD-1, CTLA-4 and DAPI in FFPE tissue using the TSA Opal system. Sections where then scanned and analysed using the Vectra 3 quantitative imaging system from Perkin-Elmer. We could simultaneously detect HIV-1 RNA and DNA, in combination with up to seven cellular markers. In agreement with previous studies both vRNA and DNA could be detected in LN tissue both on and off ART and we found co-localisation of vRNA with FoxP3 and CTLA-4 consistent with Tregs being a potential reservoir for HIV-1 on ART.

Materials & Methods

Cell lines

ACH-2 cells (subclone A3.01) obtained from NIH AIDS reagent program contain an integrated copy of HIV-1 and although commonly used as a model for HIV-1 latency, have evidence of multiple diverse integration sites consistent with some low level virus replication [79]. ACH-2 cells were cultured in Roswell Park Memorial (RPMI) 1640 supplemented with 10 mM N-2-Hydroxyethylpiperazine-N′-2-ethanesulfonic acid (HEPES), 2 mM L-glutamine, 10%; heat inactivated fetal bovine serum (FBS). The parental cell line, Jurkat cells (clone E6-1) were cultured in RPMI 1640 (RF10) supplemented with 2 mM L-glutamine, 1% Penicillin-Streptomycin and 10% FBS.

The J-Lat isoclone 6.3 contains a single copy of integrated HIV-1 which lacks multiple HIV-1 genes including envelope but includes both Tat and green fluorescent protein (GFP) open reading frames both under the control of the HIV-1 promoter in the 5' long terminal repeat (LTR) [562]; NIH AIDS reagent program]. The cell line was cultured in RPMI 1640, 10% FBS, supplemented with penicillin (100 U/ml) and streptomycin (100µg/ml). All cells were maintained in a humidified incubator at 37 °C with 5% CO2.

ACH-2 cells were mixed with uninfected Jurkat cells to obtain serial dilutions of 10-20 $x10^6$ total cells at different ratios of infected to uninfected cells of 1:2, 1:10 and 0:1. J-Lat cells were mixed with uninfected Jurkat cells at a ratio of 1:2. For some experiments, ACH-2 and J-Lat 6.3 cells were first stimulated with phorbol myristyl acetate (PMA; 10nM) for 24 hours and then diluted with Jurkats at a ratio of 1:2.

An *in vitro* HIV-1 latency model using resting CD4$^+$ T-cells and monocytes

Resting CD4$^+$ T-cells and monocytes from peripheral blood mononuclear cells (PBMC) collected from healthy donors (Australian Red Cross, Melbourne, Australia), were infected with NL4.3 which contained the CCR5–using envelope protein from AD8 and expressed GFP (GFP) in place of the nef protein or under the control of an internal ribosome entry site (IRES) element (NL(AD8)Δnef-GFP and NL(AD8) IRES–GFP respectively) were produced by transfection of 293T-cells at a multiplicity of infection (MOI) of 0.5 as determined by limiting dilution in phytohemagglutinin (PHA)-activated PBMC as previously reported [563]. Resting CD4$^+$ T-cells were isolated by negative selection using a panel of monoclonal antibodies and magnetic bead sorting (autoMACS; Miltenyi Biotec, San Diego, CA) as previously described [564]. Monocytes (CD14$^+$) were isolated from syngeneic donors using positive selection for CD14 on by magnetic bead sorting (autoMACS; Miltenyi Biotec). Monocytes with a purity ≥95% and resting CD4$^+$ T-cells with a purity of >98% were used. Resting CD4$^+$ T-cells were cultured alone or with syngeneic monocytes at a ratio of 10:1 for 24 h in the presence of IL-2 (2 U/ml; Roche Diagnostics, Mannheim, Germany) and Staphylococcus enterotoxin B (SEB) (10 ng/ml) before infection with either reporter virus for 2 h. After washing, cells were cultured for five days in IL-2 (2 U/ml) supplemented media without additional SEB. Productive infection was measured by flow cytometry at day five post infection. Monocytes were excluded by gating for HLA-DR^{lo} CD3$^+$ T cells. CD4$^+$ T cells that were non-productively infected (EGFP$^-$) were sorted by flow cytometry using a FACSAria (BD Biosciences, San Jose, CA). Latent infection was determined following activation of 200,000 sorted CD4$^+$ T cells (EGFP$^-$) with immobilized anti-CD3 (7 μg/ml; Beckman Coulter, Brea, CA) in 10% RPMI 1640 medium with

antibiotics (penicillin–streptomycin–glutamine; RF10) supplemented with soluble CD28 (7 μg/ml; BD Biosciences). Sorted cells were harvested 72 h after stimulation in RF10 media supplemented with IL-2 (10U/ml) and IL-7 (1ng/ml) with anti-CD3/CD28 and raltegravir 1 μM; National Institutes of Health AIDS Reagent Program) was added to media to prevent spreading infection. The expression of inducible virus was quantified by GFP expression using flow cytometry (FACSCalibur; BD Biosciences).

Fixation and Embedding of Cell Pellets in Paraffin

Cells were washed in PBS and fixed in 4% paraformaldehyde (PFA) at room temperature for 24 hours with mild aggregation on a slow speed rocker. Fixed cells were washed to remove PFA, which was replaced with 80% ethanol, on a slow speed rocker for mixing. Cells were then washed and in a drop wise manner, suspended in liquefied Histogel biopsy gel (Fisher Scientific, Hampton, New Hampshire) pre-warmed to 50 °C in a water bath and centrifuged for five minutes at 2,000x g. After centrifugation, cells were cooled for 5-10 minutes at 4 °C in covered by 80% ethanol and the cell pellet was paraffin embedded.

Human Subjects

Four participants underwent elective surgical resection of LNs. All participants were PLWH and were either naïve to ART (n=2; with HIV-1 RNA >150000 copies/ml) or on suppressive ART (n=2; defined as HIV-1 RNA <90 copies/ml for at least 2 years). LNs were collected at the Centro de Investigación en Enfermedades Infecciosas (CIENI-IN ER), Mexico City, Mexico and the study was approved by the local human and research ethics committee (B03-16). Clinical details are provided in Supplementary Table 1.

Histology and Immunohistochemistry

Immunohistochemistry was performed on FFPE LN tissue using a peroxidase-based method on 5 μm sections on Superfrost® plus microscope slides (Thermo Scientific). Specimen slides were incubated at 60 °C for 45-60 minutes for the melting and fixing of specimens onto microscope slides. In order to deparaffinise, slides were washed in xylene and rehydrated in ethanol of 100% to 70%. Slides were then treated with hydrogen peroxidase (Chem-Supply, Gillman, Australia) in 0.3% H_2O_2 (v/v) in double-distilled H_2O (ddH_2O) for 15 minutes at room temperature. Heat induced epitope retrieval was then performed until boiling was achieved, followed with 90 °C for 15 minutes by microwave treatment (MWT) in the appropriate retrieval buffer optimised for each target epitope. Specimens were then blocked using Background Sniper (Biocare Medical, Concord, CA) for 15 minutes prior to primary antibody application.

HIV-1-1 RNA and DNA target probes

The HIV-1 RNA probe used was designed to hybridize to viral RNA in gag, pol, vif, vpr, tat, rev, env, nef, and vpx genes (vRNA anti-sense probe, ACD catalog: ADV416111) as well as HIV-1 DNA probe targeting the Gag-Pol coding region (vDNA sense probe, ACD catalog: ADV425531). All probes were purchased from Advances Cell Diagnostics (ACD Newark, CA) and a complete list of the sequence of each probe used has been previously published [297].

HIV-1- RNA and DNA *in situ* hybridization

For the detection of vRNA and vDNA, we used the RNAscope 2.5 brown kit[297], with some modifications [297]. In brief, probes were visualized by hybridizing with preamplifiers, amplifiers in a humidified HybEZ oven, and finally, fluorescent label

with TSA amplification system (Perkin Elmer, Waltham, Massachusetts). Pre-amplifier 1 was hybridized at 40 °C for 30 min. Following washing of samples twice, then hybridized with Amplifier two in a humidified at 40 °C for 15 min. Again following two washes, amplifier three was hybridized at 40 °C for 30 min. After a further two washes, Amplifier four was hybridized at 40 °C for 15 min, washed twice, following hybridization of Amplifier five for 30 minutes at 40 °C, again with two washes and lastly incubation of Amplifier 6 for 15 minutes at 40 °C for 15 minutes with a final two washes. For vRNA detection, slides were first washed once in Tris Buffered saline (TBS) with Tween (VWR International, Radnor, Pennsylvania) and incubated for 4 minutes with either 3,3'-diaminobenzidine (DAB) for 5-10 minutes or TSA dyes. TSA dye 520 (1:700) was used for 4 minutes for labelling of vRNA, TSA dye 570 (1:700) for two minutes for labelling of vDNA and washed twice in TBS-Tween for five minutes. Lastly, slides were incubated with either DAPI (Perkin Elmer) or counterstained with hematoxylin and eosin (H&E) for one-two minutes. Slides were incubated with DAPI (1:2) for either four (human LN tissue) or six minutes (cell lines or primary model of latency). For the removal of DAPI, slides were washed twice with TBS-Tween for five minutes.

Simultaneous detection of vDNA and vRNA

In order to visualize vDNA and $vRNA^{+}$ cell simultaneously, we combined both DNA and RNAscope (DNA/RNAscope). Following fixation and pretreatment as described for RNA and DNAscope [297], slides were incubated for two hours at 40 °C with RNA probes as described previously, following amplification, washes, labelling with TSA 520 (1:700) for four minutes and MWT retrieval. For vDNA, slides were hybridized with HIV-1 DNA sense probes overnight at 40 °C, followed by amplification,

washes, labelling with TSA 570 (1:700) for two minutes and counterstained with DAPI.

Multiplex immunohistochemistry (OPAL™)

Rabbit monoclonal antibodies to CD4 (Cell Marque, Rocklin, CA) clone 104R-1, 1/100, high pH retrieval), mouse monoclonal antibody to FoxP3 (Abcam, Cambridge, UK) , clone IgG1, 1/1000, high pH retrieval), mouse polyclonal antibody to PD-1 (Abcam, IgG1 Nat105, 1/500, low pH retrieval), mouse monoclonal antibody to CTLA-4 (MyBiosource, San Diego, CA) IgG2a/k, 1/100, high pH retrieval) were used. Antibodies were diluted using a background-reducing antibody diluent buffer S3022 (Agilent, Santa Clara, CA). A horseradish hydrogen peroxidase (HRP) linked anti-mouse and anti-rabbit secondary antibody, EnvisionTM HRP (Agilent), was used for each primary antibody species according to the manufacturer's recommendation. Immunofluorescent signal was visualized using the TSA amplification system, OPAL™ 7-color fluorescent IHC kit (Perkin Elmer), TSA dyes 540, 620, 650, and 690 (1:50) for ten minutes, counterstained with Spectral DAPI. All slides were imaged on the Vectra® 3 Quantitative Pathology Imaging System (Perkin Elmer). Images were then examined using color separation and inForm® Software v2.1 (Perkin Elmer). All slides were scanned on the Vectra at 10X magnification to select for high-powered imaging at 20X (resolution of 0.5 μm per pixel) using Phenochart (Perkin Elmer).

Quantitative image analysis

HALO® image analysis software from Indica Labs (versions 2.0, Albuquerque, New Mexico) was used for quantitative IHC assessment of the number of cells positive for each stain as described above, including $vDNA^+$ and $vRNA^+$ cells in each

compartment and the number of cells with different co-localization. For the evaluation of probe signals for both vDNA and $vRNA^+$ cells in cell lines, primary T-cells and LN tissue samples, HALO's Fluorescence *in Situ* Hybridization (FISH) probing module was used to quantify co-expression of fluorescent HIV-1 DNA and RNA probes on a per cell basis and cell classification of each probe (0, 1^+, 2^+, 3^+ and 4^+) using ACD guidelines for scoring.

Statistical analysis

Statistical analysis was performed, and graphs plotted using Graphpad Prism (version 8.2.1, GraphPad Software, La Jolla, CA). Given the small sample numbers, we assumed normality and used a Two-tailed paired t-test to determine difference in vDNA and $vRNA^+$ cells between unstimulated and stimulated ACH-2 and J-Lat cells. Details of significant differences between data groups have been described in each figure legend and *P* values less than 0.05 was considered significant.

Results

Identification of latent and productively infected cells using HIV-1 DNA and RNA probes in cell lines

We first optimised our method for tissue analyses using the T-cell lines ACH-2 and J-Lats. We used ACH-2 cells which contains 2 integrated copies of HIV-1-1 DNA [79] and have evidence of low level virus replication [79]. These cells were diluted in the uninfected parental Jurkat cell line. Latently infected cells were defined as $vDNA^+$, vRNA- cells and productively infected cells as $vDNA^+$ $vRNA^+$ or vDNA- $vRNA^+$ cells. We assessed the specificity for each probe for HIV-1 RNA and HIV-1 DNA using the *in situ* hybridization (ISH) assays (RNAscope and DNAscope).

We detected no signals using the no probe control (Supplemental Fig. S1A, i) and uninfected Jurkat cells alone (Supplemental Fig. S2.1A, ii). When unstimulated ACH-2 cells were diluted at a ratio of 1:10 in uninfected Jurkat cells, we were able to detect $vRNA^+$ cells with chromogen diaminobenzidine (DAB), as a brown signal in 10% of cells, indicating highly specific detection of productively infected cells. The brown cells were densely stained, encompassing the entire cell body (Supplemental Fig. S2.1A, iii). Similar results were obtained with a higher ratio of infected cells and a corresponding increase in DAB positive or $vRNA^+$ cells (Supplemental Fig. S2.1A, iv).

We then evaluated HIV-1 DNA probes using the same samples. With the DNAscope probes, we demonstrated no DAB positive signals in the no probe control (Supplemental Fig.2.1B, i) and in Jurkat cells (Supplemental Fig. S2.1B, ii). When we used the HIV-1 DNA probes in mixtures of PMA-activated ACH-2 and Jurkat

cells, there were punctuate signals of one or two dots (vDNA$^+$ cells) within the nucleus. The frequency of cells visually scored as vDNA$^+$ decreased accordingly with the proportion of diluted PMA-activated ACH-2 with uninfected Jurkat cells (Supplemental Fig. S2.1B, iii and iv, black arrows). Collectively, this data indicate that the HIV-1 RNA probes could detect vRNA$^+$ cells and vDNA in PMA-stimulated ACH-2 cells as previously reported [297].

After successfully identifying vDNA and vRNA$^+$ cells by bright field microscopy using DAB, we next sought to identify both HIV-1 DNA and/or RNA using dual ISH and IHC and imaged on the multispectral imaging platform Vectra (Perkin-Elmer). This approach was further investigated in combination with the TSA system, which has previously demonstrated to be more sensitive than conventional DAB or fluorescence IHC [565], but has been difficult to simultaneously examine HIV-1 RNA and DNA with cellular markers (mIHC >5-plex) [566,567].

We normalized the background to a no probe control (Fig. 1A, i), and detected green vRNA$^+$ cells, when ACH2 were at a frequency of 1 in 10 uninfected Jurkat cells (Fig. 1A, ii). We used a similar approach for DNA probes using a no probe control (Fig. 1B, i) and detected red vDNA$^+$ cells as one or multiple distinct punctuate red dots within the nuclei (Fig. 2.1B, ii). To determine whether both RNA and DNA probes could be detected simultaneously, we used a dilution of ACH-2 at a frequency of 1 ACH-2 cell to 1 uninfected Jurkat cells, and detected vRNA$^+$ cells (green) within the cytoplasm (Fig. 2.1C, i,iv) and punctuate dots in red, indicative of vDNA$^+$ cells (Fig. 2.1C, ii, iii). In these cultures, we could detect both productive (vRNA$^+$ vDNA$^+$, white arrow 1.) and latent infection (vRNA- vDNA$^+$ cells, white arrow 2).

Quantification of probes in cell lines

We next quantified the number of vDNA and/or $vRNA^+$ cells using Halo imaging analysis software in the infected cell lines, ACH-2 and J-Lat which were either unstimulated or stimulated with PMA. Simultaneous visualization of $vDNA^+$ (red) and/ or $vRNA^+$ cells (green) was possible in ACH-2 (Fig. 2.2A) and J-Lat cell lines (Fig. 2.2B). Both fluorescence signals for HIV-1 DNA and RNA were visible in unstimulated and stimulated ACH-2 cells (Fig. 2.2A) and there was a significant increase in the number of vDNA and $vRNA^+$ cells in both latently and productively infected cells after stimulation (Fig. 2.2C). In unstimulated J-Lat cells, the majority of cells were $vDNA^+$ cells (red) (Fig. 2.2B) with the number of $vRNA^+$ cells significantly increasing after stimulation (Fig. 2.2D). These data are consistent with ACH-2 cells being infected with replication competent virus [79,568] while J-Lat cells are infected with replication defective virus, however, once these cells are stimulated the activation of the LTR leads to expression of viral RNA [569]. After stimulation with PMA, the ratio of vRNA to $vDNA^+$ cells increased in both ACH-2 and J-Lat cells (Fig. 2.2E). We used the Halo analysis software to quantify the number of HIV-1 DNA and RNA positive probe signals in each cell. HIV-1 DNA and/or RNA probe signals were quantified using ACD recommended RNAscope scoring guideline which consist of cells that are 0^+ (no probe signal), 1^+ (1-3 probes), 2^+ (4-9 probes), 3^+ (10-13 probes) and 4^+ (>14). In the ACH-2 cells, we observed multiple copies with both DNA and RNA probes within each cell, mainly in the 1^+ and 2^+ categories (Fig. 2.2F) with the frequency of DNA and RNA increasing in both categories after stimulation (Fig. 2.2G). In the J-Lat cells, HIV-1 DNA^+ cells were in the 1^+ expression category with a few HIV-1 RNA^+ cells (Fig. 2.2H). Following stimulation, the number of HIV-1 DNA and RNA cells increased and were mostly in

the 1^+ expression category (Fig. 2.2I). One interesting observation while utilizing image analysis on the Halo platform, we were able to enumerate multiple copies of vDNA in J-Lat 6.3 cells pre and post-activation, despite there being no evidence that suggests that these cells contain multiple copies[79].

HIV-1 RNA and DNA detection in an *in vitro* model of inducible latency

We next investigated expression of virus using the DNA and RNA probes and the TSA system in an *in vitro* infection model for HIV-1 latency [69]. Resting $CD4^+$T-cells were cultured in the presence and absence or syngeneic monocytes, with all culture media being supplemented with IL-2 (2 U/mL). Following 24 h of culture, $CD4^+$ T-cells alone and $CD4^+$T-cells-monocytes co-cultures were infected with NL (AD8)-nef/eGFP at an MOI of 0.5 for 2 h (Fig. 2.3A). These cells were then collected and processed to generate FFPE blocks. We did not observe $vDNA^+$ nor $vRNA^+$ cells in $CD4^+$T-cells alone or $CD4^+$T-cells-monocytes co-cultures 2 h following infection (Fig. 2.3B i and ii). At day 5 post-infection, the GFP $^+$ cells contained both vRNA (green) and/or vDNA (red) $^+$ cells consistent with productively infected cells (Fig. 2.4B, iii). In contrast, GFP- cells contained few $vRNA^+$ cells and the majority of cells contained integrated $vDNA^+$, suggesting that these cells were latently infected (Fig. 2.3B, iv). Finally, 3 days following activation of GFP- cells, ie at day 8, we observed an increase in $vRNA^+$ (green) and/or vDNA $^+$ cells, (red) (Fig. 2.3B, v), consistent with inducible latent infection.

To address the efficiency of viral detection using our mIHC approach, we quantified the proportion of productive, latent and inducible infection in our *in vitro* model of latency (Fig. 2.3C). In productive infection, we found similar levels of $vDNA^+$ and $vRNA^+$ cells. In latent infection, we detected a higher frequency of $vDNA^+$ cells

compared to vRNA$^+$ cells. After activating these latent cells (inducible infection), we observed an increase in vRNA$^+$ cells, with roughly equivalent levels of vDNA$^+$ cells when we compared cultures pre- and post-stimulation (Fig. 2.3C). Finally, we examined the ratio of vRNA$^+$ to vDNA$^+$ cells and observed a significant decrease in the ratio of vRNA$^+$ to vDNA$^+$ cells in latent cells compared to productive and inducible infection (Fig. 2.3D). Together these findings are consistent with the establishment of latency in this *in vitro* cell model, and that following stimulation, expression of viral RNA was induced using DNAscope and RNAscope.

Visualization of vDNA and vRNA in LN tissue from PLWH on ART

We next evaluated FFPE LN tissue from PLWH on ART using RNAscope and DNAscope and the TSA detection system. We observed vRNA$^+$ cells in LN tissue (Fig.2.4A, white arrows) located in the B cell follicles, as previously described [297,570,571]. Using DNAscope in combination with the TSA system, we detected punctuate signals within the nuclei (Fig. 2.4B, white arrows) indicative of HIV-1 provirus. We detected both productively infected cells, i.e vDNA$^+$ and vRNA$^+$ cells (Fig. 2.4C, ii, arrow 1) as well as latently infected cells, i.e vDNA$^+$ cells only (Fig. 2.4C, ii, second arrow). Finally, we quantified the frequency of productive and latent cells in LN tissue from PLWH on and off ART. Both vDNA$^+$ and vRNA$^+$ cells were detected in all samples, with less frequent vDNA$^+$ and vRNA$^+$ cells on ART compared to those off ART (Fig. 2.4D). In addition, the vRNA$^+$ to vDNA$^+$ ratio was lower on ART compared to off ART. Together, this suggests that the frequency of HIV-1 RNA is less than the frequency of HIV-1 DNA in PLWH on ART.

Co-expression of cell markers in productive and latently infected cells

To identify if IC markers such as PD-1 and CTLA-4 were co-located with latent or productively infected cells, we performed a multiplex assay with TSA, combining ISH and IHC to examine FFPE LN tissue from PLWH on and off ART. Slides were stained first for RNA and DNA, followed by antibodies to CD4, FoxP-3, PD-1 and CTLA-4 with imaging on the Vectra multispectral IHC imaging platform (Fig.2.5). We were able to demonstrate latent infection ($vDNA^+$ and vRNA- cells) co-expressing the cellular markers CD4, CTLA-4 and PD-1 (Fig. 2.5, arrow 1) and a productively infected cell ($vDNA^+$ and $vRNA^+$ cells) co-expressing CD4, PD-1 and CTLA-4 (Fig. 2.5, arrow 2).

Altogether, we successfully combined RNAscope/DNAscope approaches with numerous cellular markers and demonstrated the capacity to perform detailed quantitative immunophenotypic analysis of cellular reservoirs in HIV-1 infected treated patients. This approach is a sensitive tool to assess phenotype, activation, latency, and location in lymphoid tissues.

Discussion

Despite the extensive use of flow cytometry (FACS) for characterizing immune subsets, FACS does not reveal the spatial location of these cells or the cellular immune neighborhood, which are potentially essential indicators for understanding where and how HIV-1 can persist on ART. Advances in multiparameter imaging for nucleic acid and proteins are rapidly changing the field of pathology, enabling a more detailed description of the anatomic and cellular sites of HIV-1 persistence on ART. The development of RNAscope and DNAscope has allowed the detection of vDNA and $vRNA^{+}$ cells in FFPE tissue, discriminating between $vDNA^{+}$ cells that are transcriptionally silent ($vRNA^{-}$) and cells that are actively transcribing viral RNA ($vRNA^{+}$) [297]. In combination with IHC, co-expression of vDNA is seen in immune subsets in histological sites [297,309].

Despite the advances in combining ISH with IHC, to our knowledge this is the first demonstration of >5-plex mIHC with detection of HIV-1 DNA and RNA in FFPE tissue. To achieve this, we have modified the already established RNAscope and DNAscope approaches by incorporating the TSA system from Perkin Elmer and extended with TSA based mIHC. The previous studies of HIV-1 combining ISH and IHC have used TSA with fluorescence antibodies and chromogenic staining [297,309,567]. The combination of high sensitivity of TSA based fluorescence detection and dilute protease step allows the detection of the attenuated immunohistochemical signal seen with combination of ISH and IHC [566]. The additional intracellular marker FoxP3 and surface markers has been used to identify Treg with greater specificity than that used in the previous studies where the number of phenotyping markers was limited [309].

We first demonstrated that these technologies can be applied to *in vitro* cell models of HIV-1 latency. We first optimized this approach using latently infected cell lines and primary cells. Using this approach, we detected multiple copies of HIV-1 DNA in each cell. One potential explanation for this is that the probes are targeting a small portion of the HIV-1 genome, and as a result, a few double Z-probe pairs bound to the same integrated HIV-1 genome can be detected. This was recently also observed in a study in which two copies of $vDNA^+$ signal were found in a J-Lat 10.6 cell [572]. In LN tissue from PLWH, both vRNA and $vDNA^+$ cells were detected, however, there was a lower ratio of vRNA: vDNA in individuals on ART compared to off ART. This is consistent with studies showing that RNA^+ cells are substantially reduced by ART (29–31).

LIMITATIONS

The presence of $vRNA^+$ cells does not distinguish between cells with intact and defective proviruses. As a result, the reservoir size of intact virus could be overestimated in LNs in PLWH on ART using this approach. At the time of this study, this method was restricted to simultaneously detect up to seven markers. Therefore, we were restricted from incorporating additional markers for further characterization of the reservoir. Confocal imaging platforms require a longer time to acquire whole slide images (reviewed in [576]). However on the other hand, Vectra imaging platform circumvents this issue, but this is done by utilizing a lower resolution for scanning whole slide images and does not support high resolution imaging of whole slides. In addition, manual staining was used for this method, which increases the chances of staining errors as this method is laborious.

CONCLUSION

Using the TSA fluorescent 7-plex platform consisting of probes for HIV-1 DNA and HIV-1 RNA and antibodies to CD4, FoxP3, CTLA-4, PD-1 and DAPI in one single tissue, we developed a technique to further characterize cells that are either latently or productively infected. Combining ISH and IHC can offer new insights into HIV-1 persistence on ART in tissue. Furthermore, this technique can be applied to a wide range of viruses and pathological studies. An automative staining system such as the Leica Bond RX™ [577], which diminishes the possibility of staining errors and variation, could be adapted for this study. Future studies could include additional panels of markers to allow for further characterization of tissue which could potentially provide more insight into the HIV reservoir in tissue (Vectra® Polaris™ Imaging System).

Acknowledgements

We acknowledge the participants who donated their LNs for this study, Dr. Mauricio González-Navarro and Dr. Fernanda Torres-Ruiz for performing the LN biopsies (Centro de Investigación en Enfermdades Infecciosas, Mexico City, Mexico). We thank Caroline Tumpach and Michael Roche for providing us with cells (RMIT, Melbourne Australia and Peter Doherty Institute, Melbourne Australia), Dr. Andreas Behren (Olivia Newton John Cancer Institute) for using his lab and imaging facility, Metta Jana, Rejhan Idriza and Cameron Skinner for the analysis and imaging facility (Petermac, Melbourne, Australia), Dr. Byron Martina for proof-reading (Erasmus MC, Rotterdam, The Netherlands), T. Luka, C. Li for flow cytometric cell sorting (University of Melbourne Flow Cytometry Facility, Melbourne, Australia).

Author contributions

ZR PC and SL designed the study and the experimental plan, ZR conducted experiments, imaging and data analysis. PR GR MG and ST, CT, MW collected and processed the patient tissue. RP performed experiments on in vitro infected primary T cells, CD, JE, CT and MW provided support with imaging and quantitation. PC SL and VE provided intellectual input during the analysis. ZR drafted the manuscript with input from PC, SL and CD. All authors reviewed and provided input for the final manuscript.

Figure legends

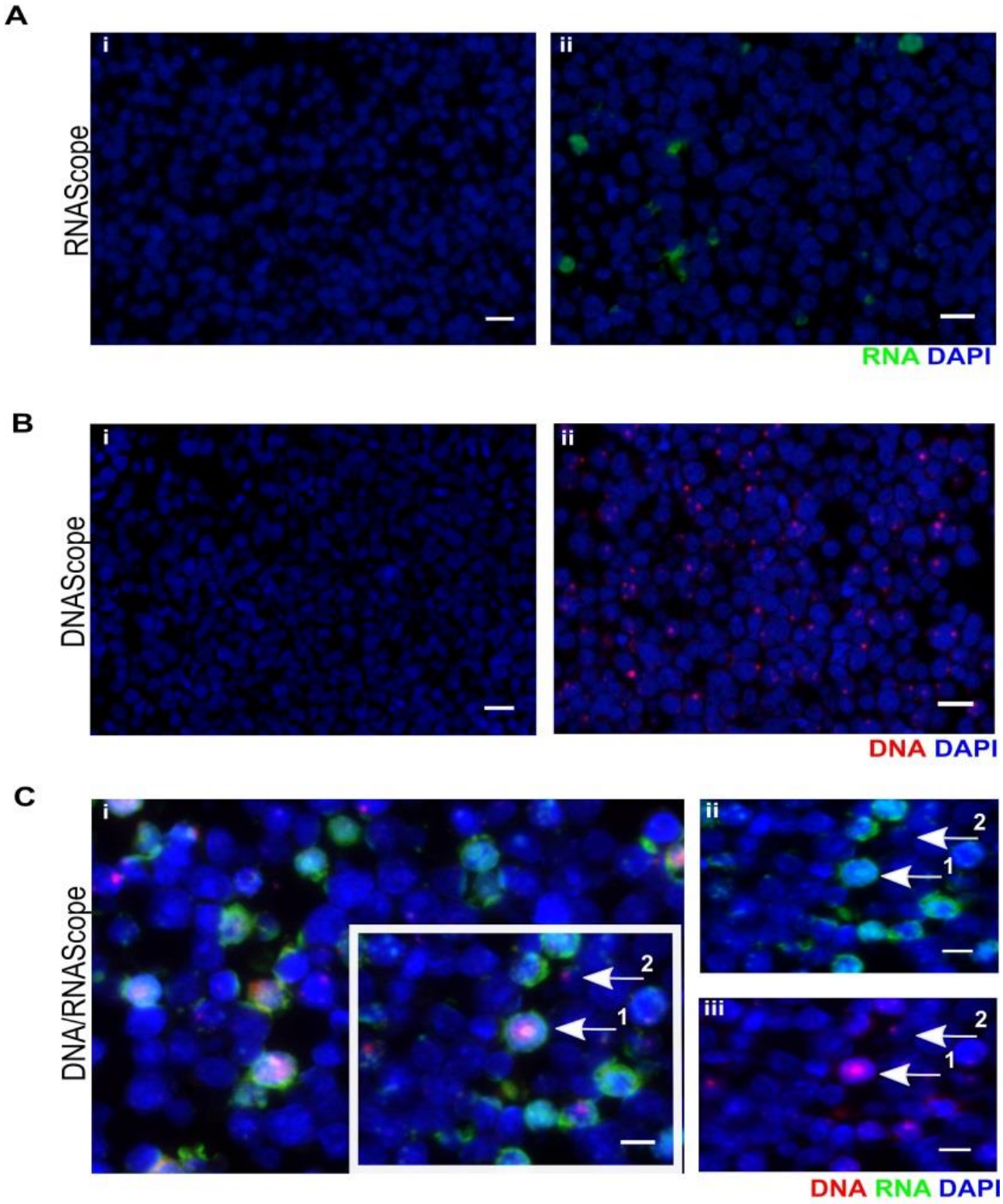

Figure 2.1. Assessment of HIV-1 RNA and DNA probes in ACH-2 cells using immunofluorescence detection. ACH2 cells were diluted 1:10 with uninfected Jurkat cells and hybridised with either (A) RNA (green) or (B) DNA (red) probes. The left

panels contain no target probe controls. (C) (i) Unmixed composite image of both RNA and DNA probes showing simultaneous detection of vRNA and $vDNA^+$ in a cell, consistent with a productively infected cell (white arrow 1) and a $vDNA^+$ cell, consistent with a latently infected cell (white arrow 2) (ii) vRNA probe only indicated in green and (iii) vDNA probe only indicated in red. All specimens were counterstained with DAPI nuclear staining in blue and all micrographs were taken at 40X magnification on the Vectra ®. Scale bars are 20μm.

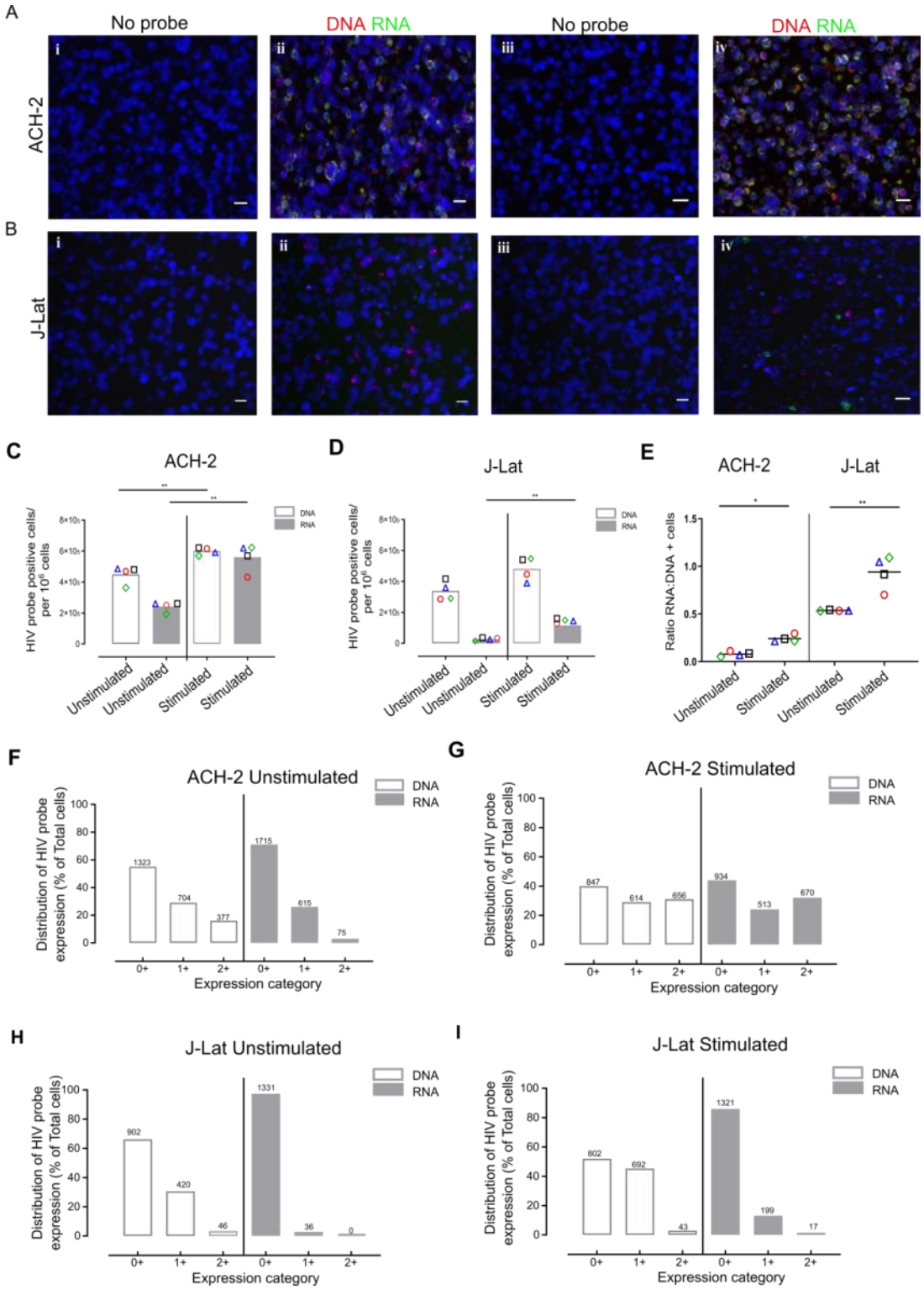

Figure 2.2. Sensitivity of HIV-1 DNA and RNA probes in unstimulated and stimulated ACH-2 cells and J-Lat cells. Representative image of **(**A) ACH2 and (B) J-Lat cells that were (i) unstimulated and stained with no probe control (ii) unstimulated and

hybridized with HIV-1 DNA and RNA probes (iii) stimulated with PMA and stained with no probe control and (iv) stimulated with PMA and hybridized with HIV-1 DNA and RNA probes. DAPI was used for nuclear counterstain and all micrographs were taken at 20X magnification on the Vectra®. Scale bars are 20 µm. Proportion of $vDNA^+$ and $vRNA^+$ cells in unstimulated and stimulated (C) ACH-2 and (D) J-Lat cells. (E) Ratio of $vDNA^+$ and $vRNA^+$ cells in unstimulated and stimulated ACH-2 and J-Lat cells. (C-E). Each color represents a region of interest. Columns represent the mean of four regions. Proportion of cells that express different frequencies of vRNA and vDNA based on the ACD scoring system of grade 0 to 2 defined as the number of RNA and DNA copies for (F) unstimulated ACH-2; (G) stimulated ACH2; (H) unstimulated J-Lats; and (I) stimulated J-Lats. Columns represent the mean of three regions of interest and the numbers above each column represents the mean value. Comparisons between conditions were performed with a t-test. * $P < 0.05$; ** $P < 0.01$.

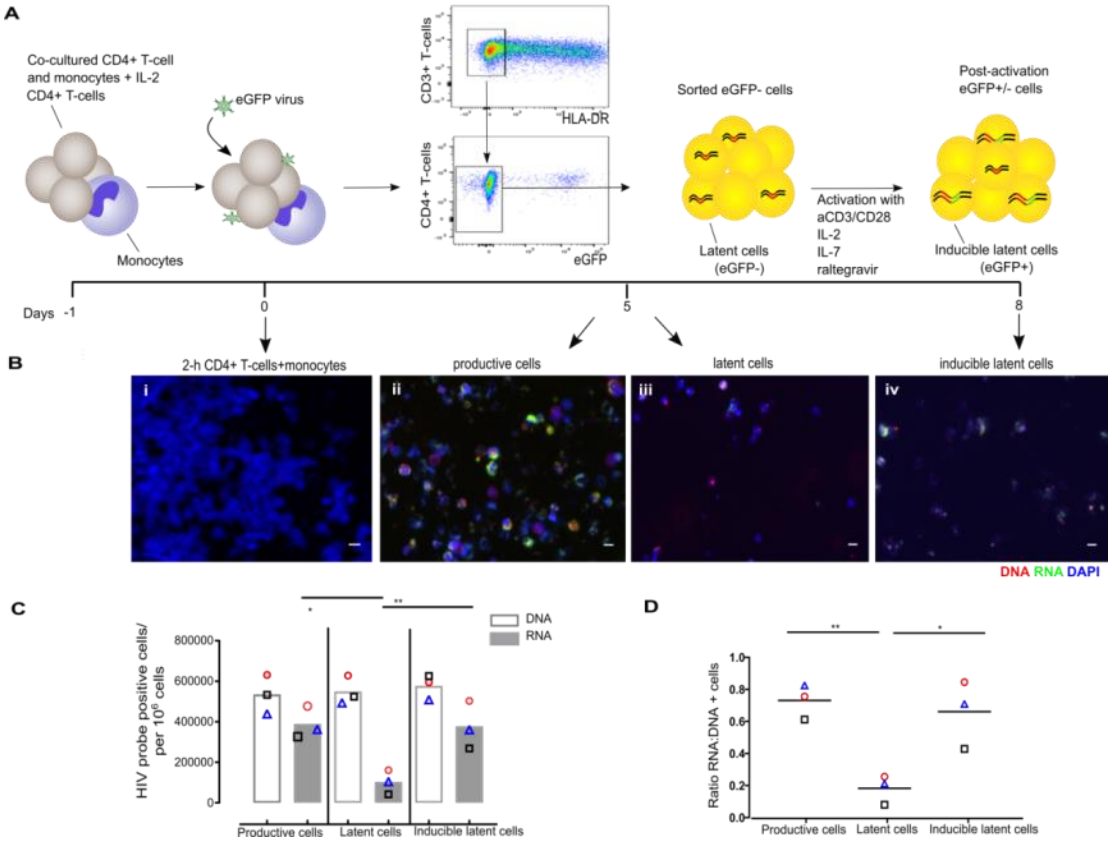

Figure 2.3. HIV-1 DNA and RNA probes to detect latent and productive infection in an *in vitro* latency model. (A) Schematic diagram of experimental approach. Resting $CD4^+$ T cells (orange) were cultured with monocytes (grey) for 24 hours and infected with NL(AD8)-□nef/GFP virus (green) at an MOI of 0.5 for 2 hours. Non-productively infected (GFP-) cells were sorted at day 5 post infection and the number of productively infected (GFP^+) cells was determined by flow cytometry. Sorted GFP- cells were stimulated with anti-$CD3/CD28^+$$IL\text{-}7^+$$IL\text{-}2^+$raltegravir for 3 days to induce expression of virus from latently infected cells. Cells were harvested at 2 hours, day 5 and 8 and formalin-fixed and paraffin-embedded (FFPE), sectioned and stained for vRNA and vDNA as indicated by black arrows. (B) Representative image of vDNA (red) and vRNA (green) showing (i) T-cells alone; (ii) T-cells and monocytes; (iii) $eGFP^+$ T-cells and monocytes; (iv) eGFP- T-cells; and (v) activated eGFP- T-cells. (C) Mean number of $vDNA^+$ (open column) and $vRNA^+$ (grey column) cells when analysing GFP^+ (productive), GFP- (latent) and inducible GFP^+ cells. (D) Mean ratio of $vRNA^+$ and DNA^+ cells in the same cell populations. DAPI was used for nuclear counterstain and all micrographs were taken at 20X magnification on the Vectra. The lower limit of detection of each assay is represented by a dotted line. Columns represent the mean of sections per slide. Each coloured symbol in panels C and D represents a region of interest. Scale bars are 20 µm. T-test; mean; * P <0.05; ** P <0.01.

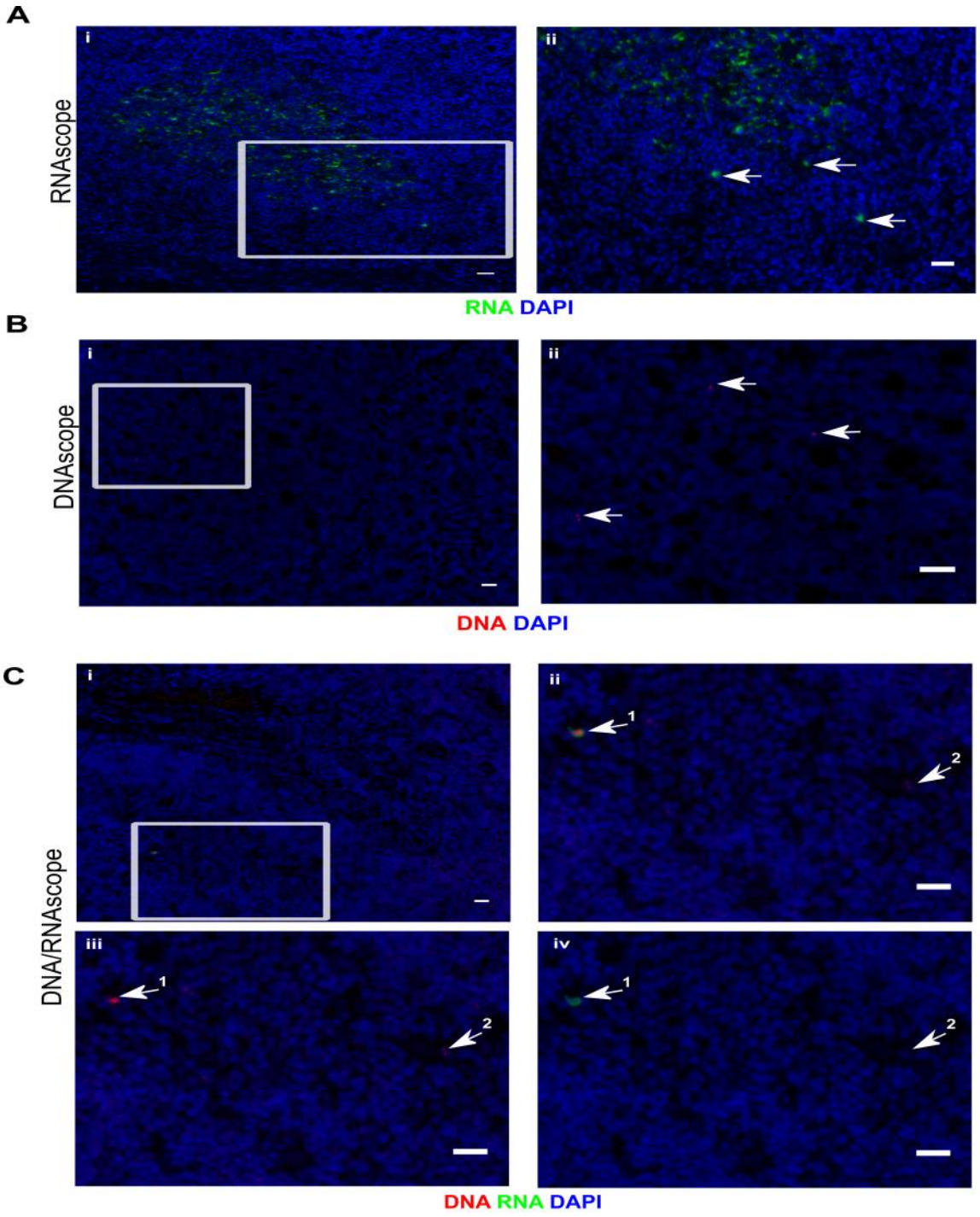
A
RNAscope
i
ii
RNA DAPI
B
DNAscope
i
ii
DNA DAPI
C
DNA/RNAscope
i
ii
iii
iv
1
2
DNA RNA DAPI
D
HIV probe positive cells/ per 10^6 cells
1×10^6
1×10^5
1×10^4
1×10^3
1×10^2
DNA
RNA
patient 1
patient 2
patient 3
patient 4
Off ART
On ART
DNA/RNA Ratio
0.7
0.5
0.1
0.2

Figure 2.4. HIV-1 RNA and DNA probes to detect HIV-1 persistence in LNs from PLWH. Representative image of LN tissue from a person living with HIV-1 off ART using (i) low and (ii) high magnification with (A) HIV-1 RNA probes demonstrating vRNA (green) in the BCF region (white arrows); (B) HIV-1 DNA probes demonstrating vDNA (red) as a punctate mark (white arrows); and (C) both HIV-1 RNA and DNA probes showing vRNA (green), vDNA (red) and DAPI (blue) with the magnified image indicating simultaneous detection of both vDNA and $vRNA^+$ cells (arrow 1) and single detection of $vDNA^+$ cells (arrow 2). Additional panels show an unmixed composite image for (iii) $vDNA^+$ cells and (iv) $vRNA^+$ cells. (D) The number of $vRNA^+$ and $vDNA^+$ cells in LN tissue from 4 HIV-1-infected participants (2 on ART and 2 off ART), with the mean number from four sections shown as a column. The ratio of vRNA and $vDNA^+$ cells is shown as a number. Each symbol represents a region of interest. All specimens were subjected to DAPI nuclear staining, shown in blue and all micrographs were taken at 20X magnification on Vectra® multispectral IHC imaging platform. Scale bars are 10 μm.

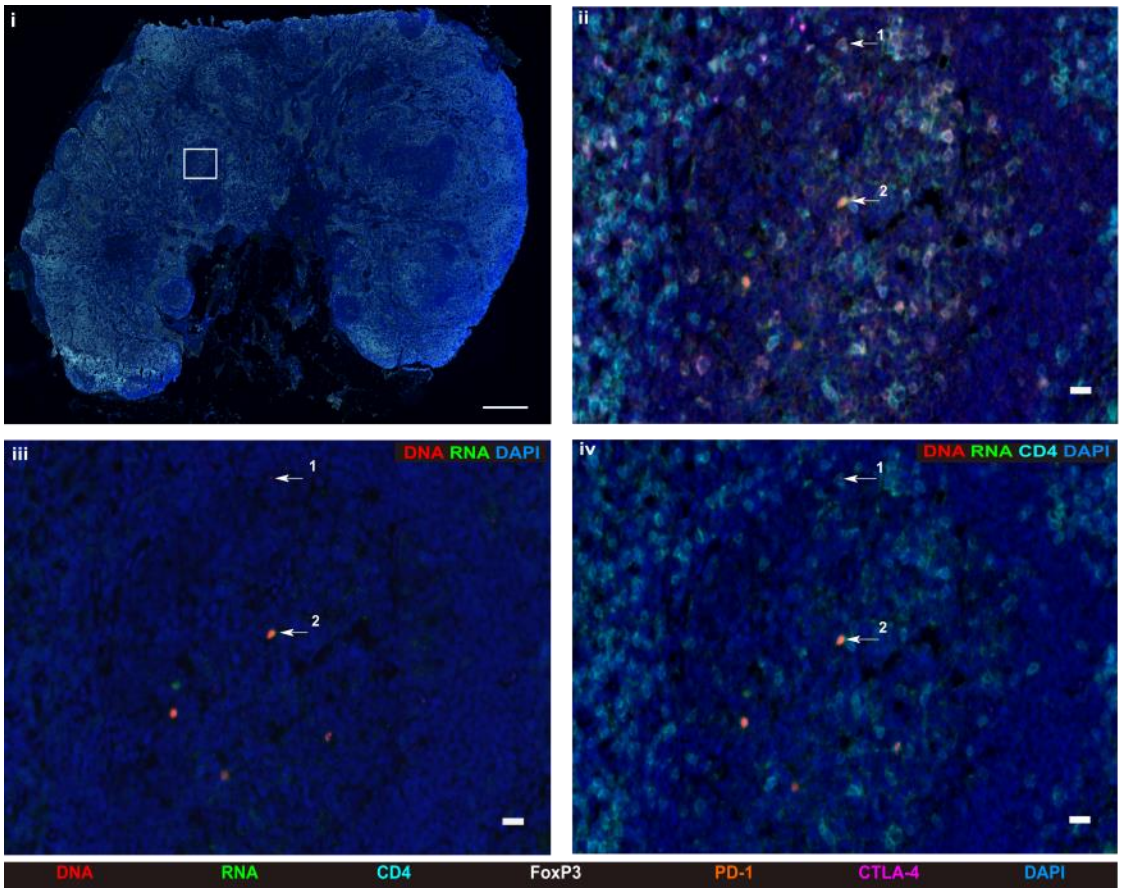

Figure 2.5. Multiplex detection with HIV-1 RNA and DNA probes and surface markers in LN tissue from PLWH. Representative images of LN tissue sections from a person living with HIV-1 off ART depicting simultaneous detection of HIV-1 DNA (red) and RNAscope (green) in combination with antibodies to CD4 (cyan), FoxP3 (white), CTLA-4 (magenta) and PD-1 (orange). (i) Whole slide scan and (ii) composite image (enlarged section of whole slide scan, white box) depicting colocalization of $vDNA^+$ cell (arrow 1) with $CD4^+$ T cells, PD-1 and CTLA-4 and $vDNA^+$ and $vRNA^+$ cell (arrow 2) with $CD4^+$ T cells, PD-1 and CTLA-4. Representative unmixed composite images of (iii) HIV-1 DNA and RNA and (iv) HIV-1 DNA, RNA and $CD4^+$ T-cells. DAPI was used for nuclear counterstain and micrographs were taken at 10X (whole slide scan) and 20 X magnifications using the Vectra™ multispectral imaging software. Scale bars are 500 µm (whole slide scan) and 20 µm.

Supplementary Figures

Supplementary Table S2.1. Site of Biopsy. Clinical characteristics of LNs from PLWH on and off ART

Patient	Classification	Type of biopsy	Gender	Age	Months on ART	$CD4^+$ T cells (cells/ μl)	$CD8^+$ T cells (cells/ μl)	viral load (copies/ml)
1	Off ART	Inguinal	M	37	-	391	1158	1,781,250
2	Off ART	Cervical	M	33	-	368	1776	6,326,452
3	On ART	Inguinal	M	54	58	336	1467	98
4	On ART	Cervical	M	32	27	355	653	<40

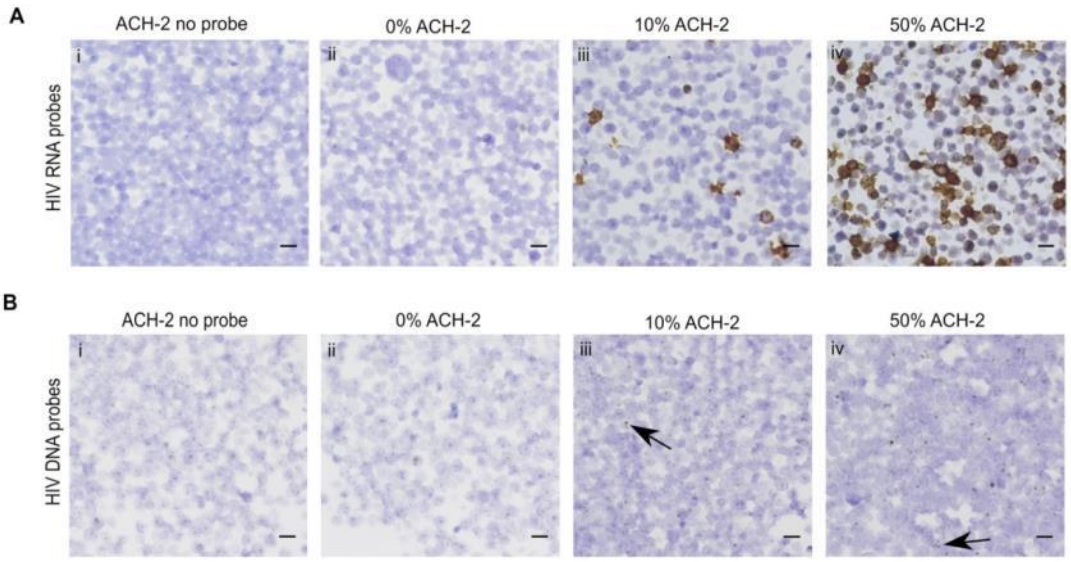

Supplementary Figure S2.1. Assessment of HIV-1 RNA and DNA probes in ACH-2 cells with chromogen diaminobenzidine (DAB). (A) Representative bright field microscope image showing ACH-2 cells in varying ratios with uninfected Jurkat cells labelled with either (A) HIV-1 RNA or (B) HIV-1 DNA probes. Negative controls included (i) no probe using either ACH-2 cells diluted 1:1 with Jurkat cells or (ii) Jurkat cells alone. Positive controls included ACH-2 cells diluted either (iii) 1:10 or (iv) 1:1 with Jurkat cells. Positive signals are brown and diffuse for RNA and punctate for DNA (black arrow). Nuclei were counterstained with hematoxylin. Original magnification 40x using bright field microscopy. Scale bars are 20μm.

Chapter 3: CTLA-4 and PD-1 are expressed on infected T-cells including Tregs in lymph node tissue from people living with HIV-1 on suppressive antiviral therapy

3.1 INTRODUCTION

Identifying which cellular subsets that preferentially harbour HIV-1 in individuals on suppressive ART is important for understanding the mechanisms of HIV-1 persistence and for developing strategies for its elimination. Memory $CD4^+$ T-cell subsets in blood and tissue, can be characterized by the presence of immune checkpoints (ICs) such as, lymphocyte activation gene 3 (LAG-3), T-cell immunoglobulin ITIM domain (TIGIT), programme death receptor-1 (PD-1) and cytotoxic T lymphocyte antigen-4 (CTLA-4). In people living with HIV-1 (PLWH) on ART, we and others have shown that $CD4^+$ T-cells that express ICs are enriched for latent HIV-1 [156]. Our lab has assessed the effects of anti-PD-1 in resting $CD4^+$ T-cells *in vitro* and showed that blocking PD-1 inhibits the establishment of HIV-1 latency [555]. In addition, we and others have shown that blockade of the ICs, PD-1 and CTLA-4 either alone or in combination have the capacity to reverse HIV-1 latency [578]. Using an *in vitro* model of HIV-1 latency, we recently showed that combining antibodies to PD-1 and CTLA-4, in combination with a second stimulus reversed latency and this was comparable in potency to the latency reversal agent (LRA)

bryostatin and more potent than the LRAs JQ1 (a bromodomain inhibitor) and histone deacetylase inhibitor (HDACi) romidepsin [578].

Studies examining the effects of anti-CTLA4 in PLWH on ART are less common but in one case report, latency reversal activity was associated with increased levels in cell-associated unspliced (CA-US) HIV-1 RNA [539]. In addition, a follow up study in our lab showed the same effect on the HIV-1 reservoir but instead using anti-PD-1, which also resulted in a significant increase in CA-US HIV-1 RNA [555], however, these results could not be repeated in other studies using anti-PD-1 or anti-PDL-1 [544]. Dual blockade of PD-1 and CTLA-4 was shown to have a significant effect in reducing the size of the SIV reservoir in lymph nodes (LNs) from ART treated macaques than either PD-1 and CTLA-4 alone [533]. More recently, it was found that in PLWH on ART with cancer, combined blockade of CTLA-4 and PD-1 modestly reversed HIV-1 latency (n=7), whereas anti-PD-1 alone did not activate HIV-1 from latency (n=33) [579].

There are multiple new approaches to quantify HIV-1 persistence in tissue compartments from PLWH. One such approach is a highly sensitive *in situ* hybridization (ISH) assay to detect viral RNA or DNA (termed RNAscope and DNAscope respectively) using formalin-fixed paraffin embedded (FFPE) LN tissue from SIV-infected non-human primate (NHP) before and following suppressive ART [297]. In LN tissue, $CD4^+$ C-X-C Motif Chemokine Receptor 5 ($CXCR5^+$) $PD\text{-}1^+$ T-cells, residing in the B-cell follicle (BCF) region, a subset of follicular helper T-cells (Tfh), have been shown to contribute to viral persistence [131]. In PLWH on ART, LN tissue $PD\text{-}1^+$ Tfh cells have been reported to produce greater levels of infectious HIV-1 and have more virus transcription compared to $CD4^+$ $CXCR5^+PD\text{-}1^-$ Tfh cells

and $CD4^+CXCR5^-$ $PD\text{-}1^-$ cells in blood [131]. In addition, a recent study of NHP infected with SIV on suppressive ART, demonstrated that $CTLA\text{-}4^+$ $PD\text{-}1^-$ cells were enriched with SIV and these cells were found outside the BCF [155]. Taken together, these data suggest that $PD\text{-}1^+$ and $CTLA\text{-}4^+$ cells harbor HIV-1 but reside in different regions of LN tissue.

Given that regulatory T-cells (Tregs) express high levels of CTLA-4, our main question here was to determine if Tregs are also a reservoir of HIV-1 in LN tissue from PLWH on ART and whether findings in relation to $CTLA\text{-}4^+$ cells and SIV persistence in NHPs were similar in human studies. Prior studies of PLWH on ART, have shown that in blood, HIV-1 was significantly higher in Tregs compared to nonTregs [434,437,580]. Unlike other T-cell subsets, Tregs represent a small population of T-cells (varying from 0.2 to 7%) [581–583] and are not always sampled in sufficiently high numbers to allow for certain clinical applications such as cell sorting. Therefore, a method such as IHC was utilized here to study this rare population.

We hypothesized that HIV-1 is enriched in cells expressing PD-1 and CTLA-4 and that in LN tissue from PLWH on ART, Tregs bordering the T-cell zone (TCZ) and the BCF are enriched for HIV-1. We quantified virus in $FoxP3^+$ $CXCR5^+$ Tregs, also known as T-follicular regulatory (Tfr) cells [584]. We used an already established multiplex method (Chapter 2) which combines detection of viral RNA and DNA using ISH RNA/DNAscope in combination with immunohistochemistry (IHC). This allowed for assessment of co-expression of surface markers $CTLA\text{-}4^+PD\text{-}1^+FoxP3^+$ to identify Tregs. We aimed to distinguish between cells based on either IC expression or Treg phenotype. We found that the frequency of HIV-1 infection was

higher in Tregs compared to nonTregs, however, the overall contribution of infected Tregs to the overall reservoir size remains small. Although the difference of HIV-1 between IC^+ and IC^- expressing cells was minimal on ART, virus was detected in CTLA-4^+ Tregs and these cells were distributed between the BCF and the TCZ cells in PLWH on ART. Future studies that aim to eradicate HIV-1 will need to address the persistence of the virus in LN anatomical sites such as the BCF and the TCZ.

3.2 MATERIAL AND METHODS

3.2.1 HUMAN SUBJECTS

LNs were obtained from a cohort of PLWH, as pointed out in chapter 2. Seven participants underwent elective surgical resection of LN, either inguinal or cervical. All participants were PLWH and were either naïve to ART (n=4; with HIV-1 RNA >30,739 copies/ml) or on suppressive ART (n=3; defined as HIV-1 RNA <98 copies/ml for at least 2 years). LNs were collected at the Centro de Investigacion en Enfermedades Infecciosas (CIENI-IN ER), Mexico City, Mexico and the study was approved by the local human and research ethics committee (B03-16). Clinical details are provided in Table 3.1.

Table 3.1. Site of Biopsy

Patient	Classification	Type of biopsy	Gender	Age	Months on ART	$CD4^+$ T cells (cells/µl)	$CD8^+$ T cells (cells/µl)	viral load (copies/ml)
1	Off ART	Inguinal	M	37	-	391	1158	1,781,250
2	Off ART	Cervical	M	33	-	368	1776	6,326,452
3	Off ART	Cervical	M	35	-	491	2284	30,739
4	Off ART	Cervical	M	24	-	316	1772	643,922
5	On ART	Cervical	M	32	24	1104	775	<40
6	On ART	Cervical	M	32	27	355	651	<40
7	On ART	Inguinal	M	54	58	336	1467	98

3.2.2 HISTOLOGY AND IMMUNOHISTOCHEMISTRY

Immunohistochemistry was performed on FFPE LN tissue using a peroxidase-based method on 5 μm sections on Superfrost® plus microscope slides (Thermo Scientific). Specimen slides were incubated at 60 °C for 45-60 minutes for the melting and fixing of specimens onto microscope slides. To deparaffinise, slides were washed in xylene and rehydrated in ethanol of 100% to 70%. Slides were then treated with hydrogen peroxidase (Chem-Supply, Gillman, Australia) in 0.3% H_2O_2 (v/v) in double-distilled H_2O (ddH_2O) for 15 minutes at room temperature. Heat induced epitope retrieval was then performed until boiling was achieved, followed

with 90°C for 15 minutes by microwave treatment (MWT) in the appropriate retrieval buffer optimised for each target epitope. Specimens were then blocked using Background Sniper (Biocare Medical, Concord, CA) for 15 minutes prior to primary antibody application.

3.2.3 HIV RNA AND DNA TARGET PROBES

The HIV-1 RNA probes used were designed to hybridize to viral RNA in gag, pol, vif, vpr, tat, rev, env, nef, and vpx genes (vRNA anti-sense probe, ACD catalog: ADV416111) as well as HIV-1 DNA probe targeting the Gag-Pol coding region (vDNA sense probe, ACD catalog: ADV425531). All probes were purchased from Advances Cell Diagnostics (ACD Newark, CA) and a complete list of the sequence of each probe used has been previously published [297].

3.2.4 HIV RNA AND DNA *IN SITU* HYBRIDIZATION

For the detection of vRNA and vDNA, we used the RNAscope 2.5 brown kit[297], with some modifications [297]. In brief, probes were visualized by hybridizing with preamplifiers, amplifiers in a humidified HybEZ oven, and finally, fluorescent label with TSA amplification system (Perkin Elmer, Waltham, Massachusetts). Pre-amplifier 1 was hybridized at 40 °C for 30 min. Following washing of samples twice, then hybridized with Amplifier two in a humidified at 40 °C for 15 min. Again, following two washes, amplifier three was hybridized at 40 °C for 30 min. After a further two washes, Amplifier four was hybridized at 40 °C for 15 min, washed twice, following hybridization of Amplifier five for 30 minutes at 40 °C, again with two washes and lastly incubation of Amplifier 6 for 15 minutes at 40 °C for 15 minutes with a final two washes.

For vRNA detection, slides were first washed once in Tris Buffered saline (TBS) with Tween (VWR International, Radnor, Pennsylvania) and incubated for 4 minutes with either 3,3'-diaminobenzidine (DAB) for 5-10 minutes or TSA dyes. TSA dye 520 (1:700) was used for 4 minutes for labelling of vRNA, TSA dye 570 (1:700) for two minutes for labelling of vDNA and washed twice in TBS-Tween for five minutes. Lastly, slides were incubated with either DAPI (Perkin Elmer) or counterstained with hematoxylin and eosin (H&E) for one-two minutes. Slides were incubated with DAPI (1:2) for four (human LN tissue). For the removal of DAPI, slides were washed twice with TBS-Tween for five minutes.

3.2.5 SIMULTANEOUS DETECTION OF VDNA AND VRNA

In order to visualize vDNA and $vRNA^+$ cell simultaneously, we combined both DNA and RNAscope (DNA/RNAscope). Following fixation and pretreatment as described for RNA and DNAscope[297], slides were incubated for two hours at 40 °C with RNA probes as described previously, following amplification, washes, labelling with TSA 520 (1:700) for four minutes and MWT retrieval. For vDNA, slides were hybridized with HIV-1 DNA sense probes overnight at 40 °C, followed by amplification, washes, labelling with TSA 570 (1:700) for two minutes and counterstained with DAPI.

3.2.6 MULTIPLEX IMMUNOHISTOCHEMISTRY (OPAL™)

Rabbit monoclonal antibodies to CD4 (Cell Marque, Rocklin, CA) clone 104R-1, 1/100, high pH retrieval), mouse monoclonal antibody to FoxP3 (Abcam, Cambridge, UK), clone IgG1, 1/1000, high pH retrieval), mouse polyclonal antibody to PD-1 (Abcam, IgG1 Nat105, 1/500, low pH retrieval), mouse monoclonal antibody to CTLA-4 (MyBiosource, San Diego, CA) IgG2a/k, 1/100, high pH retrieval) were used. Antibodies were diluted using a background-reducing antibody diluent buffer S3022 (Agilent, Santa Clara, CA). A horseradish hydrogen peroxidase (HRP) linked anti-mouse and anti-rabbit secondary antibody, EnvisionTM HRP (Agilent), was used for each primary antibody species according to the manufacturer's recommendation. Immunofluorescent signal was visualized using the TSA amplification system, OPAL™ 7-color fluorescent IHC kit (Perkin Elmer), TSA dyes 540, 620, 650, and 690 (1:50) for ten minutes, counterstained with Spectral DAPI. All slides were imaged on the Vectra® 3 Quantitative Pathology Imaging System (Perkin Elmer). Images were then examined using color separation on inForm® Software v2.1 (Perkin Elmer). All slides were scanned on the Vectra at 10x magnification using Phenochart (Perkin Elmer) in order to select for high-powered imaging at 20x (resolution of 0.5 μm per pixel).

3.2.7 QUANTITATIVE IMAGE ANALYSIS

HALO™ image analysis software from Indica Labs (versions 2.0, Albuquerque, New Mexico) was used for multispectral images prepared by inForm in LN sections (Fig.S3.1, i). The cell-based segmentation algorithm was used to

accurately segment nuclear DAPI counterstained cells (Fig.S3.1, ii). Once segmentation was verified, the HALO's Highplex Fluorescence algorithm was designed for each fluorescent probe using adjustable thresholding for positive signals [585]. Signals were determined by comparing the Opal single stains with the multiplex signal [586]. Negative control slides consisted of primary antibodies (excluding Opal), LN tissue from HIV-1 negative individuals and LN tissue from PLWH incubated with ACD negative control probes. Only cells above the positive threshold were scored. This approach allowed for the evaluation of cell phenotypes (DAPI, DNA, RNA, CD4, FoxP3, PD-1 and CTLA-4) and subsets (Tregs, nonTregs and nonCD4 expressing PD-$1^{+/-}$ and CTLA-$4^{+/-}$) (Fig.3.0, iii). Regions of interest (ROI) containing TCZs and BCFs were manually selected by drawing, and any tissue or staining artefacts were excluded. The same algorithm design was used for each ROI per slide based on staining intensity and adjusted for each patient to account for staining variability.

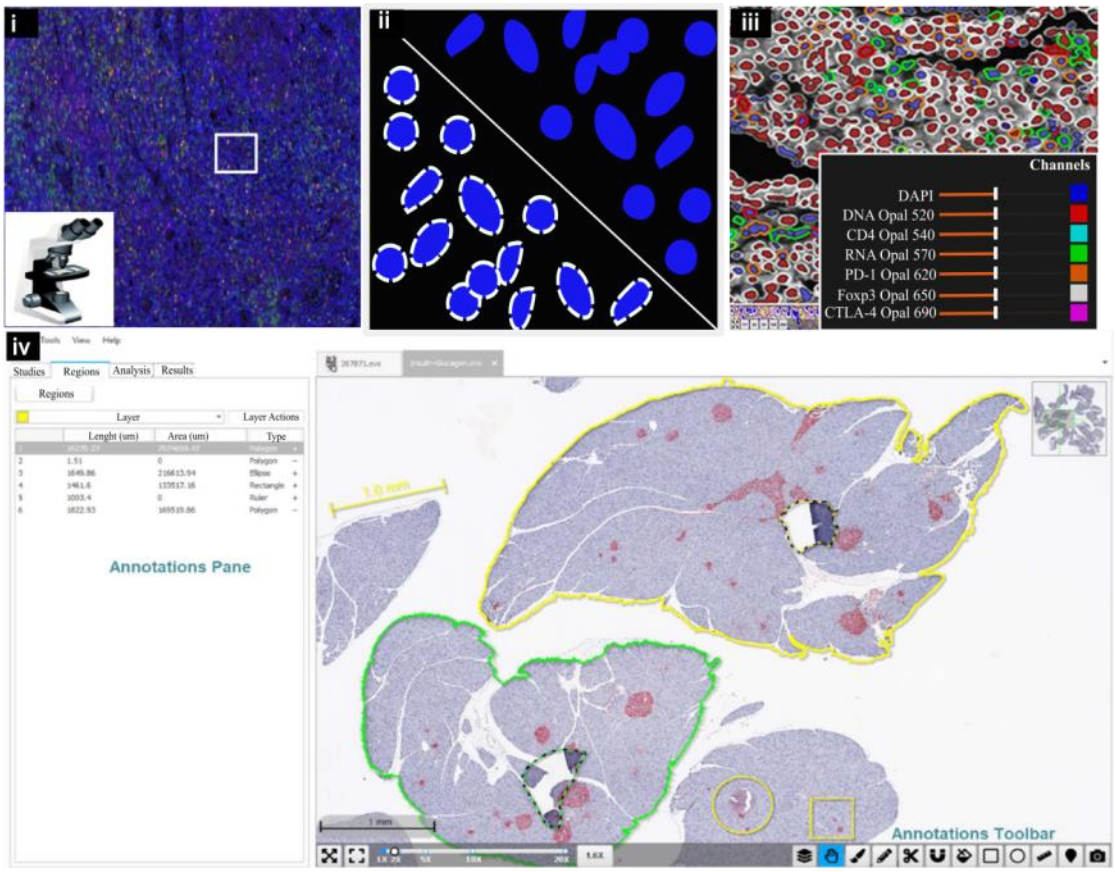

Figure 3.0 Workflow illustration of image analysis platform Indica Labs HALO™ software. i) Multiplex images are taken using Vectra 3.0™ multispectral

microscopy and prepared by inForm® cell analysis software to quantify expression of HIV-1 RNA, DNA, CD4, FoxP3, PD-1 and CTLA-4 in LN tissue. ii) Individual cells are defined by DAPI counter stain using the HALO cell segmentation option. Blue DAPI counter-stained cells surrounded by white doted lines represent segmented cells. iii) The HALO Highplex Fluorescence module allows for pixel based colocalisation analysis using adjustable thresholding. In the mark-up image, by manually adjusting the intensity threshold for each biomarker (iii, sub image on the right), cells positive for each biomarker becomes coloured. iv) Image example using the HALO's Highplex phenotyping algorithm, which allows users to select regions of interest (shown in the yellow and green layers), analysis of of positively scored cells and results. Inclusion areas are depicted as solid lines and exclusion areas depicted as dashed lines.

3.2.8 STATISTICAL ANALYSIS

Statistical analysis was performed, and graphs plotted using Graphpad Prism (version 8.2.1, GraphPad Software, La Jolla, CA). Given the small sample numbers, we assumed normality and used a Two-tailed paired t-test to determine difference in T-cell subsets. Details of significant differences between data groups have been described in each figure legend and *P* values less than 0.05 was considered significant.

3.3 RESULTS

3.3.1 MEASURING THE DISTRIBUTION OF IMMUNE CELLS IN LNS FROM PLWH PRIOR TO AND FOLLOWING ART USING IMAGING

Previous studies have examined HIV-1 persistence in PLWH on ART using a combination of ISH and mIHC in LN tissue [155,219,297]. Although these studies have provided evidence as to where HIV-1 persists during ART, prior studies were limited to a five-color panel of immunofluorescence in tissue. To address this, we examined LNs from PLWH prior to and following ART using a multiparameter analysis of HIV-1 RNA and DNA as described in Chapter 2 of this thesis. Histological sections from FFPE LN (either inguinal or cervical) were stained for HIV-1 RNA and DNA. Tregs were identified using previously described markers i.e., FoxP3. We examined expression of ICs given previous studies showing enrichment of HIV-1 in PLWH on ART in $CD4^+$ T-cells expressing PD-1 and CTLA-4 [199,309,459,555,578]. We defined productively infected cells as $vDNA^+vRNA^+$ and latently infected cell as $vDNA^+$ $vRNA^-$ cells.

We analysed both the paracortex region (the TCZ; defined by the yellow dotted lines) and the cortical region (the BCF; defined by the white dotted lines) for the distribution of immune cells (Fig. 3.1A). We then quantified total cells ($DAPI^+$ cells), double negative cells i.e., CD4neg ($CD4^-$ $FoxP3^-$), single positive cells, i.e., CD4pos ($CD4^+$ $FoxP3^-$), nonTregs ($CD4^+$ $FoxP3^-$) and Tregs ($CD4^+$ $FoxP3^+$). The total number of events were quantified within the BCF and the TCZ (Fig. 3.1B) in PLWH prior- to and during ART.

We observed a higher number of cells in the TCZ compared to the BCF (Fig.3.1B). The frequency of $CD4^+$ T-cells was higher in the TCZ compared to the BCF (i.e 43% vs 36%, respectively). The majority of the $CD4^+$ T-cell population were non-Tregs (Fig.3.1B). The frequency of the non-Tregs was higher in the TCZ compared to the BCF (i.e., 97% vs 94%, respectively; Fig.3.1B). We detected a small population of Tregs in these tissues. Tregs were located along the T-cell and B-cell (T:B) border with 3% in the BCF, with the majority located in the TCZ (6%) (Fig.3.1A&B).

We then looked at the distribution of productively and latently infected cells using RNA/DNAscope. Given the small numbers of participants, we are only able to describe trends and not apply any statistical tests. We found a similar frequency of

HIV-1 RNA$^+$ and/ or DNA$^+$ cells in the BCF and TCZ (Fig.3.1C) in participants both prior to and following ART. In addition, cells that were positive for HIV-1 were evenly distributed in both PLWH on and off ART (Fig.3.1D). Lastly, when we looked at the frequency of HIV-1$^+$ cells per million of total cells, there was a higher frequency of HIV-1 RNA$^+$ and/ or DNA$^+$ cells in the BCFs compared to the TCZ in four out of four PLWH prior-to ART and in two out of three in PLWH during ART (Fig. 3.1E & Suppl. Fig 3.1). Overall, in agreement with the literature [155,163], our results show that HIV-1-infected cells can be found distributed between the BCF and the TCZ, with the BCFs containing a higher frequency of infected cells per million total cells.

A

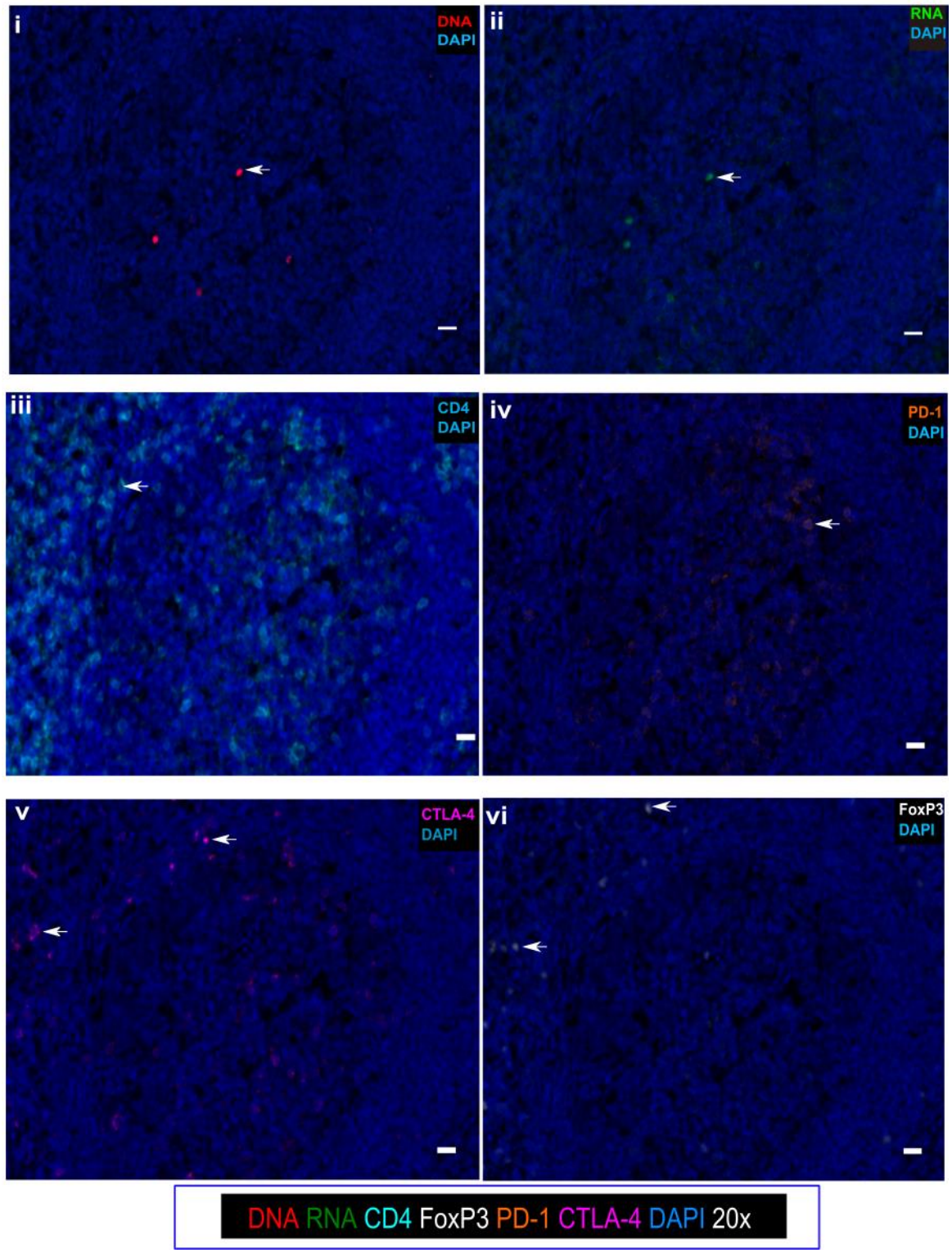
i
DNA
DAPI
ii
RNA
DAPI
iii
CD4
DAPI
iv
PD-1
DAPI
v
CTLA-4
DAPI
vi
FoxP3
DAPI
DNA RNA CD4 FoxP3 PD-1 CTLA-4 DAPI 20x

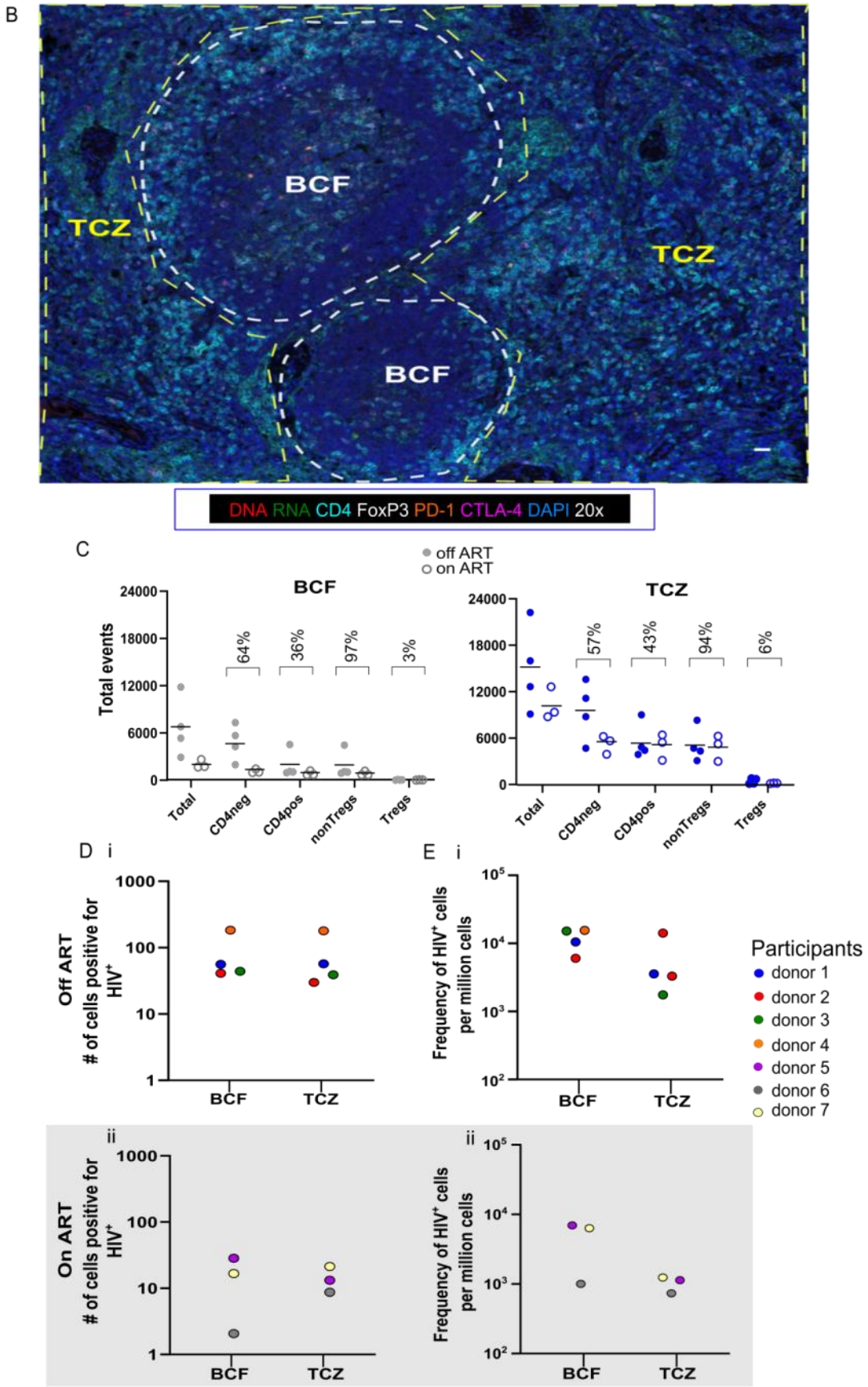
B
BCF
TCZ
TCZ
BCF
DNA RNA CD4 FoxP3 PD-1 CTLA-4 DAPI 20x
C
off ART
on ART
BCF
TCZ
Total events
24000
18000
12000
6000
0
64%
36%
97%
3%
57%
43%
94%
6%
Total
CD4neg
CD4pos
nonTregs
Tregs
D i
Off ART
# of cells positive for HIV+
1000
100
10
1
BCF
TCZ
ii
On ART
# of cells positive for HIV+
E i
Frequency of HIV+ cells per million cells
10^5
10^4
10^3
10^2
Participants
donor 1
donor 2
donor 3
donor 4
donor 5
donor 6
donor 7

Figure 3.1 Distribution of total and HIV-1-infected immune cells in the TCZ and BCF of LN tissues collected from PLWH prior to and following ART. FFPE sections of the LNs were prepared from a Mexican cohort of PLWH (3 on and 4 off ART). HIV-1 RNA^+ and/ or DNA^+ cells were visualized by mIHC (Method, Section 3.2.6). Quantification of the HIV-1 RNA^+ and/ or DNA^+ cells was carried out using RNA/DNAscope and imaging on the HALO analysis software (Method, Section 3.2.7). DAPI was used for nuclear counterstain of the cells in each zone, and micrographs were taken at 20x magnification using the Vectra™ multispectral imaging software (Method, Section 3.2.6). For each donor, four regions of interest (ROIs) were taken. A) Representative unmixed composite image of a LN section from a participant off ART, depicting single detection of (i) HIV-1 DNA (red) and (ii) RNAs (green), (iii) CD4 (cyan), (iv) FoxP3 (white), (v) PD-1 (orange) and (vi) CTLA-4 (magenta). DAPI was used for nuclear counterstain and all micrographs were taken at 20X magnification using the Vectra™ multispectral imaging software. Scale =10 μm. B) Representative multiplex image of LN tissue of a participant off ART depicting simultaneous detection of HIV-1 DNA and RNA in combination with antibodies for CD4, Treg marker FoxP3, and ICs CTLA-4 and PD-1 distributed between the TCZs (yellow dotted lines) and the BCFs (white dotted lines). C) Images were analysed with HALO to quantify the total events (number) of HIV-1 RNA^+ and/ or DNA^+ positive cells and denoted as total cells ($DAPI^+$), CD4neg ($CD4^-$ $FoxP3^-$), CD4pos ($CD4^+$), nonTregs ($CD4^+FoxP3^-$) and Tregs ($CD4^+$ $FoxP3^+$) in the BCF (grey symbols) or TCZ (blue symbols) from participants off ART (closed symbol) and on ART (open symbol). D) The absolute number of HIV-1 RNA^+ and/ or DNA^+ positive cells on total cells prior-to ART (i) and on ART (ii) and (E) the frequency of infection compared with the total amount of HIV-1 RNA^+ and/ or DNA^+ cells is shown as log 10 for PLWH off ART (i) and on ART (ii) in TCZ and the BCF of LN. Each participant is shown by a different colour (n=7 subjects). Grey shaded area highlights people living with HIV-1 on ART. TCZ: T-cell zone; BCF: B-cell follicle.

3.3.2 TREGS CONTAIN A HIGHER FREQUENCY OF HIV-1 INFECTION COMPARED TO OTHER T-CELL SUBSETS

To determine the contribution of Tregs to the total number of HIV-1-infected cells in LNs, we next divided the cells into subpopulations of T-cells expressing ICs i.e., CTLA-4 and PD-1 as well as FoxP3. Based on this analysis, cells in the LN tissue were divided into $CD4^{+}FoxP3^{+}$ Tregs, $CD4^{+}$ $FoxP3^{-}$ nonTregs and CD4neg T-cells ($CD4^{-}FoxP3^{-}$cells). We found $FoxP3^{+}$ expression was predominantly seen near the T:B border (Fig. 3.2 i, yellow arrows). In contrast, cells that did not express FoxP3 and defined as nonTregs were located within the BCF and the TCZ (Fig. 3.2A, ii, white and yellow arrows, respectively). Cells that did not express CD4 and defined as CD4neg ($CD4^{-}$ $FoxP3^{-}$) were found between the BCF and the TCZ (Fig. 3.2 iii, white and yellow arrows, respectively).

We then used the same approach as described earlier to understand the distribution of productively and latently infected cells in the BCF and TCZ according to the T-cell phenotype in LNs prior-to and during ART (Fig. 3.2 B&C). In LN from participants both off and on ART, the highest frequency of $HIV\text{-}1^{+}$ cells were found in the Treg population of cells, followed by nonTregs and by CD4neg cells (Fig. 3.2). In participants off ART, the frequency of infected Tregs was higher in the BCF (circles) compared to the TCZ (triangles; Fig 3.2 B, i) but this distinction was not observed in LN from participants on ART (Fig 3.2B, ii). Interestingly, Tregs were the least frequent cell in both the TCZ or BCF for participants off and on ART (Fig. 3.2C, i & ii). Together these data demonstrate preferential HIV-1 infection in Tregs in PWLH prior-to or during ART, but given the low frequency of these cells, their overall contribution to the total pool of infected cells is low (5.11%, off ART and 3.9%, on ART).

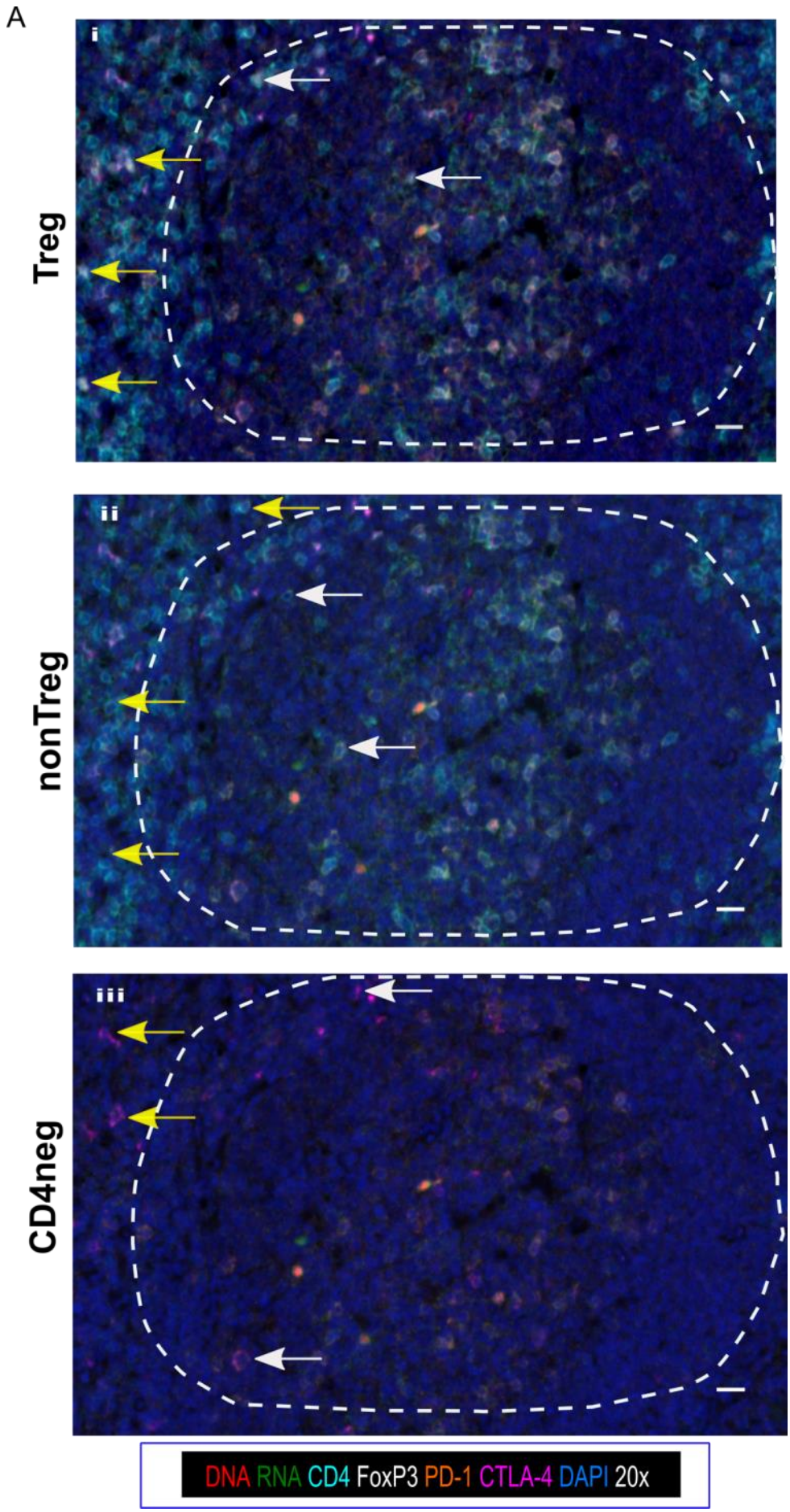
A
i
Treg
ii
nonTreg
iii
CD4neg
DNA RNA CD4 FoxP3 PD-1 CTLA-4 DAPI 20x

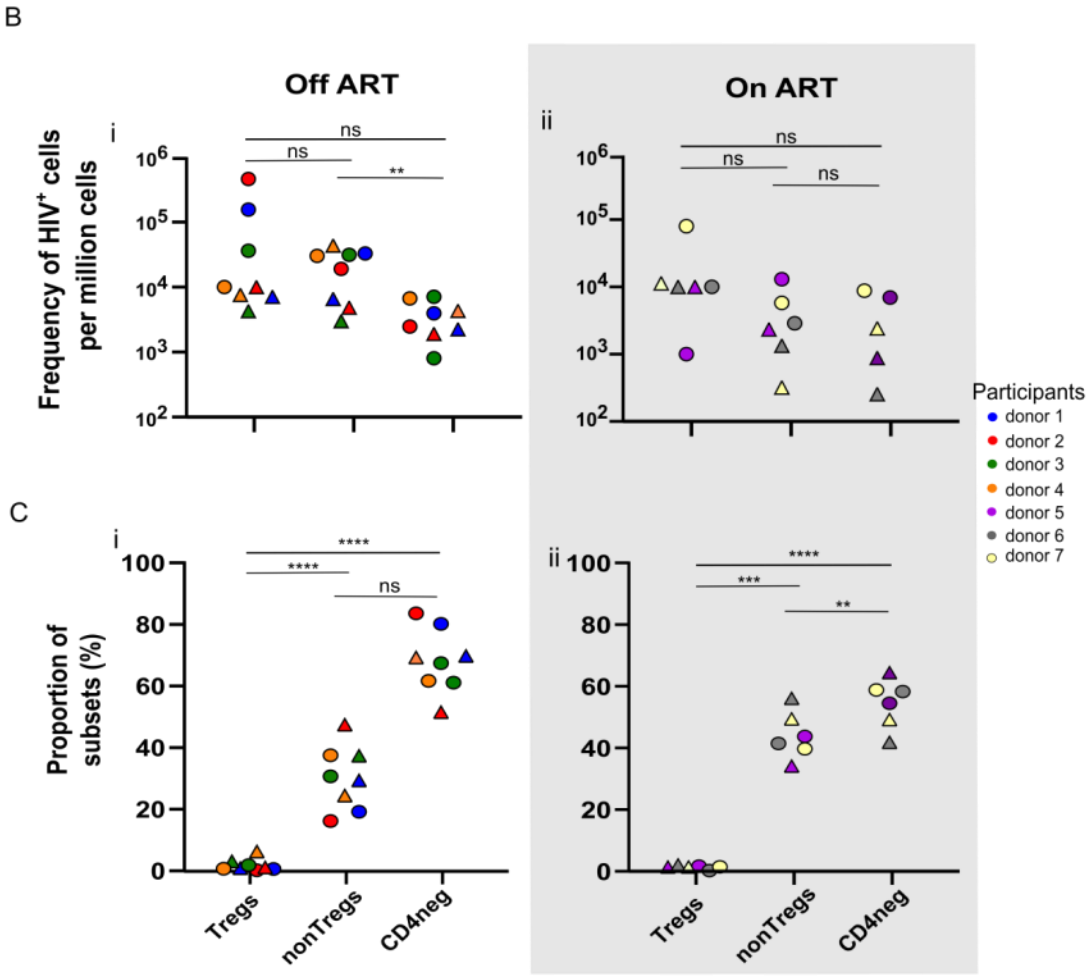

Figure 3.2. Distribution of infected Tregs and nonTregs in LNs. A) Representative multiplex images of a LN in a participant off ART, from a Mexican cohort in PLWH (3 on and 4 off ART). mIHC image (Method, Section 3.2.6) of HIV-1 DNA (red) and RNA (green) using RNA/DNAscope in combination with IHC of T-cell populations with expression markers CD4 (cyan), Treg marker FoxP3 (white), and ICs CTLA-4 (magenta) and PD-1 (orange). (i) The location of Tregs is shown between the BCF (white arrows) and the TCZ (yellow arrows), (ii) nonTregs distrubuted between the BCF (white arrows) and the TCZ (yellow arrows) and (iii) nonCD4 cells within the BCF (white arrows) and the TCZ (yellow arrows). DAPI was used for nuclear counterstain and micrographs were taken at 20x magnification using the Vectra™ multispectral imaging software. Scale =20 μm. For each donor, four ROIs were taken. B) The frequency of HIV-1 RNA^+ and/ or DNA^+ in infected subsets prior-to ART (i) and on ART (ii) was examined with HALO (Method, Section 3.2.7) using cells positively scored to identify CD4neg cells, Tregs and nonTregs. C) The

proportion of HIV-1 RNA^+ and/ or DNA^+ infected cells in participants prior-to ART (i) and on ART (ii) was examined with HALO (Method, Section 3.2.7) using cell positively scored to identify CD4neg cells, Tregs and nonTregs in participants prior-to ART. The samples are colour coded (n=7 subjects) in either the BCF (closed circle) or the TCZ (closed triangle). *p < 0.05; **p < 0.01; ***p < 0.001; ****p < 0.0001 and ns (no significance).

3.3.3 CELLS EXPRESSING PD-1$^+$ ARE MORE FREQUENTLY INFECTED COMPARED TO CTLA-4$^+$ CELLS

We and others have shown that in blood and LN tissue from PLWH on ART, HIV-1 is enriched in PD-1$^+$ and CTLA-4$^+$ CD4$^+$ T-cells [199,556]. Similar findings have been observed in SIV-infected non-human primates on ART [155]. To determine if cells expressing ICs i.e., PD-1 and CTLA-4 are enriched for HIV-1 and to identify their location within LN, we combined RNA/DNAscope with mIHC and assessed the same LNs from PLWH prior-to and during ART.

We found that nonTregs contained the majority of PD-1$^+$ cells, whereas CTLA-4$^+$ cells consisted of Tregs in participants prior to- and during ART (Fig. 3.3A). We next compared the frequency of infected cells in PD-1 positive and negative cells and did the same for CTLA-4 positive and negative cells in the BCF and TCZ (Fig. 3.3B). In PLWH off ART, virus was more commonly detected in PD-1$^+$ compared to PD-1$^-$ cells in the TCZ, while there was no difference between CTLA-4$^+$ and CTLA-4$^-$ cells in the BCF and the TCZ. In contrast, in PLWH on ART, there was no enrichment of virus in PD-1$^+$ compared to PD-1$^-$ cells and there was a trend to more virus in PD-1$^-$ cells in the BCF and the TCZ. In both PLWH off ART and PLWH on ART there was no difference in virus in CTLA-4$^+$ compared to CTLA-4$^-$ cells.

As expected, the frequency of infected cells was higher in LN from participants off ART compared to on ART. We examined the number of infected cells in PD-1$^+$ and CTLA-4$^+$ cells (Fig 3.3C). In the PD-1$^+$ cells in participants off ART, infected cells were most common in total cells, followed by non-Tregs followed by Tregs. A similar pattern was observed in the CTLA-4$^+$ cells. Infected cells were found in both the BCF and TCZ. In participants on ART, detection of infected cells in either PD-1$^+$ or CTLA-4$^+$ cells was dramatically reduced compared to participants off ART. For PD-1$^+$ cells, one of three participants had detectable virus in PD-1$^+$ nonTregs and this was only in the BCF. For CTLA-4$^+$ cells, one of three participants had detectable virus in CTLA-4$^+$ Tregs and only in the both the BCF and the TCZ. These data demonstrate that virus persistence in participants on ART has a very different distribution to participants off ART and that when virus persists in Tregs, these are CTLA-4$^+$ and found in the BCF and the TCZ.

Altogether these results suggest that nonTregs expressing PD-1^{+} were more frequently infected in participants prior-to ART compared to Tregs. In PLWH on ART, we saw no enrichment of virus in PD-1^{+} cells, in contrast to other publications [199,459,555]. Although numbers were small, we saw clear enrichment of virus in PLWH on ART in CTLA-4^{+} Tregs located in the BCF and the TCZ, consistent with similar descriptions in a NHP model[155].

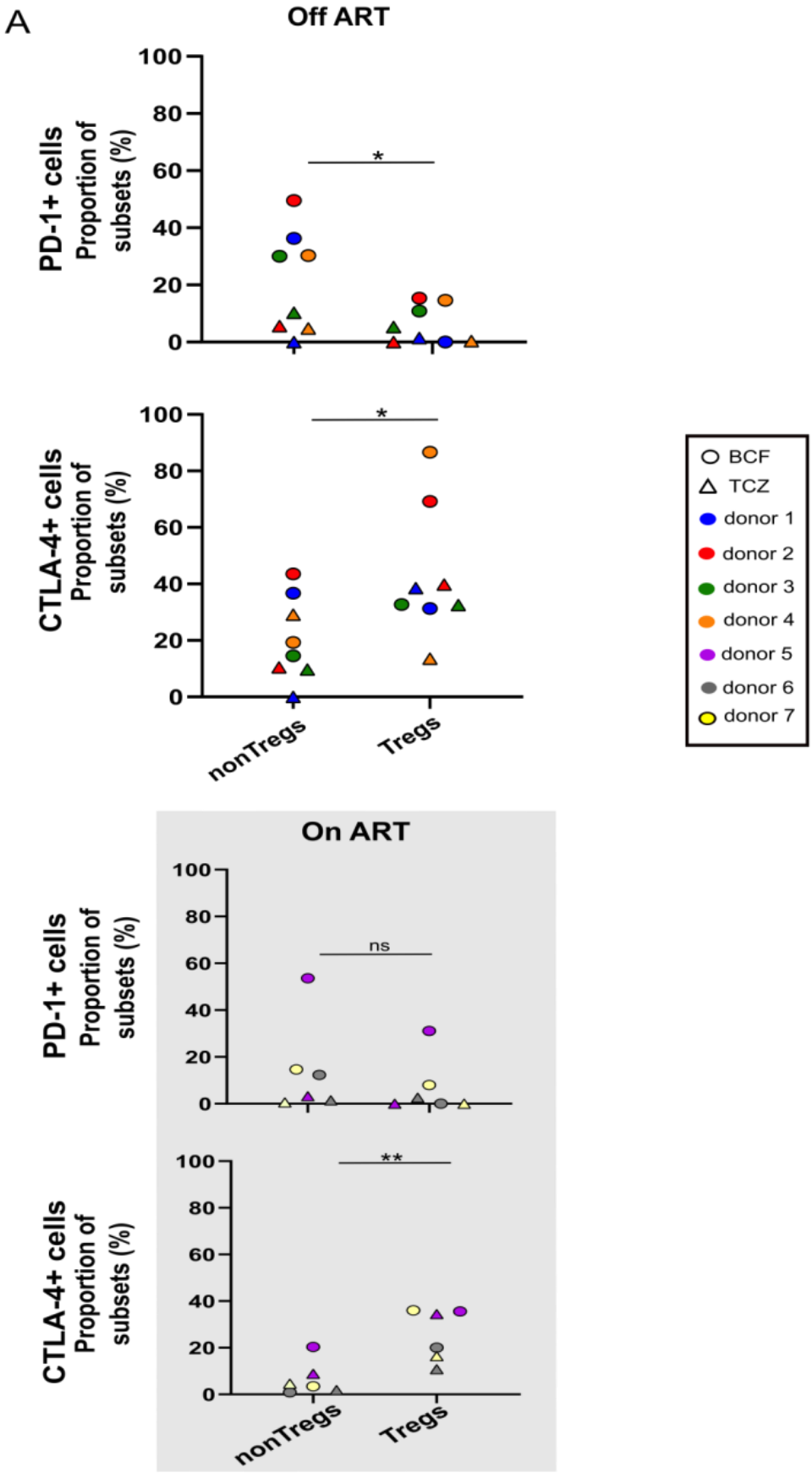
A
Off ART
PD-1+ cells
Proportion of subsets (%)
100
80
60
40
20
0
*
CTLA-4+ cells
Proportion of subsets (%)
100
80
60
40
20
0
*
nonTregs
Tregs
BCF
TCZ
donor 1
donor 2
donor 3
donor 4
donor 5
donor 6
donor 7
On ART
PD-1+ cells
Proportion of subsets (%)
100
80
60
40
20
0
ns
CTLA-4+ cells
Proportion of subsets (%)
100
80
60
40
20
0
**
nonTregs
Tregs

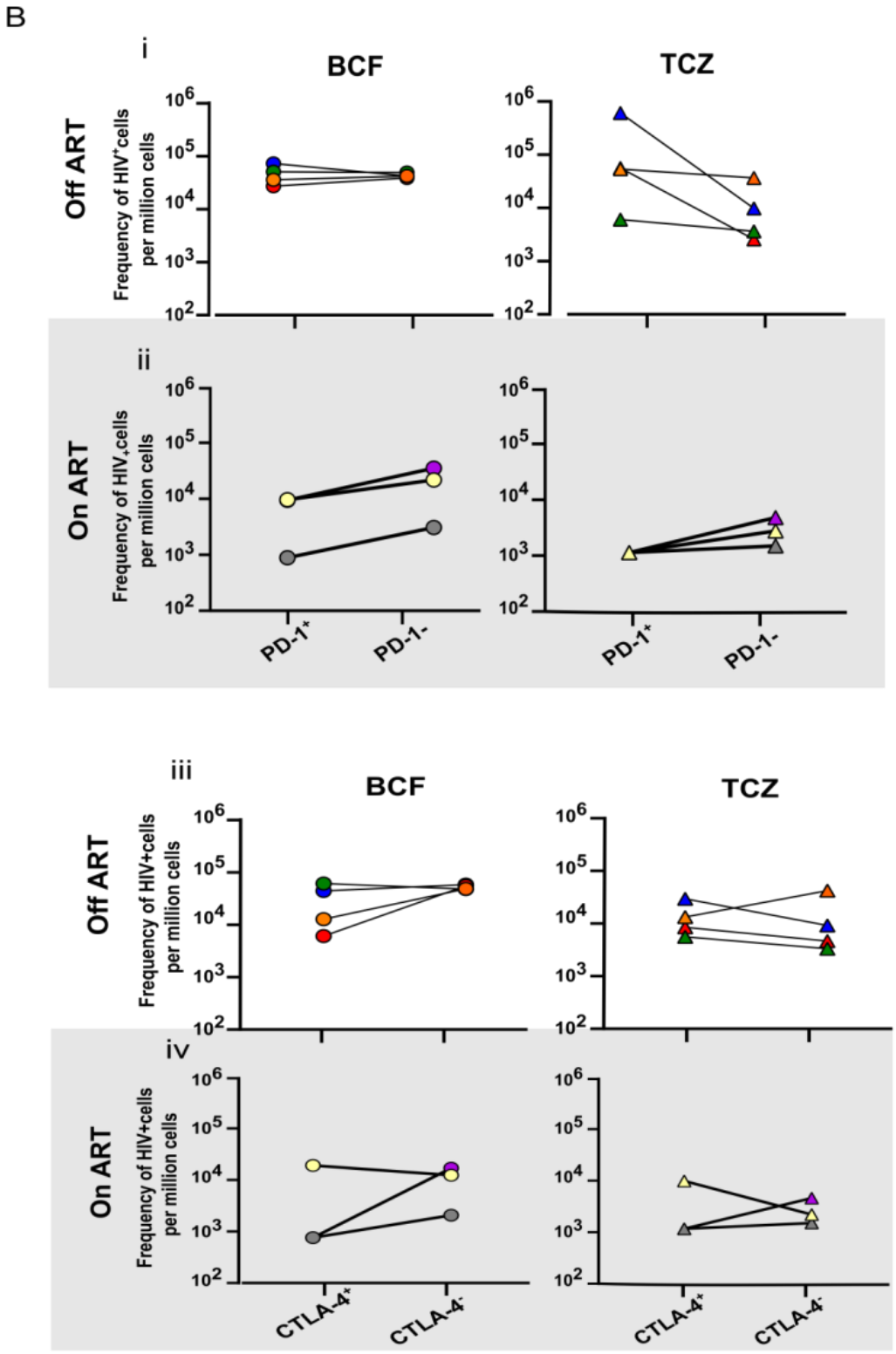

Figure 3.3. Distribution of PD-1$^+$ and CTLA-4$^+$ HIV-1-infected cells in LNs tissue. Cells were stained using mIHC (Method, Section 3.2.6) and RNA/DNAscope following image analysis of LNs sections. Each section was quantified using HALO analysis software (Method, Section 3.2.7). Quantitative imaging analysis of LNs from participants

prior-to (n=4) or post ART (n=3) showing the frequency of HIV-1 infection in cells expressing ICs. A) The proportion of PD-$1^{+/-}$ CTLA-$4^{+/-}$in infected subsets prior-to and post ART (grey shaded area) was examined with HALO (Method, Section 3.2.7) using cells positively scored to quantify PD-$1^{+/-}$ CTLA-$4^{+/-}$ expression on Tregs and nonTregs. The samples are colour coded (n=7 subjects). B) Plots show the frequency of HIV-1 infection in matched PD-1^{+} or CTLA4^{+} expression in LNs in participants prior-to or post ART (grey shaded areas). Cells were stained with ICs and quantified using HALO analysis software (Method, Section 3.2.7). C) Plot shows the frequency of HIV-1 RNA^{+} and/ or DNA^{+} infected total cells ($DAPI^{+}$), CD4neg ($CD4^{-}$ $FoxP3^{-}$), CD4pos ($CD4^{+}$), nonTregs ($CD4^{+}$ $FoxP3^{-}$) and Tregs ($CD4^{+}$ $FoxP3^{+}$) that expressed PD-1^{+} and/or CTLA-4^{+} prior-to or during ART. Mean of four ROIs were taken for each donor. The samples are colour coded (n=7 subjects) in either the BCF (closed circle) or the TCZ (closed triangle).

3.4 DISCUSSION

In this study, we used RNA/DNA scope and imaging established in our lab (Chapter 2) which allowed us to define Tregs and their relationship with ICs such as PD-1 and CTLA-4 in the BCF and TCF regions of the LNs of PLWH prior-or during ART. We showed that in both PLWH on ART and off ART; 1. virus was detected in both the BCF and TCZ with similar frequency; 2. infection of Tregs was more common than non Tregs; 3 the frequency of Tregs was low so the contribution of infected Tregs to the overall reservoir size is small; and 4. the overall frequency of infection was higher in PLWH off ART compared to on ART.

When we examined the relationship between Treg markers and ICs, we found that 1. PD-1 was predominantly expressed on nonTregs; 2. CTLA-4 was expressed at higher levels on Tregs than non-Tregs; 3. There was minimal enrichment of virus in PD-1^+ compared to PD-1^- cells or CTLA-4^+ cells compared to CTLA-4^- cells both on ART; and 4 persistent virus was detected on ART in CTLA-4^+ Tregs located in the BCF and the TCZ, similar to findings in NHP [309].

Our data demonstrated a higher frequency of HIV-1 infected cells both RNA^+ and/ or DNA^+ in the BCF than TCZ (Fig. 3.1E). This was shown with a similar pattern in PLWH prior to- and during ART, which suggests that the BCF is a site of ongoing HIV-1 replication in LNs [297]. However, we found that the TCZ also contained HIV-1 infected both RNA^+ and/or DNA^+. This observation suggests that the enrichment of HIV-1 infection can be found outside the follicles, as shown in SIV-infected NHP on ART [309].

Using our imaging analysis, we further looked at the compartmentalization of the T-cells in the BCF and the TCZ and their relationship with HIV-1 infection (Fig. 3.1B). We showed that nonTregs are predominantly found in the BCF and express more PD-1 on their surface than CTLA-4 (Fig.3.3A). Our data is in agreement with the literature which shows that $CD4^+$ T-cells (nonTregs) characterized by the expression of cell surface receptors ($CD4^+$ PD-$1^{+/-}$ CTLA-$4^{+/-}$) are the major source of persistent and infectious HIV-1, particularly in LN from PLWH on ART [131,587,588].

When we compared Tregs to nonTregs, we found that Tregs contained higher levels of HIV-1 than nonTregs, this was also observed in two studies which demonstrated an abundance of HIV-1 DNA in Tregs compared to nonTregs in

PBMCs from PLWH that were either treatment naïve[438] and on ART[437,438]. In addition, our data confirms what other groups have reported, which is that $CD4^+$ $PD\text{-}1^{+/-}$ $CTLA\text{-}4^{+/-}$ nonTregs contain frequently infected HIV-1 RNA^+ and/or DNA^+ cells in ART naïve participants [131,587,588]. Our data which shows an enrichment of HIV-1 in $CD4^+$ $FoxP3^+$ or $CTLA\text{-}4^{+/-}$ $PD\text{-}1^{+/-}$Tregs identified in the BCF, makes us speculate that these Tregs are Tfr cells which next to CXCR5 and Bcl6, also express $CD4^+$ $FoxP3^+$ or $CTLA\text{-}4^{+/-}PD\text{-}1^{+/-}$ and are capable of gaining entry to the BCFs through the expressing of CXCR5[584]. Additionally, these cells share similar phenotypic characteristic with Tfr cells, where the expression of CTLA-4 was shown to correlate with these cells [589].

We found that Tregs contained the highest frequency of infection, particularly in the BCF, in participants on and off ART. Although we didn't specifically measure CXCR5 expression which defines Tfr cells, we speculate that these Tregs are a subset of Tfr cells [584]. Tfr and Tfh cells differ by the presence or absence of FoxP3 and high or low levels of PD-1 and CTLA-4. In *vivo* and *ex vivo* studies have demonstrated that Tfr cells are more permissive to HIV-1 R5-tropic HIV-1 infection compared to Tfh cell which may be mediated by their high expression of CD4 and CXCR5 [407].

Early initiation of ART has shown to be associated with a lower HIV-1 reservoir in $CD4^+$ T-cells [590] and a decay of $PD\text{-}1^+$ cells in the LN over time [131]. Of note, in this cohort, the initiation and duration of ART varied amongst participants. Another essential factor to take into consideration is the donor variation between PLWH. Published data has shown that age i.e. plays an important role in subset contribution during HIV-1 [591]. Furthermore, CD4neg cells can resemble Tfh cells or macrophages which have lost their surface expression [592].

Although we found evidence of infected Tregs, there appeared to be no difference between those on and off ART. However, we found no difference between the number of infected Tregs with PD-1 and CTLA-4, but this remained challenging to examine due to the low number of cells and cohort size.

3.4.1 LIMITATIONS

This is the first systematic characterisation of HIV-1 location in LN based on expression of Treg markers and the ICs PD-1 and CTLA-4. A major limitation of this work is the small sample size analysed and further work would be needed to ensure any differences were statistically significant. We had limited LN material from participants that could be evaluated. This was largely due to the manner the samples were prepared. Time in formalin is a variable which can impact sensitive detection of viral RNA and proteins. In these studies, we only included samples that were prepared using a method that preserved detection of viral RNA.

Although we did detect CTLA-4 predominantly on Tregs and other subsets, CTLA-4 expression is retained considerably longer on Tregs and other T-cells and can be found on the membrane and cytoplasm of the cell [593,594]. The algorithm used on the HALO analysis software was set on membrane staining and not cytoplasmic expression and this could potentially explain why CTLA-4 expression is low in T-cells which constitutively internalize CTLA-4.

The Tregs identified led us to believe that they might be Tfr cells. However, our data could not provide their phenotype as we only looked at Tregs as a bulk population and not subsets of Tregs. Therefore, including other markers such as CXCR5 and Bcl6 in future studies would be useful to fully determine their phenotype. This also applies to the nonTregs seen which had a Tfh cell-like phenotype due to their location and expressesion of CXCR5 and Bcl6. These issues deserve further empirical study.

3.4.2 CONCLUSION

Besides blood, lymphoid tissue such as gut associated lymphoid tissue and LNs is reported as an essential anatomical site where the majority of $CD4^+$ T-cells reside [574]. Tregs have been identified previously as a reservoir during HIV-1 persistence in blood in PLWH on ART, however these studies have been limited to blood [201,595]. Most importantly, we demonstrate that Tregs are enriched for virus compared to non Tregs both on and off ART. In participants on ART, we showed that $PD\text{-}1^+$ cells were not enriched for infection in LN tissue and that virus can certainly persist

outside the BCF, largely in CTLA-4^{+} cells. Future studies should include additional phenotyping to include CXCR5 and BCL6 to fully understand the relationship of Tregs to Tfh and Tfr. We conclude that HIV-1 persistence in cells outside the BCF needs to be considered in eradication strategies.

3.5 SUPPLEMENTARY FIGURES

Supplementary Table 3.1 Percentage of infected cells in each subset

Off ART	**BCF**	**%**	**TCZ**	**%**
HIV DNA^+ RNA^+ $PD\text{-}1^+$	105/2548	4.0	32/1288	2.0
HIV DNA^+ RNA^+ $CTLA\text{-}4^+$	41/1957	2.0	30/2600	1.0
HIV DNA^+ RNA^+ $CD4^+$ $FoxP3^+$ (Tregs)	l13/182	7.1	10/1736	0.6
HIV DNA^+ RNA^+ $CD4^+$ $FoxP3^-$ (nonTregs)	218/7258	2.9	212/20418	1.0
HIV DNA^+ RNA^+ $CD4^-$	92/197217	0.5	83/38212	0.2

On ART	**BCF**	**%**	**TCZ**	**%**
HIV DNA^+ RNA^+ $PD\text{-}1^+$	7/819	1.0	0/215	0.0
HIV DNA^+ RNA^+ $CTLA\text{-}4^+$	1/295	0.3	3/742	0.4
HIV DNA^+ RNA^+ $CD4^+$ $FoxP3^+$ (Tregs)	2 /75	2.7	2/496	0.4
HIV DNA^+ RNA^+ $CD4^+$ $FoxP3^-$ (nonTregs)	21/2533	0.8	16/14482	0.1
HIV DNA^+ RNA^+ $CD4^-$	19/3429	1.0	21/15783	0.1

Chapter 4: HIV-1 persists preferentially in memory CTLA-4$^+$ CD4$^+$ T-cells

4.1 INTRODUCTION

Analysing LN tissue is critically important to fully understand HIV-1 persistence in PLWH on ART given: 1. the low penetration of ART into lymphoid tissue [596] as cessation of ART resulted in viral rebound originating from the lymphatic tissue[597], 2. anatomic compartments in the LNs such as BCF are immune-privileged sites restricting migration of HIV-1-specific CD8$^+$ T-cells [598] and 3. the majority of T-cells reside in the LNs and are functionally distinct from those in blood [599].

In addition, multiple studies have shown that LN PD-1$^+$ cells, the majority of which are follicular helper T-cells (Tfh), harbor the majority of HIV-1 DNA and replication-competent HIV-1 in PLWH on ART [131]. In contrast, in ART-treated SIV-infected rhesus macaques CTLA-4$^+$ cells were enriched for SIV DNA and these infected cells were primary located in the T-cell zone (TCZ) and not within the B-cell follicle (BCF) of the LN [155]. The CTLA-4$^+$ cellular subset within the TCZ of the LN tissue has never been studied in PLWH on ART.

In this study, we sought to determine whether blood and LN CD4$^+$ T cells subsets defined by their expression of PD-1 and CTLA-4 preferentially harbor HIV-1 in PLWH on ART. We showed that although there was enrichment of HIV-1 DNA in memory CD4$^+$ T-cells expressing CTLA-4, there was no significant difference between the blood and the LN. In addition, we combined RNA/DNAscope with multiplex immunohistochemistry (mIHC) to provide insight into spatial distribution of the HIV-1 reservoir in LN tissue, and found enrichment of HIV-1 in PD-1$^-$CTLA-4$^+$ cells located in either the BCFs or the TCZs in PLWH on ART. We conclude that CTLA-4 is indeed an important marker for HIV-1 enrichment and identifies a pool of infected cells distinct from PD-1$^+$ cells.

4.2 METHODS

4.2.1 STUDY PARTICIPANTS AND SAMPLE COLLECTION

We enrolled 11 PLWH receiving suppressive ART (see clinical characteristics in Table 1) at The Alfred Hospital, Melbourne, Australia (n=11). Inclusion criteria were documented HIV-1-1 infection, aged 18 years or older and receiving combination ART with plasma HIV-1 RNA <50 copies/mL for at least 3 years. Due to leukapheresis and LN biopsy procedures, we excluded individuals with skin infection at inguinal area; current lower extremity, gastrointestinal or genitourinary infection; chronic venous stasis or lymphedema of lower extremities; blood coagulation disorders or conditions requiring anticoagulant therapy; liver cirrhosis; weight <50 kg or body mass index (BMI) >35; blood pressure >160/100 mmHg or <100/70 mmHg; pregnant or breast feeding; or any with clinically significant cardiac or cerebrovascular disease. Leukapheresis procedures were performed at The Alfred Hospital (n=11) and excisional LN biopsies were performed at The Avenue Hospital, Melbourne, Australia. The time between the two procedures ranged from 6 to 50 days. LN biopsies were performed by an experienced surgeon using general anaesthesia.

Table 4.1 Clinical characteristics of PLWH

Participant ID	Age (years)	Gender	Race	HIV diagnosis	Years since HIV diagnosis	CD4+ count (cells/uL)	CD4% (%)	CD8+ count (cells/uL)	CD8% (%)	Nadir CD4+ count (cells/uL)	ART regimen	VL (copies/mL)	Peak VL (copies/mL)	Duration VL<50 (years)	Leuka-pheresis	LN biopsy
PRA001	64	Male	Caucasian	1985	31.7	403	24	1061	63	10	ATV, TDF/FTC	<20	148,430	14.1	Yes	Yes
PRA002	48	Male	Caucasian	2006	10.9	1460	47	793	26	698	ABC/3TC, EFV	<20	N/A	N/A	Yes	No
PRA003	49	Male	Caucasian	1997	20.3	833	31	767	29	218	TDF/FTC, DRV, RTV	<20	78,300	11.5	Yes	Yes
PRA004	55	Male	Caucasian	1996	21.1	1036	40	1069	42	266	TAF/FTC, DTG	<20	100,000	11.1	Yes	No
PRA005	49	Male	Caucasian	2003	13.7	388	28	717	51	168	TAF/FTC, MVC	<20	147,000	12.0	Yes	Yes
PRA006	48	Male	Caucasian	2011	6.8	864	38	864	39	538	EVG/TAF/FTC/COBI	<20	118,800	6.1	Yes	Yes
PRA007	47	Male	Caucasian	2001	16.4	705	32	1034	47	122	DRV/COBI, TAF/FTC	<20	548,000	6.5	Yes	Yes
PRA008	38	Male	Other (PNG)	2006	11.2	281	25	328	30	168	EVG/TAF/FTC/COBI	<20	63,300	8.7	Yes	Yes
PRA009	49	Male	Caucasian	2010	7.5	474	25	1085	56	42	EVG/TAF/FTC/COBI	<20	211,930	7.0	Yes	Yes
PRA010	48	Male	Caucasian	2000	17.6	484	28	895	52	411	TAF, FTC, RPV	<20	N/A	N/A	Yes	No
PRA011	53	Male	Caucasian	2004	14.2	735	37	810	41	300	ABC/3TC, EFV	<20	365,000	11.2	Yes	Yes
Mean (sd)	**53 (9.3)**	**N/A**	**N/A**	**N/A**	**19.5 (9.0)**	**623 (284)**	**35 (7.1)**	**671 (270)**	**38 (10.6)**	**222 (183)**	**N/A**		**155,366 (135,841)**	**9.4 (2.8)**	**N/A**	**N/A**

4.2.2 PROCESSING OF EXCISED LNS AND SORTING OF LNMCS

To disaggregate lymph node mononuclear cells (LNMCs) from LN biopsy tissue, we initially stored LN samples in RPMI 1640 media (Life Technologies, Carlsbad, CA, USA) supplemented with 15% heat-inactivated Fetal Bovine Serum (FBS, Bovogen, Keilor East, VIC, AUS), 10mM HEPES buffer (Life Technologies, Cat no 15630-080), 1X Penicillin-Streptomycin-Glutamine (Life Technologies, Cat no 10378016) on ice in a 4°C cold room overnight for processing the following day. Using sterile disposable scalpels and forceps, LN tissue was torn apart and minced to obtain small fragments. Minced node tissue was transferred to a 70-micron nylon cell strainer (Bio-Strategy Laboratory Products PTY LTD, Tullamarine, VIC, AUS, Cat no 352350) inserted into a 50 mL collection tube. Remaining tissue within the cell strainer was further grinded to allow cells to pass through and then passed through a second strainer with a 40-micron filter (Bio-Strategy Laboratory Products PTY LTD, Cat no 352340). Cells were then transferred to conical tubes and centrifuged at 400g for 10 minutes. In case of significant presence of red blood cells, these were lysed with ACK lysing buffer (Life Technologies). Cells were then resuspended in warm DNase media (RPMI with 1% FBS and 100 ug/mL DNase I [Sigma Aldrich, St. Louis, MO, USA, Cat no DN25-100mg]) at 10 million cells/mL, centrifuged at 400g for 10 minutes and resuspended at desired concentration for sorting or immunophenotyping. Following isolation of LNMCs from LN biopsies, unfrozen cells were labelled with the following antibodies and fluorophores all from BD Biosciences (Franklin Lakes, NJ, USA): anti-CD3 BV711 (Cat no 563725), CD4 FITC (Cat no 561842), CD45RA PE-Cy7 (Cat no 337167), PD1 BV421 (Cat no 562516) and CTLA4 PE (Cat no 557301) and sorted on a BD FACS Aria cell sorter. We collected 4 different subsets of LN memory $CD4^+$ T-cells defined as double positive ($CD3^+CD4^+CD45RA^-PD\text{-}1^+CTLA\text{-}4^+$), PD-1 single positive (SP) ($CD3^+CD4^+CD45RA^-PD\text{-}1^+CTLA\text{-}4^-$), CTLA-$4^+$ SP ($CD3^+CD4^+CD45RA^-PD\text{-}1^-CTLA\text{-}4^+$) and double negative ($CD3^+CD4^+CD45RA^-PD1^-CTLA4^-$).

4.2.3 ISOLATION OF BLOOD MEMORY $CD4^+$ T CELLS AND CELL SORTING

Following leukapheresis, peripheral blood mononuclear cells (PBMCs) and plasma were isolated using standard Ficoll procedures and cryopreserved in liquid nitrogen. To isolate memory $CD4^+$ T-cells from PBMCs obtained by leukapheresis, we subsequently thawed PBMCs and used a magnetic bead negative selection kit from BioLegend that depleted non-$CD4^+$ memory T-cells with a biotin antibody cocktail consisting of anti-CD8a, anti-CD11b, anti-CD14, anti-CD16, anti-CD19, anti-CD20, anti-CD36, anti-CD45RA, anti-CD56, anti-CD123, anti-CD235ab and TC γ/δ (MojoSort Human CD4 memory T-cell isolation kit, BioLegend, San Diego, CA, USA, Cat no 480064). Memory $CD4^+$ T cells were then labelled with the following antibodies and fluorophores all from BD Biosciences: anti-CD3 BV711, CD4 FITC, CD45RA PE-Cy7, PD-1 BV421 and CTLA-4 PE and sorted on a BD FACS Aria Fusion. We collected 4 different subsets defined as double positive ($CD3^+CD4^+CD45RA^-PD\text{-}1^+CTLA\text{-}4^+$), PD-$1^+$ SP ($CD3^+CD4^+CD45RA^-PD\text{-}1^+CTLA\text{-}4^-$), CTLA-$4^+$ SP ($CD3^+CD4^+CD45RA^-PD1^-CTLA\text{-}4^+$) and double negative ($CD3^+CD4^+CD45RA^-PD\text{-}1^-CTLA\text{-}4^-$).

4.2.4 FLOW CYTOMETRY ON T-CELL SUBSETS

The flow cytometry gating strategy used to analyse the distribution of PD-1 and CTLA-4 in memory $CD4^+$ T-cell subsets derived from blood and LNs are shown in (Fig. 4.1A). This involved gating on live $CD3^+CD4^+$ T-cells negative for CD45RA, followed by gating on PD-1 and CTLA-4 to obtain 4 populations of memory $CD4^+$ T cells defined by their expression of PD-1 and CTLA-4, i.e. DN $PD1^-CTLA4^-$, SP PD-1^+CTLA-4^-, SP $PD1^-$CTLA-4^+ and DP PD-1^+CTLA4^+ on their surface (Fig. 4A). In PBMCs this was performed on cells that were enriched for CD45RA- memory $CD4^+$ T-cells using negative selection (MojoSort Human CD4 memory T-cell isolation kit, BioLegend, San Diego, CA, USA, Cat no 480064).

4.2.5 IMMUNOPHENOTYPING

Before sorting cells, we used flow cytometry to assess the distribution of the 4 subsets of memory $CD4^+$ T cells in blood and LN based on their expression of PD1 and CTLA-4. For this we used the same antibodies as described for cell sorting and fluorescence minus one (FMO) control and ran samples on a BD LSR Fortessa flow cytometer. Gates were set based on the FMOs and then adjusted by comparing

CD45RA versus PD-1 and CD45RA versus CTLA-4 populations as this was found to be a more accurate way of determining the populations. Flow Jo version 10 was used for analysing acquired data.

4.2.6 QUANTIFICATION OF TOTAL HIV-1 DNA, CA-US HIV-1 RNA, CA-MS HIV-1 RNA

To quantify levels of cell-associated HIV-1 RNA and DNA, memory $CD4^+$ T-cells sorted based on their expression of PD-1 and CTLA-4 subsets were lysed and lysates stored at -80 until analyses. We extracted RNA from lysates using the Qiagen All-prep kit (Qiagen, Hilden, Germany). Cell associated unspliced (CA-US) HIV-1 RNA was then quantified in four replicates using a semi-nested real-time quantitative polymerase chain reaction (RT-PCR) as previously described[600]. Primers used for 1st and 2nd round amplified HIV-1-1 RNA copy numbers, which were standardized to cellular input using the 18S TaqMan gene Expression Assay (Applied Biosystems, Foster City, CA USA). For all samples, a non-RT control was included. If this control was positive, results for this sample were excluded from the analysis. Cell associated multiple spliced (CA-MS) HIV-1 RNA was measured using RT-PCR with primers and probes as described previously [578]. Total HIV-1 RNA and DNA were isolated from AllPrep extraction kit and CA total HIV-1-DNA was analysed in triplicate with cell lysates using primers SL19/SL20 and SL30 probes to detect either HIV DNA or HIV RNA. The 18S Taqman probe was used as house keeping gene for total cellular RNA as previously described [601]. HIV DNA copy numbers were standardized to cellular equivalents through quantification of CCR5.

4.2.7 HISTOLOGY AND IMMUNOHISTOCHEMISTRY

After using LN tissue for sorting, the remaining LNs were embedded and snap frozen in optimum cutting temperature (OCT) compound (Sakura) and stored at -80°C before FFPE and sectioning. Immunohistochemistry was performed on FFPE LN tissue using a peroxidase-based method on 5 μm sections on Superfrost® plus microscope slides (Thermo Scientific). Specimen slides were incubated at 60 °C for 45-60 minutes for the melting and fixing of specimens onto microscope slides. In order to deparaffinise, slides were washed in xylene and rehydrated in ethanol of 100% to 70%. Slides were then treated with hydrogen peroxidase (Chem-Supply, Gillman, Australia) in 0.3% H_2O_2 (v/v) in double-distilled H_2O (ddH_2O) for 15 minutes at room temperature. Heat induced epitope retrieval was then performed

until boiling was achieved, followed with 90°C for 15 minutes by microwave treatment (MWT) in the appropriate retrieval buffer optimised for each target epitope. Specimens were then blocked using Background Sniper (Biocare Medical, Concord, CA) for 15 minutes prior to primary antibody application.

4.2.8 HIV-1-1 RNA AND DNA TARGET PROBES

The HIV-1 RNA probe used was designed to hybridize to viral RNA in gag, pol, vif, vpr, tat, rev, env, nef, and vpx genes (vRNA anti-sense probe, ACD catalog: ADV416111) as well as HIV-1 DNA probe targeting the Gag-Pol coding region (vDNA sense probe, ACD catalog: ADV425531). All probes were purchased from Advances Cell Diagnostics (ACD Newark, CA) and a complete list of the sequence of each probe used has been previously published [297].

4.2.9 HIV-1-1 RNA AND DNA *IN SITU* HYBRIDIZATION

For the detection of vRNA and vDNA, we used the RNAscope 2.5 brown kit [297], with some modifications [297]. In brief, probes were visualized by hybridizing with preamplifiers, amplifiers in a humidified HybEZ oven, and finally, fluorescent label with TSA amplification system (Perkin Elmer, Waltham, Massachusetts). LNs that were stored in OCT and FFPE were stained for HIV-1 RNA and DNA.

4.2.10 MULTIPLEX IMMUNOHISTOCHEMISTRY (OPAL™)

Rabbit monoclonal antibodies to CD4 (Cell Marque, Rocklin, CA) clone 104R-1, 1/100, high pH retrieval), mouse monoclonal antibody to FoxP3 (Abcam, Cambridge, UK), clone IgG1, 1/1000, high pH retrieval), mouse polyclonal antibody to PD-1 (Abcam, IgG1 Nat105, 1/500, low pH retrieval), mouse monoclonal antibody to CTLA-4 (MyBiosource, San Diego, CA) IgG2a/k, 1/100, high pH retrieval) were used. Sectioned LN tissues were stained using IHC with CD4, PD-1 and CTLA-4 and DAPI, followed by imaging on the Vectra multispectral IHC imaging (as described in Chapter 3, Methods 3.2.7).

4.2.11 QUANTITATIVE IMAGE ANALYSIS

HALO™ image analysis software from Indica Labs (versions 2.0, Albuquerque, New Mexico) was used for multispectral images prepared by inForm in LN samples (described in chapter 3.2.7) Cells below the positive threshold were not scored and cells above the positive threshold are scored. Using the HALO analysis software, $CD4^+$ T-cells were divided into PD-1 and/or CTLA-4, i.e., DN

PD1^{-}CTLA4^{-}, SP PD1^{+}CTLA4^{-}, SP PD1^{-}CTLA-4^{+} and DP PD-1^{+}CTLA4^{+} in both the TCZ and the BCF of LNs. In addition, further characterization of subsets, i.e. Tregs, nonTregs and nonCD4, (as described in Chapter 3, Methods 3.2.7).

4.2.12 STATISTICAL ANALYSES

We performed pairwise comparisons across the individual subsets using paired t-test or Wilcoxon matched-pairs signed rank test, depending on data distribution. We investigated associations of HIV-1 persistence measures and baseline characteristics using Spearman or Pearson correlation depending on data distribution. All statistical analyses were performed in Prism 8 (version 8.4.3).

4.2.13 STUDY APPROVALS

The study was approved by Human Research Ethics Committees at The Alfred and Avenue Hospitals in Melbourne. The study was also registered at and approved by the University of Melbourne Ethics Committee. The study was conducted in accordance with the principles of the Declaration of Helsinki (1996) and the principles described in the Food and Drug Administration regulations and the Department of Health and Human Services regulations for the protection of human participants. Each participant provided written informed consent.

4.3 RESULTS

4.3.1 STUDY PARTICIPANTS AND CLINICAL DETAILS

Eleven participants were recruited for this study. Their clinical characteristics are summarized in Table 4.1. In brief, all 11 participants >18 years were males who had been on suppressive ART for at least three years with undetectable viral load (<20 or <40 copies/mL). The mean duration of suppressed plasma HIV-1 RNA prior to study entry was 9.4 years (95% confidence interval (CI) 8.1-10.8) and mean nadir $CD4^+$ T cell count was 222 cells/uL (95% CI 138-305). Ten participants consented to both leukapheresis and excisional biopsy of an inguinal LN under general anaesthetic, and one participant consented only to leukapheresis. Four of ten participants (40%) that underwent excisional LN biopsy developed a seroma at the surgical site 7-17 days after the procedure, which all fully resolved after 4-8 weeks. One participant developed a local infection following LN biopsy, which also fully resolved after treatment with antibiotics. In two participants, the excised LN tissue did not contain any $CD3^+$ T-cells and could not be used for the study. We therefore analysed paired LN and leukapheresis samples from 8 individuals and leukapheresis samples only for three individuals.

4.3.2 FLOW CYTOMETRY AND QUANTITATIVE IMAGING OF ICS SUBSETS IN HUMAN BLOOD AND LN

Memory $CD4^+$ T-cells cells were found in all four populations in blood and LNs, but with a higher frequency of CTLA-4 negative subsets than CTLA-4 positive subsets (Fig.4.1B, first and second image). When comparing the relative frequency of each subset across blood and LNs, we found that double negative cells were more frequent in blood compared to LN, whereas DP cells were more frequent in the LN compared to blood (Fig.4.1B, third image).

We also employed *in situ* hybridization (ISH) using RNA/DNAscope (Fig. 4.2,as pointed out in Chapter 3) with IHC to analyse the distribution of all four subsets in LN tissue with a method that also allowed us to assess the location of cellular subsets within LN tissue. With this methodology we assessed LN tissue from two individuals (PRADA 6 and PRADA 11) and found that double negative and SP PD-1neg $CTLA\text{-}4^+$ constituted the majority of cells in both the TCZ and the BCF, whereas double positive $PD\text{-}1^+CTLA\text{-}4^+$ cells were found at a much lower frequency

(Fig. 4.1D). Next, we compared flow cytometry data (memory $CD4^+$ T-cells) with IHC (total $CD4^+$ T-cells) to assess whether these two approaches to quantifying cellular subsets defined by PD-1 and CTLA-4 yielded different results. We found that PD-1^- subsets were identified at a higher frequency using IHC, whereas PD-1^+ subsets were identified at a higher frequency using flow cytometry (Fig. 4.1E).

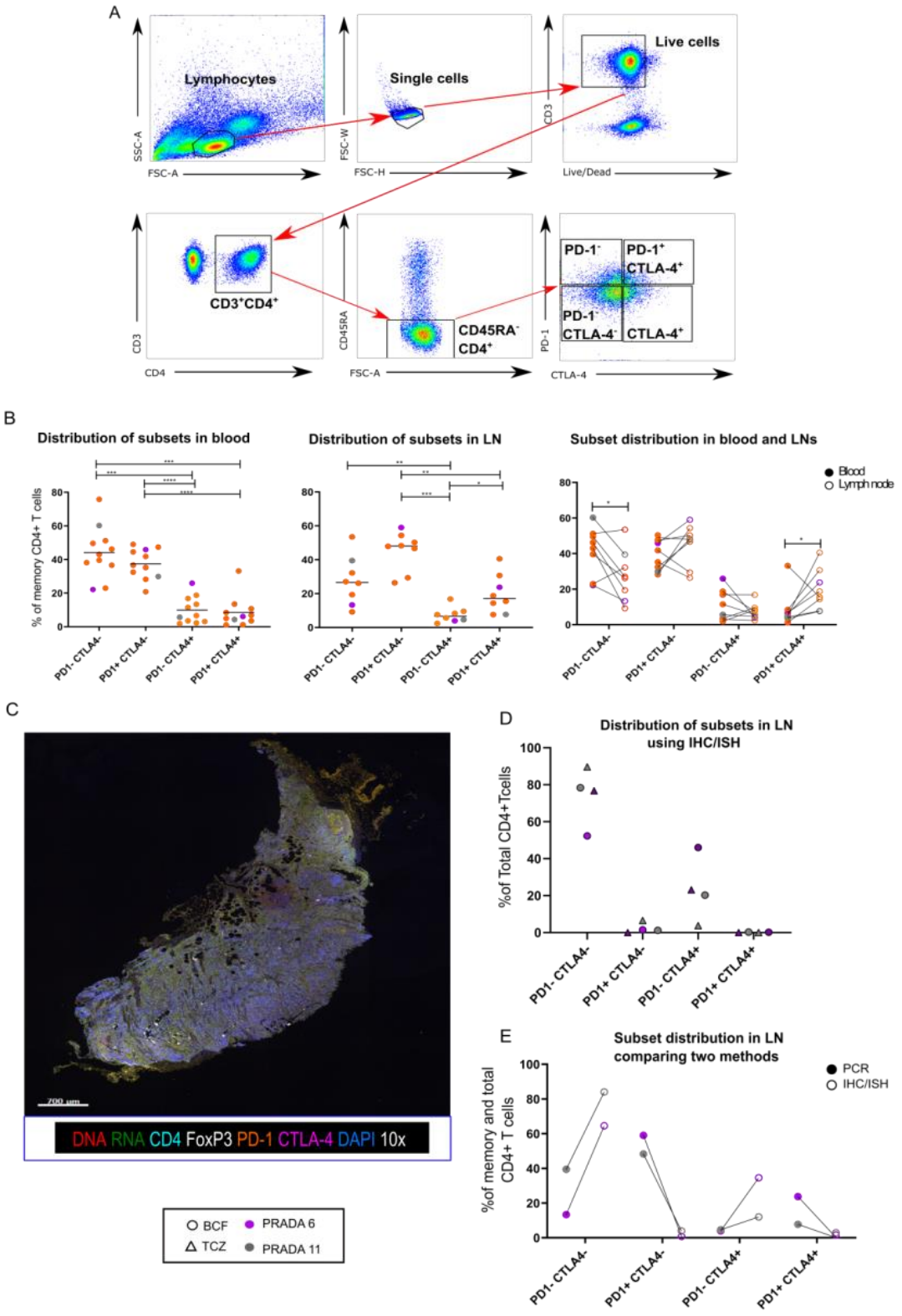

Figure 4.1. Memory CD4$^+$ T-cells in PLWH on ART express ICs and harbor HIV-1 DNA. A) Sorting strategy to collect memory CD4$^+$ T-cells expressing PD-1 or CTLA-4. B) The percentage showing the distribution of CD4$^+$ T-cells expressing PD-1 and CTLA-4 in matched blood (n=11, first figure), LNs (n=8, second figure) and comparison between blood and LNs (last figure) using flow cytometry. C) FFPE sections from LNs were

prepared from two PLWH on ART that were part of this study cohort. HIV-1 RNA^+ and/ or DNA^+ cells were stained in combination with the Opal system (Method, Section 4.2.9). Quantification of the HIV-1 RNA^+ and/ or DNA^+ cells was carried out using RNA/DNAscope and imaging on the HALO analysis software (Method, Section 4.2.10). DAPI was used for nuclear counterstain of the cells in each zone, and micrographs were taken at 10 and 20x magnification using the Vectra™ multispectral imaging software (Method, Section 4.2.10). Scale =500 µm. For each donor, two regions of interest were taken. Representative of multiplex IHC composite image (10x) of a participant on ART (PRADA011), depicting simultaneous detection of HIV-1 DNA (red) and RNA (green) in combination with antibodies for T-cell expression markers CD4 (cyan), Treg marker FoxP3 (white), and ICs markers CTLA-4 (magenta) and PD-1 (orange) in dotted lines. D) Images were analysed with HALO to quantify the distribution of $CD4^+$ T-cells expressing $PD\text{-}1^{+/-}$ /$CTLA\text{-}4^{+/-}$ (alone or in combination) on ART in either the BCF (closed circle) or the TCZ (closed triangle). E) The percentage of memory $CD4^+$ T-cells subsets using PCR and RNA/DNAscope with multiplex IHC. Data from subsets with fewer than (10.000) sorted cells were excluded when undetectable. Sample averages are indicated by the horizontal bar on each graph, and Wilcoxon matched pairs signed-rank test were used to compare the distribution between blood, LNs and two methods; sorted subsets (full circles) and RNA/DNAscope with IHC (closed circles) between samples from the same individuals. The data showed as log10. Each participant is shown by a different colour (n=2 subjects). *$p < 0.05$; **$p < 0.01$; ***$p < 0.001$; ****$p < 0.0001$. Samples are colour coded for each memory $CD4^+$ T-cell subset. LN: lymph node; FC: flow cytometry; IHC: immunohistochemistry; ISH: *in situ* hybridization.

4.3.3 CD4$^+$ T-CELLS IN BLOOD THAT EXPRESS CTLA-4 ARE ENRICHED FOR HIV-1

DNA and RNA were extracted from memory CD4$^+$ T-cells that were derived from LN tissue and sorted according to their expression of PD-1 and CTLA-4. We then quantified the frequency of cells containing HIV-1 DNA across all four subsets.

To address whether the frequency of infected cells might differ between blood and LN memory CD4$^+$ T-cell PD-1/CTLA-4 subsets, we directly compared the level of HIV-1 DNA within each subset across LN and blood. We found that the level of HIV-1 DNA was significantly higher in memory CD4$^+$ T-cells expressing CTLA-4 compared to double negative and SP PD-1$^+$ cells in blood, this trend was also demonstrated in LN but did not reach statistical significance (Fig. 4.2A-B). Furthermore, when we compared blood and LN cells within each PD-1/CTLA-4 subset, we found that the frequency of cells containing HIV-1 DNA was not significantly different across the tissue types (Fig. 4.2C).

Next, we investigated whether *in situ* hybridization (ISH) RNA/DNAscope combined with multiplex immunohistochemistry (mIHC) would provide a similar estimate of the frequency cells containing HIV-1 as compared to PCR performed on sorted PD-1/CTLA-4 subsets. This comparison indicated that the ISH approach generally found HIV-1$^+$ cells at a lower frequency, except for the PD-1neg CTLA-4$^+$ subset in one participant (Fig. 4.2 D).

We then examined the frequency of HIV-1 infection (HIV-1 RNA$^+$ and HIV-1 DNA$^+$ cells combined) using both RNA$^+$ and/ or DNA$^+$ cells expressing PD-1 and/or CTLA-4. Cells in the LN tissue were divided into Tregs, nonTregs and CD4neg T-cells in both the BCF and/or TCZ. We found HIV-1 in CTLA-4$^+$ cells in both nonTregs, Tregs and CD4neg cells in BCF and/or TCZ in one out of the two participants (Fig. 4.2E, i). In the total PD-1$^+$ cells from the same participant, infected cells were rarely found and only seen in total cells or in CD4neg cells in the BCF (Fig. 4.2E, ii).

Lastly, we compared nonTregs and Tregs across all four subsets of PD-1/CTLA-4 cells (Fig. 4.2 F). This showed that for both Tregs and nonTregs, HIV-1$^+$ infection was primarily seen in CTLA-4$^+$ SP cells in and was identified both in the BCF and the TCZ although not consistently across both donors (Fig. 4.3F, i).

Altogether these data demonstrate that HIV-1 can be preferentially found in FoxP3^{+} CTLA-4^{+} expressing cells, although these cells make up only a small part of the reservoir, and HIV-1 was found less frequently in PD-1^{+} cells which were found in the BCFs. These findings are aligned with previous observations that cells expressing PD-1^{+} and CTLA-4^{+} contribute to the HIV-1 reservoir [155,199,459,555].

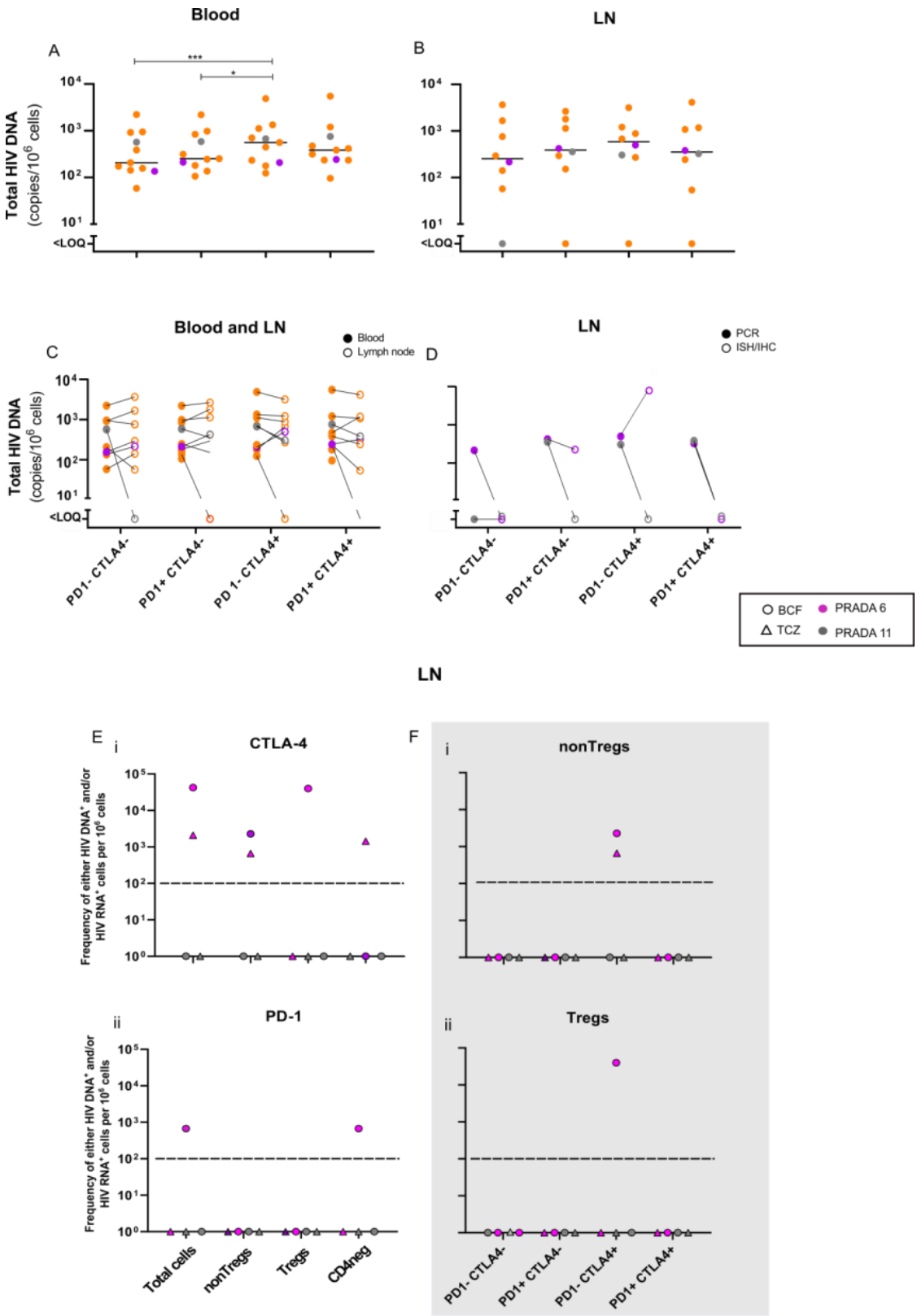

Figure 4.2. The frequency of CD4$^+$ T-cell subsets producing HIV-1 RNA and DNA in HIV-1 infected individuals on ART using. A-C) Representative total HIV-1 DNA quantities from PD-1 and/or CTLA-4 sorted subsets (alone or in combination)

in blood and/or LNs from participants on ART. D) Data shows total HIV-1 DNA and/or RNA in sorted subsets using flow cytometry (closed circles) or subsets quantified using RNA/DNAscope in combination with ISH and IHC (empty circles) in LNs from individuals on ART. E) Frequency of HIV-1 RNA^+ and/ or DNA^+ in $PD\text{-}1^+$ subsets (i) and $CTLA\text{-}4^+$ subsets (ii). F) Frequency of HIV-1 RNA^+ and/ or DNA^+ in nonTregs (i) and Tregs (ii) across $CD4^+$ T-cell subsets expressing PD-1/CTLA-4 in LNs using the IHC/ISH method. Data from subsets with fewer than (10.000) sorted cells were excluded when undetectable. Wilcoxon matched pairs signed-rank test were used to compare the distribution between blood, LNs and two methods; sorted subsets (full circles) and RNA/DNAscope with IHC (closed circles) between samples from the same participants. The data showed as log10. All study participant are shown in a uniform colour (orange), except for the two participants which were further used to compare PCR with ISH/IHC (n=2 subjects, grey or purple). *$p < 0.05$; **$p < 0.01$; ***$p < 0.001$; ****$p < 0.0001$. LN: lymph node; FC: flow cytometry; IHC: immunohistochemistry; ISH: *in situ* hybridization.

4.3.4 CD4$^+$ T-CELLS IN BLOOD THAT CO-EXPRESS PD-1 AND CTLA-4 ARE ENRICHED FOR CA US AND MS HIV-1 RNA

Cell associated HIV-1 RNA in PLWH on ART is frequently used as an important marker of the the transcriptional activity of the reservoir [602,603]. CA-US HIV-1 RNA has also been shown to predict the time to viral rebound following cessation of ART in another study [604]. In comparison, multiply-spliced HIV-1 RNA (MS HIV-1 RNA) transcripts are usually absent in latently infected cells but are produced upon viral reactivation, emphasising that cells containing MS RNA are enriched for functional virus [605].

We quantified the level of CA-US HIV-1 RNA in all PD-1/CTLA-4 subsets in blood and LN from PLWH on ART to investigate whether any cellular subset was enriched for HIV-1measurable RNA levels (Fig. 4.3). We found moderately higher levels of CA-US HIV-1 RNA within PD-1negCTLA-4$^+$ cells in blood, however we did not see any statistically significant differences between blood and LN tissue in any of the four subsets (Fig.4.3A). We next measured MS HIV-1 RNA but found that these transcripts were rarely detectable in blood and LN samples from all ART treated PLWH (Fig. 3B).

In summary, these data identify subsets of memory CD4$^+$ T-cells which express CA-US but cells containing MS HIV-1 RNA were very infrequent. Also, there were no significant differences in the transcriptional activity between blood and LN across all four subsets. Of note, we could only assess LN samples obtained for MS HIV-1 RNA for no more than three individuals compared to cells obtained from the blood.

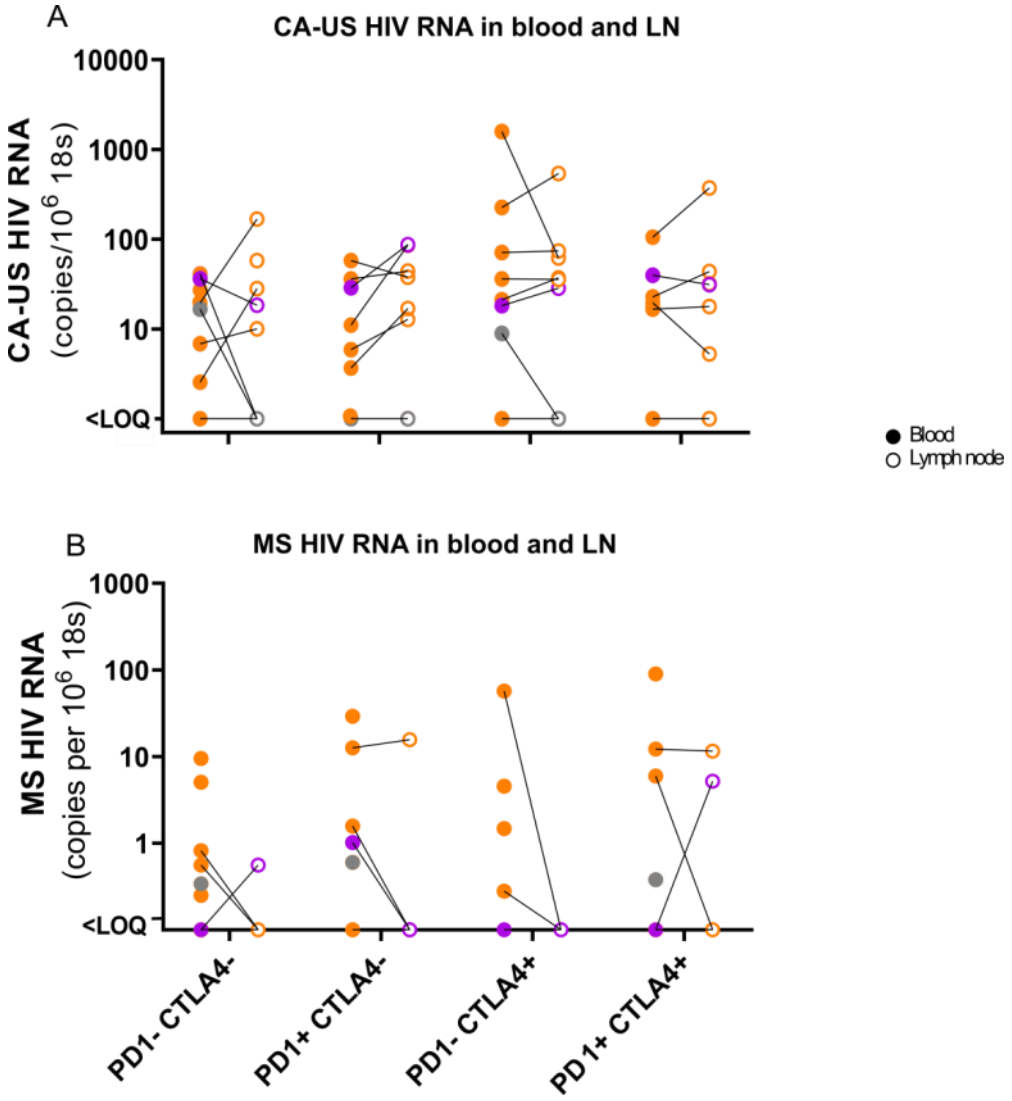

Figure 4.3. The frequency of CD4⁺ T-cell subsets producing HIV-1 RNA and DNA in HIV-1 infected individuals on ART. A) CA-US HIV-1 DNA was quantified by qPCR from memory CD4⁺ T-cell sorted subsets in blood and LN and presented as copy number per million 18S RNA. B) Frequency of memory CD4⁺ T-cells expressing MS HIV-1 RNA per million in sorted ICs subsets unstimulated in blood and LN. Data from subsets with fewer than (10.000) sorted cells were excluded when undetectable. Wilcoxon matched pairs signed-rank test were used to compare the distribution between blood, LNs between samples from the same individuals. The data showed CA-US HIV-1 RNA and MS HIV-1 RNA as log10. All study participants are shown in a uniform colour (orange), except for the two participants (n=2 subjects, grey or purple). *$p < 0.05$; **$p < 0.01$; ***$p < 0.001$; ****$p < 0.0001$. Samples are colour coded for each memory CD4⁺ T-cell subset. LN: lymph node; CA-US HIV-1 RNA: cell-associated unspliced HIV-1 RNA; MS HIV-1 RNA: multiply-spliced HIV-1 RNA.

4.4 DISCUSSION

We aimed to determine the contribution of cells expressing PD-1 and/or CTLA-4 to the HIV-1 reservoir in blood and LN tissue in PLWH on ART, using both PCR quantification of HIV-1 DNA and RNA as well as IHC. We demonstrate that in PLWH on ART; 1. a significant enrichment of HIV-1 DNA in $CD4^+$ memory T-cells expressing CTLA-4^+ cells in blood compared to single positive PD-1^+ and DN cells and a modest increase of HIV-1 DNA in CTLA-4^+ cells compared to SP PD-1^+, double positive and double negative cells; 2. we did not identify any differences between blood and LNs in levels of HIV-1 DNA, cell-associated HIV-1 DNA, US HIV-1 RNA or MS HIV-1 RNA; 3. using ISH/IHC we demonstrated that CTLA-4^+ infected cells were found in both the TCZ and BCF of the LN and included both Tregs and non Tregs. Virus was also detected in PD-1^+ cells but at a lower frequency than CTLA-4^+ cells.

Previous studies have done similar analyses but there are important differences worth highlighting; 1. limited in sorted subsets in LNs, 2. were only performed in SIV-rhesus macaques other than humans, 3. did not sort for PD-1 alone [131] or 4. did not further characterize CTLA-4^+ cells found in the follicles [155].

We observed a significant enrichment of HIV-1 DNA in memory $CD4^+$ T-cells expressing CTLA-4^+ cells compared to single positive PD-1^+ and double negative cells in blood. There was no enrichment of HIV-1 in single positive CTLA-4^+ cells in LN compared to double negative, double positive and single positive PD-1 subsets. In addition, IHC result suggests that CTLA-4^+ cells are distributed between the TCZ and the BCFs of the LN in PLWH on ART, highlighting the importance between both regions. Infected Tregs identified in the BCF, share a similar phenotype as follicular Tregs ($FoxP3^+$ CTLA-4^+) which are located in the mantel zone region of the follicles [606]. The persistence of HIV-1 in PLWH on ART in Tregs and nonTregs within the TCZ and BCFs could be explained by the anatomical location of the BCF, which has shown to be an immune-privileged site, restricting entry of HIV-1-specific cytotoxic T-cells [607] and potentially also due to impaired ART penetration into LN tissue compared to blood [596].

Although we only examined two participants with IHC, our findings are consistent with a previous study which identified preferential viral persistence in a subset of memory $CD4^+$ T-cells expressing CTLA-4^+ cells in SIV-infected NHPs on suppressive ART [155]. Notably, HIV-1 infected single positive PD-1^+ cells from the same

participant were only seen in total cells or in CD4neg cells. We speculate that these CD4neg cells are in fact a subset of $CD4^+$ T-cells, i.e., Tfh cells which have lost their surface expression and are mainly found in the BCF. A previous study demonstrated that PD-1-expressing memory $CD4^+$ T-cells contained high levels of HIV-1 DNA and that the majority of replication-competent and infectious HIV-1 were found in LN $PD\text{-}1^+$ cells, many of which are Tfh cells[131]. However, this study did not look at PD-1 solely, instead this was performed on total double positive $PD\text{-}1^+$ $CTLA\text{-}4^+$ CXCR5 $CD4^+$ T-cell populations in blood and LN [131].

4.4.1 LIMITATIONS

There are some limitations of our study that require consideration. First, of the 11 participants enrolled, we were only able to acquire LN memory $CD4^+$ T-cells from 8 individuals, which limited our ability to detect minor differences in HIV-1 persistence between PD-1/CTLA-4 subsets in LN tissue. Second, as memory $CD4^+$ T-cells expressing CTLA-4 were relatively rare and due to the limited number of memory $CD4^+$ T-cells that were collected in a single LN, we were not able to analyse as many $CTLA\text{-}4^+$ as $CTLA\text{-}4^-$ cells in tissue. Thirdly, due to reports demonstrating that the majority of proviruses are defective [608], it is important to address whether persistent HIV-1 on ART is inducible across the PD-1/CTLA-4 subsets, but this was not possible in this study due to limited cell numbers of sorted LNs. Fourthly, we were only able to perform IHC/ISH in two individuals, as LNs were first frozen in OCT and then FFPE allowing for water in LNs to turn into ice crystals during snap-freezing, as a result affecting the tissue structure and limiting us in analysing more regions of interest. Finally, when comparing sorted cells with IHC/ISH methods across all four subsets, $CD4^+CD45RA^-$ was used to characterize memory $CD4^+$ T-cells for the sorted cells, however, only CD4 antibody was used for IHC/ISH.

4.4.2 CONCLUSION

These observations demonstrate direct quantification of measures of HIV-1 persistence within purified subsets of memory $CD4^+$ T-cells defined by their expression of PD-1 and CTLA-4 in a human cohort. The ability to perform these analyses in both blood and LN tissue furthermore enabled investigations of the anatomical location of infected cellular subsets within LN tissue.

In conclusion, our results suggest that the frequency of infected cells is higher in memory $CD4^+$ T-cells that express SP CTLA-4 in blood and LNs. When we used IHC/ISH for characterising the reservoir, we demonstrated that infected single positive CTLA-4^+ infected cells can be found in the BCF and the TCZ. Most importantly, nonTregs and Tregs enriched for HIV-1 were in PD-1^- CTLA-4^+ subsets found in both the BCFs and TCZs. Therefore, these findings provide the rationale to develop safe strategies to target PD-1/CTLA-4 to eliminate the reservoir and/or potentially targeting infected cells in the BCFs using antiviral chimeric antigen receptors (CAR) T-cells engineered with homing receptors that will enhance migration into the BCFs.

Chapter 5: **Discussion**

5.1 SUMMARY

In summary, this thesis demonstrated the successful establishment of a microscopic multiplex IHC method that is based on the combination of ISH and IHC with the possibility of whole-slide analysis of HIV-1 RNA, DNA, and immune cells. In addition, ISH/IHC could be applied to cell lines, in *vitro models* of latency and LN tissue from PLWH to study HIV-1 persistence with colocalization of HIV-1 DNA and RNA in the same tissue section. Also, using this method, we were able to distinguish cells based on their IC expression or Treg phenotype and showed that Tregs were infected with HIV-1 more frequently than nonTregs. However, further studies are needed to confirm these observations, as the overall contribution of infected Tregs to the overall reservoir remains small. This makes studying Tregs very challenging when comparing the size of the reservoir to other subsets, as most quantitative analysis, such as the qVOA, TILDA and the intact proviral DNA assay (IPDA) require at least one million $CD4^+$ T-cells and preferably much more (Section 1.7).

We extended this study by comparing the contribution of cells expressing programmed cell death protein-1 (PD-1) and/or cytotoxic T-lymphocyte-associated protein 4 (CTLA-4) to the HIV-1 reservoir in LN and blood from PLWH on ART. Using both PCR quantification and ISH/IHC, we demonstate that memory $CD4^+$ T-cells that express single positive (SP) CTLA-4 had a higher frequency of infected cells in blood and LNs and were distributed in the BCF and the TCZ in LNs. Most importantly, nonTregs and Tregs enriched for HIV-1 were in $PD\text{-}1^-CTLA\text{-}4^+$ subsets found in both the BCFs and TCZs.

5.2 ESTABLISHING A MULTIPARAMETER IHC ANALYSIS PLATFORM TO DEFINE THE HIV-1 RESERVOIR IN LN

While several advances have been made towards understanding the tissue reservoir using multi-color flow cytometric analysis, application of this method has

been hampered by technical limitations such as measuring multiple parameters due to spectral overlap and the ability to provide contextual information of cells that are infected and their anatomical location. Although *in situ* immunofluorescence overcome these limitations, they have been restricted by the number of markers to characterize the reservoir by confocal microscopy [155]. We have addressed these limitations and modified the already established RNAscope and DNAscope method by incorporating the tyramide signal amplification (TSA) system with multiplex IHC (mIHC). This allowed us to detect $vDNA^+$ and $vRNA^+$ cells in latent cell lines (ACH2 and J-Lats), in an *in vitro* model established in our lab, and in LN from PLWH on and off ART that were formalin-fixed paraffin embedded (FFPE) (Section 2.3).

Using the TSA system, we were able to successfully distinguish between HIV-1 infected cells ($vDNA^+$) cells that are transcriptionally silent ($vRNA^-$) and cells that are actively transcribing viral RNA ($vRNA^+$), as well as determine number of copies of proviruses in each cell (Section 2.3). Surprisingly, when we used J-Lat cells to determine if the imaging software Halo (Section 3.2.5) could accurately quantify the number of proviruses in each cell, we found limitations because of the probes used. First, there were multiple copies detected per cell. The sense HIV-1 DNA probes used in this study (Section 2.4) only targets half the viral genome (4.5kb) [297]. Second, another possible limitation of the probes used is that cells will be represented in multiple sections (3-5μm) and targets under-represented. The analysis could miss information whether molecules are expressed in the same cell due to section thickness in the z-axis [609]. Therefore, further research is needed to overcome this. Z-stack image analysis, which gives a greater depth of field, can be used for proximal location to determine whether molecules are expressed in the same cell or the location of the cell [610].

We have successfully developed a 7-plex platform using the TSA fluorescent system to detect cellular phenotype allowing us to characterize the HIV-1 reservoir in LN from PLWH on and off ART. Using this method, we simultaneously detected seven markers including HIV-1 DNA and RNA in a single FFPE tissue slide using multispectral Vectra imaging, while providing important contextual information. This important new method may provide a better understanding of the reservoir phenotype and predominate location, which has been limited in a previous study [155].

Although this platform allows us to distinguish $vRNA^+$ cells from $vDNA^+$ cells, one of the limitations is that this method does not detect ongoing viral replication and reactivation of latent cells. However, a new approach, termed Basescope promises to address these limitation in FFPE tissue, by identifying exon splice junctions[298].

5.3 LN AS A SANCTUARY SITE FOR HIV-1 REPLICATION

Increasing evidence has shown the importance of lymphoid tissue including GALT and LN as important sites for persistence of the latent reservoir [219,265]. A more in depth analysis using *in situ* (ISH) imaging approaches revealed that infected cells can be found distributed in different anatomical locations, including the B-cell follicle (BCFs) in PLWH [131,297] and the T-cell zones (TCZs) in SIV-infected macaque[155]. Although a more recent study has looked at LNs during HIV-1 persistence, cells were isolated as single cells which loses important spatial details such as their location [285]. We used our ISH/IHC method to simultaneously look at both the BCF and the TCZ in PLWH, to compare the distribution of the viral reservoir in these sites. Our data is consistent with what has been reported, which is that HIV-1 can be detected in both BCF and the TCZ. However, these studies have only looked at tissue regions from SIV-infected macaques and not humans [131,155]. Although our numbers were too small to allow for formal statistical comparison, we found a higher frequency of HIV-1-infected cells in the BCF compared to the TCZ (Fig. 3.1E), confirming the BCF as the primary site of HIV-1 persistence in PLWH on ART. Early studies have pointed out the persistence of HIV-1 in lymphoid tissue, where the BCFs [131,155,297] may be functioning as an immune-privileged site with restricted access of HIV-1-specific cytotoxic $CD8^+$ T-cells [212,588]. In this model, only $CD8^+$ T-cells that express chemokine receptor CXCR5 on their surface can selectively enter the BCF and eliminate infected cells [212,611].

One potential explanation for continuous detection of both HIV-1 DNA and RNA in LN tissue, is the low penetration of ART into LN tissue compared to blood [612]. In addition, drug penetration is dependent on the size of the lymphoid lobule (cortex and paracortex region) due to immune activation [596]. New strategies that specifically deliver ART to LNs should be explored in the future. One approach is to use nanoformulations. Nanoformulations can enhance drug penetration and function as a nanodrug by taking nanoparticles up into cells via endocytosis[613], releasing drugs to LNs and clearing infected cells [614]. Despite the increasing interest, there are

still significant gaps in knowledge of the underlying mechanisms, i.e., drug release. Additionally, chimeric antigen receptors (CAR) T-cells that target the HIV-1 envelope could also play a role by enhancing their localisation to the BCFs [615,616]. A recent study further explored this novel approach by developing an *ex vivo* BCF migration assay and showed that CAR-T/CXCR5 selectively migrated into the BCF and lead to *in vitro* viral suppression [617]. Although this study design has shown promising results in an animal model, there are still some challenges to take into consideration. One of the main challenges is the potential risk of CAR-T-cells becoming infected as the CD4 receptors are genetically modified to construct anti-HIV-1 CARs responses and the need for antigenic stimulation of latent cells in the BCFs.

5.4 TREGS AS A RESERVOIR DURING HIV-1 PERSISTENCE

There are ongoing studies investigating other T-cell subsets, i.e., Tregs and their potential contribution to the HIV-1 reservoir. To date, only a few studies have shown that Tregs are infected by HIV-1 *in vivo*, thereby potentially contributing to the HIV-1 reservoir [437,438,618]. Although there has been evidence of Tregs containing HIV-1 in lymphoid tissue, little is known about their distribution during HIV-1 persistence in tissue. Using our ISH/IHC method, we found that Tregs are indeed a reservoir for HIV-1 infection and are more frequently infected compared to nonTregs (Section 3.3). Our approach using TSA and RNA/DNA scope demonstrated the distribution of infected cells in LN and that infected Tregs were found in both TCZ and BCF, however, they were found predominantly in the BCF in PLWH on and off ART (Section 3.3). Due to a restricted panel, we were unable to further investigate the phenotype of infected Tregs found in the BCFs, however, we speculate that these cells could potentially be follicular regulatory T-cells (Tfr) cells, a unique subset of Tregs [401]. A previous study, which also looked at HIV-1 persistence in LNs, showed infection of a $CD4^+$ T-cell subset that was suggested to be Tfr cells, however Tregs were sorted based on immune checkpoints (ICs) expression and not FoxP3 or CXCR5 to confirm these cells were indeed Tregs [155]. Another study demonstrated that Tfr cells in the BCFs were expanded in PLWH compared to non-infected participants. Tfr cells are able to impair the function of follicular helper (Tfh) cells [619] as binding of HIV-1 to the CD4 receptor enhances their suppressive functions [620].

There has been conflicting results concerning the frequency of Tregs in HIV-1-infected participants on and off ART [425,427,429,621–624], which may be related to the lack of consistent phenotypic markers used to characterize Tregs. In our study we did not observe any significant differences in Tregs frequency between PLWH on or off ART (Fig. 3.2).

When combined with the before mentioned human studies, which clearly demonstrate replication-competent HIV-1- in peripheral blood Tregs, there is strong evidence that Tregs can contribute to the HIV-1- reservoir. In the future, it will be important to determine whether strategies that specifically target Tregs could be used. One such approach could be using Ontak which targets human $CD25^{+}$ cells by binding to IL-2 fused with diphtheria toxin, subsequently leading to cell death [514].

5.5 OVERALL CONTRIBUTION OF TREGS TO THE HIV-1 RESERVOIR

There have been a few studies demonstrating the quantitative contribution of Tregs to the HIV-1 reservoir [435,437,438]. We have shown that the frequency of infection was higher in PLWH off ART compared to those on ART. However, the frequency of Tregs was small, so the contribution of infected Tregs to the overall reservoir size is small (Fig. 3.2 and Fig 4.3). Therefore, it is worth improving methods that will deliver a high Treg yield during Treg isolation processing. Another potential solution for studying Tregs is single-cell analysis which will circumvent the issue of low frequency of Tregs as this technology particularly characterises rare cell populations based on their gene expression profiles [625].

5.5.1 TREG PROPERTIES THAT CONTRIBUTE TO HIV-1 PERSISTENCE

We have demonstrated that Tregs are indeed a reservoir for HIV-1 in lymphoid tissue and that HIV-1 is potentially higher in Tregs compared to nonTregs (Fig. 3.2). There are several potential mechanisms by which Tregs may be enriched for HIV-1. A previous study provided evidence for their susceptibility to HIV-1 infection through high expression of CCR5 [626]. This study also showed that their survival was promoted by FoxP3-mediated inhibition of the HIV-1 long-terminal repeat, ultimately contributing to the establishment of latency [626]. Another potential

explanation is that FoxP3 expression may downregulate the apoptosis-mediating surface antigen, also known as Fas and Fas ligand production, increasing their survival as Tregs become resistant to apoptosis [627,628]. Exposure of Tregs to HIV-1 also promoted their survival in an *in vitro* model through a CD4-gp12 depedent pathaway, resulting in an increase of Tregs with active viral replication [194]. Paiardini and colleagues also demonstatred Tregs as a potential reservoir in an *ex vivo* study using SIV-infected rhesus macaques (RM) in which they found that memory $CD4^+$ T-cells expressing $CTLA\text{-}4^+PD\text{-}1^-$, which phenotypically overlap with Tregs, contained higher levels of anti-apoptotic Bcl2, promoting their survival [155].

Additionally, the depletion of $CD4^+CD25^+$ Tregs also provided evidence for their survival in which the depletion of Tregs led to an increase of cytotoxic T-cell granzyme-B [437] and an increase of activation markers in PLWH on ART during $CD4^+CD25^+CD127^-$ Treg depletion [438].

5.5.2 IMMUNE CHECKPOINT (IC) CONTRIBUTION TO HIV-1 PERSISTENCE

Our data showed an enrichment of HIV-1 in $CD4^+$ T-cells that express ICs in blood and in LNs in PLWH on and off ART (Fig. 3.3, 4.2 & 4.3). This data supports other observations which have demonstrated that ICs play a role for HIV-1 persistence, likely through HIV-1-associated immune exhaustion and establishing and maintaining HIV-1 latent reservoirs [131,555,629]. We demonstrated that cells in PLWH off ART frequently expressed more PD-1 and CTLA-4 than cells obtained from PLWH on ART (Fig. 3.3A). Tregs in PLWH express significantly higher levels of PD-1, T-cell immunoglobulin and mucin-domain containing-3 (TIM-3), CTLA-4, and lymphocyte activation gene 3 (LAG3) compared with those from PLWH on ART or healthy individuals [630–633]. This was also demonstrated in an *in vitro* study in which the presence of HIV-1 enhanced CTLA-4 expression on Tregs [634]. It was also found that T- cells residing within the LN compartment exhibited even greater levels of inhibitory receptors when compared to the peripheral blood [635].

In addition to their role in HIV-1-associated immune exhaustion, several studies have also shown expression of PD-1 and other ICs, i.e., LAG3 and T-cell immunoglobulin and ITIM domain (TIGIT) play a role for HIV-1 persistence on ART. In samples obtained from PLWH on ART, $CD4^+$ T-cells co-expressing these

markers were highly enriched for HIV-1 as demonstrated by a significant positive correlation between expression of ICs and the higher frequency of integrated HIV-1 DNA and also an gradual enrichment of HIV-1 in cells expressing multiple markers [459,636,637]. It has also been shown that LN PD-1$^+$ cells from PLWH on ART, the majority of which were characterized as Tfh cells, were enriched for HIV-1 DNA [131] and that CTLA-4$^+$ cells are enriched for SIV DNA [155].

In addition CTLA-4 expression can lead to activation or cross linking by upregulating Bcl2 and as a result prevent apoptosis by limiting Fasl-FasL expression [627]. In summary, the co-expression or single expression of ICs is associated with HIV-1 persistence and is a key mechanism for the functional impairment of HIV-1-specific T-cells.

5.6 ICS IN CURE STRATEGIES

Blockade of co-inhibitors such as PD-1 and CTLA-4 have produced clinically significant antitumor effects in clinical cancer trials by augmenting tumour-directed T-cell responses. Such therapy may also have a role in eliminating HIV-1 reservoirs although therapeutic efficacy remains to be demonstrated and there are concerns of immune-related adverse effects. Using an *in vitro* model of HIV-1 latency, we recently showed that anti-PD1 and anti-CTLA4 could reverse HIV-1 latency, but the antibodies had different target cells with anti-PD1 targeting non-proliferating and anti-CTLA4 targeting proliferating infected CD4$^+$ T-cells [578]. In SIV infected non-human primates on suppressive ART, anti-PD1 in combination with anti-CTLA4 was more effective than anti-PD1 alone in reversing SIV latency and inducing plasma viremia leading to a reduced frequency of latent infection in blood and LN CD4$^+$ T cells. We recently observed similar results in a cohort of PLWH on ART with cancer, where combination therapy with anti-PD1 and anti-CTLA4 significantly increased HIV-1 production in latently infected cells, which was not seen with anti-PD1 alone (Rasmussen CID, in press).

5.7 FUTURE DIRECTIONS

Having demonstrated that HIV-1 can persist in both PD-1$^+$ and CTLA-4$^+$ cells in both the BCF and TCZ from PLWH on ART, further studies that investigate targeting cells expressing ICs and Tregs should be pursued. These approaches include; 1. the depletion of Tregs through targeting CD25 which can significantly

decrease Tregs, as previously shown [515]; 2. targeting CCR4 receptor on Tregs which demonstrated a decrease in LNs [520]; 3. targeting GITR, which can downregulate Treg function, [638] and diminish Tregs [639] in cancer models; 4. targeting ICs with anti-CTLA-4 (ipilimumab) which has been shown to reverse latency in an HIV-infected individual on ART [539] and in SIV-infected non-human primates on ART [533]. In addition, CAR T-cells are a promising approach for targeting infected cells in the BCFs that persists on ART, that is worth further exploration, despite the limitations such as adverse events and off target effects [510].

Basescope, a recent ISH advancement to the RNAscope technique has been developed by ACD. Although very similar, this approach differs by its ability to incorporate an additional signal amplification step to increase the sensitivity without increasing background noise. Additionally, this assay requires only 1-6 double Z probe pairs to target RNA sequences as short as 50 bp [640]. Although there are no studies using Basescope for the detection of HIV in tissue from PLWH on ART, this approach could be used to detect MS HIV RNAs, determining whether HIV-infected cells in FFPE is a surrogate for intact and/or replication-competent virus expressed either constitutively or after stimulation, as we recently demonstrated using whole blood [641].

5.8 CONCLUDING REMARKS

The findings of this thesis are aligned with recent data performed in our lab, showing that HIV-1 is enriched in cells that express ICs [555].

In conclusion, my work has established several new techniques to better understand where HIV-1 persists in tissue in PLWH on ART. We developed a technique to differentiate between latently and productively infected cells using both *in vitro* models and patient tissue. Furthermore, using the TSA system, we could further phenotype the infected cells. We demonstrated that HIV-1 can persist in both PD-1^+ and CTLA-4^+ cells in both the BCF and TCZ. Although Tregs are also infected, they were only a subset of total CTLA-4^+ cells. New tools to characterise the reservoir are still needed and the work in this thesis provides further insight into the role of both immune checkpoints and Tregs.

Bibliography

1. Barré-Sinoussi, F. *et al.* Isolation of a T-lymphotropic retrovirus from a patient at risk for acquired immune deficiency syndrome (AIDS). *Science* **220**, 868–871 (1983).
2. Frank, T. D. *et al.* Global, regional, and national incidence, prevalence, and mortality of HIV, 1980–2017, and forecasts to 2030, for 195 countries and territories: a systematic analysis for the Global Burden of Diseases, Injuries, and Risk Factors Study 2017. *The Lancet HIV* **6**, e831–e859 (2019).
3. World Health Organization. *World health statistics 2014.* (World Health Organization, 2014).
4. HowAIDSchangedeverything/factsheet. (2014).
5. Granich, R. *et al.* Trends in AIDS Deaths, New Infections and ART Coverage in the Top 30 Countries with the Highest AIDS Mortality Burden; 1990–2013. *PLoS ONE* **10**, (2015).
6. Chun, T.-W. *et al.* In vivo fate of HIV-1-infected T cells: Quantitative analysis of the transition to stable latency. *Nat Med* **1**, 1284–1290 (1995).
7. Hosmane, N. N. *et al.* Proliferation of latently infected CD4+ T cells carrying replication-competent HIV-1: Potential role in latent reservoir dynamics. *Journal of Experimental Medicine* **214**, 959–972 (2017).
8. Dolutegravir-Based or Low-Dose Efavirenz–Based Regimen for the Treatment of HIV-1. *New England Journal of Medicine* **381**, 816–826 (2019).
9. Venter, W. D. F. *et al.* Dolutegravir plus Two Different Prodrugs of Tenofovir to Treat HIV. *New England Journal of Medicine* **381**, 803–815 (2019).

10. Granich, R. *et al.* Trends in AIDS Deaths, New Infections and ART Coverage in the Top 30 Countries with the Highest AIDS Mortality Burden; 1990–2013. *PLoS One* **10**, (2015).
11. Muesing, M. A. *et al.* Nucleic acid structure and expression of the human AIDS/lymphadenopathy retrovirus. *Nature* **313**, 450–458 (1985).
12. Bubeck, D. *et al.* The Structure of the Poliovirus 135S Cell Entry Intermediate at 10-Angstrom Resolution Reveals the Location of an Externalized Polypeptide That Binds to Membranes. *J Virol* **79**, 7745–7755 (2005).
13. Strebel, K. HIV accessory proteins versus host restriction factors. *Curr Opin Virol* **3**, 692–699 (2013).
14. Malim, M. H. & Emerman, M. HIV-1 accessory proteins--ensuring viral survival in a hostile environment. *Cell Host Microbe* **3**, 388–398 (2008).
15. Turner, B. G. & Summers, M. F. Structural biology of HIV. *J. Mol. Biol.* **285**, 1–32 (1999).
16. Gallo, R., Wong-Staal, F., Montagnier, L., Haseltine, W. A. & Yoshida, M. HIV/HTLV gene nomenclature. *Nature* **333**, 504 (1988).
17. Willey, R. L., Bonifacino, J. S., Potts, B. J., Martin, M. A. & Klausner, R. D. Biosynthesis, cleavage, and degradation of the human immunodeficiency virus 1 envelope glycoprotein gp160. *Proc Natl Acad Sci U S A* **85**, 9580–9584 (1988).
18. Ashorn, P. *et al.* An inhibitor of the protease blocks maturation of human and simian immunodeficiency viruses and spread of infection. *Proc. Natl. Acad. Sci. U.S.A.* **87**, 7472–7476 (1990).

19. Cohen, E. A., Dehni, G., Sodroski, J. G. & Haseltine, W. A. Human immunodeficiency virus vpr product is a virion-associated regulatory protein. *J. Virol.* **64**, 3097–3099 (1990).

20. Sato, A., Igarashi, H., Adachi, A. & Hayami, M. Identification and localization of vpr gene product of human immunodeficiency virus type 1. *Virus Genes* **4**, 303–312 (1990).

21. Zhu, P. *et al.* Distribution and three-dimensional structure of AIDS virus envelope spikes. *Nature* **441**, 847–852 (2006).

22. Liu, J., Bartesaghi, A., Borgnia, M. J., Sapiro, G. & Subramaniam, S. Molecular architecture of native HIV-1 gp120 trimers. *Nature* **455**, 109–113 (2008).

23. Kwong, P. D. *et al.* Structure of an HIV gp120 envelope glycoprotein in complex with the CD4 receptor and a neutralizing human antibody. *Nature* **393**, 648–659 (1998).

24. Rizzuto, C. D. *et al.* A conserved HIV gp120 glycoprotein structure involved in chemokine receptor binding. *Science* **280**, 1949–1953 (1998).

25. Vandegraaff, N. & Engelman, A. Molecular mechanisms of HIV integration and therapeutic intervention. *Expert Rev Mol Med* **9**, 1–19 (2007).

26. Brasey, A. *et al.* The leader of human immunodeficiency virus type 1 genomic RNA harbors an internal ribosome entry segment that is active during the G2/M phase of the cell cycle. *J. Virol.* **77**, 3939–3949 (2003).

27. Klotman, M. E. *et al.* Kinetics of expression of multiply spliced RNA in early human immunodeficiency virus type 1 infection of lymphocytes and monocytes. *Proc. Natl. Acad. Sci. U.S.A.* **88**, 5011–5015 (1991).

28. Purcell, D. F. & Martin, M. A. Alternative splicing of human immunodeficiency virus type 1 mRNA modulates viral protein expression, replication, and infectivity. *J Virol* **67**, 6365–6378 (1993).
29. Stoltzfus, C. M. & Madsen, J. M. Role of viral splicing elements and cellular RNA binding proteins in regulation of HIV-1 alternative RNA splicing. *Curr. HIV Res.* **4**, 43–55 (2006).
30. Marco, A. de *et al.* Structural Analysis of HIV-1 Maturation Using Cryo-Electron Tomography. *PLOS Pathogens* **6**, e1001215 (2010).
31. Colin, L. & Van Lint, C. Molecular control of HIV-1 postintegration latency: implications for the development of new therapeutic strategies. *Retrovirology* **6**, 111 (2009).
32. Rambaut, A., Posada, D., Crandall, K. A. & Holmes, E. C. The causes and consequences of HIV evolution. *Nature Reviews Genetics* **5**, 52–61 (2004).
33. Mitsuya, H., Yarchoan, R. & Broder, S. Molecular targets for AIDS therapy. *Science* **249**, 1533–1544 (1990).
34. Shukla, E. & Chauhan, R. Host-HIV-1 Interactome: A Quest for Novel Therapeutic Intervention. *Cells* **8**, 1155 (2019).
35. Wang, H.-G. H., Williams, R. E. & Lin, P.-F. A novel class of HIV-1 inhibitors that targets the viral envelope and inhibits CD4 receptor binding. *Curr. Pharm. Des.* **10**, 1785–1793 (2004).
36. Cahn, P., Fink, V. & Patterson, P. Fostemsavir: a new CD4 attachment inhibitor. *Current Opinion in HIV and AIDS* **13**, 341–345 (2018).
37. Urano, E. *et al.* Resistance to Second-Generation HIV-1 Maturation Inhibitors. *J. Virol.* **93**, (2019).

38. Tang, C. *et al.* Antiviral inhibition of the HIV-1 capsid protein. *J. Mol. Biol.* **327**, 1013–1020 (2003).

39. Fricke, T., Buffone, C., Opp, S., Valle-Casuso, J. & Diaz-Griffero, F. BI-2 destabilizes HIV-1 cores during infection and Prevents Binding of CPSF6 to the HIV-1 Capsid. *Retrovirology* **11**, 120 (2014).

40. Margolis, D. A. & Boffito, M. Long-acting antiviral agents for HIV treatment. *Curr Opin HIV AIDS* **10**, 246–252 (2015).

41. Sok, D. & Burton, D. R. Recent progress in broadly neutralizing antibodies to HIV. *Nature Immunology* **19**, 1179–1188 (2018).

42. Kuznetsov, Y. G., Victoria, J. G., Robinson, W. E. & McPherson, A. Atomic force microscopy investigation of human immunodeficiency virus (HIV) and HIV-infected lymphocytes. *J. Virol.* **77**, 11896–11909 (2003).

43. Jacobson, J. M. *et al.* Safety, Pharmacokinetics, and Antiretroviral Activity of Multiple Doses of Ibalizumab (formerly TNX-355), an Anti-CD4 Monoclonal Antibody, in Human Immunodeficiency Virus Type 1-Infected Adults. *Antimicrob Agents Chemother* **53**, 450–457 (2009).

44. Henderson, L. E. *et al.* Gag proteins of the highly replicative MN strain of human immunodeficiency virus type 1: posttranslational modifications, proteolytic processings, and complete amino acid sequences. *J Virol* **66**, 1856–1865 (1992).

45. Wiegers, K. *et al.* Sequential steps in human immunodeficiency virus particle maturation revealed by alterations of individual Gag polyprotein cleavage sites. *J. Virol.* **72**, 2846–2854 (1998).

46. Pettit, S. C., Henderson, G. J., Schiffer, C. A. & Swanstrom, R. Replacement of the P1 Amino Acid of Human Immunodeficiency Virus Type 1 Gag Processing

Sites Can Inhibit or Enhance the Rate of Cleavage by the Viral Protease. *J Virol* **76**, 10226–10233 (2002).

47. Smith, P. F. *et al.* Phase I and II study of the safety, virologic effect, and pharmacokinetics/pharmacodynamics of single-dose 3-o-(3',3'-dimethylsuccinyl)betulinic acid (bevirimat) against human immunodeficiency virus infection. *Antimicrob. Agents Chemother.* **51**, 3574–3581 (2007).
48. HIV-1 Gag Polymorphisms Determine Treatment Response to Bevirimat (PA-457). http://www.natap.org/2008/ResisWksp/ResisWksp_23.htm.
49. Hwang, C. *et al.* Antiviral Activity, Safety, and Exposure-Response Relationships of GSK3532795, a Second-Generation Human Immunodeficiency Virus Type 1 Maturation Inhibitor, Administered as Monotherapy or in Combination With Atazanavir With or Without Ritonavir in a Phase 2a Randomized, Dose-Ranging, Controlled Trial (AI468002). *Clin. Infect. Dis.* **65**, 442–452 (2017).
50. Park, J. & Morrow, C. D. Mutations in the protease gene of human immunodeficiency virus type 1 affect release and stability of virus particles. *Virology* **194**, 843–850 (1993).
51. Yant, S. R. *et al.* A highly potent long-acting small-molecule HIV-1 capsid inhibitor with efficacy in a humanized mouse model. *Nature Medicine* **25**, 1377–1384 (2019).
52. Pierson, T. C. *et al.* Intrinsic stability of episomal circles formed during human immunodeficiency virus type 1 replication. *J. Virol.* **76**, 4138–4144 (2002).
53. Pierson, T. C. *et al.* Molecular characterization of preintegration latency in human immunodeficiency virus type 1 infection. *J. Virol.* **76**, 8518–8531 (2002).

54. Williams, S. A. & Greene, W. C. Regulation of HIV-1 latency by T-cell activation. *Cytokine* **39**, 63–74 (2007).

55. Zhou, Y., Zhang, H., Siliciano, J. D. & Siliciano, R. F. Kinetics of human immunodeficiency virus type 1 decay following entry into resting CD4+ T cells. *J. Virol.* **79**, 2199–2210 (2005).

56. Whitney, J. B. & Brad Jones, R. In Vitro and In Vivo Models of HIV Latency. *Adv. Exp. Med. Biol.* **1075**, 241–263 (2018).

57. Siliciano, R. F. & Greene, W. C. HIV Latency. *Cold Spring Harb Perspect Med* **1**, (2011).

58. Shan, L. *et al.* Transcriptional Reprogramming during Effector-to-Memory Transition Renders CD4+ T Cells Permissive for Latent HIV-1 Infection. *Immunity* **47**, 766-775.e3 (2017).

59. Agosto, L. M., Herring, M. B., Mothes, W. & Henderson, A. J. HIV-1-Infected CD4+ T Cells Facilitate Latent Infection of Resting CD4+ T Cells through Cell-Cell Contact. *Cell Reports* **24**, 2088–2100 (2018).

60. Elsheikh, M. M., Tang, Y., Li, D. & Jiang, G. Deep latency: A new insight into a functional HIV cure. *EBioMedicine* **45**, 624–629 (2019).

61. Finzi, D. *et al.* Latent infection of CD4 + T cells provides a mechanism for lifelong persistence of HIV-1, even in patients on effective combination therapy. *Nature Medicine* **5**, 512 (1999).

62. Cameron, P. U. *et al.* Establishment of HIV-1 latency in resting CD4+ T cells depends on chemokine-induced changes in the actin cytoskeleton. *Proc Natl Acad Sci U S A* **107**, 16934–16939 (2010).

63. Pace, M. J. *et al.* Directly Infected Resting CD4+T Cells Can Produce HIV Gag without Spreading Infection in a Model of HIV Latency. *PLOS Pathogens* **8**, e1002818 (2012).

64. Chavez, L., Calvanese, V. & Verdin, E. HIV Latency Is Established Directly and Early in Both Resting and Activated Primary CD4 T Cells. *PLoS Pathog.* **11**, e1004955 (2015).

65. Vatakis, D. N., Kim, S., Kim, N., Chow, S. A. & Zack, J. A. Human immunodeficiency virus integration efficiency and site selection in quiescent CD4+ T cells. *J. Virol.* **83**, 6222–6233 (2009).

66. Lindqvist, B., Akusjärvi, S. S., Sönnerborg, A., Dimitriou, M. & Svensson, J. P. Chromatin maturation of the HIV-1 provirus in primary resting CD4+ T cells. *PLOS Pathogens* **16**, e1008264 (2020).

67. DeMaster, L. K. *et al.* A Subset of CD4/CD8 Double-Negative T Cells Expresses HIV Proteins in Patients on Antiretroviral Therapy. *J. Virol.* **90**, 2165–2179 (2015).

68. Pace, M. J. *et al.* Directly Infected Resting CD4+T Cells Can Produce HIV Gag without Spreading Infection in a Model of HIV Latency. *PLoS Pathog* **8**, (2012).

69. Evans, V. A. *et al.* Myeloid Dendritic Cells Induce HIV-1 Latency in Non-proliferating CD4+ T Cells. *PLOS Pathogens* **9**, e1003799 (2013).

70. Kumar, N. A. *et al.* Myeloid Dendritic Cells induce HIV latency in proliferating CD4+ T-cells. *J Immunol* **201**, 1468–1477 (2018).

71. Shen, A. *et al.* Endothelial cell stimulation overcomes restriction and promotes productive and latent HIV-1 infection of resting CD4+ T cells. *J. Virol.* **87**, 9768–9779 (2013).

72. Saleh, S. *et al.* CCR7 ligands CCL19 and CCL21 increase permissiveness of resting memory CD4+ T cells to HIV-1 infection: a novel model of HIV-1 latency. *Blood* **110**, 4161–4164 (2007).

73. Saleh, S. *et al.* HIV integration and the establishment of latency in CCL19-treated resting CD4+ T cells require activation of NF-κB. *Retrovirology* **13**, (2016).

74. Colin, L. & Lint, C. V. Molecular control of HIV-1 postintegration latency: implications for the development of new therapeutic strategies. *Retrovirology* **6**, 111 (2009).

75. Debyser, Z., Vansant, G., Bruggemans, A., Janssens, J. & Christ, F. Insight in HIV Integration Site Selection Provides a Block-and-Lock Strategy for a Functional Cure of HIV Infection. *Viruses* **11**, (2018).

76. Crooks, A. M. *et al.* Precise Quantitation of the Latent HIV-1 Reservoir: Implications for Eradication Strategies. *J Infect Dis* **212**, 1361–1365 (2015).

77. Liu, R., Simonetti, F. R. & Ho, Y.-C. The forces driving clonal expansion of the HIV-1 latent reservoir. *Virology Journal* **17**, 4 (2020).

78. Coiras, M., López-Huertas, M. R., Pérez-Olmeda, M. & Alcamí, J. Understanding HIV-1 latency provides clues for the eradication of long-term reservoirs. *Nat. Rev. Microbiol.* **7**, 798–812 (2009).

79. Symons, J. *et al.* HIV integration sites in latently infected cell lines: evidence of ongoing replication. *Retrovirology* **14**, (2017).

80. Archin, N. M., Sung, J. M., Garrido, C., Soriano-Sarabia, N. & Margolis, D. M. Eradicating HIV-1 infection: seeking to clear a persistent pathogen. *Nat Rev Microbiol* **12**, 750–764 (2014).

81. Cameron, P. U. *et al.* Dendritic cells exposed to human immunodeficiency virus type-1 transmit a vigorous cytopathic infection to CD4+ T cells. *Science* **257**, 383–387 (1992).

82. Rezaei, S. D. *et al.* The Pathway To Establishing HIV Latency Is Critical to How Latency Is Maintained and Reversed. *Journal of Virology* **92**, (2018).

83. Marini, A., Harper, J. M. & Romerio, F. An in vitro system to model the establishment and reactivation of HIV-1 latency. *J Immunol* **181**, 7713–7720 (2008).

84. Tyagi, M., Pearson, R. J. & Karn, J. Establishment of HIV Latency in Primary CD4+ Cells Is due to Epigenetic Transcriptional Silencing and P-TEFb Restriction. *Journal of Virology* **84**, 6425–6437 (2010).

85. Kim, M. *et al.* A primary CD4 + T cell model of HIV-1 latency established after activation through the T cell receptor and subsequent return to quiescence. *Nature Protocols* **9**, 2755–2770 (2014).

86. Swiggard, W. J. *et al.* Human Immunodeficiency Virus Type 1 Can Establish Latent Infection in Resting CD4+ T Cells in the Absence of Activating Stimuli. *J Virol* **79**, 14179–14188 (2005).

87. Bosque, A. & Planelles, V. Studies of HIV-1 latency in an ex vivo model that uses primary central memory T cells. *Methods* **53**, 54–61 (2011).

88. Chomont, N., DaFonseca, S., Vandergeeten, C., Ancuta, P. & Sékaly, R.-P. Maintenance of CD4+ T-cell memory and HIV persistence: keeping memory, keeping HIV. *Curr Opin HIV AIDS* **6**, 30–36 (2011).

89. Wang, F.-X. *et al.* IL-7 is a potent and proviral strain–specific inducer of latent HIV-1 cellular reservoirs of infected individuals on virally suppressive HAART. *J Clin Invest* **115**, 128–137 (2005).

90. T W Chun, L. C. Chun, T.-W. et al. Quantitation of latent tissue reservoirs and total body load in HIV-1 infection. Nature 387, 183-188. *Nature* **387**, 183–8 (1997).

91. Kiepiela, P. *et al.* CD8+ T-cell responses to different HIV proteins have discordant associations with viral load. *Nat. Med.* **13**, 46–53 (2007).

92. Demers, K. R. *et al.* Temporal Dynamics of CD8+ T Cell Effector Responses during Primary HIV Infection. *PLoS Pathog.* **12**, e1005805 (2016).

93. Perdomo-Celis, F., Velilla, P. A., Taborda, N. A. & Rugeles, M. T. An altered cytotoxic program of CD8+ T-cells in HIV-infected patients despite HAART-induced viral suppression. *PLoS One* **14**, (2019).

94. Helleberg, M. *et al.* Course and Clinical Significance of CD8+ T-Cell Counts in a Large Cohort of HIV-Infected Individuals. *J. Infect. Dis.* **211**, 1726–1734 (2015).

95. Youngblood, B., Wherry, E. J. & Ahmed, R. Acquired transcriptional programming in functional and exhausted virus-specific CD8 T cells. *Curr Opin HIV AIDS* **7**, 50–57 (2012).

96. Hoffmann, M. *et al.* Exhaustion of Activated CD8 T Cells Predicts Disease Progression in Primary HIV-1 Infection. *PLoS Pathog* **12**, (2016).

97. Migueles, S. A. *et al.* Lytic granule loading of CD8+ T cells is required for HIV-infected cell elimination associated with immune control. *Immunity* **29**, 1009–1021 (2008).

98. Yan, J. *et al.* HIV-Specific CD8+ T Cells from Elite Controllers Are Primed for Survival. *J Virol* **87**, 5170–5181 (2013).

99. Betts, M. R. *et al.* Analysis of Total Human Immunodeficiency Virus (HIV)-Specific CD4+ and CD8+ T-Cell Responses: Relationship to Viral Load in Untreated HIV Infection. *J Virol* **75**, 11983–11991 (2001).

100. Shan, L. *et al.* Stimulation of HIV-1-specific cytolytic T lymphocytes facilitates elimination of latent viral reservoir after virus reactivation. *Immunity* **36**, 491–501 (2012).

101. Cockerham, L. R. *et al.* Programmed death-1 expression on CD4+ and CD8+ T cells in treated and untreated HIV disease. *AIDS* **28**, 1749–1758 (2014).

102. Conway, J. M. & Ribeiro, R. M. Modeling the immune response to HIV infection. *Curr Opin Syst Biol* **12**, 61–69 (2018).

103. Sevilya, Z. *et al.* Killing of Latently HIV-Infected CD4 T Cells by Autologous CD8 T Cells Is Modulated by Nef. *Front. Immunol.* **9**, (2018).

104. Younes, S.-A. *et al.* HIV-1 viremia prevents the establishment of interleukin 2-producing HIV-specific memory CD4+ T cells endowed with proliferative capacity. *J. Exp. Med.* **198**, 1909–1922 (2003).

105. Dyer, W. B. *et al.* Mechanisms of HIV non-progression; robust and sustained CD4+ T-cell proliferative responses to p24 antigen correlate with control of viraemia and lack of disease progression after long-term transfusion-acquired HIV-1 infection. *Retrovirology* **5**, 112 (2008).

106. Jacobs, E. S. *et al.* Cytokines Elevated in HIV Elite Controllers Reduce HIV Replication In Vitro and Modulate HIV Restriction Factor Expression. *J Virol* **91**, (2017).

107. Riou, C. *et al.* Restoration of CD4+ responses to co-pathogens in HIV-infected individuals on antiretroviral therapy is dependent on T cell memory phenotype. *J Immunol* **195**, 2273–2281 (2015).

108. Adland, E. *et al.* Recovery of effective HIV-specific CD4+ T-cell activity following antiretroviral therapy in paediatric infection requires sustained suppression of viraemia. *AIDS* **32**, 1413–1422 (2018).

109. Sun, Y. *et al.* The investigation of CD4+T-cell functions in primary HIV infection with antiretroviral therapy. *Medicine (Baltimore)* **96**, (2017).

110. Mavigner, M. *et al.* CD8 Lymphocyte Depletion Enhances the Latency Reversal Activity of the SMAC Mimetic AZD5582 in ART-Suppressed Simian Immunodeficiency Virus-Infected Rhesus Macaques. *Journal of Virology* **95**, (2021).

111. McBrien, J. B. *et al.* Robust and persistent reactivation of SIV and HIV by N-803 and depletion of CD8+ cells. *Nature* **578**, 154–159 (2020).

112. Betts, M. R. *et al.* HIV nonprogressors preferentially maintain highly functional HIV-specific CD8+ T cells. *Blood* **107**, 4781–4789 (2006).

113. Betts, M. R. *et al.* Analysis of Total Human Immunodeficiency Virus (HIV)-Specific CD4+ and CD8+ T-Cell Responses: Relationship to Viral Load in Untreated HIV Infection. *J Virol* **75**, 11983–11991 (2001).

114. Deng, K. *et al.* Broad CTL response is required to clear latent HIV-1 due to dominance of escape mutations. *Nature* **517**, 381–385 (2015).

115. Pereyra, F. *et al.* HIV control is mediated in part by CD8+ T-cell targeting of specific epitopes. *J Virol* **88**, 12937–12948 (2014).

116. Arora, J. *et al.* HIV peptidome-wide association study reveals patient-specific epitope repertoires associated with HIV control. *PNAS* **116**, 944–949 (2019).

117. Khoury, G. *et al.* Persistence of integrated HIV DNA in CXCR3+CCR6+memory CD4+ T cells in HIV-infected individuals on antiretroviral therapy. *AIDS* **30**, 1511–1520 (2016).

118. Telwatte, S. *et al.* Gut and blood differ in constitutive blocks to HIV transcription, suggesting tissue-specific differences in the mechanisms that govern HIV latency. *PLOS Pathogens* **14**, e1007357 (2018).
119. Bukrinsky, M. I., Stanwick, T. L., Dempsey, M. P. & Stevenson, M. Quiescent T lymphocytes as an inducible virus reservoir in HIV-1 infection. *Science* **254**, 423–427 (1991).
120. Chun, T.-W. *et al.* Presence of an inducible HIV-1 latent reservoir during highly active antiretroviral therapy. *PNAS* **94**, 13193–13197 (1997).
121. Chun, T. W. *et al.* Quantification of latent tissue reservoirs and total body viral load in HIV-1 infection. *Nature* **387**, 183–188 (1997).
122. Borrow, P. *et al.* Antiviral pressure exerted by HIV-1-specific cytotoxic T lymphocytes (CTLs) during primary infection demonstrated by rapid selection of CTL escape virus. *Nat. Med.* **3**, 205–211 (1997).
123. Warren, J. A. *et al.* Quantifying Virus Escape from T Cells in the Latent HIV Reservoir. *The Journal of Immunology* **202**, 197.14-197.14 (2019).
124. Chomont, N. *et al.* HIV reservoir size and persistence are driven by T cell survival and homeostatic proliferation. *Nature Medicine* **15**, 893–900 (2009).
125. Wightman, F. *et al.* Both CD31+ and CD31- Naive CD4+ T Cells Are Persistent HIV Type 1-Infected Reservoirs in Individuals Receiving Antiretroviral Therapy. *J Infect Dis* **202**, 1738–1748 (2010).
126. Roche, M. *et al.* CXCR4-Using HIV Strains Predominate in Naive and Central Memory CD4+ T Cells in People Living with HIV on Antiretroviral Therapy: Implications for How Latency Is Established and Maintained. *Journal of Virology* **94**, (2020).

127. Zerbato, J. M. *et al.* Establishment and Reversal of HIV-1 Latency in Naive and Central Memory CD4+ T Cells In Vitro. *Journal of Virology* **90**, 8059–8073 (2016).

128. Chomont, N. *et al.* HIV reservoir size and persistence are driven by T cell survival and homeostatic proliferation. *Nat Med* **15**, 893–900 (2009).

129. Buzon, M. J. *et al.* HIV-1 persistence in CD4+ T cells with stem cell-like properties. *Nat. Med.* **20**, 139–142 (2014).

130. Buzon, M. J. *et al.* Long-term antiretroviral treatment initiated at primary HIV-1 infection affects the size, composition, and decay kinetics of the reservoir of HIV-1-infected CD4 T cells. *J. Virol.* **88**, 10056–10065 (2014).

131. Banga, R. *et al.* PD-1(+) and follicular helper T cells are responsible for persistent HIV-1 transcription in treated aviremic individuals. *Nat. Med.* **22**, 754–761 (2016).

132. Nutt, S. L. & Tarlinton, D. M. Germinal center B and follicular helper T cells: siblings, cousins or just good friends? *Nat. Immunol.* **12**, 472–477 (2011).

133. Chtanova, T. *et al.* T follicular helper cells express a distinctive transcriptional profile, reflecting their role as non-Th1/Th2 effector cells that provide help for B cells. *J. Immunol.* **173**, 68–78 (2004).

134. Perreau, M. *et al.* Follicular helper T cells serve as the major CD4 T cell compartment for HIV-1 infection, replication, and production. *J Exp Med* **210**, 143–156 (2013).

135. Lindqvist, M. *et al.* Expansion of HIV-specific T follicular helper cells in chronic HIV infection. *J. Clin. Invest.* **122**, 3271–3280 (2012).

136. Boily-Larouche, G. *et al.* CD161 identifies polyfunctional Th1/Th17 cells in the genital mucosa that are depleted in HIV-infected female sex workers from Nairobi, Kenya. *Sci Rep* **7**, 11123 (2017).

137. Darcis, G. *et al.* CD32+CD4+ T Cells Are Highly Enriched for HIV DNA and Can Support Transcriptional Latency. *Cell Reports* **30**, 2284-2296.e3 (2020).

138. Moreno-Fernandez, M. E., Zapata, W., Blackard, J. T., Franchini, G. & Chougnet, C. A. Human Regulatory T Cells Are Targets for Human Immunodeficiency Virus (HIV) Infection, and Their Susceptibility Differs Depending on the HIV Type 1 Strain. *J Virol* **83**, 12925–12933 (2009).

139. Dunay, G. A. *et al.* Assessment of the HIV-1 reservoir in CD4+ regulatory T cells by a Droplet Digital PCR based approach. *Virus Research* **240**, 107–111 (2017).

140. Zalar, A. *et al.* Macrophage HIV-1 infection in duodenal tissue of patients on long term HAART. *Antiviral Res.* **87**, 269–271 (2010).

141. Yona, S. *et al.* Fate Mapping Reveals Origins and Dynamics of Monocytes and Tissue Macrophages under Homeostasis. *Immunity* **38**, 79–91 (2013).

142. James, K. S. *et al.* Measuring the contribution of γδ T cells to the persistent HIV reservoir. *AIDS* **34**, 363–371 (2020).

143. Soriano-Sarabia, N. *et al.* Peripheral Vγ9Vδ2 T Cells Are a Novel Reservoir of Latent HIV Infection. *PLoS Pathog* **11**, (2015).

144. Li, G. *et al.* HIV-1 infection depletes human CD34+CD38- hematopoietic progenitor cells via pDC-dependent mechanisms. *PLoS Pathog.* **13**, e1006505 (2017).

145. Louache, F. *et al.* Role of human immunodeficiency virus replication in defective in vitro growth of hematopoietic progenitors. *Blood* **80**, 2991–2999 (1992).

146. Majka, M. *et al.* Bone marrow CD34(+) cells and megakaryoblasts secrete beta-chemokines that block infection of hematopoietic cells by M-tropic R5 HIV. *J. Clin. Invest.* **104**, 1739–1749 (1999).

147. Majka, M. *et al.* The limited infectability by R5 HIV of CD34(+) cells from thymus, cord, and peripheral blood and bone marrow is explained by their ability to produce beta-chemokines. *Exp. Hematol.* **28**, 1334–1342 (2000).

148. McNamara, L. A., Ganesh, J. A. & Collins, K. L. Latent HIV-1 infection occurs in multiple subsets of hematopoietic progenitor cells and is reversed by NF-κB activation. *J. Virol.* **86**, 9337–9350 (2012).

149. Zaikos, T. D. *et al.* Hematopoietic Stem and Progenitor Cells Are a Distinct HIV Reservoir that Contributes to Persistent Viremia in Suppressed Patients. *Cell Rep* **25**, 3759-3773.e9 (2018).

150. Churchill, M. J. *et al.* Use of laser capture microdissection to detect integrated HIV-1 DNA in macrophages and astrocytes from autopsy brain tissues. *J. Neurovirol.* **12**, 146–152 (2006).

151. Barat, C. *et al.* Astrocytes sustain long-term productive HIV-1 infection without establishment of reactivable viral latency. *Glia* **66**, 1363–1381 (2018).

152. Narasipura, S. D., Kim, S. & Al-Harthi, L. Epigenetic Regulation of HIV-1 Latency in Astrocytes. *Journal of Virology* **88**, 3031 (2014).

153. Ko, A. *et al.* Macrophages but not Astrocytes Harbor HIV DNA in the Brains of HIV-1-Infected Aviremic Individuals on Suppressive Antiretroviral Therapy. *J Neuroimmune Pharmacol* **14**, 110–119 (2019).

154. Hashimoto, M. *et al.* Fibrocytes Differ from Macrophages but Can Be Infected with HIV-1. *The Journal of Immunology* **195**, 4341–4350 (2015).

155. McGary, C. S. *et al.* CTLA-4+PD-1- Memory CD4+ T Cells Critically Contribute to Viral Persistence in Antiretroviral Therapy-Suppressed, SIV-Infected Rhesus Macaques. *Immunity* **47**, 776-788.e5 (2017).

156. Fromentin, R. *et al.* CD4+ T Cells Expressing PD-1, TIGIT and LAG-3 Contribute to HIV Persistence during ART. *PLOS Pathogens* **12**, e1005761 (2016).

157. Khoury, G. *et al.* Persistence of integrated HIV DNA in CXCR3+CCR6+ memory CD4+ T-cells in HIV-infected individuals on antiretroviral therapy. *AIDS* **30**, 1511–1520 (2016).

158. McBride, K. *et al.* The Majority of HIV Type 1 DNA in Circulating CD4+ T Lymphocytes Is Present in Non-Gut-Homing Resting Memory CD4+ T Cells. *AIDS Res Hum Retroviruses* **29**, 1330–1339 (2013).

159. Descours, B. *et al.* CD32a is a marker of a CD4 T-cell HIV reservoir harbouring replication-competent proviruses. *Nature* **543**, 564–567 (2017).

160. Pérez, L. *et al.* Conflicting evidence for HIV enrichment in CD32 + CD4 T cells. *Nature* **561**, E9–E16 (2018).

161. Osuna, C. E. *et al.* Evidence that CD32a does not mark the HIV-1 latent reservoir. *Nature* **561**, E20–E28 (2018).

162. Martin, G. E. *et al.* CD32-Expressing CD4 T Cells Are Phenotypically Diverse and Can Contain Proviral HIV DNA. *Front Immunol* **9**, 928 (2018).

163. Estes, J. D. *et al.* Defining total-body AIDS-virus burden with implications for curative strategies. *Nat. Med.* **23**, 1271–1276 (2017).

164. Churchill, M. J. *et al.* Extensive astrocyte infection is prominent in human immunodeficiency virus-associated dementia. *Ann. Neurol.* **66**, 253–258 (2009).

165. Tso, F. Y. *et al.* Brain is a potential sanctuary for subtype C HIV-1 irrespective of ART treatment outcome. *PLoS ONE* **13**, e0201325 (2018).

166. Schnell, G., Spudich, S., Harrington, P., Price, R. W. & Swanstrom, R. Compartmentalized Human Immunodeficiency Virus Type 1 Originates from Long-Lived Cells in Some Subjects with HIV-1–Associated Dementia. *PLOS Pathogens* **5**, e1000395 (2009).

167. da Fonseca, A. C. C. *et al.* The impact of microglial activation on blood-brain barrier in brain diseases. *Front Cell Neurosci* **8**, 362 (2014).

168. Eisfeld, C., Reichelt, D., Evers, S. & Husstedt, I. CSF Penetration by Antiretroviral Drugs. *CNS Drugs* **27**, 31–55 (2013).

169. Yadav, A. & Collman, R. G. CNS Inflammation and Macrophage/Microglial Biology Associated with HIV-1 Infection. *J Neuroimmune Pharmacol* **4**, 430–447 (2009).

170. Asahchop, E. L. *et al.* Reduced antiretroviral drug efficacy and concentration in HIV-infected microglia contributes to viral persistence in brain. *Retrovirology* **14**, 47 (2017).

171. Wallet, C. *et al.* Microglial Cells: The Main HIV-1 Reservoir in the Brain. *Front Cell Infect Microbiol* **9**, (2019).

172. Gray, L. R. *et al.* HIV-1 entry and trans-infection of astrocytes involves CD81 vesicles. *PLoS ONE* **9**, e90620 (2014).

173. Micci, L. *et al.* CD4 depletion in SIV-infected macaques results in macrophage and microglia infection with rapid turnover of infected cells. *PLoS Pathog.* **10**, e1004467 (2014).

174. Bozzi, G. *et al.* No evidence of ongoing HIV replication or compartmentalization in tissues during combination antiretroviral therapy: Implications for HIV eradication. *Science Advances* **5**, eaav2045 (2019).

175. Joseph, S. B. *et al.* Human Immunodeficiency Virus Type 1 RNA Detected in the Central Nervous System (CNS) After Years of Suppressive Antiretroviral Therapy Can Originate from a Replicating CNS Reservoir or Clonally Expanded Cells. *Clin. Infect. Dis.* **69**, 1345–1352 (2019).

176. Debes, G. F. *et al.* CC chemokine receptor 7 required for T lymphocyte exit from peripheral tissues. *Nat Immunol* **6**, 889–894 (2005).

177. Sallusto, F., Lenig, D., Förster, R., Lipp, M. & Lanzavecchia, A. Two subsets of memory T lymphocytes with distinct homing potentials and effector functions. *Nature* **401**, 708–712 (1999).

178. Association of antiretroviral therapy with detection of HIV-... : AIDS. *LWW* http://journals.lww.com/aidsonline/Fulltext/2000/03310/Association_of_antiretroviral_therapy_with.1.aspx.

179. Pantaleo, G. *et al.* Lymphoid organs function as major reservoirs for human immunodeficiency virus. *Proc. Natl. Acad. Sci. U.S.A.* **88**, 9838–9842 (1991).

180. Chun, T.-W. *et al.* Persistence of HIV in Gut-Associated Lymphoid Tissue despite Long-Term Antiretroviral Therapy. *J Infect Dis.* **197**, 714–720 (2008).

181. Science Magazine: Sign In. http://www.sciencemag.org/content/280/5362/427.long.

182. Heesters, B. A. *et al.* Follicular Dendritic Cells Retain Infectious HIV in Cycling Endosomes. *PLoS Pathog* **11**, (2015).

183. Gunn, M. D. *et al.* A chemokine expressed in lymphoid high endothelial venules promotes the adhesion and chemotaxis of naive T lymphocytes. *Proc Natl Acad Sci U S A* **95**, 258–263 (1998).

184. Folkvord, J. M., Armon, C. & Connick, E. Lymphoid follicles are sites of heightened human immunodeficiency virus type 1 (HIV-1) replication and reduced antiretroviral effector mechanisms. *AIDS Res. Hum. Retroviruses* **21**, 363–370 (2005).

185. von Andrian, U. H. & Mempel, T. R. Homing and cellular traffic in lymph nodes. *Nature Reviews Immunology* **3**, 867–878 (2003).

186. Mondino, A., Khoruts, A. & Jenkins, M. K. The anatomy of T-cell activation and tolerance. *Proc Natl Acad Sci U S A* **93**, 2245–2252 (1996).

187. Rubin, P. & Hansen, J. T. *TNM Staging Atlas with Oncoanatomy*. (Lippincott Williams & Wilkins, 2013).

188. Fletcher, C. V. *et al.* Persistent HIV-1 replication is associated with lower antiretroviral drug concentrations in lymphatic tissues. *Proc. Natl. Acad. Sci. U.S.A.* **111**, 2307–2312 (2014).

189. Fukazawa, Y. *et al.* B cell follicle sanctuary permits persistent productive simian immunodeficiency virus infection in elite controllers. *Nat. Med.* **21**, 132–139 (2015).

190. Connick, E. *et al.* CTL fail to accumulate at sites of HIV-1 replication in lymphoid tissue. *J. Immunol.* **178**, 6975–6983 (2007).

191. Li, S. *et al.* Simian Immunodeficiency Virus-Producing Cells in Follicles Are Partially Suppressed by CD8+ Cells In Vivo. *J Virol* **90**, 11168–11180 (2016).

192. He, R. *et al.* Follicular CXCR5- expressing CD8(+) T cells curtail chronic viral infection. *Nature* **537**, 412–428 (2016).

193. Shen, J. *et al.* A Subset of CXCR5+CD8+ T Cells in the Germinal Centers From Human Tonsils and Lymph Nodes Help B Cells Produce Immunoglobulins. *Front. Immunol.* **9**, (2018).

194. Nilsson, J. *et al.* HIV-1–driven regulatory T-cell accumulation in lymphoid tissues is associated with disease progression in HIV/AIDS. *Blood* **108**, 3808–3817 (2006).

195. Andersson, J. *et al.* Cutting Edge: The Prevalence of Regulatory T Cells in Lymphoid Tissue Is Correlated with Viral Load in HIV-Infected Patients. *The Journal of Immunology* **174**, 3143–3147 (2005).

196. Ji, J. & Cloyd, M. W. HIV-1 binding to CD4 on CD4+CD25+ regulatory T cells enhances their suppressive function and induces them to home to, and accumulate in, peripheral and mucosal lymphoid tissues: an additional mechanism of immunosuppression. *Int Immunol* **21**, 283–294 (2009).

197. Yero, A. *et al.* Differential Dynamics of Regulatory T-Cell and Th17 Cell Balance in Mesenteric Lymph Nodes and Blood following Early Antiretroviral Initiation during Acute Simian Immunodeficiency Virus Infection. *J Virol* **93**, (2019).

198. Riou, C. *et al.* Restoration of CD4+ responses to co-pathogens in HIV-infected individuals on antiretroviral therapy is dependent on T cell memory phenotype. *J Immunol* **195**, 2273–2281 (2015).

199. Banga, R. *et al.* PD-1(+) and follicular helper T cells are responsible for persistent HIV-1 transcription in treated aviremic individuals. *Nat. Med.* **22**, 754–761 (2016).

200. Porichis, F. *et al.* Immune Checkpoint Blockade Restores HIV-Specific CD4 T Cell Help for NK Cells. *J. Immunol.* **201**, 971–981 (2018).

201. Jiao, Y.-M. *et al.* CD4+CD25+CD127 regulatory cells play multiple roles in maintaining HIV-1 p24 production in patients on long-term treatment: HIV-1 p24-producing cells and suppression of anti-HIV immunity. *Int. J. Infect. Dis.* **37**, 42–49 (2015).

202. Kinter, A. *et al.* Suppression of HIV-specific T cell activity by lymph node CD25+ regulatory T cells from HIV-infected individuals. *Proc. Natl. Acad. Sci. U.S.A.* **104**, 3390–3395 (2007).

203. Yates, A., Stark, J., Klein, N., Antia, R. & Callard, R. Understanding the slow depletion of memory CD4+ T cells in HIV infection. *PLoS Med.* **4**, e177 (2007).

204. Moreno-Fernandez, M. E., Rueda, C. M., Rusie, L. K. & Chougnet, C. A. Regulatory T cells control HIV replication in activated T cells through a cAMP-dependent mechanism. *Blood* **117**, 5372–5380 (2011).

205. Mylvaganam, G. H. *et al.* Diminished viral control during simian immunodeficiency virus infection is associated with aberrant PD-1hi CD4 T cell enrichment in the lymphoid follicles of the rectal mucosa. *J. Immunol.* **193**, 4527–4536 (2014).

206. Petrovas, C. & Koup, R. A. T follicular helper cells and HIV/SIV-specific antibody responses. *Curr Opin HIV AIDS* **9**, 235–241 (2014).

207. Hong, J. J., Amancha, P. K., Rogers, K., Ansari, A. A. & Villinger, F. Spatial Alterations between CD4+ T Follicular Helper, B, and CD8+ T Cells during Simian Immunodeficiency Virus Infection: T/B Cell Homeostasis, Activation,

and Potential Mechanism for Viral Escape. *The Journal of Immunology* **188**, 3247–3256 (2012).

208. Sage, P. T., Francisco, L. M., Carman, C. V. & Sharpe, A. H. The receptor PD-1 controls follicular regulatory T cells in the lymph nodes and blood. *Nat. Immunol.* **14**, 152–161 (2013).
209. Sage, P. T., Alvarez, D., Godec, J., von Andrian, U. H. & Sharpe, A. H. Circulating T follicular regulatory and helper cells have memory-like properties. *J. Clin. Invest.* **124**, 5191–5204 (2014).
210. Li, G. *et al.* Regulatory T Cells Contribute to HIV-1 Reservoir Persistence in CD4+ T Cells Through Cyclic Adenosine Monophosphate-Dependent Mechanisms in Humanized Mice In Vivo. *J. Infect. Dis.* **216**, 1579–1591 (2017).
211. He, R. *et al.* Follicular CXCR5-expressing CD8 + T cells curtail chronic viral infection. *Nature* **537**, 412–416 (2016).
212. Li, S. *et al.* Simian Immunodeficiency Virus-Producing Cells in Follicles Are Partially Suppressed by CD8+ Cells In Vivo. *J Virol* **90**, 11168–11180 (2016).
213. Perdomo-Celis, F., Feria, M. G., Taborda, N. A. & Rugeles, M. T. Induction of Follicular-Like CXCR5+ CD8+ T Cells by TGF-β1/IL-23 Is Limited During HIV Infection. *Viral Immunology* **32**, 278–288 (2019).
214. Petrovas, C. *et al.* Follicular CD8 T cells accumulate in HIV infection and can kill infected cells in vitro via bispecific antibodies. *Sci Transl Med* **9**, (2017).
215. Connick, E. *et al.* Compartmentalization of simian immunodeficiency virus replication within secondary lymphoid tissues of rhesus macaques is linked to disease stage and inversely related to localization of virus-specific CTL. *J. Immunol.* **193**, 5613–5625 (2014).

216. Mowat, A. M. & Viney, J. L. The anatomical basis of intestinal immunity. *Immunol. Rev.* **156**, 145–166 (1997).

217. Ma, H., Tao, W. & Zhu, S. T lymphocytes in the intestinal mucosa: defense and tolerance. *Cellular & Molecular Immunology* **16**, 216–224 (2019).

218. Chun, T.-W. *et al.* Persistence of HIV in Gut-Associated Lymphoid Tissue despite Long-Term Antiretroviral Therapy. *J Infect Dis* **197**, 714–720 (2008).

219. Estes, J. D. *et al.* Defining total-body AIDS-virus burden with implications for curative strategies. *Nat. Med.* **23**, 1271–1276 (2017).

220. Anderson, J. L. *et al.* Human Immunodeficiency Virus (HIV)–Infected CCR6+ Rectal CD4+ T Cells and HIV Persistence On Antiretroviral Therapy. *J Infect Dis* **221**, 744–755 (2020).

221. Yukl, S. *et al.* Differences in HIV Burden and Immune Activation within the Gut of HIV+ Patients on Suppressive Antiretroviral Therapy. *J Infect Dis* **202**, 1553–1561 (2010).

222. Veazey, R. S. *et al.* Gastrointestinal tract as a major site of CD4+ T cell depletion and viral replication in SIV infection. *Science* **280**, 427–431 (1998).

223. Guadalupe, M. *et al.* Severe CD4+ T-cell depletion in gut lymphoid tissue during primary human immunodeficiency virus type 1 infection and substantial delay in restoration following highly active antiretroviral therapy. *J. Virol.* **77**, 11708–11717 (2003).

224. Mattapallil, J. J. *et al.* Massive infection and loss of memory CD4+ T cells in multiple tissues during acute SIV infection. *Nature* **434**, 1093–1097 (2005).

225. Mehandru, S. & Dandekar, S. Role of the gastrointestinal tract in establishing infection in primates and humans. *Curr Opin HIV AIDS* **3**, 22–27 (2008).

226. Niess, J. H. & Reinecker, H.-C. Dendritic cells in the recognition of intestinal microbiota. *Cellular Microbiology* **8**, 558–564 (2006).

227. Mattapallil, J. J. *et al.* Massive infection and loss of memory CD4+ T cells in multiple tissues during acute SIV infection. *Nature* **434**, 1093–1097 (2005).

228. Brenchley, J. M. *et al.* CD4+ T cell depletion during all stages of HIV disease occurs predominantly in the gastrointestinal tract. *J. Exp. Med.* **200**, 749–759 (2004).

229. Brenchley, J. M. *et al.* CD4+ T cell depletion during all stages of HIV disease occurs predominantly in the gastrointestinal tract. *J. Exp. Med.* **200**, 749–759 (2004).

230. Khoury, G. *et al.* Human Immunodeficiency Virus Persistence and T-Cell Activation in Blood, Rectal, and Lymph Node Tissue in Human Immunodeficiency Virus-Infected Individuals Receiving Suppressive Antiretroviral Therapy. *J. Infect. Dis.* **215**, 911–919 (2017).

231. Thornhill, J. P. *et al.* CD32 expressing doublets in HIV-infected gut-associated lymphoid tissue are associated with a T follicular helper cell phenotype. *Mucosal Immunology* **12**, 1212–1219 (2019).

232. Asmuth, D. M. *et al.* Tissue Pharmacologic and Virologic Determinants of Duodenal and Rectal Gastrointestinal-Associated Lymphoid Tissue Immune Reconstitution in HIV-Infected Patients Initiating Antiretroviral Therapy. *J. Infect. Dis.* **216**, 813–818 (2017).

233. Fletcher, C. V. *et al.* Persistent HIV-1 replication is associated with lower antiretroviral drug concentrations in lymphatic tissues. *Proc Natl Acad Sci U S A* **111**, 2307–2312 (2014).

234. Bruner, K. M. *et al.* Defective proviruses rapidly accumulate during acute HIV-1 infection. *Nat. Med.* **22**, 1043–1049 (2016).

235. Lee, G. Q. *et al.* Clonal expansion of genome-intact HIV-1 in functionally polarized Th1 $CD4^+$ T cells. *J Clin Invest* **127**, 2689–2696 (2017).

236. Hiener, B. *et al.* Identification of Genetically Intact HIV-1 Proviruses in Specific CD4+ T Cells from Effectively Treated Participants. *Cell Reports* **21**, 813–822 (2017).

237. Ho, Y.-C. *et al.* Replication-competent non-induced proviruses in the latent reservoir increase barrier to HIV-1 cure. *Cell* **155**, 540–551 (2013).

238. Ho, Y.-C. *et al.* Replication-competent non-induced proviruses in the latent reservoir increase barrier to HIV-1 cure. *Cell* **155**, 540–551 (2013).

239. Pollack, R. A. *et al.* Defective HIV-1 proviruses are expressed and can be recognized by cytotoxic T lymphocytes which shapes the proviral landscape. *Cell Host Microbe* **21**, 494-506.e4 (2017).

240. Bruner, K. M. *et al.* Defective proviruses rapidly accumulate during acute HIV-1 infection. *Nature Medicine* **22**, 1043–1049 (2016).

241. Ho, Y.-C. *et al.* Replication-competent noninduced proviruses in the latent reservoir increase barrier to HIV-1 cure. *Cell* **155**, 540–551 (2013).

242. Barton, K. M. & Palmer, S. E. How to Define the Latent Reservoir: Tools of the Trade. *Curr HIV/AIDS Rep* **13**, 77–84 (2016).

243. Bruner, K. M. *et al.* A novel quantitative approach for measuring the reservoir of latent HIV-1 proviruses. *Nature* **566**, 120–125 (2019).

244. Peluso, M. J. *et al.* Differential decay of intact and defective proviral DNA in HIV-1–infected individuals on suppressive antiretroviral therapy. *JCI Insight* **5**, (2020).

245. Stone, M. *et al.* Assessing the Suitability of Next-Generation Viral Outgrowth Assays to Measure Human Immunodeficiency Virus 1 Latent Reservoir Size. *J Infect Dis* doi:10.1093/infdis/jiaa089.

246. Pasternak, A. O. *et al.* Highly sensitive methods based on seminested real-time reverse transcription-PCR for quantitation of human immunodeficiency virus type 1 unspliced and multiply spliced RNA and proviral DNA. *J Clin Microbiol* **46**, 2206–2211 (2008).

247. Salasc, F. *et al.* A novel, sensitive dual-indicator cell line for detection and quantification of inducible, replication-competent latent HIV-1 from reservoir cells. *Scientific Reports* **9**, 19325 (2019).

248. Ho, Y.-C. *et al.* Replication-competent noninduced proviruses in the latent reservoir increase barrier to HIV-1 cure. *Cell* **155**, 540–551 (2013).

249. Hosmane, N. N. *et al.* Proliferation of latently infected CD4+ T cells carrying replication-competent HIV-1: Potential role in latent reservoir dynamics. *J Exp Med* **214**, 959–972 (2017).

250. Jiang, C. *et al.* Distinct viral reservoirs in individuals with spontaneous control of HIV-1. *Nature* **585**, 261–267 (2020).

251. Rothenberger, M. K. *et al.* Large number of rebounding/founder HIV variants emerge from multifocal infection in lymphatic tissues after treatment interruption. *Proc. Natl. Acad. Sci. U.S.A.* **112**, E1126-1134 (2015).

252. Lerner, P. *et al.* The gut mucosal viral reservoir in HIV-infected patients is not the major source of rebound plasma viremia following interruption of highly active antiretroviral therapy. *J. Virol.* **85**, 4772–4782 (2011).

253. Josefsson, L. *et al.* Single Cell Analysis of Lymph Node Tissue from HIV-1 Infected Patients Reveals that the Majority of CD4+ T-cells Contain One HIV-1 DNA Molecule. *PLoS Pathog* **9**, (2013).

254. von Stockenstrom, S. *et al.* Longitudinal Genetic Characterization Reveals That Cell Proliferation Maintains a Persistent HIV Type 1 DNA Pool During Effective HIV Therapy. *J Infect Dis* **212**, 596–607 (2015).

255. Josefsson, L. *et al.* The HIV-1 reservoir in eight patients on long-term suppressive antiretroviral therapy is stable with few genetic changes over time. *PNAS* **110**, E4987–E4996 (2013).

256. De Scheerder, M.-A. *et al.* HIV Rebound Is Predominantly Fueled by Genetically Identical Viral Expansions from Diverse Reservoirs. *Cell Host Microbe* **26**, 347-358.e7 (2019).

257. Joos, B. *et al.* HIV rebounds from latently infected cells, rather than from continuing low-level replication. *PNAS* **105**, 16725–16730 (2008).

258. McManus, W. R. *et al.* HIV-1 in lymph nodes is maintained by cellular proliferation during antiretroviral therapy. *J Clin Invest* **129**, 4629–4642 (2019).

259. Haddad, D. N. *et al.* Evidence for late stage compartmentalization of HIV-1 resistance mutations between lymph node and peripheral blood mononuclear cells. *AIDS* **14**, 2273–2281 (2000).

260. Günthard, H. F. *et al.* Residual human immunodeficiency virus (HIV) Type 1 RNA and DNA in lymph nodes and HIV RNA in genital secretions and in cerebrospinal fluid after suppression of viremia for 2 years. *J. Infect. Dis.* **183**, 1318–1327 (2001).

261. Pasternak, A. O. *et al.* Modest nonadherence to antiretroviral therapy promotes residual HIV-1 replication in the absence of virological rebound in plasma. *J. Infect. Dis.* **206**, 1443–1452 (2012).

262. Van Gulck, E. *et al.* Immune and viral correlates of 'secondary viral control' after treatment interruption in chronically HIV-1 infected patients. *PLoS ONE* **7**, e37792 (2012).

263. Spudich, S. *et al.* Persistent HIV-infected cells in cerebrospinal fluid are associated with poorer neurocognitive performance. *J Clin Invest* **129**, 3339–3346 (2019).

264. Fletcher, C. V. *et al.* Persistent HIV-1 replication is associated with lower antiretroviral drug concentrations in lymphatic tissues. *PNAS* **111**, 2307–2312 (2014).

265. Lorenzo-Redondo, R. *et al.* Persistent HIV-1 replication maintains the tissue reservoir during therapy. *Nature* **530**, 51–56 (2016).

266. Hatano, H. *et al.* Increase in 2–Long Terminal Repeat Circles and Decrease in D-dimer After Raltegravir Intensification in Patients With Treated HIV Infection: A Randomized, Placebo-Controlled Trial. *J Infect Dis* **208**, 1436–1442 (2013).

267. Rasmussen, T. A. *et al.* The effect of antiretroviral intensification with dolutegravir on residual virus replication in HIV-infected individuals: a randomised, placebo-controlled, double-blind trial. *The Lancet HIV* **5**, e221–e230 (2018).

268. Darcis, G. *et al.* Detectability of HIV Residual Viremia despite Therapy Is Highly Associated with Treatment with a Protease Inhibitor-Based

Combination Antiretroviral Therapy. *Antimicrobial Agents and Chemotherapy* **64**, (2020).

269. Tosiano, M. A., Jacobs, J. L., Shutt, K. A., Cyktor, J. C. & Mellors, J. W. A Simpler and More Sensitive Single-Copy HIV-1 RNA Assay for Quantification of Persistent HIV-1 Viremia in Individuals on Suppressive Antiretroviral Therapy. *Journal of Clinical Microbiology* **57**, (2019).
270. Darcis, G., Berkhout, B. & Pasternak, A. O. Differences in HIV Markers between Infected Individuals Treated with Different ART Regimens: Implications for the Persistence of Viral Reservoirs. *Viruses* **12**, (2020).
271. Darcis, G. *et al.* Detectability of HIV Residual Viremia despite Therapy Is Highly Associated with Treatment with a Protease Inhibitor-Based Combination Antiretroviral Therapy. *Antimicrobial Agents and Chemotherapy* **64**, (2020).
272. Maldarelli, F. *et al.* HIV latency. Specific HIV integration sites are linked to clonal expansion and persistence of infected cells. *Science* **345**, 179–183 (2014).
273. Bui, J. K. *et al.* Proviruses with identical sequences comprise a large fraction of the replication-competent HIV reservoir. *PLoS Pathog* **13**, (2017).
274. Mendoza, P. *et al.* Antigen-responsive CD4+ T cell clones contribute to the HIV-1 latent reservoir. *J Exp Med* **217**, (2020).
275. Gantner, P. *et al.* Single-cell TCR sequencing reveals phenotypically diverse clonally expanded cells harboring inducible HIV proviruses during ART. *Nature Communications* **11**, 4089 (2020).
276. Bui, J. K. *et al.* Proviruses with identical sequences comprise a large fraction of the replication-competent HIV reservoir. *PLoS Pathog.* **13**, e1006283 (2017).

277. Lorenzi, J. C. C. *et al.* Paired quantitative and qualitative assessment of the replication-competent HIV-1 reservoir and comparison with integrated proviral DNA. *Proc. Natl. Acad. Sci. U.S.A.* **113**, E7908–E7916 (2016).

278. Hosmane, N. N. *et al.* Proliferation of latently infected CD4+ T cells carrying replication-competent HIV-1: Potential role in latent reservoir dynamics. *J. Exp. Med.* **214**, 959–972 (2017).

279. Pinzone, M. R. *et al.* Longitudinal HIV sequencing reveals reservoir expression leading to decay which is obscured by clonal expansion. *Nature Communications* **10**, 728 (2019).

280. Elias K. Halvas, J. W. M. HIV-1 viremia not suppressible by antiretroviral therapy can originate from large T cell clones producing infectious virus. *J Clin Invest* (2020).

281. Kearney, M. F. *et al.* Lack of detectable HIV-1 molecular evolution during suppressive antiretroviral therapy. *PLoS Pathog.* **10**, e1004010 (2014).

282. Kearney, M. F. *et al.* Origin of Rebound Plasma HIV Includes Cells with Identical Proviruses That Are Transcriptionally Active before Stopping of Antiretroviral Therapy. *J Virol* **90**, 1369–1376 (2016).

283. Mok, H. P. *et al.* No evidence of ongoing evolution in replication competent latent HIV-1 in a patient followed up for two years. *Scientific Reports* **8**, 2639 (2018).

284. Reeves, D. B. *et al.* A majority of HIV persistence during antiretroviral therapy is due to infected cell proliferation. *Nature Communications* **9**, 1–16 (2018).

285. McManus, W. R. *et al.* HIV-1 in lymph nodes is maintained by cellular proliferation during antiretroviral therapy. *J Clin Invest* **129**, 4629–4642.

286. Bruner, K. M. *et al.* A quantitative approach for measuring the reservoir of latent HIV-1 proviruses. *Nature* **566**, 120 (2019).

287. Hiener, B. *et al.* Identification of Genetically Intact HIV-1 Proviruses in Specific CD4+ T Cells from Effectively Treated Participants. *Cell Rep* **21**, 813–822 (2017).

288. Imamichi, H. *et al.* Defective HIV-1 proviruses produce novel protein-coding RNA species in HIV-infected patients on combination antiretroviral therapy. *Proc. Natl. Acad. Sci. U.S.A.* **113**, 8783–8788 (2016).

289. Finzi, D. *et al.* Identification of a reservoir for HIV-1 in patients on highly active antiretroviral therapy. *Science* **278**, 1295–1300 (1997).

290. Falcinelli, S. D., Ceriani, C., Margolis, D. M. & Archin, N. M. New Frontiers in Measuring and Characterizing the HIV Reservoir. *Front. Microbiol.* **10**, (2019).

291. Rutsaert, S. *et al.* In-depth validation of total HIV-1 DNA assays for quantification of various HIV-1 subtypes. *Scientific Reports* **8**, 17274 (2018).

292. Bosman, K. J. *et al.* Development of sensitive ddPCR assays to reliably quantify the proviral DNA reservoir in all common circulating HIV subtypes and recombinant forms. *J Int AIDS Soc* **21**, (2018).

293. Lee, M., Kim, W.-K., Kuroda, M. J., Pal, R. & Chung, H. K. Development of real-time PCR for quantitation of simian immunodeficiency virus 2-LTR circles. *J. Med. Primatol.* **45**, 215–221 (2016).

294. Hebberecht, L. *et al.* Single genome sequencing of near full-length HIV-1 RNA using a limiting dilution approach. *Journal of Virological Methods* **274**, 113737 (2019).

295. Plantin, J., Massanella, M. & Chomont, N. Inducible HIV RNA transcription assays to measure HIV persistence: pros and cons of a compromise. *Retrovirology* **15**, 9 (2018).

296. Darcis, G. *et al.* Detectability of HIV Residual Viremia despite Therapy Is Highly Associated with Treatment with a Protease Inhibitor-Based Combination Antiretroviral Therapy. *Antimicrobial Agents and Chemotherapy* **64**, (2020).

297. Deleage, C. *et al.* Defining HIV and SIV Reservoirs in Lymphoid Tissues. *Pathog Immun* **1**, 68–106 (2016).

298. Deleage, C., Chan, C. N., Busman-Sahay, K. & Estes, J. D. Next-generation in situ hybridization approaches to define and quantify HIV and SIV reservoirs in tissue microenvironments. *Retrovirology* **15**, (2018).

299. Histopathology of the Lymph Nodes. https://www.ncbi.nlm.nih.gov/pmc/articles/PMC1892634/.

300. Aguzzi, A. & Krautler, N. J. Characterizing follicular dendritic cells: A progress report. *Eur. J. Immunol.* **40**, 2134–2138 (2010).

301. Josefsson, L. *et al.* Single Cell Analysis of Lymph Node Tissue from HIV-1 Infected Patients Reveals that the Majority of CD4+ T-cells Contain One HIV-1 DNA Molecule. *PLOS Pathogens* **9**, e1003432 (2013).

302. Rato, S., Rausell, A., Muñoz, M., Telenti, A. & Ciuffi, A. Single-cell analysis identifies cellular markers of the HIV permissive cell. *PLOS Pathogens* **13**, e1006678 (2017).

303. John, H. A., Birnstiel, M. L. & Jones, K. W. RNA-DNA Hybrids at the Cytological Level. *Nature* **223**, 582 (1969).

304. Herrington, C. S., Burns, J., Graham, A. K., Evans, M. & McGee, J. O. Interphase cytogenetics using biotin and digoxigenin labelled probes I: relative sensitivity of both reporter molecules for detection of HPV16 in CaSki cells. *J. Clin. Pathol.* **42**, 592–600 (1989).

305. Bauman, J. G., Wiegant, J., Borst, P. & van Duijn, P. A new method for fluorescence microscopical localization of specific DNA sequences by in situ hybridization of fluorochromelabelled RNA. *Exp. Cell Res.* **128**, 485–490 (1980).

306. Gulley, M. L. Molecular Diagnosis of Epstein-Barr Virus-Related Diseases. *J Mol Diagn* **3**, 1–10 (2001).

307. Wang, F. *et al.* RNAscope. *J Mol Diagn* **14**, 22–29 (2012).

308. Wang, F. *et al.* RNAscope. *J Mol Diagn* **14**, 22–29 (2012).

309. McGary, C. S. *et al.* CTLA-4+PD-1- Memory CD4+ T Cells Critically Contribute to Viral Persistence in Antiretroviral Therapy-Suppressed, SIV-Infected Rhesus Macaques. *Immunity* **47**, 776-788.e5 (2017).

310. Jonkman, J. & Brown, C. M. Any Way You Slice It—A Comparison of Confocal Microscopy Techniques. *J Biomol Tech* **26**, 54–65 (2015).

311. Nishizuka, Y. & Sakakura, T. Thymus and reproduction: sex-linked dysgenesia of the gonad after neonatal thymectomy in mice. *Science* **166**, 753–755 (1969).

312. Sakaguchi, S., Sakaguchi, N., Asano, M., Itoh, M. & Toda, M. Immunologic self-tolerance maintained by activated T cells expressing IL-2 receptor alpha-chains (CD25). Breakdown of a single mechanism of self-tolerance causes various autoimmune diseases. *J. Immunol.* **155**, 1151–1164 (1995).

313. Amsen, D. *et al.* Instruction of Distinct CD4 T Helper Cell Fates by Different Notch Ligands on Antigen-Presenting Cells. *Cell* **117**, 515–526 (2004).

314. Nunes-Cabaço, H., Caramalho, Í., Sepúlveda, N. & Sousa, A. E. Differentiation of human thymic regulatory T cells at the double positive stage. *European Journal of Immunology* **41**, 3604–3614 (2011).

315. Gottschalk, R. A., Corse, E. & Allison, J. P. TCR ligand density and affinity determine peripheral induction of Foxp3 in vivo. *J. Exp. Med.* **207**, 1701–1711 (2010).

316. Li, C., Ebert, P. J. R. & Li, Q.-J. T Cell Receptor (TCR) and Transforming Growth Factor β (TGF-β) Signaling Converge on DNA (Cytosine-5)-methyltransferase to Control forkhead box protein 3 (foxp3) Locus Methylation and Inducible Regulatory T Cell Differentiation. *J. Biol. Chem.* **288**, 19127–19139 (2013).

317. Qian, Z. *et al.* Engineered Regulatory T Cells Coexpressing MHC Class II:Peptide Complexes Are Efficient Inhibitors of Autoimmune T Cell Function and Prevent the Development of Autoimmune Arthritis. *The Journal of Immunology* **190**, 5382–5391 (2013).

318. Belizário, J. E., Brandão, W., Rossato, C. & Peron, J. P. Thymic and Postthymic Regulation of Naïve CD4+ T-Cell Lineage Fates in Humans and Mice Models. *Mediators Inflamm* **2016**, (2016).

319. Hori, S., Nomura, T. & Sakaguchi, S. Control of regulatory T cell development by the transcription factor Foxp3. *Science* **299**, 1057–1061 (2003).

320. Komatsu, N. *et al.* Pathogenic conversion of Foxp3+ T cells into TH17 cells in autoimmune arthritis. *Nat. Med.* **20**, 62–68 (2014).

321. Gavin, M. A. *et al.* Single-cell analysis of normal and FOXP3-mutant human T cells: FOXP3 expression without regulatory T cell development. *Proc. Natl. Acad. Sci. U.S.A.* **103**, 6659–6664 (2006).

322. Allan, S. E. *et al.* Activation-induced FOXP3 in human T effector cells does not suppress proliferation or cytokine production. *Int. Immunol.* **19**, 345–354 (2007).

323. Wang, J., Ioan-Facsinay, A., van der Voort, E. I. H., Huizinga, T. W. J. & Toes, R. E. M. Transient expression of FOXP3 in human activated nonregulatory CD4+ T cells. *Eur. J. Immunol.* **37**, 129–138 (2007).

324. Vadasz, Z. *et al.* The Expansion of CD25highIL-10highFoxP3high B Regulatory Cells Is in Association with SLE Disease Activity. *Journal of Immunology Research* **2015**, (2015).

325. Liu, V. C. *et al.* Tumor Evasion of the Immune System by Converting CD4+CD25− T Cells into CD4+CD25+ T Regulatory Cells: Role of Tumor-Derived TGF-β. *The Journal of Immunology* **178**, 2883–2892 (2007).

326. Luo, X. *et al.* Dendritic cells with TGF-β1 differentiate naïve CD4+CD25− T cells into islet-protective Foxp3+ regulatory T cells. *PNAS* **104**, 2821–2826 (2007).

327. Luo, X. *et al.* Cutting Edge: TGF-β-Induced Expression of Foxp3 in T cells Is Mediated through Inactivation of ERK. *The Journal of Immunology* **180**, 2757–2761 (2008).

328. Bettelli, E., Dastrange, M. & Oukka, M. Foxp3 interacts with nuclear factor of activated T cells and NF-κB to repress cytokine gene expression and effector functions of T helper cells. *PNAS* **102**, 5138–5143 (2005).

329. Vaeth, M. *et al.* Dependence on nuclear factor of activated T-cells (NFAT) levels discriminates conventional T cells from Foxp3+ regulatory T cells. *Proc. Natl. Acad. Sci. U.S.A.* **109**, 16258–16263 (2012).

330. Grinberg-Bleyer, Y. *et al.* NF-κB c-Rel Is Crucial for the Regulatory T Cell Immune Checkpoint in Cancer. *Cell* **170**, 1096-1108.e13 (2017).

331. Chambers, E. S. *et al.* Serum 25-dihydroxyvitamin D levels correlate with CD4+Foxp3+ T-cell numbers in moderate/severe asthma. *Journal of Allergy and Clinical Immunology* **130**, 542–544 (2012).

332. Urry, Z. *et al.* The role of 1α,25-dihydroxyvitamin D3 and cytokines in the promotion of distinct Foxp3+ and IL-10+ CD4+ T cells. *Eur. J. Immunol.* **42**, 2697–2708 (2012).

333. Chambers, E. S. *et al.* 1α,25-dihydroxyvitamin D3 in combination with transforming growth factor-β increases the frequency of $Foxp3^+$ regulatory T cells through preferential expansion and usage of interleukin-2. *Immunology* **143**, 52–60 (2014).

334. Valmori, D., Merlo, A., Souleimanian, N. E., Hesdorffer, C. S. & Ayyoub, M. A peripheral circulating compartment of natural naive $CD4^+$ Tregs. *J Clin Invest* **115**, 1953–1962 (2005).

335. Konkel, J. E. *et al.* Transforming Growth Factor-β Signaling in Regulatory T Cells Controls T Helper-17 Cells and Tissue-Specific Immune Responses. *Immunity* **46**, 660–674 (2017).

336. Hsu, P. *et al.* IL-10 Potentiates Differentiation of Human Induced Regulatory T Cells via STAT3 and Foxo1. *J. Immunol.* **195**, 3665–3674 (2015).

337. Lane, N., Robins, R. A., Corne, J. & Fairclough, L. Regulation in chronic obstructive pulmonary disease: the role of regulatory T-cells and Th17 cells. *Clin. Sci.* **119**, 75–86 (2010).

338. Mason, G. M. *et al.* Phenotypic Complexity of the Human Regulatory T Cell Compartment Revealed by Mass Cytometry. *J. Immunol.* **195**, 2030–2037 (2015).

339. Ng, W. F. *et al.* Human CD4(+)CD25(+) cells: a naturally occurring population of regulatory T cells. *Blood* **98**, 2736–2744 (2001).

340. Dieckmann, D., Plottner, H., Berchtold, S., Berger, T. & Schuler, G. Ex vivo isolation and characterization of CD4(+)CD25(+) T cells with regulatory properties from human blood. *J. Exp. Med.* **193**, 1303–1310 (2001).

341. Kmieciak, M. *et al.* Human T cells express CD25 and Foxp3 upon activation and exhibit effector/memory phenotypes without any regulatory/suppressor function. *Journal of Translational Medicine* **7**, 89 (2009).

342. Liu, W. *et al.* CD127 expression inversely correlates with FoxP3 and suppressive function of human CD4+ T reg cells. *J Exp Med* **203**, 1701–1711 (2006).

343. Yu, N. *et al.* CD4(+)CD25 (+)CD127 (low/-) T cells: a more specific Treg population in human peripheral blood. *Inflammation* **35**, 1773–1780 (2012).

344. Mahalingam, J. *et al.* CD4+ T Cells Expressing Latency-Associated Peptide and Foxp3 Are an Activated Subgroup of Regulatory T Cells Enriched in Patients with Colorectal Cancer. *PLOS ONE* **9**, e108554 (2014).

345. Lee, J. H., Lydon, J. P. & Kim, C. H. Progesterone suppresses the mTOR pathway and promotes generation of induced regulatory T cells with increased stability. *Eur J Immunol* **42**, 2683–2696 (2012).

346. Xiao, X. *et al.* GITR subverts Foxp3+ Tregs to boost Th9 immunity through regulation of histone acetylation. *Nat Commun* **6**, (2015).

347. Barsheshet, Y. *et al.* CCR8+FOXp3+ Treg cells as master drivers of immune regulation. *Proc Natl Acad Sci U S A* **114**, 6086–6091 (2017).

348. Ellis, G. I., Reneer, M. C., Vélez-Ortega, A. C., McCool, A. & Martí, F. Generation of Induced Regulatory T Cells from Primary Human Naïve and Memory T Cells. *J Vis Exp* (2012) doi:10.3791/3738.

349. Chen, L. *et al.* Diminished Frequency and Function of CD4+CD25high Regulatory T Cells Associated with Active Uveitis in Vogt-Koyanagi-Harada Syndrome. *Invest. Ophthalmol. Vis. Sci.* **49**, 3475–3482 (2008).

350. Salvany-Celades, M. *et al.* Three Types of Functional Regulatory T Cells Control T Cell Responses at the Human Maternal-Fetal Interface. *Cell Reports* **27**, 2537-2547.e5 (2019).

351. Klein, S., Kretz, C. C., Krammer, P. H. & Kuhn, A. CD127low/- and FoxP3+ Expression Levels Characterize Different Regulatory T-Cell Populations in Human Peripheral Blood. *Journal of Investigative Dermatology* **130**, 492–499 (2010).

352. Venken, K. *et al.* Natural naive CD4+CD25+CD127low regulatory T cell (Treg) development and function are disturbed in multiple sclerosis patients: recovery of memory Treg homeostasis during disease progression. *J. Immunol.* **180**, 6411–6420 (2008).

353. Niedźwiecki, M. *et al.* CD4+CD25highCD127low/−FoxP3+ Regulatory T Cell Subpopulations in the Bone Marrow and Peripheral Blood of Children with ALL: Brief Report. *J Immunol Res* **2018**, (2018).

354. Zhang, X. *et al.* Decreased regulatory T‐cell frequency and interleukin‐35 levels in patients with rheumatoid arthritis. *Experimental and Therapeutic Medicine* **16**, 5366–5372 (2018).

355. Pesenacker, A. M. *et al.* Treg gene signatures predict and measure type 1 diabetes trajectory. *JCI Insight* **4**,.

356. Li, L. *et al.* Increased frequency of regulatory T cells in the peripheral blood of patients with endometrioid adenocarcinoma. *Oncology Letters* **18**, 1424–1430 (2019).

357. Simonetta, F. *et al.* Increased CD127 expression on activated FOXP3+CD4+ regulatory T cells. *Eur. J. Immunol.* **40**, 2528–2538 (2010).

358. Mazzucchelli, R. & Durum, S. K. Interleukin-7 receptor expression: intelligent design. *Nat. Rev. Immunol.* **7**, 144–154 (2007).

359. Faller, E. M., Sugden, S. M., McVey, M. J., Kakal, J. A. & MacPherson, P. A. Soluble HIV Tat protein removes the IL-7 receptor alpha-chain from the surface of resting CD8 T cells and targets it for degradation. *J. Immunol.* **185**, 2854–2866 (2010).

360. Moniuszko, M. *et al.* Decreased number of CD4+ and CD8+ T cells that express the interleukin-7 receptor in blood and tissues of SIV-infected macaques. *Virology* **356**, 188–197 (2006).

361. Nemes, E. *et al.* Immunophenotype of HIV+ patients during CD4 cell-monitored treatment interruption: role of the IL-7/IL-7 receptor system. *AIDS* **20**, 2021–2032 (2006).

362. Miyara, M. *et al.* Functional Delineation and Differentiation Dynamics of Human CD4+ T Cells Expressing the FoxP3 Transcription Factor. *Immunity* **30**, 899–911 (2009).

363. Zhu Ling *et al.* Elevated Methylation of FOXP3 (Forkhead Box P3)-TSDR (Regulatory T-Cell–Specific Demethylated Region) Is Associated With

Increased Risk for Adverse Outcomes in Patients With Acute Coronary Syndrome. *Hypertension* **74**, 581–589 (2019).

364. Arroyo Hornero, R. *et al.* CD45RA Distinguishes CD4+CD25+CD127−/low TSDR Demethylated Regulatory T Cell Subpopulations With Differential Stability and Susceptibility to Tacrolimus-Mediated Inhibition of Suppression. *Transplantation* **101**, 302–309 (2017).
365. Sato, K. *et al.* Spatially selective depletion of tumor-associated regulatory T cells with near-infrared photoimmunotherapy. *Sci Transl Med* **8**, 352ra110 (2016).
366. Onda, M., Kobayashi, K. & Pastan, I. Depletion of regulatory T cells in tumors with an anti-CD25 immunotoxin induces CD8 T cell-mediated systemic antitumor immunity. *PNAS* **116**, 4575–4582 (2019).
367. Simonetta, F. & Bourgeois, C. CD4+FOXP3+ Regulatory T-Cell Subsets in Human Immunodeficiency Virus Infection. *Front. Immunol.* **4**, (2013).
368. Ferreira, R. C. *et al.* Cells with Treg-specific FOXP3 demethylation but low CD25 are prevalent in autoimmunity. *Journal of Autoimmunity* **84**, 75–86 (2017).
369. Smigiel, K. S. *et al.* CCR7 provides localized access to IL-2 and defines homeostatically distinct regulatory T cell subsets. *J. Exp. Med.* **211**, 121–136 (2014).
370. Li, M. O. & Rudensky, A. Y. T cell receptor signalling in the control of regulatory T cell differentiation and function. *Nature Reviews Immunology* **16**, 220–233 (2016).
371. Chen, W. & Konkel, J. E. TGF-beta and 'adaptive' Foxp3(+) regulatory T cells. *J Mol Cell Biol* **2**, 30–36 (2010).

372. Tone, Y. *et al.* Smad3 and NFAT cooperate to induce Foxp3 expression through its enhancer. *Nat. Immunol.* **9**, 194–202 (2008).

373. Arroyo Hornero, R. *et al.* CD45RA Distinguishes CD4+CD25+CD127−/low TSDR Demethylated Regulatory T Cell Subpopulations With Differential Stability and Susceptibility to Tacrolimus-Mediated Inhibition of Suppression. *Transplantation* **101**, 302 (2017).

374. Venken, K. *et al.* Natural Naive CD4+CD25+CD127low Regulatory T Cell (Treg) Development and Function Are Disturbed in Multiple Sclerosis Patients: Recovery of Memory Treg Homeostasis during Disease Progression. *The Journal of Immunology* **180**, 6411–6420 (2008).

375. Gagliani, N. *et al.* Coexpression of CD49b and LAG-3 identifies human and mouse T regulatory type 1 cells. *Nature Medicine* **19**, 739–746 (2013).

376. Jia, X. *et al.* Decreased number and impaired function of type 1 regulatory T cells in autoimmune diseases. *Journal of Cellular Physiology* **234**, 12442–12450 (2019).

377. Chen, Y., Kuchroo, V. K., Inobe, J., Hafler, D. A. & Weiner, H. L. Regulatory T cell clones induced by oral tolerance: suppression of autoimmune encephalomyelitis. *Science* **265**, 1237–1240 (1994).

378. Tordesillas, L. *et al.* Epicutaneous immunotherapy induces gastrointestinal LAP+ regulatory T cells and prevents food-induced anaphylaxis. *J. Allergy Clin. Immunol.* **139**, 189-201.e4 (2017).

379. Bollyky, P. L. *et al.* CD44 co-stimulation promotes FoxP3+ regulatory T-cell persistence and function via production of IL-2, IL-10 and TGF-beta. *J Immunol* **183**, 2232–2241 (2009).

380. Schmidleithner, L. *et al.* Enzymatic Activity of HPGD in Treg Cells Suppresses Tconv Cells to Maintain Adipose Tissue Homeostasis and Prevent Metabolic Dysfunction. *Immunity* **50**, 1232-1248.e14 (2019).

381. Campbell, D. J. Control of regulatory T cell migration, function and homeostasis. *J Immunol* **195**, 2507–2513 (2015).

382. Linterman, M. A. *et al.* Foxp3 + follicular regulatory T cells control the germinal center response. *Nature Medicine* **17**, 975–982 (2011).

383. Sambucci, M., Gargano, F., Guerrera, G., Battistini, L. & Borsellino, G. One, No One, and One Hundred Thousand: T Regulatory Cells' Multiple Identities in Neuroimmunity. *Front. Immunol.* **10**, (2019).

384. Chung, Y. *et al.* Follicular regulatory T cells expressing Foxp3 and Bcl-6 suppress germinal center reactions. *Nat. Med.* **17**, 983–988 (2011).

385. Wollenberg, I. *et al.* Regulation of the germinal center reaction by Foxp3+ follicular regulatory T cells. *J. Immunol.* **187**, 4553–4560 (2011).

386. Vaeth, M. *et al.* Follicular regulatory T cells control humoral autoimmunity via NFAT2-regulated CXCR5 expression. *J. Exp. Med.* **211**, 545–561 (2014).

387. Chung, Y. *et al.* Follicular regulatory T cells expressing Foxp3 and Bcl-6 suppress germinal center reactions. *Nature Medicine* **17**, 983–988 (2011).

388. Sage, P. T., Francisco, L. M., Carman, C. V. & Sharpe, A. H. The receptor PD-1 controls follicular regulatory T cells in the lymph nodes and blood. *Nat. Immunol.* **14**, 152–161 (2013).

389. Wing, J. B. *et al.* A distinct subpopulation of CD25− T-follicular regulatory cells localizes in the germinal centers. *PNAS* **114**, E6400–E6409 (2017).

390. Aloulou, M. *et al.* Follicular regulatory T cells can be specific for the immunizing antigen and derive from naive T cells. *Nat Commun* **7**, 10579 (2016).

391. Interleukin-10 from CD4+ follicular regulatory T cells promotes the germinal center response | Science Immunology. https://immunology.sciencemag.org/content/2/16/eaan4767.

392. Xie, M. M. *et al.* Follicular regulatory T cells inhibit the development of granzyme B–expressing follicular helper T cells. *JCI Insight* **4**,.

393. Sage, P. T., Francisco, L. M., Carman, C. V. & Sharpe, A. H. The receptor PD-1 controls follicular regulatory T cells in the lymph nodes and blood. *Nat. Immunol.* **14**, 152–161 (2013).

394. Aloulou, M. & Fazilleau, N. Regulation of B cell responses by distinct populations of CD4 T cells. *Biomedical Journal* **42**, 243–251 (2019).

395. Sage, P. T. & Sharpe, A. H. T Follicular Regulatory Cells in the Regulation of B cell Responses. *Trends Immunol* **36**, 410–418 (2015).

396. Sayin, I. *et al.* Spatial distribution and function of T follicular regulatory cells in human lymph nodes. *J Exp Med* **215**, 1531–1542 (2018).

397. Wing, J. B. *et al.* A distinct subpopulation of CD25- T-follicular regulatory cells localizes in the germinal centers. *Proc. Natl. Acad. Sci. U.S.A.* **114**, E6400–E6409 (2017).

398. Maceiras, A. R. *et al.* T follicular helper and T follicular regulatory cells have different TCR specificity. *Nat Commun* **8**, 15067 (2017).

399. Huang, Y. *et al.* Follicular regulatory T cells: a novel target for immunotherapy? *Clinical & Translational Immunology* **9**, e1106 (2020).

400. Sage, P. T., Alvarez, D., Godec, J., von Andrian, U. H. & Sharpe, A. H. Circulating T follicular regulatory and helper cells have memory-like properties. *J. Clin. Invest.* **124**, 5191–5204 (2014).

401. Shen, E. *et al.* Control of Germinal Center Localization and Lineage Stability of Follicular Regulatory T Cells by the Blimp1 Transcription Factor. *Cell Rep* **29**, 1848-1861.e6 (2019).

402. Wing, J. B., Tekgüç, M. & Sakaguchi, S. Control of Germinal Center Responses by T-Follicular Regulatory Cells. *Front Immunol* **9**, (2018).

403. Jiang, Q. *et al.* FoxP3+CD4+ regulatory T cells play an important role in acute HIV-1 infection in humanized Rag2−/−γC−/− mice in vivo. *Blood* **112**, 2858–2868 (2008).

404. Sato, K. *et al.* HIV-1 Vpr Accelerates Viral Replication during Acute Infection by Exploitation of Proliferating CD4+ T Cells In Vivo. *PLOS Pathogens* **9**, e1003812 (2013).

405. Moreno-Fernandez, M. E., Zapata, W., Blackard, J. T., Franchini, G. & Chougnet, C. A. Human regulatory T cells are targets for human immunodeficiency Virus (HIV) infection, and their susceptibility differs depending on the HIV type 1 strain. *J. Virol.* **83**, 12925–12933 (2009).

406. Sato, K. *et al.* HIV-1 Vpr Accelerates Viral Replication during Acute Infection by Exploitation of Proliferating CD4+ T Cells In Vivo. *PLOS Pathogens* **9**, e1003812 (2013).

407. Miller, S. M. *et al.* Follicular Regulatory T Cells Are Highly Permissive to R5-Tropic HIV-1. *Journal of Virology* **91**, (2017).

408. Jiao, Y. *et al.* The decrease of regulatory T cells correlates with excessive activation and apoptosis of CD8+ T cells in HIV-1-infected typical progressors, but not in long-term non-progressors. *Immunology* **128**, e366–e375 (2009).

409. Nikolova, M. *et al.* Subset- and Antigen-Specific Effects of Treg on CD8+ T Cell Responses in Chronic HIV Infection. *PLoS Pathog* **12**, (2016).

410. Angin, M. *et al.* Preserved Function of Regulatory T Cells in Chronic HIV-1 Infection Despite Decreased Numbers in Blood and Tissue. *J Infect Dis* **205**, 1495–1500 (2012).

411. Ji, J. & Cloyd, M. W. HIV-1 binding to CD4 on CD4+CD25+ regulatory T cells enhances their suppressive function and induces them to home to, and accumulate in, peripheral and mucosal lymphoid tissues: an additional mechanism of immunosuppression. *Int Immunol* **21**, 283–294 (2009).

412. Presicce, P. *et al.* Frequency of circulating regulatory T cells increases during chronic HIV infection and is largely controlled by highly active antiretroviral therapy. *PLoS ONE* **6**, e28118 (2011).

413. Schulze Zur Wiesch, J. *et al.* Comprehensive analysis of frequency and phenotype of T regulatory cells in HIV infection: CD39 expression of FoxP3+ T regulatory cells correlates with progressive disease. *J. Virol.* **85**, 1287–1297 (2011).

414. Chachage, M. *et al.* CD25+ FoxP3+ Memory CD4 T Cells Are Frequent Targets of HIV Infection In Vivo. *Journal of Virology* **90**, 8954–8967 (2016).

415. Ambada, G. N. *et al.* Phenotypic characterization of regulatory T cells from antiretroviral-naive HIV-1-infected people. *Immunology* **151**, 405–416 (2017).

416. Song, J.-W. *et al.* Expression of CD39 Is Correlated With HIV DNA Levels in Naïve Tregs in Chronically Infected ART Naïve Patients. *Front. Immunol.* **10**, (2019).

417. Allers, K. *et al.* Gut Mucosal FOXP3+ Regulatory CD4+ T Cells and Nonregulatory CD4+ T Cells Are Differentially Affected by Simian Immunodeficiency Virus Infection in Rhesus Macaques. *Journal of Virology* **84**, 3259–3269 (2010).

418. Angin, M. *et al.* Preserved function of regulatory T cells in chronic HIV-1 infection despite decreased numbers in blood and tissue. *J. Infect. Dis.* **205**, 1495–1500 (2012).

419. Wiesch, J. S. zur *et al.* Comprehensive Analysis of Frequency and Phenotype of T Regulatory Cells in HIV Infection: CD39 Expression of FoxP3+ T Regulatory Cells Correlates with Progressive Disease. *Journal of Virology* **85**, 1287–1297 (2011).

420. Simonetta, F. *et al.* Early and Long-Lasting Alteration of Effector CD45RA−Foxp3high Regulatory T-Cell Homeostasis During HIV Infection. *J Infect Dis.* **205**, 1510–1519 (2012).

421. Apoil, P. A. *et al.* FOXP3 mRNA levels are decreased in peripheral blood CD4+ lymphocytes from HIV-positive patients. *J. Acquir. Immune Defic. Syndr.* **39**, 381–385 (2005).

422. Andersson, J. *et al.* The prevalence of regulatory T cells in lymphoid tissue is correlated with viral load in HIV-infected patients. *J. Immunol.* **174**, 3143–3147 (2005).

423. Xing, S. *et al.* Increased turnover of FoxP3high regulatory T cells is associated with hyperactivation and disease progression of chronic HIV-1 infection. *J. Acquir. Immune Defic. Syndr.* **54**, 455–462 (2010).

424. Montes, M. *et al.* Normalization of FoxP3(+) regulatory T cells in response to effective antiretroviral therapy. *J. Infect. Dis.* **203**, 496–499 (2011).

425. Saison, J. *et al.* Increased Regulatory T-Cell Percentage Contributes to Poor CD4+ Lymphocytes Recovery: A 2-Year Prospective Study After Introduction of Antiretroviral Therapy. *Open Forum Infect Dis* **2**, (2015).

426. Hunt, P. W. *et al.* A low T regulatory cell response may contribute to both viral control and generalized immune activation in HIV controllers. *PLoS ONE* **6**, e15924 (2011).

427. Kolte, L. *et al.* Increased levels of regulatory T cells (Tregs) in human immunodeficiency virus-infected patients after 5 years of highly active anti-retroviral therapy may be due to increased thymic production of naive Tregs. *Clin Exp Immunol* **155**, 44–52 (2009).

428. Ndhlovu, L. C. *et al.* IL-2 Immunotherapy to Recently HIV-1 Infected Adults Maintains the Numbers of IL-17 Expressing CD4+ T (TH17) Cells in the Periphery. *J Clin Immunol* **30**, 681–692 (2010).

429. Caruso, M. P. *et al.* Impact of HIV-ART on the restoration of Th17 and Treg cells in blood and female genital mucosa. *Scientific Reports* **9**, 1978 (2019).

430. Grützner, E. M. *et al.* Treatment Intensification in HIV-Infected Patients Is Associated With Reduced Frequencies of Regulatory T Cells. *Front Immunol* **9**, (2018).

431. Angin, M. *et al.* HIV-1 Infection Impairs Regulatory T-Cell Suppressive Capacity on a Per-Cell Basis. *J Infect Dis* **210**, 899–903 (2014).

432. Pion, M., Jaramillo-Ruiz, D., Martínez, A., Muñoz-Fernández, M. A. & Correa-Rocha, R. HIV infection of human regulatory T cells downregulates Foxp3 expression by increasing DNMT3b levels and DNA methylation in the FOXP3 gene. *AIDS* **27**, 2019–2029 (2013).

433. Tran, T.-A. *et al.* Resting Regulatory CD4 T Cells: A Site of HIV Persistence in Patients on Long-Term Effective Antiretroviral Therapy. *PLoS ONE* **3**, e3305 (2008).

434. Jiao, Y.-M. *et al.* CD4+CD25+CD127 regulatory cells play multiple roles in maintaining HIV-1 p24 production in patients on long-term treatment: HIV-1 p24-producing cells and suppression of anti-HIV immunity. *International Journal of Infectious Diseases* **37**, 42–49 (2015).

435. Dunay, G. A. *et al.* Assessment of the HIV-1 reservoir in CD4+ regulatory T cells by a Droplet Digital PCR based approach. *Virus Research* **240**, 107–111 (2017).

436. Li, G. *et al.* Regulatory T Cells Contribute to HIV-1 Reservoir Persistence in CD4+ T Cells Through Cyclic Adenosine Monophosphate-Dependent Mechanisms in Humanized Mice In Vivo. *J. Infect. Dis.* **216**, 1579–1591 (2017).

437. Tran, T.-A. *et al.* Resting Regulatory CD4 T Cells: A Site of HIV Persistence in Patients on Long-Term Effective Antiretroviral Therapy. *PLoS One* **3**, (2008).

438. Jiao, Y.-M. *et al.* CD4+CD25+CD127 regulatory cells play multiple roles in maintaining HIV-1 p24 production in patients on long-term treatment: HIV-1 p24-producing cells and suppression of anti-HIV immunity. *Int. J. Infect. Dis.* **37**, 42–49 (2015).

439. Allers, K. *et al.* Gut mucosal FOXP3+ regulatory CD4+ T cells and Nonregulatory CD4+ T cells are differentially affected by simian immunodeficiency virus infection in rhesus macaques. *J. Virol.* **84**, 3259–3269 (2010).

440. Qin, S. *et al.* Novel immune checkpoint targets: moving beyond PD-1 and CTLA-4. *Molecular Cancer* **18**, 155 (2019).

441. Rotte, A., Jin, J. Y. & Lemaire, V. Mechanistic overview of immune checkpoints to support the rational design of their combinations in cancer immunotherapy. *Annals of Oncology* **29**, 71–83 (2018).

442. Chomont, N. *et al.* HIV reservoir size and persistence are driven by T cell survival and homeostatic proliferation. *Nature Medicine* **15**, 893–900 (2009).

443. EVANS, V. A. *et al.* PD-1 contributes to the establishment and maintenance of HIV-1 latency. *AIDS* **32**, 1491–1497 (2018).

444. Marhelava, K., Pilch, Z., Bajor, M., Graczyk-Jarzynka, A. & Zagozdzon, R. Targeting Negative and Positive Immune Checkpoints with Monoclonal Antibodies in Therapy of Cancer. *Cancers (Basel)* **11**, (2019).

445. Murakami, N. & Riella, L. V. Co-Inhibitory Pathways and Their Importance in Immune Regulation: *Transplantation* **98**, 3–14 (2014).

446. Linsley, P. S. *et al.* Intracellular trafficking of CTLA-4 and focal localization towards sites of TCR engagement. *Immunity* **4**, 535–543 (1996).

447. Schneider, H. *et al.* Cytolytic T lymphocyte-associated antigen-4 and the TCR zeta/CD3 complex, but not CD28, interact with clathrin adaptor complexes AP-1 and AP-2. *J. Immunol.* **163**, 1868–1879 (1999).

448. Schneider, H. & Rudd, C. E. Diverse Mechanisms Regulate the Surface Expression of Immunotherapeutic Target CTLA-4. *Front Immunol* **5**, (2014).

449. Jago, C. B., Yates, J., Câmara, N. O. S., Lechler, R. I. & Lombardi, G. Differential expression of CTLA-4 among T cell subsets. *Clin. Exp. Immunol.* **136**, 463–471 (2004).

450. Schwartz, R. H. Costimulation of T lymphocytes: the role of CD28, CTLA-4, and B7/BB1 in interleukin-2 production and immunotherapy. *Cell* **71**, 1065–1068 (1992).

451. Matheu, M. P. *et al.* Imaging regulatory T cell dynamics and CTLA4-mediated suppression of T cell priming. *Nat Commun* **6**, 6219 (2015).

452. Schwartz, R. H. Costimulation of T lymphocytes: the role of CD28, CTLA-4, and B7/BB1 in interleukin-2 production and immunotherapy. *Cell* **71**, 1065–1068 (1992).

453. Kinter, A. *et al.* Suppression of HIV-specific T cell activity by lymph node CD25+ regulatory T cells from HIV-infected individuals. *Proc Natl Acad Sci U S A* **104**, 3390–3395 (2007).

454. Sabins, N. C., Harman, B. C., Barone, L. R., Shen, S. & Santulli-Marotto, S. Differential Expression of Immune Checkpoint Modulators on In Vitro Primed CD4+ and CD8+ T Cells. *Front. Immunol.* **7**, (2016).

455. Yuzefpolskiy, Y., Baumann, F. M., Penny, L. A., Kalia, V. & Sarkar, S. Signaling through PD-1 on CD8 T cells is critical for antigen-independent maintenance of immune memory. *The Journal of Immunology* **196**, 129.6-129.6 (2016).

456. Ma, J. *et al.* PD1Hi CD8+ T cells correlate with exhausted signature and poor clinical outcome in hepatocellular carcinoma. *Journal for ImmunoTherapy of Cancer* **7**, 331 (2019).

457. Dong, Y. *et al.* CD4+ T cell exhaustion revealed by high PD-1 and LAG-3 expression and the loss of helper T cell function in chronic hepatitis B. *BMC Immunol* **20**, (2019).

458. Programmed cell death-1 contributes to the establishment and maintenance of HIV-1 latency. - Abstract - Europe PMC. https://europepmc.org/article/PMC/6026054.

459. Fromentin, R. *et al.* CD4+ T Cells Expressing PD-1, TIGIT and LAG-3 Contribute to HIV Persistence during ART. *PLOS Pathogens* **12**, e1005761 (2016).

460. Gupta, R. K. *et al.* HIV-1 remission following CCR5Δ32/Δ32 haematopoietic stem-cell transplantation. *Nature* **568**, 244–248 (2019).

461. Hütter, G. *et al.* Long-Term Control of HIV by CCR5 Delta32/Delta32 Stem-Cell Transplantation. *New England Journal of Medicine* **360**, 692–698 (2009).

462. Styczyński, J. *et al.* Death after hematopoietic stem cell transplantation: changes over calendar year time, infections and associated factors. *Bone Marrow Transplantation* **55**, 126–136 (2020).

463. International AIDS Society Scientific Working Group on HIV Cure *et al.* Towards an HIV cure: a global scientific strategy. *Nat. Rev. Immunol.* **12**, 607–614 (2012).

464. Deeks, S. G. HIV: Shock and kill. *Nature* **487**, 439–440 (2012).

465. Marsden, M. D. & Zack, J. A. Eradication of HIV: current challenges and new directions. *J. Antimicrob. Chemother.* **63**, 7–10 (2009).

466. Richman, D. D. *et al.* The challenge of finding a cure for HIV infection. *Science* **323**, 1304–1307 (2009).

467. Rasmussen, T. A. *et al.* Panobinostat, a histone deacetylase inhibitor, for latent-virus reactivation in HIV-infected patients on suppressive antiretroviral therapy: a phase 1/2, single group, clinical trial. *Lancet HIV* **1**, e13-21 (2014).

468. Xu, W. *et al.* Advancements in Developing Strategies for Sterilizing and Functional HIV Cures. *Biomed Res Int* **2017**, 6096134 (2017).

469. Ahlenstiel, C. L., Symonds, G., Kent, S. J. & Kelleher, A. D. Block and Lock HIV Cure Strategies to Control the Latent Reservoir. *Front Cell Infect Microbiol* **10**, (2020).

470. Yoshida, M., Kudo, N., Kosono, S. & Ito, A. Chemical and structural biology of protein lysine deacetylases. *Proc. Jpn. Acad., Ser. B, Phys. Biol. Sci.* **93**, 297–321 (2017).

471. Archin, N. M. *et al.* Administration of vorinostat disrupts HIV-1 latency in patients on antiretroviral therapy. *Nature* **487**, 482–485 (2012).

472. Archin, N. M. *et al.* Administration of vorinostat disrupts HIV-1 latency in patients on antiretroviral therapy. *Nature* **487**, 482–485 (2012).

473. Elliott, J. H. *et al.* Activation of HIV transcription with short-course vorinostat in HIV-infected patients on suppressive antiretroviral therapy. *PLoS Pathog.* **10**, e1004473 (2014).

474. Rasmussen, T. A. *et al.* Panobinostat, a histone deacetylase inhibitor, for latent-virus reactivation in HIV-infected patients on suppressive antiretroviral therapy: a phase 1/2, single group, clinical trial. *The Lancet HIV* **1**, e13–e21 (2014).

475. Wei, D. G. *et al.* Histone deacetylase inhibitor romidepsin induces HIV expression in CD4 T cells from patients on suppressive antiretroviral therapy at concentrations achieved by clinical dosing. *PLoS Pathog.* **10**, e1004071 (2014).

476. Søgaard, O. S. *et al.* The Depsipeptide Romidepsin Reverses HIV-1 Latency In Vivo. *PLoS Pathog.* **11**, e1005142 (2015).

477. Mehla, R. *et al.* Bryostatin Modulates Latent HIV-1 Infection via PKC and AMPK Signaling but Inhibits Acute Infection in a Receptor Independent Manner. *PLoS One* **5**, (2010).

478. Pérez, M. *et al.* Bryostatin-1 synergizes with histone deacetylase inhibitors to reactivate HIV-1 from latency. *Curr. HIV Res.* **8**, 418–429 (2010).

479. Mehla, R. *et al.* Bryostatin Modulates Latent HIV-1 Infection via PKC and AMPK Signaling but Inhibits Acute Infection in a Receptor Independent Manner. *PLoS ONE* **5**, e11160 (2010).

480. Sánchez-Duffhues, G. *et al.* Activation of latent HIV-1 expression by protein kinase C agonists. A novel therapeutic approach to eradicate HIV-1 reservoirs. *Curr Drug Targets* **12**, 348–356 (2011).

481. Banerjee, C. *et al.* BET bromodomain inhibition as a novel strategy for reactivation of HIV-1. *J Leukoc Biol* **92**, 1147–1154 (2012).

482. Bisgrove, D. A., Mahmoudi, T., Henklein, P. & Verdin, E. Conserved P-TEFb-interacting domain of BRD4 inhibits HIV transcription. *Proc. Natl. Acad. Sci. U.S.A.* **104**, 13690–13695 (2007).

483. Suzuki, K. *et al.* Prolonged transcriptional silencing and CpG methylation induced by siRNAs targeted to the HIV-1 promoter region. *J RNAi Gene Silencing* **1**, 66–78 (2005).

484. Méndez, C., Ledger, S., Petoumenos, K., Ahlenstiel, C. & Kelleher, A. D. RNA-induced epigenetic silencing inhibits HIV-1 reactivation from latency. *Retrovirology* **15**, 67 (2018).

485. Jin, H. *et al.* Shutdown of HIV-1 Transcription in T Cells by Nullbasic, a Mutant Tat Protein. *mBio* **7**, (2016).

486. Jin, H. *et al.* Shutdown of HIV-1 Transcription in T Cells by Nullbasic, a Mutant Tat Protein. *mBio* **7**, (2016).

487. Apolloni, A. *et al.* A mutant Tat protein provides strong protection from HIV-1 infection in human CD4+ T cells. *Hum Gene Ther* **24**, 270–282 (2013).

488. Lin, M.-H. *et al.* A HIV-1 Tat mutant protein disrupts HIV-1 Rev function by targeting the DEAD-box RNA helicase DDX1. *Retrovirology* **11**, 121 (2014).

489. Jin, H. *et al.* Strong In Vivo Inhibition of HIV-1 Replication by Nullbasic, a Tat Mutant. *mBio* **10**, (2019).

490. Mousseau, G. *et al.* An analog of the natural steroidal alkaloid cortistatin A potently suppresses Tat-dependent HIV transcription. *Cell Host Microbe* **12**, 97–108 (2012).

491. Mousseau, G. *et al.* The Tat Inhibitor Didehydro-Cortistatin A Prevents HIV-1 Reactivation from Latency. *mBio* **6**, e00465 (2015).

492. Kessing, C. F. *et al.* In Vivo Suppression of HIV Rebound by Didehydro-Cortistatin A, a 'Block-and-Lock' Strategy for HIV-1 Treatment. *Cell Rep* **21**, 600–611 (2017).

493. Mediouni, S. *et al.* The Tat inhibitor didehydro-cortistatin A suppresses SIV replication and reactivation. *FASEB J* **33**, 8280–8293 (2019).

494. Pfeffer, C. M. & Singh, A. T. K. Apoptosis: A Target for Anticancer Therapy. *Int J Mol Sci* **19**, (2018).

495. Gyrd-Hansen, M. *et al.* IAPs contain an evolutionarily conserved ubiquitin-binding domain that regulates NF-kappaB as well as cell survival and oncogenesis. *Nat. Cell Biol.* **10**, 1309–1317 (2008).

496. Wang, J. & Li, W. Discovery of Novel Second Mitochondria-Derived Activator of Caspase Mimetics as Selective Inhibitor of Apoptosis Protein Inhibitors. *J Pharmacol Exp Ther* **349**, 319–329 (2014).

497. Derakhshan, A., Chen, Z. & Waes, C. V. Therapeutic small-molecules target inhibitor of apoptosis proteins in cancers with deregulation of extrinsic and intrinsic cell death pathways. *Clin Cancer Res* **23**, 1379–1387 (2017).

498. Honeycutt, J. B. *et al.* Macrophages sustain HIV replication in vivo independently of T cells. *J. Clin. Invest.* **126**, 1353–1366 (2016).

499. Campbell, G. R., To, R. K., Zhang, G. & Spector, S. A. SMAC mimetics induce autophagy-dependent apoptosis of HIV-1-infected macrophages. *Cell Death & Disease* **11**, 1–14 (2020).

500. Pache, L. *et al.* BIRC2/cIAP1 Suppresses HIV-1 Transcription and Can Be Targeted by Smac Mimetics to Promote Reversal of Viral Latency. *Cell Host Microbe* **18**, 345–353 (2015).

501. Pache, L. *et al.* Pharmacological Activation of Non-canonical NF-κB Signaling Activates Latent HIV-1 Reservoirs In Vivo. *CR Med* **1**, (2020).

502. Altfeld, M. & Gale Jr, M. Innate immunity against HIV-1 infection. *Nat Immunol* **16**, 554–562 (2015).

503. Darcis, G. *et al.* An In-Depth Comparison of Latency-Reversing Agent Combinations in Various In Vitro and Ex Vivo HIV-1 Latency Models Identified Bryostatin-1+JQ1 and Ingenol-B+JQ1 to Potently Reactivate Viral Gene Expression. *PLoS Pathog.* **11**, e1005063 (2015).

504. Acchioni, C. *et al.* Alternate NF-κB-Independent Signaling Reactivation of Latent HIV-1 Provirus. *Journal of Virology* **93**, (2019).

505. Gane, E. J. *et al.* The oral toll-like receptor-7 agonist GS-9620 in patients with chronic hepatitis B virus infection. *J. Hepatol.* **63**, 320–328 (2015).

506. Borducchi, E. N. *et al.* Ad26/MVA therapeutic vaccination with TLR7 stimulation in SIV-infected rhesus monkeys. *Nature* **540**, 284–287 (2016).

507. Lim, S.-Y. *et al.* TLR7 agonists induce transient viremia and reduce the viral reservoir in SIV-infected rhesus macaques on antiretroviral therapy. *Sci Transl Med* **10**, (2018).

508. Prete, G. Q. D. *et al.* TLR7 agonist administration to SIV-infected macaques receiving early initiated cART does not induce plasma viremia. *JCI Insight* **4**, (2019).

509. Meås, H. Z. *et al.* Sensing of HIV-1 by TLR8 activates human T cells and reverses latency. *Nature Communications* **11**, 1–16 (2020).

510. Sadowski, I. & Hashemi, F. B. Strategies to eradicate HIV from infected patients: elimination of latent provirus reservoirs. *Cell. Mol. Life Sci.* **76**, 3583–3600 (2019).

511. Voss, K. & Snow, A. L. Transient FOXP3 upregulation protects human conventional T cells from restimulation-induced cell death during activation-induced proliferation. *The Journal of Immunology* **198**, 124.3-124.3 (2017).

512. Dao, T. *et al.* Depleting T regulatory cells by targeting intracellular Foxp3 with a TCR mimic antibody. *Oncoimmunology* **8**, (2019).

513. Wiendl, H. & Gross, C. C. Modulation of IL-2Rα with daclizumab for treatment of multiple sclerosis. *Nat Rev Neurol* **9**, 394–404 (2013).

514. Wang, Z. *et al.* Ontak-like human IL-2 fusion toxin. *J Immunol Methods* **448**, 51–58 (2017).

515. Pandrea, I. *et al.* Cutting edge: Experimentally induced immune activation in natural hosts of simian immunodeficiency virus induces significant increases in viral replication and CD4+ T cell depletion. *J. Immunol.* **181**, 6687–6691 (2008).

516. Ma, D. *et al.* Simian Immunodeficiency Virus SIVsab Infection of Rhesus Macaques as a Model of Complete Immunological Suppression with Persistent Reservoirs of Replication-Competent Virus: Implications for Cure Research. *Journal of Virology* **89**, 6155–6160 (2015).

517. Pandrea, I. *et al.* Functional Cure of SIVagm Infection in Rhesus Macaques Results in Complete Recovery of CD4+ T Cells and Is Reverted by CD8+ Cell Depletion. *PLOS Pathogens* **7**, e1002170 (2011).

518. Peraino, J. S. *et al.* Diphtheria toxin-based bivalent human IL-2 fusion toxin with improved efficacy for targeting human CD25(+) cells. *J. Immunol. Methods* **405**, 57–66 (2014).

519. Wang, Z. *et al.* Diphtheria-toxin based anti-human CCR4 immunotoxin for targeting human CCR4(+) cells in vivo. *Mol Oncol* **9**, 1458–1470 (2015).

520. Wang, Z. *et al.* Treg depletion in non-human primates using a novel diphtheria toxin-based anti-human CCR4 immunotoxin. *Molecular Oncology* **10**, 553–565 (2016).

521. Noordam, L. *et al.* Low-dose cyclophosphamide depletes circulating naïve and activated regulatory T cells in malignant pleural mesothelioma patients synergistically treated with dendritic cell-based immunotherapy. *Oncoimmunology* **7**, (2018).

522. Camisaschi, C. *et al.* Effects of cyclophosphamide and IL-2 on regulatory CD4+ T cell frequency and function in melanoma patients vaccinated with

HLA-class I peptides: impact on the antigen-specific T cell response. *Cancer Immunol Immunother* **62**, 897–908 (2013).

523. Bartlett, J. A. *et al.* Addition of cyclophosphamide to antiretroviral therapy does not diminish the cellular reservoir in HIV-infected persons. *AIDS Res. Hum. Retroviruses* **18**, 535–543 (2002).

524. Leach, D. R., Krummel, M. F. & Allison, J. P. Enhancement of Antitumor Immunity by CTLA-4 Blockade. *Science* **271**, 1734–1736 (1996).

525. Elsas, A. van, Hurwitz, A. A. & Allison, J. P. Combination Immunotherapy of B16 Melanoma Using Anti–Cytotoxic T Lymphocyte–Associated Antigen 4 (Ctla-4) and Granulocyte/Macrophage Colony-Stimulating Factor (Gm-Csf)-Producing Vaccines Induces Rejection of Subcutaneous and Metastatic Tumors Accompanied by Autoimmune Depigmentation. *J Exp Med* **190**, 355–366 (1999).

526. Freeman, G. J. *et al.* Engagement of the PD-1 immunoinhibitory receptor by a novel B7 family member leads to negative regulation of lymphocyte activation. *J. Exp. Med.* **192**, 1027–1034 (2000).

527. Iwai, Y., Terawaki, S. & Honjo, T. PD-1 blockade inhibits hematogenous spread of poorly immunogenic tumor cells by enhanced recruitment of effector T cells. *Int. Immunol.* **17**, 133–144 (2005).

528. Grosso, J. F. & Jure-Kunkel, M. N. CTLA-4 blockade in tumor models: an overview of preclinical and translational research. *Cancer Immun* **13**, (2013).

529. Hodi, F. S. *et al.* Improved Survival with Ipilimumab in Patients with Metastatic Melanoma. *New England Journal of Medicine* **363**, 711–723 (2010).

530. Larkin, J. *et al.* Five-Year Survival with Combined Nivolumab and Ipilimumab in Advanced Melanoma. *N. Engl. J. Med.* **381**, 1535–1546 (2019).

531. Selby, M. J. *et al.* Preclinical Development of Ipilimumab and Nivolumab Combination Immunotherapy: Mouse Tumor Models, In Vitro Functional Studies, and Cynomolgus Macaque Toxicology. *PLoS One* **11**, (2016).

532. Choi, J. *et al.* Combined VLA-4–Targeted Radionuclide Therapy and Immunotherapy in a Mouse Model of Melanoma. *J Nucl Med* **59**, 1843–1849 (2018).

533. Harper, J. *et al.* CTLA-4 and PD-1 dual blockade induces SIV reactivation without control of rebound after antiretroviral therapy interruption. *Nature Medicine* **26**, 519–528 (2020).

534. Gay, C. L. *et al.* Clinical Trial of the Anti-PD-L1 Antibody BMS-936559 in HIV-1 Infected Participants on Suppressive Antiretroviral Therapy. *J Infect Dis* **215**, 1725–1733 (2017).

535. Ruzevick, J. *et al.* A Patient with HIV Treated with Ipilimumab and Stereotactic Radiosurgery for Melanoma Metastases to the Brain. *Case Rep Oncol Med* **2013**, 946392 (2013).

536. Burke, M. M. *et al.* Case Report: response to ipilimumab in a patient with HIV with metastatic melanoma. *J. Clin. Oncol.* **29**, e792-794 (2011).

537. Guihot, A. *et al.* Drastic decrease of the HIV reservoir in a patient treated with nivolumab for lung cancer. *Annals of Oncology* **29**, 517–518 (2018).

538. Le Garff, G. *et al.* Transient HIV-specific T cells increase and inflammation in an HIV-infected patient treated with nivolumab. *AIDS* **31**, 1048–1051 (2017).

539. Wightman, F. *et al.* Effect of ipilimumab on the HIV reservoir in an HIV-infected individual with metastatic melanoma. *AIDS* **29**, 504–506 (2015).

540. Fromentin, R. *et al.* PD-1 blockade potentiates HIV latency reversal ex vivo in CD4 + T cells from ART-suppressed individuals. *Nature Communications* **10**, 814 (2019).

541. Cecchinato, V. *et al.* Immune Activation Driven by CTLA-4 Blockade Augments Viral Replication at Mucosal Sites in Simian Immunodeficiency Virus Infection. *J Immunol* **180**, 5439–5447 (2008).

542. Velu, V. *et al.* Enhancing SIV-Specific Immunity In Vivo by PD-1 Blockade. *Nature* **458**, 206–210 (2009).

543. Lavolé, A. *et al.* PD-1 blockade in HIV-infected patients with lung cancer: a new challenge or already a strategy? *Ann. Oncol.* **29**, 1065–1066 (2018).

544. Scully, E. P. *et al.* Inconsistent HIV reservoir dynamics and immune responses following anti-PD-1 therapy in cancer patients with HIV infection. *Ann Oncol* **29**, 2141–2142 (2018).

545. Davar, D., Wilson, M., Pruckner, C. & Kirkwood, J. M. PD-1 Blockade in Advanced Melanoma in Patients with Hepatitis C and/or HIV. *Case Rep Oncol Med* **2015**, 737389 (2015).

546. Hosmane, N. N. *et al.* Proliferation of latently infected CD4+ T cells carrying replication-competent HIV-1: Potential role in latent reservoir dynamics. *J. Exp. Med.* **214**, 959–972 (2017).

547. Brooks, D. G. *et al.* Molecular characterization, reactivation, and depletion of latent HIV. *Immunity* **19**, 413–423 (2003).

548. Hermankova, M. *et al.* Analysis of Human Immunodeficiency Virus Type 1 Gene Expression in Latently Infected Resting CD4+ T Lymphocytes In Vivo. *Journal of Virology* **77**, 7383–7392 (2003).

549. Chun, T. W., Engel, D., Mizell, S. B., Ehler, L. A. & Fauci, A. S. Induction of HIV-1 replication in latently infected CD4+ T cells using a combination of cytokines. *J. Exp. Med.* **188**, 83–91 (1998).

550. Yukl, S. A. *et al.* Differences in HIV burden and immune activation within the gut of HIV-positive patients receiving suppressive antiretroviral therapy. *J. Infect. Dis.* **202**, 1553–1561 (2010).

551. Chun, T.-W. *et al.* Persistence of HIV in gut-associated lymphoid tissue despite long-term antiretroviral therapy. *J. Infect. Dis.* **197**, 714–720 (2008).

552. Yukl, S. A. *et al.* The distribution of HIV DNA and RNA in cell subsets differs in gut and blood of HIV-positive patients on ART: implications for viral persistence. *J. Infect. Dis.* **208**, 1212–1220 (2013).

553. Takahashi, T. *et al.* Immunologic Self-Tolerance Maintained by Cd25+Cd4+Regulatory T Cells Constitutively Expressing Cytotoxic T Lymphocyte–Associated Antigen 4. *J Exp Med* **192**, 303–310 (2000).

554. Amarnath, S. *et al.* Regulatory T cells and human myeloid dendritic cells promote tolerance via programmed death ligand-1. *PLoS Biol.* **8**, e1000302 (2010).

555. Evans, V. A. *et al.* Programmed cell death-1 contributes to the establishment and maintenance of HIV-1 latency. *AIDS* **32**, 1491–1497 (2018).

556. Fromentin, R. *et al.* PD-1 blockade potentiates HIV latency reversal ex vivo in CD4 + T cells from ART-suppressed individuals. *Nature Communications* **10**, 1–7 (2019).

557. Fukazawa, Y. *et al.* B cell follicle sanctuary permits persistent productive simian immunodeficiency virus infection in elite controllers. *Nat. Med.* **21**, 132–139 (2015).

558. Rallón, N. *et al.* Expression of PD-1 and Tim-3 markers of T-cell exhaustion is associated with CD4 dynamics during the course of untreated and treated HIV infection. *PLoS ONE* **13**, e0193829 (2018).

559. Vendrame, E. *et al.* TIGIT is upregulated by HIV-1 infection and marks a highly functional adaptive and mature subset of natural killer cells. *AIDS* **34**, 801–813 (2020).

560. CTLA-4+PD-1- Memory CD4+ T Cells Critically Contribute to Viral Persistence in Antiretroviral Therapy-Suppressed, SIV-Infected Rhesus Macaques. - PubMed - NCBI. https://www-ncbi-nlm-nih-gov.ezp.lib.unimelb.edu.au/pubmed/29045906.

561. Wee, Y. T. F. *et al.* An integrated automated multispectral imaging technique that simultaneously detects and quantitates viral RNA and immune cell protein markers in fixed sections from Epstein-Barr virus-related tumours. *Ann Diagn Pathol* **37**, 12–19 (2018).

562. Jordan, A., Bisgrove, D. & Verdin, E. HIV reproducibly establishes a latent infection after acute infection of T cells in vitro. *EMBO J.* **22**, 1868–1877 (2003).

563. Reed, L. J. & Muench, H. A SIMPLE METHOD OF ESTIMATING FIFTY PER CENT ENDPOINTS. *Am J Epidemiol* **27**, 493–497 (1938).

564. Evans, V. A. *et al.* Myeloid Dendritic Cells Induce HIV-1 Latency in Non-proliferating CD4+ T Cells. *PLOS Pathogens* **9**, e1003799 (2013).

565. Stack, E. C., Wang, C., Roman, K. A. & Hoyt, C. C. Multiplexed immunohistochemistry, imaging, and quantitation: A review, with an assessment of Tyramide signal amplification, multispectral imaging and multiplex analysis. *Methods* **70**, 46–58 (2014).

566. Millar, M. Mixed Multiplex Staining: Automated RNAscope™ and OPAL™ for Multiple Targets. *Methods Mol. Biol.* **2148**, 277–298 (2020).

567. Vasquez, J. J. *et al.* Elucidating the Burden of HIV in Tissues Using Multiplexed Immunofluorescence and In Situ Hybridization: Methods for the Single-Cell Phenotypic Characterization of Cells Harboring HIV In Situ. *J Histochem Cytochem* **66**, 427–446 (2018).

568. Emiliani, S. *et al.* A point mutation in the HIV-1 Tat responsive element is associated with postintegration latency. *Proc. Natl. Acad. Sci. U.S.A.* **93**, 6377–6381 (1996).

569. Zhang, W., Svensson Akusjärvi, S., Sönnerborg, A. & Neogi, U. Characterization of Inducible Transcription and Translation-Competent HIV-1 Using the RNAscope ISH Technology at a Single-Cell Resolution. *Front. Microbiol.* **9**, (2018).

570. Tacchetti, C. *et al.* HIV is trapped and masked in the cytoplasm of lymph node follicular dendritic cells. *Am J Pathol* **150**, 533–542 (1997).

571. Fletcher, C. V. *et al.* Persistent HIV-1 replication is associated with lower antiretroviral drug concentrations in lymphatic tissues. *PNAS* **111**, 2307–2312 (2014).

572. Ukah, O. B. *et al.* Visualization of HIV-1 RNA Transcription from Integrated HIV-1 DNA in Reactivated Latently Infected Cells. *Viruses* **10**, (2018).

573. Denton, P. W. *et al.* Targeted cytotoxic therapy kills persisting HIV infected cells during ART. *PLoS Pathog.* **10**, e1003872 (2014).

574. Estes, J. D. *et al.* Defining total-body AIDS-virus burden with implications for curative strategies. *Nature medicine* **23**, 1271–1276 (2017).

575. Henrich, T. J. *et al.* HIV-1 persistence following extremely early initiation of antiretroviral therapy (ART) during acute HIV-1 infection: An observational study. *PLoS Med* **14**, (2017).

576. Elliott, A. D. Confocal Microscopy: Principles and Modern Practices. *Curr Protoc Cytom* **92**, e68 (2020).

577. Anderson, C. M. *et al.* Fully Automated RNAscope In Situ Hybridization Assays for Formalin-Fixed Paraffin-Embedded Cells and Tissues. *J Cell Biochem* **117**, 2201–2208 (2016).

578. Sluis, R. M. V. der *et al.* Combination Immune Checkpoint Blockade to Reverse HIV Latency. *The Journal of Immunology* **204**, 1242–1254 (2020).

579. IMPACT OF ANTI-PD-1 AND ANTI-CTLA-4 ON THE HIV RESERVOIR IN VIVO: THE AMC-095 STUDY. *CROI Conference* https://www.croiconference.org/abstract/impact-of-anti-pd-1-and-anti-ctla-4-on-the-hiv-reservoir-in-vivo-the-amc-095-study/.

580. Jiao, Y. *et al.* The decrease of regulatory T cells correlates with excessive activation and apoptosis of CD8+ T cells in HIV-1-infected typical progressors, but not in long-term non-progressors. *Immunology* **128**, e366–e375 (2009).

581. Zhang, W. *et al.* An innovative method to generate a Good Manufacturing Practice-ready regulatory T-cell product from non-mobilized leukapheresis donors. *Cytotherapy* **17**, 1268–1279 (2015).

582. Blache, C. *et al.* Reduced frequency of regulatory T cells in peripheral blood stem cell compared to bone marrow transplantations. *Biol. Blood Marrow Transplant.* **16**, 430–434 (2010).

583. Gregg, R. *et al.* The number of human peripheral blood CD4+ CD25high regulatory T cells increases with age. *Clin. Exp. Immunol.* **140**, 540–546 (2005).

584. Linterman, M. A. *et al.* Foxp3+ follicular regulatory T cells control the germinal center response. *Nat. Med.* **17**, 975–982 (2011).

585. Horai, Y. *et al.* Quantification of histopathological findings using a novel image analysis platform. *Journal of Toxicologic Pathology* **32**, 319–327 (2019).

586. Stack, E. C., Wang, C., Roman, K. A. & Hoyt, C. C. Multiplexed immunohistochemistry, imaging, and quantitation: A review, with an assessment of Tyramide signal amplification, multispectral imaging and multiplex analysis. *Methods* **70**, 46–58 (2014).

587. Lindqvist, M. *et al.* Expansion of HIV-specific T follicular helper cells in chronic HIV infection. *J Clin Invest* **122**, 3271–3280 (2012).

588. Perreau, M. *et al.* Follicular helper T cells serve as the major CD4 T cell compartment for HIV-1 infection, replication, and production. *J Exp Med* **210**, 143–156 (2013).

589. Sayin, I. *et al.* Spatial distribution and function of T follicular regulatory cells in human lymph nodes. *J Exp Med* **215**, 1531–1542 (2018).

590. Persaud, D. *et al.* Absence of detectable HIV-1 viremia after treatment cessation in an infant. *The New England Journal of Medicine* **369**, 1828–1835 (2013).

591. Heigele, A., Joas, S., Regensburger, K. & Kirchhoff, F. Increased susceptibility of CD4+ T cells from elderly individuals to HIV-1 infection and apoptosis is associated with reduced CD4 and enhanced CXCR4 and FAS surface expression levels. *Retrovirology* **12**, 86 (2015).

592. Graziani-Bowering, G. M. & Filion, L. G. Down Regulation of CD4 Expression following Isolation and Culture of Human Monocytes. *Clin. Diagn. Lab. Immunol.* **7**, 182–191 (2000).

593. Qureshi, O. S. *et al.* Constitutive clathrin-mediated endocytosis of CTLA-4 persists during T cell activation. *J. Biol. Chem.* **287**, 9429–9440 (2012).

594. Takahashi, T. *et al.* Immunologic Self-Tolerance Maintained by Cd25+Cd4+Regulatory T Cells Constitutively Expressing Cytotoxic T Lymphocyte–Associated Antigen 4. *J Exp Med* **192**, 303–310 (2000).

595. Tran, T.-A. *et al.* Resting Regulatory CD4 T Cells: A Site of HIV Persistence in Patients on Long-Term Effective Antiretroviral Therapy. *PLoS ONE* **3**, e3305 (2008).

596. Jagarapu, A., Piovoso, M. J. & Zurakowski, R. An Integrated Spatial Dynamics—Pharmacokinetic Model Explaining Poor Penetration of Anti-retroviral Drugs in Lymph Nodes. *Front. Bioeng. Biotechnol.* **8**, (2020).

597. Rothenberger, M. K. *et al.* Large number of rebounding/founder HIV variants emerge from multifocal infection in lymphatic tissues after treatment interruption. *Proceedings of the National Academy of Sciences of the United States of America* **112**, E1126-1134 (2015).

598. Fukazawa, Y. *et al.* B cell follicle sanctuary permits persistent productive simian immunodeficiency virus infection in elite controllers. *Nat. Med.* **21**, 132–139 (2015).

599. Kim, C. H. *et al.* Subspecialization of CXCR5+ T cells: B helper activity is focused in a germinal center-localized subset of CXCR5+ T cells. *The Journal of Experimental Medicine* **193**, 1373–1381 (2001).

600. Activation of HIV Transcription with Short-Course Vorinostat in HIV-Infected Patients on Suppressive Antiretroviral Therapy. https://journals.plos.org/plospathogens/article?id=10.1371/journal.ppat.1004473 .

601. Rasmussen, T. A. *et al.* The effect of antiretroviral intensification with dolutegravir on residual virus replication in HIV-infected individuals: a randomised, placebo-controlled, double-blind trial. *Lancet HIV* **5**, e221–e230 (2018).

602. Pasternak, A. O. *et al.* Cellular Levels of HIV Unspliced RNA from Patients on Combination Antiretroviral Therapy with Undetectable Plasma Viremia Predict the Therapy Outcome. *PLOS ONE* **4**, e8490 (2009).

603. Pasternak, A. O. *et al.* Modest nonadherence to antiretroviral therapy promotes residual HIV-1 replication in the absence of virological rebound in plasma. *J. Infect. Dis.* **206**, 1443–1452 (2012).

604. Li, J. Z. *et al.* The Size of the Expressed HIV Reservoir Predicts Timing of Viral Rebound after Treatment Interruption. *AIDS* **30**, 343–353 (2016).

605. Procopio, F. A. *et al.* A Novel Assay to Measure the Magnitude of the Inducible Viral Reservoir in HIV-infected Individuals. *EBioMedicine* **2**, 874–883 (2015).

606. Vanderleyden, I., Linterman, M. A. & Smith, K. G. Regulatory T cells and control of the germinal centre response. *Arthritis Research & Therapy* **16**, 471 (2014).

607. Fryer, H. R., Wolinsky, S. M. & McLean, A. R. Increased T cell trafficking as adjunct therapy for HIV-1. *PLOS Computational Biology* **14**, e1006028 (2018).

608. Ho, Y.-C. *et al.* Replication-Competent Noninduced Proviruses in the Latent Reservoir Increase Barrier to HIV-1 Cure. *Cell* **155**, 540–551 (2013).

609. McCampbell, A. S. *et al.* Tissue Thickness Effects on Immunohistochemical Staining Intensity of Markers of Cancer. *Appl Immunohistochem Mol Morphol* (2017) doi:10.1097/PAI.0000000000000593.

610. Lugagne, J.-B. *et al.* Identification of individual cells from z-stacks of bright-field microscopy images. *Scientific Reports* **8**, 11455 (2018).

611. Leong, Y. A. *et al.* CXCR5(+) follicular cytotoxic T cells control viral infection in B cell follicles. *Nat. Immunol.* **17**, 1187–1196 (2016).

612. Fletcher, C. V. *et al.* Persistent HIV-1 replication is associated with lower antiretroviral drug concentrations in lymphatic tissues. *Proc Natl Acad Sci U S A* **111**, 2307–2312 (2014).

613. Selby, L. I., Cortez-Jugo, C. M., Such, G. K. & Johnston, A. P. R. Nanoescapology: progress toward understanding the endosomal escape of polymeric nanoparticles. *Wiley Interdiscip Rev Nanomed Nanobiotechnol* **9**, (2017).

614. Surve, D. H. & Jindal, A. B. Recent advances in long-acting nanoformulations for delivery of antiretroviral drugs. *Journal of Controlled Release* **324**, 379–404 (2020).

615. June, C. H., O'Connor, R. S., Kawalekar, O. U., Ghassemi, S. & Milone, M. C. CAR T cell immunotherapy for human cancer. *Science* **359**, 1361–1365 (2018).

616. Kalos, M. *et al.* T cells with chimeric antigen receptors have potent antitumor effects and can establish memory in patients with advanced leukemia. *Sci Transl Med* **3**, 95ra73 (2011).

617. Haran, K. P. *et al.* Simian Immunodeficiency Virus (SIV)-Specific Chimeric Antigen Receptor-T Cells Engineered to Target B Cell Follicles and Suppress SIV Replication. *Front. Immunol.* **9**, (2018).

618. Allers, K. *et al.* Gut Mucosal FOXP3+ Regulatory CD4+ T Cells and Nonregulatory CD4+ T Cells Are Differentially Affected by Simian

Immunodeficiency Virus Infection in Rhesus Macaques. *J Virol* **84**, 3259–3269 (2010).

619. Miles, B. *et al.* Follicular regulatory T cells impair follicular T helper cells in HIV and SIV infection. *Nature Communications* **6**, 8608 (2015).
620. Ji, J. & Cloyd, M. W. HIV-1 binding to CD4 on CD4+CD25+ regulatory T cells enhances their suppressive function and induces them to home to, and accumulate in, peripheral and mucosal lymphoid tissues: an additional mechanism of immunosuppression. *Int Immunol* **21**, 283–294 (2009).
621. Jiao, Y. *et al.* The decrease of regulatory T cells correlates with excessive activation and apoptosis of CD8+ T cells in HIV-1-infected typical progressors, but not in long-term non-progressors. *Immunology* **128**, e366–e375 (2009).
622. Weiss, L. *et al.* Relationship between Regulatory T Cells and Immune Activation in Human Immunodeficiency Virus-Infected Patients Interrupting Antiretroviral Therapy. *PLOS ONE* **5**, e11659 (2010).
623. Simonetta, F. *et al.* Early and long-lasting alteration of effector CD45RA(-)Foxp3(high) regulatory T-cell homeostasis during HIV infection. *J Infect Dis* **205**, 1510–1519 (2012).
624. Angin, M. *et al.* Preserved function of regulatory T cells in chronic HIV-1 infection despite decreased numbers in blood and tissue. *J Infect Dis* **205**, 1495–1500 (2012).
625. Miragaia, R. J. *et al.* Single-Cell Transcriptomics of Regulatory T Cells Reveals Trajectories of Tissue Adaptation. *Immunity* **50**, 493-504.e7 (2019).
626. Selliah, N. *et al.* FOXP3 Inhibits HIV-1 Infection of CD4 T-cells via Inhibition of LTR Transcriptional Activity. *Virology* **381**, 161–167 (2008).

627. Pandiyan, P. *et al.* CD152 (CTLA-4) Determines the Unequal Resistance of Th1 and Th2 Cells against Activation-induced Cell Death by a Mechanism Requiring PI3 Kinase Function. *J Exp Med* **199**, 831–842 (2004).

628. Weiss, E.-M. *et al.* Foxp3-mediated suppression of CD95L expression confers resistance to activation-induced cell death in regulatory T cells. *J Immunol* **187**, 1684–1691 (2011).

629. Day, C. L. *et al.* PD-1 expression on HIV-specific T cells is associated with T-cell exhaustion and disease progression. *Nature* **443**, 350–354 (2006).

630. Cao, Q., Xue, Y. & Wang, Y. [Association of PD-1 expression on CD4+ CD25 nt/hi CD127 lo regulatory T cells with disease progression in HIV-1 infected patients]. *Xi Bao Yu Fen Zi Mian Yi Xue Za Zhi* **25**, 1020–1022 (2009).

631. Elahi, S., Niki, T., Hirashima, M. & Horton, H. Galectin-9 binding to Tim-3 renders activated human CD4+ T cells less susceptible to HIV-1 infection. *Blood* **119**, 4192–4204 (2012).

632. Koch, K. *et al.* Increased Frequency of CD49b/LAG-3(+) Type 1 Regulatory T Cells in HIV-Infected Individuals. *AIDS Res Hum Retroviruses* **31**, 1238–1246 (2015).

633. Khaitan, A. *et al.* FOXP3+Helios+ regulatory T cells, immune activation and advancing disease in HIV infected children. *J Acquir Immune Defic Syndr* **72**, 474–484 (2016).

634. Ji, J. & Cloyd, M. W. HIV-1 binding to CD4 on CD4+CD25+ regulatory T cells enhances their suppressive function and induces them to home to, and accumulate in, peripheral and mucosal lymphoid tissues: an additional mechanism of immunosuppression. *Int Immunol* **21**, 283–294 (2009).

635. D'Souza, M. *et al.* Programmed death 1 expression on HIV-specific CD4+ T cells is driven by viral replication and associated with T cell dysfunction. *J Immunol* **179**, 1979–1987 (2007).

636. Chew, G. M. *et al.* TIGIT Marks Exhausted T Cells, Correlates with Disease Progression, and Serves as a Target for Immune Restoration in HIV and SIV Infection. *PLOS Pathogens* **12**, e1005349 (2016).

637. Noto, A. *et al.* CD32+ and PD-1+ Lymph Node CD4 T Cells Support Persistent HIV-1 Transcription in Treated Aviremic Individuals. *J Virol* **92**, (2018).

638. Schaer, D. A. *et al.* GITR pathway activation abrogates tumor immune suppression through loss of regulatory T cell lineage stability. *Cancer Immunol Res* **1**, 320–331 (2013).

639. Schoenhals, J. E. *et al.* Anti-glucocorticoid-induced Tumor Necrosis Factor–Related Protein (GITR) Therapy Overcomes Radiation-Induced Treg Immunosuppression and Drives Abscopal Effects. *Front. Immunol.* **9**, (2018).

640. Erben, L. & Buonanno, A. Detection and Quantification of Multiple RNA Sequences Using Emerging Ultrasensitive Fluorescent in situ Hybridization Techniques. *Curr Protoc Neurosci* **87**, e63 (2019).

641. Zerbato, J. M. *et al.* Multiply spliced HIV RNA is a predictive measure of virus production ex vivo and in vivo following reversal of HIV latency. *EBioMedicine* **65**, 103241 (2021).